

## Tandem catalysis in polymer chemistry

**Citation for published version (APA):**

As, van, B. A. C. (2007). *Tandem catalysis in polymer chemistry*. [Phd Thesis 1 (Research TU/e / Graduation TU/e), Chemical Engineering and Chemistry]. Technische Universiteit Eindhoven.  
<https://doi.org/10.6100/IR616811>

**DOI:**

[10.6100/IR616811](https://doi.org/10.6100/IR616811)

**Document status and date:**

Published: 01/01/2007

**Document Version:**

Publisher's PDF, also known as Version of Record (includes final page, issue and volume numbers)

**Please check the document version of this publication:**

- A submitted manuscript is the version of the article upon submission and before peer-review. There can be important differences between the submitted version and the official published version of record. People interested in the research are advised to contact the author for the final version of the publication, or visit the DOI to the publisher's website.
- The final author version and the galley proof are versions of the publication after peer review.
- The final published version features the final layout of the paper including the volume, issue and page numbers.

[Link to publication](#)

**General rights**

Copyright and moral rights for the publications made accessible in the public portal are retained by the authors and/or other copyright owners and it is a condition of accessing publications that users recognise and abide by the legal requirements associated with these rights.

- Users may download and print one copy of any publication from the public portal for the purpose of private study or research.
- You may not further distribute the material or use it for any profit-making activity or commercial gain
- You may freely distribute the URL identifying the publication in the public portal.

If the publication is distributed under the terms of Article 25fa of the Dutch Copyright Act, indicated by the "Taverne" license above, please follow below link for the End User Agreement:

[www.tue.nl/taverne](http://www.tue.nl/taverne)

**Take down policy**

If you believe that this document breaches copyright please contact us at:

[openaccess@tue.nl](mailto:openaccess@tue.nl)

providing details and we will investigate your claim.

# Tandem Catalysis in Polymer Chemistry

## **Proefschrift**

ter verkrijging van de graad van doctor aan de  
Technische Universiteit Eindhoven, op gezag van de  
Rector Magnificus, prof.dr.ir. C.J. van Duijn, voor een  
commissie aangewezen door het College voor  
Promoties in het openbaar te verdedigen  
op dinsdag 16 januari 2007 om 16.00 uur

door

**Bart Arnoldus Cornelis van As**

geboren te Nijmegen

Dit proefschrift is goedgekeurd door de promotor:

prof.dr. E.W. Meijer

Copromotor:

dr.ir. A.R.A. Palmans

The research described in this thesis was financially supported by the National Research School Combination Catalysis Controlled by Chemical Design.

Druk: Gildeprint Drukkerijen B.V. te Enschede

A catalogue record is available from the Library Eindhoven University of Technology

ISBN-10: 90-386-2639-8

ISBN-13: 978-90-386-2639-0

# Table of contents

## Chapter 1

### Introduction

1.1	Lipase catalysis	2
1.1.1	<i>Candida antarctica</i> Lipase B: Structure and mechanism	2
1.1.2	Lipases in polymerization chemistry	4
1.1.3	Role of water in lipase (polymerization) chemistry	5
1.1.4	Selectivity in lipase-catalyzed reactions: the enantiomeric ratio E	7
1.2	Tandem catalysis – nomenclature and considerations	9
1.2.1	Nomenclature of one-pot multicyclic reactions	9
1.2.2	Considerations and issues concerning tandem catalysis	10
1.2.3	Applications of tandem catalysis in organic chemistry	11
1.4	Ruthenium-catalyzed racemization	14
1.4.1	Catalysts available	14
1.4.2	Ruthenium-catalyzed racemization: mechanism	16
1.5	Iterative tandem catalysis	18
1.5.1	Tandem catalysis in polymer chemistry	18
1.6	Aim and scope of the thesis	19
1.7	Outline of the thesis	20
1.8	References and notes	21

## Chapter 2

### Chiral block copolymers by one-pot chemoenzymatic cascade polymerization

2.1	Introduction	26
2.1.1	Synthesis of block copolymers	26
2.1.2	Nitroxide-mediated controlled free radical polymerization	27
2.2	Block copolymers from a bifunctional initiator	29
2.3	Synthesis of block copolymers in one pot	34
2.4	One-pot chemo-enzymatic kinetic resolution polymerization	35
2.4	Conclusions	38
2.5	Experimental Section	38
2.6	References and notes	41

## Chapter 3

### Enzymatic ring-opening of $\omega$ -substituted lactones

3.1	Introduction	44
3.1.1	Enantioselectivity of lipases towards the nucleophile	44
3.1.2	Enantioselectivity of CALB toward the acyl donor	45
3.1.3	Enantioselectivity in CALB-catalyzed ring-opening of lactones	45
3.2	Enzymatic ring-opening of 6-methyl- $\epsilon$ -caprolactone	46
3.2.1	Enzymatic ring-opening of 6-methyl- $\epsilon$ -caprolactone on short timescales	47
3.2.2	Enzymatic ring-opening of 6-methyl- $\epsilon$ -caprolactone on long time scales	48
3.2.3	Effect of solvent and temperature on the insertion of ( <i>R</i> )-6-MeCL	52
3.3	Enzymatic ring-opening of other cyclic esters	54
3.3.1	Enzymatic ring-opening of lactide	56
3.4	Reversibility of enzymatic ring-opening: synthesis of both enantiomers of 6-MeCL	59
3.5	Thermodynamic analysis of the ring-opening of 6-MeCL	63
3.5.1	Thermodynamics of enantioselectivity	64
3.5.2	Thermodynamics of the enantioselectivity of CALB towards 6-MeCL	67
3.6	Conclusions	69
3.7	Experimental section	70
3.8	References	72

## Chapter 4

### Iterative tandem catalysis

4.1	Introduction	76
4.2	Selection of the catalysts: selectivity and complementarity	78
4.3	ITC of ( <i>S</i> )-6-MeCL in a one-pot system	82
4.4	Compatibility of the catalysts	84
4.4.1	Activity of the racemization catalyst in one-pot ITC	84
4.4.2	Activity of the lipase catalyst in one-pot ITC	85
4.4.3	Deactivation of the lipase under ITC conditions	86
4.4.4	Deactivation of the racemization catalyst under ITC conditions	88
4.5	Proof of principle: ITC of ( <i>S</i> )-6-MeCL in a two-pot system	90
4.6	Conclusions	94
4.7	Experimental section	95
4.8	References and notes	97

## Chapter 5

### Dynamic kinetic resolution polymerization of diols and diesters

5.1	Introduction	102
5.2	Selection of the racemization catalyst	103
5.2.1	Reference experiments with catalysts <b>1</b> and <b>2</b>	104
5.2.2	DKRP using racemization catalyst <b>1</b>	106
5.2.3	DKRP using racemization catalyst <b>2</b>	109
5.3	DKRP of other substrates	111
5.4	Optimization study of the DKRP of 1,3-diol and DIA using catalyst <b>2</b>	115
5.5	Conclusions	119
5.6	Experimental section	119
5.7	References and notes	124

## Chapter 6

### Kinetics of enzymatic ROP and ITC - Theory and practice

6.1	Introduction	128
6.2	Kinetics of lipase-catalyzed polymerizations	128
6.2.1	Michaelis-Menten kinetics	128
6.2.2	Michaelis-Menten kinetics in an enzymatic ring-opening polymerization	129
6.2.3	Experimental results	134
6.3	Application of the LH model to enzyme kinetics	136
6.3.1	Langmuir-Hinshelwood applied to a MM single substrate single product reaction	137
6.4	Kinetic evaluation of iterative tandem catalysis of (S)-6-MeCL	139
6.4.1	Kinetic behavior of one-pot ITC of (S)-6-MeCL	139
6.4.2	Application of LH kinetics to one-pot ITC of (S)-6-MeCL	142
6.4.3	Simulation of ITC based on the LH model	144
6.4	Conclusions	146
6.5	Experimental	147
6.6	References and notes	149



# 1

## Introduction



## 1.1 Lipase catalysis

The use of biocatalysis by mankind has a long history, with records of beer brewing by the Sumerians dating back as much as 6000 years. The use of Nature's catalysts – enzymes – for synthetic purposes, however, was initiated only in the second half of the 19<sup>th</sup> century. The history of the word “enzyme” itself goes back to 1877 when Wilhelm Kühne, a German scientist, coined the word after the Greek word “εν ζυμων” meaning “in leaven”. Twenty years later, a major development came with the discovery in 1897 by Eduard Büchner that yeast extracts – i.e. in the absence of living cells – also show catalytic activity. Soon after, it became apparent that enzymes even show catalytic activity in organic media.<sup>1,2</sup> In 1926, James Sumner for the first time succeeded in isolating and crystallizing an enzyme: an urease. However, biocatalysis only became commonplace with the publications of Zaks and Klivanov in the early 1980s and the development of industrial applications.<sup>3,4</sup> Nowadays, biocatalysts are an indispensable tool for the organic chemist as well as for the chemical and food processing industries. The Accelrys Biocatalysis Database currently records an impressive 46,000+ reactions involving enzymic and microbial transformations. For almost every conceivable chemical reaction a biocatalyst is available that is able to perform the desired chemistry under mild conditions, with high activity and often with chemo-, regio- or stereoselectivity.

### 1.1.1 *Candida antarctica* Lipase B: Structure and mechanism

Lipases are by far the most used enzymes in synthetic organic chemistry. Their biological function is the hydrolysis of fatty acid esters in aqueous medium. However, they are also catalytically active in esterification, transesterification and aminolysis in organic solvents.<sup>5,6</sup> Due to their simple catalytic machinery, lipases are versatile catalysts that readily perform non-natural reactions. Many lipases are activated by an oil/water interface and are inactive in a homogeneous aqueous medium. The interfacial activation of lipases exists because most of them possess a lid, which is kept closed by the surface tension of water. This lid rolls back in contact with an oil phase and the enzyme becomes active. Although the natural role of lipases does not involve enantiodiscrimination, they are inherently chiral and often act enantioselectively on the acyl donor as well as on the acceptor.

Of all available lipases, by far the most used in organic chemistry is *Candida antarctica* Lipase B (CALB). This flexible, thermostable lipase is available in immobilized form on a macroporous polymer matrix, Novozym 435 (Figure 1.1). Contrary to most other lipases, CALB does not display interfacial activation; it is one of the very few lipases where this lid structure is very small or absent. Some authors consider CALB therefore not to be a true lipase, since it behaves more like an esterase.<sup>7</sup> Like all other lipases of which the structure has been resolved at a molecular level, CALB belongs to the  $\alpha/\beta$ -hydrolase fold family of proteins.

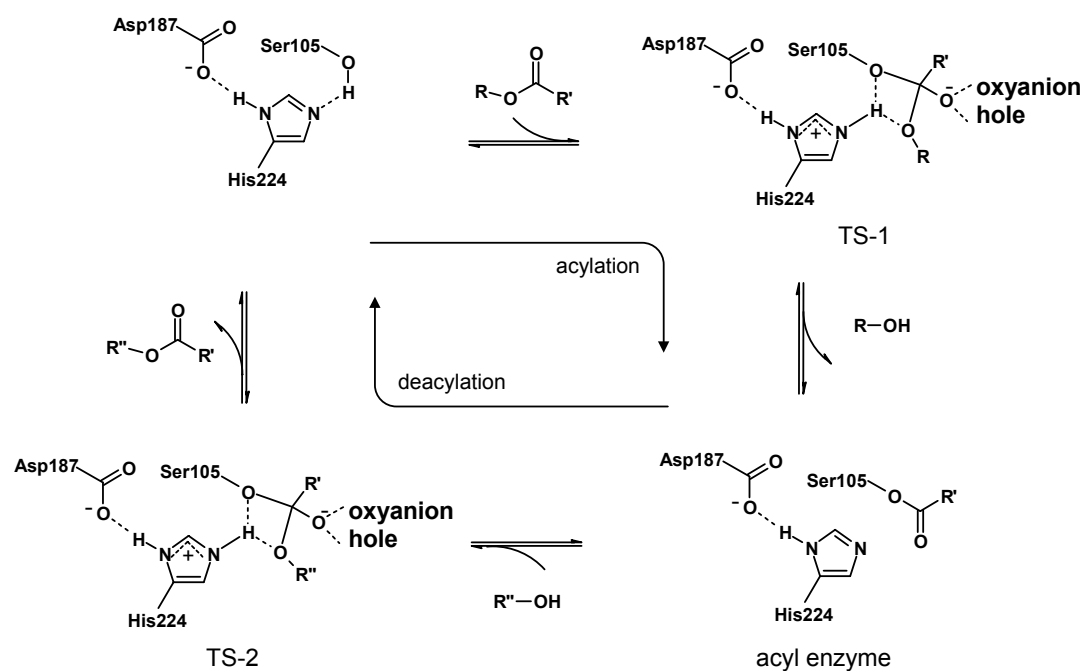
CALB consists of 317 amino acids with a molecular weight of approximately 33 kDa, which is relatively small compared to other lipases. The active site of CALB contains the so-called catalytic triad, Ser105-His224-Asp187, which is common to all serine hydrolases.



**Figure 1.1** *Novozym 435 is an immobilized preparation of CALB. The acrylic resin beads have a size of 0.3 – 1.0 mm and contain approximately 10 wt.% protein.*

The mechanism of lipases has been studied in detail.<sup>8-11</sup> Lipases belong to the class of enzymes “serine hydrolases”. These enzymes were so named as they have a highly reactive serine residue – for CALB this is Ser105 – which attacks the carboxyl group of the substrate. This results in an acyl enzyme intermediate consisting of the acyl donor covalently bound to the enzyme at this serine. The residues of the catalytic triad form a charge-transfer relay network. His224, polarized by Asp187, acts as a proton shuttle which accepts the hydrogen ion from Ser105 as it nucleophilically attacks the substrate. This is clarified in Scheme 1.1, which shows the generally accepted mechanism for CALB-catalyzed transesterification.<sup>12</sup> In the first step, the acyl donor is adsorbed in the active site of the lipase. Subsequently, the carbonyl is attacked by the serine hydroxyl residue, leading to transition state analogue TS-1. The C=O bond becomes a single bond, leaving a negative charge on the O atom (an *oxyanion*), while the fourth valency of the carbon atom is occupied by a bond with the serine oxygen. The oxyanion forms hydrogen bonds to two main chain amides of residues Thr40 and Gln106. This binding site is termed the *oxyanion hole*. The freed alcohol leaves the active site, yielding the acyl enzyme in which the acyl group is covalently bonded to the serine residue. In the subsequent deacylation, an alcohol performs a nucleophilic attack on the carbonyl group of the acyl enzyme. Again, interaction with the oxyanion hole stabilizes the transition state. Finally, the transesterification product can leave the active site, reforming the original free enzyme. The active site of CALB can be partitioned into two sides, an acyl side and an alcohol side, where the corresponding parts of the substrate will be located during catalysis.<sup>13</sup> The acyl side of the active site pocket is more spacious than the alcohol side, and it might be able to accommodate both enantiomers of chiral acyl groups. Therefore, the stereoselectivity with respect to the acyl side of the substrate is much lower than for the alcohol side.<sup>14,15</sup> Enantioselectivity towards chiral esters is the result of the lower energy of the transition state of the acylation for the favored enantiomer, while the enantioselectivity

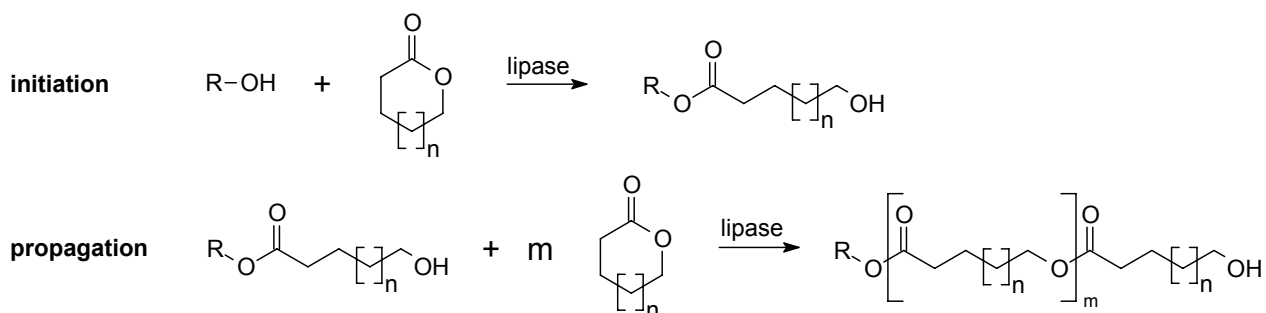
towards secondary alcohols is the result of the lower energy of the transition state of the deacylation for the favored enantiomer of the alcohol.



**Scheme 1.1** Reaction mechanism of CALB-catalyzed transesterification. TS-1 and TS-2 represent the transition state analogues in the acylation and deacylation steps, respectively.<sup>12</sup>

### 1.1.2 Lipases in polymerization chemistry

All naturally occurring polymers are produced *in vivo* by enzymatic catalysis. Therefore, it is not surprising that isolated enzymes can also show polymerization activity *in vitro*. In the past two decades, many reports have appeared on the synthesis of polymers using oxidoreductases, transferases and hydrolases.<sup>16,17</sup> The first observation was reported in 1983 by Okamura *et al.* who discovered that oligomeric species were formed in the lipase-catalyzed hydrolysis of castor oil.<sup>18</sup> Soon after, reports appeared on the synthesis of polymers with considerable molecular weight by lipase-catalyzed polycondensation of hydroxyacids,<sup>19,20</sup> and even enantioselective lipase-catalyzed polycondensations were reported.<sup>21-23</sup>



**Scheme 1.2** Lipase-catalyzed ring-opening polymerization of lactones.

The lipase-catalyzed ring-opening polymerization of lactones, which is shown in Scheme 1.2, was pioneered by Kobayashi and Knani in 1993.<sup>24,25</sup> Since then a broad range of substrates have been polymerized. Recently, our laboratories reported on the successful lipase-catalyzed polymerization of all lactones with ring sizes between 6 to 13.<sup>26</sup> Furthermore, reports have appeared on the polymerization of macrolactones (which are difficult to polymerize using chemical catalysts),<sup>26-28</sup> cyclic carbonates,<sup>29-33</sup> mixtures of diols and diesters, dicarbonates or diacids,<sup>34-39</sup> and hydroxyesters.<sup>40,41</sup> Since most lipases retain their activity in organic media under nearly anhydrous conditions, well-defined high molecular weight functionalized polymers can be obtained; e.g. poly( $\omega$ -pentadecalactone) was synthesized using CALB with a weight-averaged molecular weight  $M_w$  of 91 kDa.<sup>42</sup>

### 1.1.3 Role of water in lipase (polymerization) chemistry

Enzymes naturally perform their roles in aqueous environment. However, it has been long recognized that many enzymes show high activity in organic solvents.<sup>43</sup> Since water is the natural environment for an enzyme, it is not surprising that the water content of an organic solvent (or, more specifically, the water activity  $a_w$ ) greatly influences the activity and stability of enzymes.<sup>44-48</sup> In esterification and transesterification reactions, the presence of water leads to hydrolysis of esters. In a lipase-catalyzed ring-opening polymerization, water may be used as the initiator since the hydrolysis of a lactone leads to a hydroxyacid, which can then propagate via the formed hydroxygroup. However, the use of water initiation severely limits the control over the polymerization. Since the exact amount of water in the system is difficult to manage, the monomer / initiator ratio is uncertain and one loses control over the molecular weight of the polymer formed. Moreover, if one aims at making a functional polymer with a specific initiator (e.g. a bifunctional initiator, so a block copolymer can be formed in a second polymerization step), the presence of water leads, due to of water initiation, to unfunctionalized polymers. In these situations, it is of paramount importance to reduce the amount of water to a level as low as possible, while maintaining enzymatic activity.

#### *Enzyme hydration: three states of water*

Clark *et al.* investigated the role of water in enzymes in organic solvents through a multinuclear NMR study.<sup>49</sup> Based on the results of this study a model was proposed that describes three different states of water during enzyme hydration (Figure 1.2). First, a layer of tightly bound water molecules exists that do not exchange with the solvent (layer b1). These water molecules are necessary for retaining the tertiary structure of the enzyme. Removal of this water layer results in denaturation of the enzyme. A second hydration state exists of water molecules that are reversibly bound to the enzyme, and do exchange into the bulk solvent (layer b2). These water molecules are in equilibrium with the third state of water, free water molecules that are adsorbed on the enzyme or carrier or are dissolved in the medium (layer f).

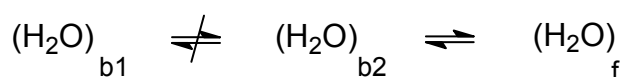


**Figure 1.2** States of enzyme hydration.

### Minimizing water initiation by enzyme drying

It is assumed that the water molecules that are loosely bound and the free water (layers b2 and f) can act as initiators in lipase-catalyzed ring-opening polymerization. To reduce water initiation to the fullest extent possible, these water layers have to be removed from enzyme and carrier by a drying protocol. It is evident that a fine balance exists between removing as much water as possible to reduce water-related side reactions and enzyme activity. In our laboratory extensive research has been carried out to determine the effect of several drying protocols on the activity of the lipase and the amount of water initiation in a benzyl alcohol-initiated polymerization of  $\epsilon$ -caprolactone (CL) in dry toluene.<sup>50</sup> Figure 1.3 shows that the optimal results were obtained by drying the enzyme for 16 hours at 50 °C, under reduced pressure (20 mbar) in presence of  $\text{P}_2\text{O}_5$ , and with molar sieves added to the reaction mixture (entry 8). Using this drying protocol, high activity was retained while the water-initiation was below detection limit (<5 %).

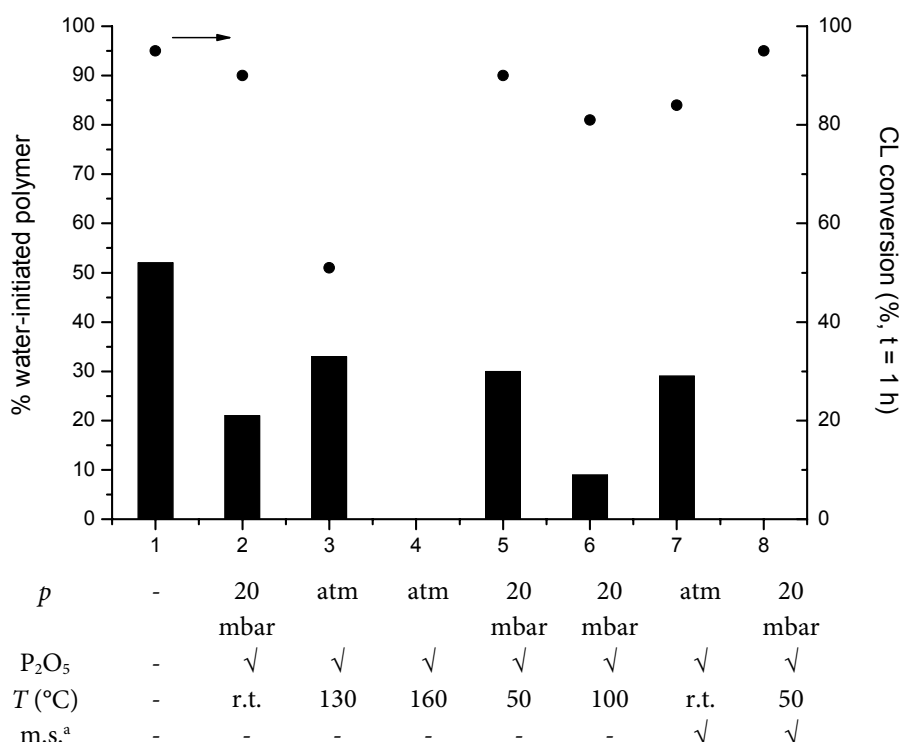


**Figure 1.3** Effect of different drying protocols on enzyme activity and amount of water initiation in a CL polymerization.<sup>50</sup> <sup>a</sup>Activated molar sieves (4 Å) were added before drying the enzyme.

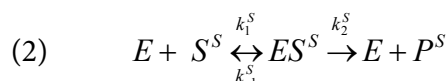
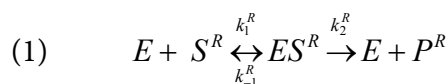
The molar sieves were kept in the reaction mixture during reaction.

### 1.1.4 Selectivity in lipase-catalyzed reactions: the enantiomeric ratio E

Although the natural role of lipases does not involve enantioselective action, they often behave stereoselectively towards chiral substrates. The enantioselectivity of a given reaction is usually described by the enantiomeric ratio E.

The enantiomeric ratio E

In an enantioselective reaction, two enantiomers can react according to Equations 1 and 2. The steady-state hypothesis gives Equation 3 (as given for S<sup>R</sup>) and rearranges, after substituting K<sub>M</sub><sup>R</sup> into Equation 4:



$$(3) \quad \frac{d[ES^R]}{dt} = 0 = k_1^R[E][S^R] - k_{-1}^R[ES^R] - k_2^R[ES^R]$$

$$(4) \quad [ES^R] = \frac{k_1^R[E][S^R]}{k_{-1}^R + k_2^R} = \frac{[E][S^R]}{K_M^R}$$

The ratio of the reaction rates for both enantiomers is then given by Equation 5. V<sub>max</sub> is the maximum velocity of the enzymatic reaction and is equal to k<sub>1</sub>·[E]<sub>0</sub> (see also Chapter 6). As a measure of the selectivity of the enzyme towards the faster reacting enantiomer, the enantiomeric ratio E was introduced by Chen *et al.*<sup>51</sup> E is defined as the ratio of specificity constants k<sub>sp</sub> of both enantiomers (Equation 6). As can be seen from Equation 5, if a racemic mixture is used, E corresponds to the ratio of the initial reaction rates of both enantiomers.

$$(5) \quad \frac{\frac{d[S^R]}{dt}}{\frac{d[S^S]}{dt}} = \frac{r^R}{r^S} = \frac{k_2^R[ES^R]}{k_2^S[ES^S]} = \frac{\frac{V_{\max}^R}{K_M^R} [S^R]}{\frac{V_{\max}^S}{K_M^S} [S^S]} = E \frac{[S^R]}{[S^S]}$$

$$(6) \quad \text{with } E = \frac{\frac{V_{\max}^R}{K_M^R}}{\frac{V_{\max}^S}{K_M^S}} = \frac{k_{sp}^R}{k_{sp}^S}$$

*Determination of the enantiomeric ratio E*

The enantiomeric ratio  $E$  can be calculated if the  $K_M$  and  $V_{max}$  of both enantiomers are known. However, in most situations those constants are not available nor easily determined. Several methods have been developed to calculate  $E$  from the  $ee$  of the remaining substrate, product and/or conversion.<sup>51,52</sup> The advantages and problems related to each of those methods have been discussed in literature.<sup>53</sup> Although calculation based on the  $ee$  of remaining substrate and product yields the most accurate result, in an enantioselective polymerization, the  $ee$  of the product can not (easily) be determined. In this situation, Equation 7 can be used, relating the  $ee$  of the remaining substrate ( $ee_s$ ) and total conversion ( $c$ ) to the enantiomeric ratio  $E$ .

$$(7) \quad E = \frac{\ln[(1-c)(1-ee_s)]}{\ln[(1-c)(1+ee_s)]} \quad \text{with } 0 < ee < 1 \quad \text{and} \quad 0 < c < 1$$

For a reliable determination of  $E$ , curve fitting should be employed using as many data points as possible. An important consideration is the sensitivity of the calculated  $E$  towards errors in measured conversion and  $ee_s$ . Figure 1.4 shows the conversion –  $ee_s$  curves for  $E$  ratios of 3, 5, 10 and 100. Clearly, at 50% conversion (conversion = 0.5 in Figure 1.4, indicated by the dotted line) the values of  $ee_s$  differ the most; measurements around 50% conversion therefore provide more valuable data than measurements at low or high conversion levels.

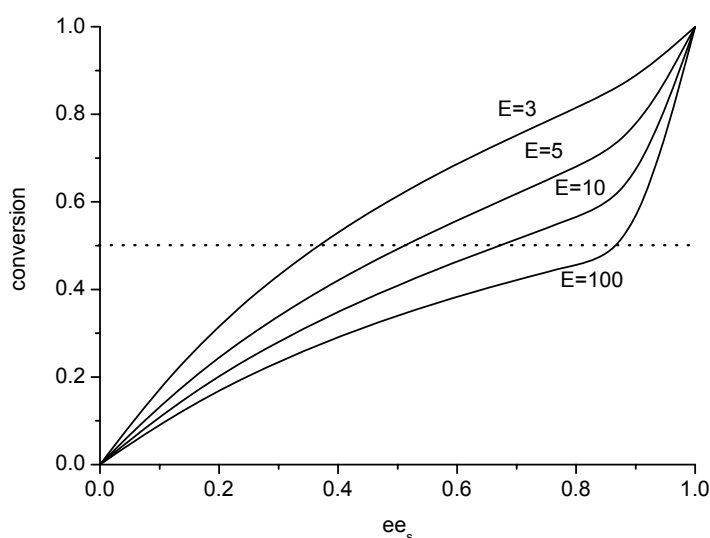


**Figure 1.4** Theoretical conversion versus  $ee_s$  curves for different  $E$  ratios

## 1.2 Tandem catalysis – nomenclature and considerations

Traditional organic and polymer synthesis of complex (macro)structures is often achieved by a step-by-step approach.<sup>54</sup> However, the integration of steps in a one-pot fashion has gained considerable interest in the past decades. The objectives for this are clear: not only can a reduction in effort, waste and energy consumption be achieved, but also the synthesis of complex products that are otherwise difficult to obtain – e.g. because of thermodynamic hurdles – comes within reach. In other words, the combination of chemistries may allow the direct synthesis of (macro)molecules with high structural complexity.<sup>55</sup> When multiple chemistries are performed in a single system, selectivity is a key issue. In many cases, it demands the simultaneous action of several highly selective catalytic systems. Perhaps the best examples of the concept of cooperating catalytic systems can be found in the human body; while reading this text your body is performing many biological processes in which multiple enzymes are working simultaneously (e.g. the multi-step glycolysis pathway which comprises the digestive conversion of glucose into energy and pyruvate<sup>56</sup>).

### 1.2.1 Nomenclature of one-pot multicatalytic reactions

The nomenclature used in literature associated with performing multiple catalytic mechanisms in one pot is confusing and frequently inconsistent. Near-synonymous terms like domino, cascade, tandem and multicatalytic have been used interchangeably. Several authors have proposed (sometimes incomplete or contradicting) definitions of each of these terms.<sup>55,57,58</sup> Fogg *et al.* recently proposed a taxonomy on one-pot procedures involving multiple catalytic events.<sup>59</sup> Although this proposal contains very stringent conditions, we adhere to the basic classification which is summarized below.

The terms *domino catalysis*, *tandem catalysis* and *cascade catalysis* are only applicable if multiple catalytic actions on a single molecule are performed in one pot and if all (pre)catalysts (masked or apparent) are present from the outset. If this is not the case, one can only speak of a *multicatalytic one-pot reaction*. This definition classifies the chemoenzymatic synthesis of chiral block copolymers as reported by Peeters *et al.* as a multicatalytic one-pot reaction, since the nickel-based catalyst for the radical polymerization is only added after the enzymatic reaction has completed.<sup>60</sup> Furthermore, *domino catalysis* applies to systems where only one catalytic mechanism operates. *Cascade catalysis* is a subcategory of domino catalysis, applying to systems with more than two transformations. *Tandem catalysis* then applies to systems where multiple catalytic mechanisms are exploited in one pot. If the catalytic mechanisms act independently, one speaks of *orthogonal tandem catalysis*. If a single catalyst acts via two different mechanisms, the term *auto-tandem catalysis* would be applicable. If a trigger is needed (e.g. by means of addition a reagent) to transform the catalyst or substrate



thereby activating the second catalytic mechanism, the term *assisted tandem catalysis* should be used. Figure 1.5 shows a flowchart for classification of one-pot reactions. In the work described in this thesis we deal with systems where multiple catalytic systems are running in one pot; therefore wherever the term tandem catalysis is mentioned, according to Fogg's taxonomy this belongs to the subcategory *orthogonal tandem catalysis*.

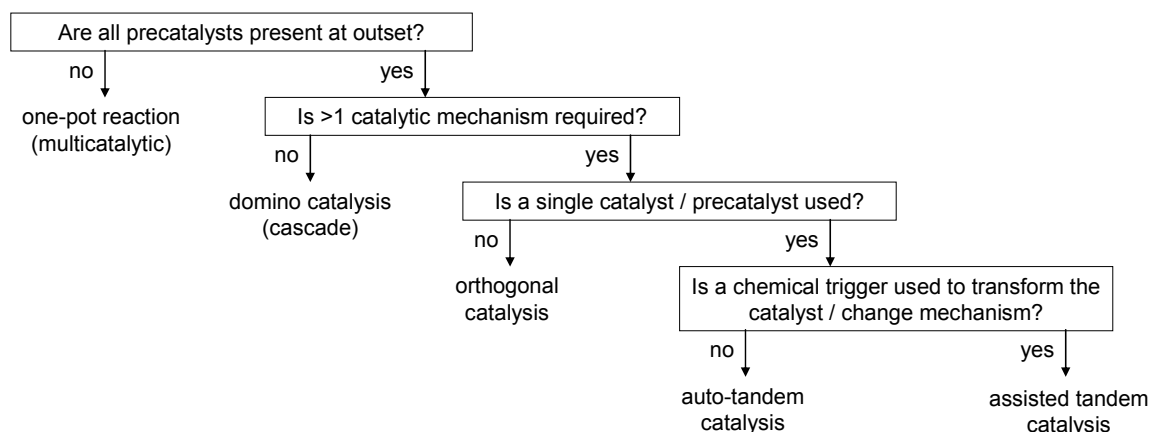


**Figure 1.5** Flowchart for classification of one-pot processes involving several catalytic mechanisms.<sup>59</sup>

## 1.2.2 Considerations and issues concerning tandem catalysis

### *Compatibility of reaction conditions*

When multiple catalysts are used, they should be mutually compatible with respect to the required reaction conditions. However, they often function optimally at different reaction conditions. This requires fine-tuning of the catalytic systems and conditions to allow for the right concerted cooperation. For example, a higher temperature might lead to faster kinetics of a homogeneous transition-metal catalyst, while enzyme specificity generally goes down with temperature. Frequently, a trade-off must be made between several competing effects.

### *Selectivity and substrate compatibility*

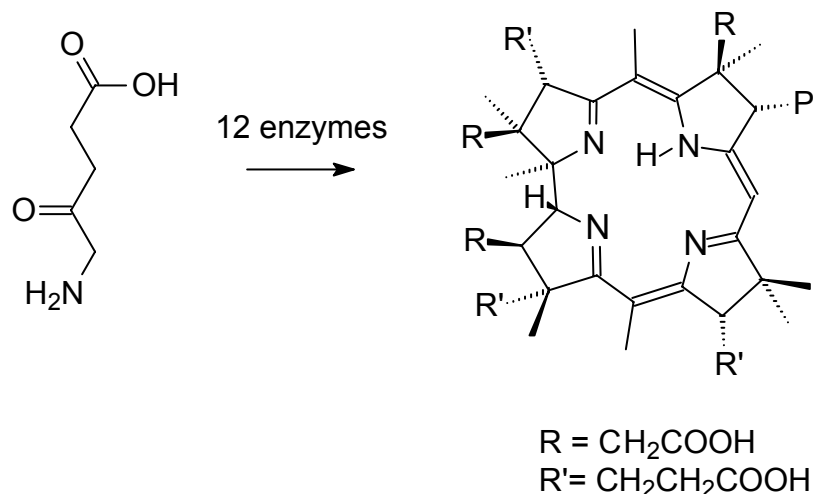
In addition, the catalytic action should be sufficiently selective and high-yielding. Since intermediate purification is left out in a one-pot reaction, imperfection in selectivity and yield is amplified when multiple processes are coupled. Side-products from one reaction step might have a detrimental effect on the activity of the other catalyst in the system. An example of this appears in the dynamic kinetic resolution process (DKR). Here, hydrolysis of acyl donor by the lipase (which always contains some trace water) results in carboxylic acid formation as a side-product. However, some ruthenium-complexes employed are deactivated by strong coordination of acids; therefore, a solid base must be added to the reaction mixture to preserve racemization activity.<sup>61</sup> Also, the combination of two catalytic processes is only

possible if they are truly orthogonal. A reactant that is consumed by one catalyst might result in unwanted side-reactions if exposed to the second catalyst. De Geus *et al.* recently reported their attempts to synthesize block copolymers in one pot by combining lipase-catalyzed ring-opening polymerization of  $\epsilon$ -caprolactone with the radical polymerization of methyl methacrylate (MMA).<sup>62</sup> They discovered, however, that MMA – being an ester – is readily transesterified by the lipase, setting free methanol. This resulted in methanol-initiated chains, as well as in chains end-capped by methacrylate-groups. Hence, no well-defined block copolymers could be obtained from a one-pot procedure.

For developing tandem catalytic processes, in-depth knowledge is required of the mechanistic characteristics of both catalytic processes, and of the interplay of the catalysts. Important questions are whether the catalysts, substrates and/or reagents affect each other, which side-reactions might play a role and whether the kinetics and reaction conditions can be matched. Kinetic measurements, therefore, are a crucial instrument in these investigations; insight into reaction rates provides invaluable information here. Since kinetics of enzyme-catalyzed (polymerization) processes are barely covered in literature, an overview of this topic is presented in Chapter 6.

### 1.2.3 Applications of tandem catalysis in organic chemistry

In the past decades, tandem catalysis has made inroads into organic synthesis. Many publications have appeared that describe the application of multiple catalysts or catalytic processes in a single system. Since several excellent reviews have appeared recently, elaborating on the many reports regarding tandem catalysis, only some instructive examples are discussed.<sup>54,55,57,59,63,64</sup> A stunning example where the action of multiple enzymes is combined – inspired by multienzymatic synthesis by Nature – is the ingenious *in vitro* synthesis of corrin, a vitamin B12 precursor from 5-aminolevulinic acid. Here, the target molecule is constructed using 12 enzymes for 17 consecutive reaction steps in a single flask, with an overall yield of 20% (Figure 1.6).<sup>65</sup>



20% yield

**Figure 1.6** Synthesis of corrin, a vitamin B12 precursor from 5-aminolevulinic acid, by 12 enzymes and 17 steps in a single vessel.<sup>65</sup>

#### Dynamic kinetic resolution

Since neither biotechnology nor metal-catalysis can replace all multistep routes, researchers seek to combine the virtues of chemical, chemocatalytic and enzymatic conversions. Perhaps the most elegant example of multidisciplinary catalysis is dynamic kinetic resolution (DKR), a process for synthesizing enantiopure products from racemic starting materials in 100% theoretical yield. Synthesis of chiral compounds can traditionally be achieved via three different strategies. First, chiral precursors from natural resources can be used – the so-called chiral pool. Second, asymmetric synthesis from prochiral precursors can be applied – mostly by using either enzymes or chiral (transition) metal-catalysts. To date, the most used method for production of chiral compounds, however, is resolution of racemates.<sup>66</sup> Resolution means the separation of a racemic mixture into its enantiomers. Generally, this is achieved by interaction with a chiral agent. Since reaction with either enantiomer proceeds via diastereomeric transition states, one enantiomer reacts faster than the other (Figure 1.7a). The major limitation of such kinetic resolution is that the maximum theoretical yield is 50% since only one enantiomer of the racemic starting material is consumed. This limitation was overcome by the development of dynamic kinetic resolution (DKR), where the remaining enantiomer is racemized *in situ* (Figure 1.7b). In DKR, the maximum theoretical yield has increased to 100%, since all of the racemic mixture can be converted to the optically pure product.

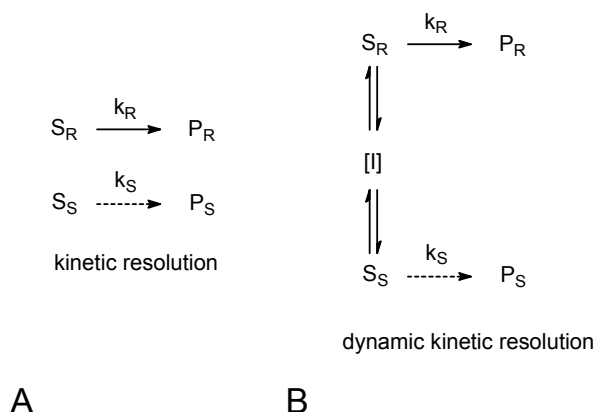


**Figure 1.7** General concept of (A) kinetic resolution and (B) dynamic kinetic resolution.  $k_R \gg k_S$ . The racemization often proceeds via an achiral intermediate (I).

The first example of DKR was reported by Noyori *et al.*, who performed stereoselective hydrogenation on chirally labile  $\beta$ -keto-esters.<sup>67</sup> Since the racemization originates from the lability of the acidic hydrogen, thus not being accomplished using a catalyst, this application of DKR is not considered tandem catalysis. The widest use of DKR, however, employs a combination of an enzyme with transition-metal catalyzed racemization to provide enantiopure secondary alcohols, carboxylic acids, esters, acetates, and  $\beta$ -hydroxy-esters.<sup>68-71</sup> Typically, ruthenium, iridium, rhodium, aluminum, vanadium or palladium catalysts are used as the racemization catalyst.<sup>72</sup> In the pioneering work of the group of Bäckvall *R*-selective lipase-catalyzed esterification of secondary alcohols is combined with ruthenium-catalyzed racemization of these secondary alcohols (Figure 1.8).

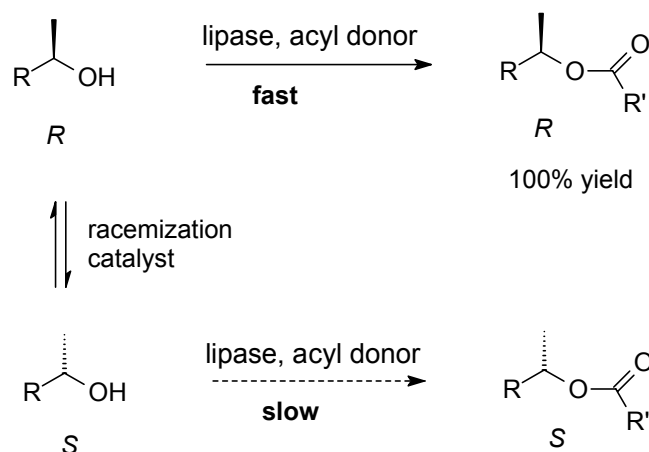


**Figure 1.8** Application of DKR for the synthesis of enantiopure secondary alcohols.

Recently, major developments have appeared in the field of ruthenium-catalyzed racemization; a short overview of the available catalysts and their respective mechanisms is

presented in section 1.4. The critical point for a successful DKR is the compatibility of both reactions and their respective kinetics. Ideally, the rate of racemization is much higher than the rate of acylation, and the latter should be highly selective. A major drawback of DKR is that the selectivity of the enzyme determines which enantiomer can be produced; to overcome this limitation, enzymes from other classes can be used which show opposite selectivity (such as *Subtilisin carlsberg*, which is classified as a peptidase, and shows *S*-selectivity in the acylation of secondary alcohols).

## 1.4 Ruthenium-catalyzed racemization

### 1.4.1 Catalysts available

Many types of racemization catalysts have been reported for use in DKR, among which ruthenium, iridium, rhodium, aluminum, vanadium and palladium complexes.<sup>72</sup> Ruthenium complexes are by far the most employed racemization catalysts in DKR due to their high activity and compatibility with lipases. Figure 1.9 shows the ruthenium-based racemization catalysts that were reportedly used successfully in DKR. In 1997, Bäckvall pioneered the DKR of secondary alcohols using a lipase as the acylating agent and a ruthenium complex for racemization.<sup>73,74</sup> The racemization catalyst employed was Shvo's diruthenium complex **1**. In the presence of this catalyst, various secondary alcohols were subjected to DKR in 20-40 hours reaction time at 70 °C with catalyst loadings of 2-5 mol.%. *p*-Chlorophenyl acetate was used as the acyl donor, since the use of common acyl donors in kinetic resolution such as vinyl acetate and isopropenyl acetate results in the formation of large quantities of acetaldehyde and acetone, respectively, which interfere with the racemization process. Kim and Park reported the DKR of various secondary alcohols using 5 mol.% of **2** as the racemization catalyst in presence of NEt<sub>3</sub> as a weak base.<sup>75</sup> A distinctive feature of this racemization system was that it only showed catalytic activity in presence of oxygen (2 mol. % was found to be optimal), but exposure to excess oxygen resulted in a loss of activity. The use of 4 mol.% of complex **3** in presence of NEt<sub>3</sub> allowed the DKR at room temperature of a wide range of allylic alcohols.<sup>76</sup> Verzijl *et al.* developed a DKR process using **1** as the catalyst. The DKR was performed at reduced pressure for selective distillation of the acyl donor residue, allowing the use of simple alkyl esters such as isopropyl butyrate instead of the costly and toxic *p*-chlorophenyl acetate.<sup>77</sup> A large scale DKR process was also developed using highly active catalyst **4**, which is readily formed *in situ* from [RuCl<sub>2</sub>(cymene)]<sub>2</sub> precursor and (*rac*)-2-phenyl-2-amino-propionamide as a ligand in presence of K<sub>2</sub>CO<sub>3</sub> as a solid base.<sup>61</sup> For most secondary alcohols, only 0.2 mol.% catalyst was sufficient for efficient DKR in 24 h at 70 °C.

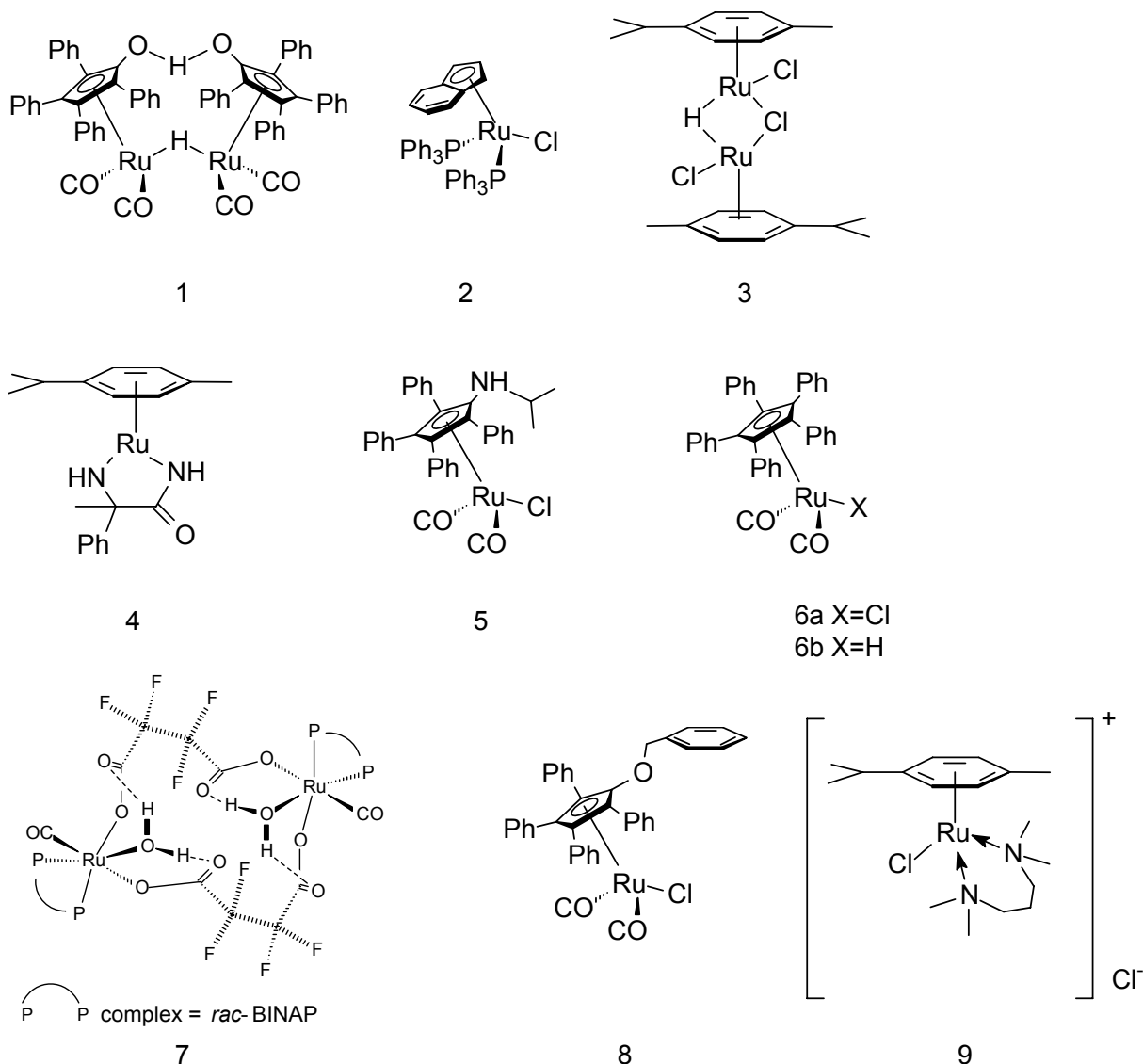


**Figure 1.9** Ruthenium-based racemization catalysts employed in dynamic kinetic resolution.

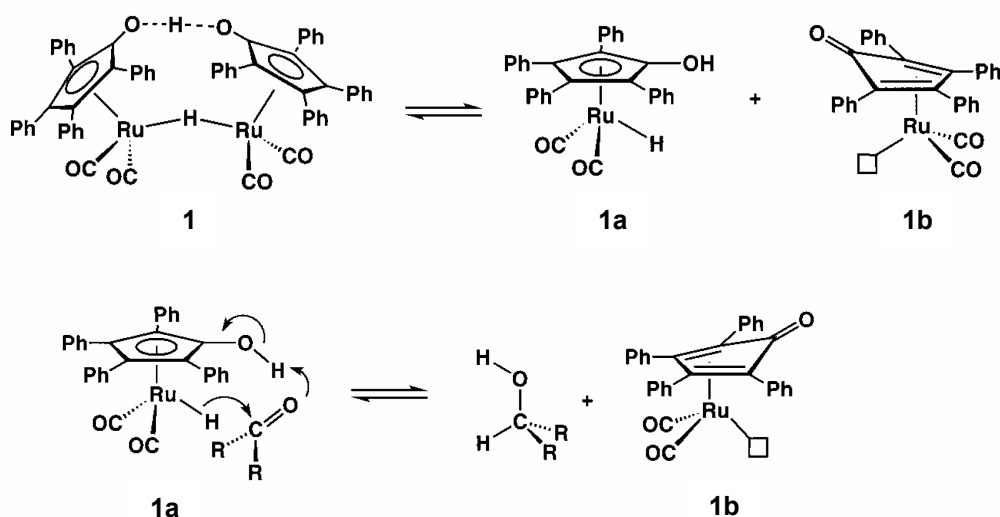
Kim and Park introduced complex **5**, which is active in presence of potassium *tert*-butoxide at room temperature, although long reaction times were required when this catalyst was applied for DKR purposes (1-7 days).<sup>78</sup> A major breakthrough in the development of room temperature DKR was the development of catalyst **6** by the Bäckvall group, which provides adequate racemization activity at room temperature.<sup>79</sup> This allows the DKR of substrates for which enantioselectivity of the lipase was insufficient at elevated temperatures; the fast activity of the catalyst resulted in reaction times of only 3-20 hours. Our laboratory recently reported on the successful DKR using **7** as the racemization catalyst.<sup>80</sup> This diruthenium complex, bearing tetrafluorosuccinate and *rac*-BINAP ligands, shows very high racemization activity at 70 °C, in presence of K<sub>2</sub>CO<sub>3</sub> as a solid base. For a variety of substrates the DKR could be carried out productively with high yields and ee's, using only 0.1 mol.%

ruthenium. The discovery of catalyst **8** allowed the DKR at room temperature under aerobic conditions.<sup>81</sup> With catalyst loadings of 4 mol.%, this catalyst allowed the DKR of a range of secondary alcohols in 20 h without the need for an inert atmosphere. Moreover, the catalyst was also attached to a polystyrene carrier; this immobilized catalyst performed similarly to the free ruthenium complex. Finally, Riermeier *et al.* recently reported **9** as a suitable catalyst for DKR.<sup>82</sup> This easily accessible Noyori-type catalyst has *N,N,N',N'*-tetramethyl-1,3-propanediamine as a ligand. While the catalytically active 16-electron complex **4** is generated by elimination of HCl, the 18-electron Ru(II)-complex **9** is not susceptible to HCl-loss by interaction with a base. However, appearing to be catalytically active as such, possibly the Ru-N bond is weak and might dissociate, leading to an electron-deficient, catalytically active 16-electron complex. The DKR of various secondary alcohols proceeds successfully, and, importantly, does not require an additional base nor inert conditions as the ruthenium-catalyst is stable to air and moisture.

#### 1.4.2 Ruthenium-catalyzed racemization: mechanism

Usually, racemization of secondary alcohols by ruthenium catalysis occurs through a dehydrogenation-hydrogenation pathway. Since the intermediate ketone species is prochiral, net racemization takes place. The first step in the catalytic cycle consists of the coordination of the alcohol (by means of an oxygen lone pair) to the electron-deficient ruthenium. This implies that only 16-electron ruthenium complexes are catalytically active. In presence of a strong base, such as potassium *tert*-butoxide, the alkoxide might coordinate to the ruthenium, rather than the alcohol.

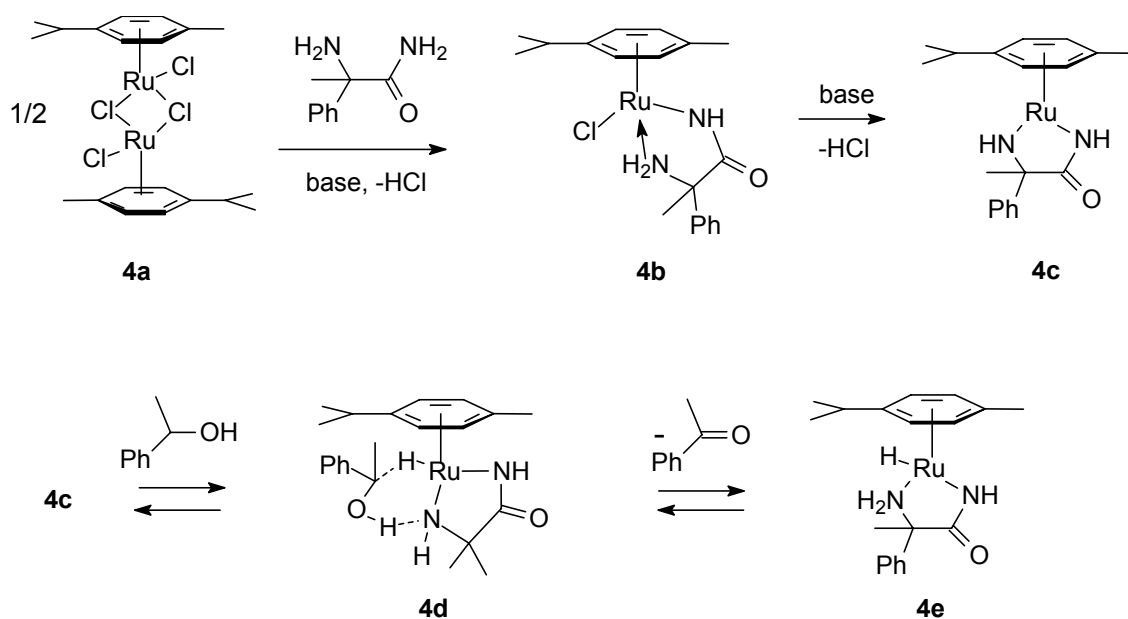
In the work described in this thesis, complexes **1** and **4** are used as the racemization catalysts. Description of the mechanistic aspects of ruthenium-catalyzed racemization is therefore focused on these two particular catalysts. Dinuclear complex **1** is a pre-catalyst that dissociates in solution at elevated temperature in an 18-electron Ru(II)-hydride complex **1a** and a 16-electron Ru(0)-complex **1b** (Scheme 1.2). A secondary alcohol can coordinate to the 16-electron complex **1b** and subsequently the corresponding (achiral) ketone and complex **1a** are formed. The ketone can react with complex **1a**, resulting in formation of the (racemized) alcohol and complex **1b**. Casey *et al.* suggested that the mechanism of oxidation and reduction proceeds via a concerted simultaneous transfer of a proton to the ketone of the cyclopentadienone ligand and a hydride to the ruthenium.<sup>83</sup>



**Scheme 1.2** Concerted mechanism for transfer hydrogenation by catalyst **1**.

Catalyst **4** is readily accessible via *in situ* complexation of commercially available  $[\text{RuCl}_2(\text{cymene})]_2$  (**4a**) with (*rac*)-2-phenyl-2-amino-propionamide in the presence of a solid base, such as  $\text{K}_2\text{CO}_3$ . Elimination of  $\text{HCl}$  provides complex **4b** bearing an anionic amido ligand. Loss of a second equivalent of  $\text{HCl}$  leads to the formation of the active 16 electron  $\text{Ru}(\text{II})$  complex **4c**. For the racemization of secondary alcohols by catalyst **4**, a metal-ligand bifunctional mechanism similar to that of analogous diamino transfer hydrogenation catalysts is proposed (Scheme 1.3).<sup>84-87,88</sup> Coordination of a secondary alcohol, such as 1-phenylethanol, leads to transition state **4d**. Dehydrogenation of the secondary alcohol results in the formation of the corresponding ketone and the hydride complex **4e**. In this step, the hydride in the  $\alpha$ -position of the alcohol is transferred to the  $\text{Ru}$ , while its  $\text{OH}$ -proton ends up on the acidic nitrogen of the amino ligand. Conversely, hydrogenation of a ketone by complex **4e** gives the corresponding alcohol with the overall transfer hydrogenation process resulting in racemization. Alternatively, hydride complex **4e** can eliminate molecular hydrogen to reform complex **4c**.





**Scheme 1.3** Synthesis of and transfer hydrogenation mechanism for catalyst 4.

## 1.5 Iterative tandem catalysis

### 1.5.1 Tandem catalysis in polymer chemistry

In contrast to the applications of tandem catalysis in organic synthetic chemistry, tandem catalysis is still rarely employed in the field of polymer chemistry.<sup>57</sup> An example is the synthesis of linear low-density polyethylene (LLDPE): one catalyst oligomerizes ethylene to  $\alpha$ -olefins, while the second catalyst polymerizes these  $\alpha$ -olefins as well as the remaining ethylene.<sup>89-94</sup> Furthermore, several examples have been reported of the synthesis of block copolymers in one pot by combining ring-opening polymerization (ROP) with radical polymerization using an unsymmetrical bifunctional initiator.<sup>50,60,62,95-101</sup> Analogously, graft copolymers can be synthesized in a one-pot procedure by using a suitable monomer.<sup>102</sup>

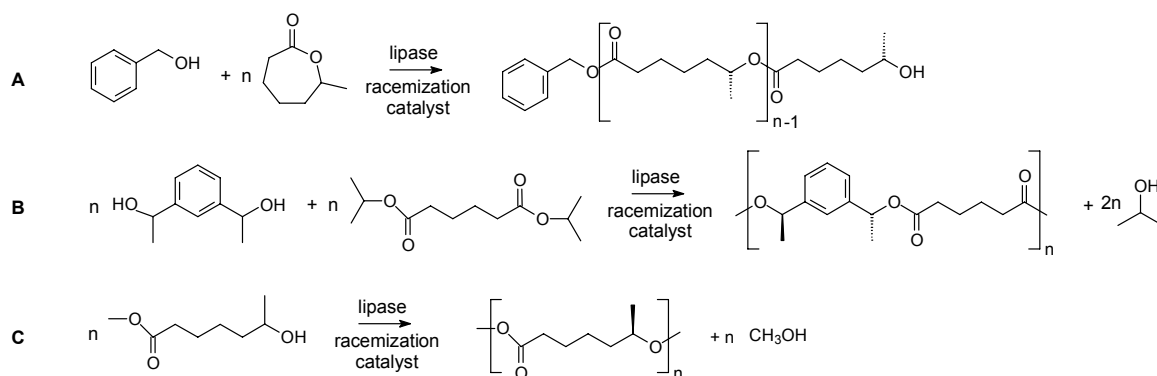
In these systems, however, the catalytic processes are not necessarily performed in one pot – if the two catalytic steps are carried out separately, a similar polymer would still result after two steps. In literature, few examples can be found where the catalytic processes involved in a polymerization are truly complementary and cannot be separated. Drent *et al.* described a copolymerization of ethylene and carbon monoxide where one palladium complex alternatively builds in both monomers via distinctively different catalytic mechanisms.<sup>103</sup> In addition, a concept called *chain shuttling polymerization* was recently introduced, where a growing chain is transferred repeatedly from one catalyst to another to achieve “multiblock” copolymer formation.<sup>104</sup> We recently introduced the term “iterative tandem catalysis” (ITC) to

describe those polymerization processes where iterative, complementary action of multiple catalytic processes is required in order to obtain polymeric materials.

## 1.6 Aim and scope of the thesis

The aim of this thesis is the development of new catalytic methods for the synthesis of highly structured polymeric materials. For this purpose, iterative tandem catalysis (ITC) is introduced as a novel polymerization method. ITC allows for the synthesis of polymeric materials with a higher structural complexity. The concept of ITC was developed together with Jeroen van Buijtenen.<sup>105</sup> In this thesis ITC is employed for the synthesis of enantiopure polyesters.

Iterative tandem catalysis (ITC) is defined as “a polymerization process in which chain growth is effectuated by a combination of two (or more) intrinsically different catalytic processes that are both compatible and complementary”. This implies that the catalytic processes must operate concurrently for propagation to occur, or, in other words, propagation by one catalyst is not possible until a transformation by another catalyst is performed. Scheme 1.4 shows the application of ITC for the synthesis of chiral polyesters by combination of enantioselective esterification of secondary alcohols with ruthenium-catalyzed racemization of secondary alcohols. Within this class of ITC, three subtypes can be envisioned. The first comprises the enzymatic ring-opening of  $\omega$ -substituted lactones, which results in a ring-opening product with a secondary alcohol group at the chain end (Scheme 1.4A). Conversion of *S*-secondary alcohols into *R*-secondary alcohols by a racemization catalyst is needed for propagation to occur, since lipases only accept *R*-secondary alcohols as the nucleophile. The second subtype involves the polycondensation of diesters with secondary diols (Scheme 1.4B). Although this system can reach 50% conversion without racemization activity, iterative activity of both catalysts is needed to obtain polymers of significant molecular weight. The third subtype is the polycondensation of AB-monomers; single molecules bearing both a secondary alcohol and an ester functionality (Scheme 1.4C). This thesis deals with subtypes A and B.



**Scheme 1.4** Variants of ITC based on the combination of enantioselective esterification and racemization.

## 1.7 Outline of the thesis

This thesis describes the use of Novozym 435 for the lipase-catalyzed ring-opening of  $\epsilon$ -caprolactone and  $\omega$ -substituted derivatives such as 6-methyl- $\epsilon$ -caprolactone. Furthermore, the synthesis of block copolymers and of chiral polyesters by tandem catalysis is discussed. Finally, the synthesis of optically pure lactones by means of enantioselective enzymatic ring-closure is described.

Chapter 2 deals with the tandem catalytic synthesis of block copolymers from a bifunctional initiator. Here, lipase-catalyzed ring-opening polymerization of  $\epsilon$ -caprolactone is combined with nitroxide-mediated controlled radical polymerization of styrene and *t*-butyl acrylate. The polymerizations were run in a two-pot as well as in a one-pot fashion. By using 4-methyl- $\epsilon$ -caprolactone as a monomer, the system was extended to the synthesis of chiral block copolymers in one pot.<sup>97</sup>

In Chapter 3 of this thesis, the enzymatic ring-opening of  $\omega$ -substituted  $\epsilon$ -caprolactones is investigated. The ring-opening of 6-methyl- $\epsilon$ -caprolactone is described extensively; the kinetic behavior on short time scales as well as on long time-scales is discussed. By means of temperature studies, the entropic and enthalpic contributions to enantioselectivity are determined. Using kinetic resolution and enzymatic ring-closure, the synthesis of both enantiomers of 6-methyl- $\epsilon$ -caprolactone with high optical purity is presented.<sup>106</sup>

In Chapter 4 the concept of iterative tandem catalysis is introduced (ITC). ITC comprises the simultaneous action of two catalytic processes to yield polymeric materials. As a proof of principle, the polymerization of (*S*)-6-methyl- $\epsilon$ -caprolactone is provided. In this system, racemization of secondary alcohols by a ruthenium catalyst is combined with lipase-catalyzed enantioselective ring-opening of lactones. With lipase catalysis only, 6-methyl- $\epsilon$ -caprolactone could not be polymerized.<sup>107</sup>

Chapter 5 describes the extension of ITC to polycondensation reactions: dynamic kinetic resolution polymerization (DKRP). A copolymerization of several aromatic diols and a diester is presented as proof of principle. The applicability of DKRP to aliphatic diols is discussed, as well as the selectivity of the lipase for these substrates. For the model compound 1,1'-(1,3-phenylene)diethanol (1,3-diol) an optimization study is presented.

Chapter 6 deals with the kinetics of enzymatic ring-opening polymerization and with the kinetics of one-pot ITC. The effect of product inhibition in an enzymatic ring-opening polymerization is investigated; also, the effect of different affinities of the enzyme towards lactone and polyester is described and investigated experimentally. Based on the Langmuir-Hinshelwood mechanism, a kinetic model is developed that describes the one-pot ITC of (S)-6-MeCL. The obtained experimental data are compared to the model.

## 1.8 References and notes

1. Hill, A.C. *J. Chem. Soc., Trans.* **1898**, 73, 634.
2. Kastle, J.H.; Loevenhart, A.S. *Am. Chem. J.* **1900**, 24, 491-525.
3. Zaks, A.; Klivanov, A.M. *Science* **1984**, 224, (4654), 1249-1251.
4. Halling, P.; Kvittingen, L. *Trends Biotechnol.* **1999**, 17, (9), 343-344.
5. Reetz, M.T. *Curr. Opin. Chem. Biol.* **2002**, 6, (2), 145-150.
6. Villeneuve, P.; Muderhwa, J.M.; Graille, J.; Haas, M.J. *J. Mol. Catal. B: Enzym.* **2000**, 9, (4-6), 113-148.
7. Martinelle, M.; Hult, K. *Biochim. Biophys. Acta* **1995**, 1251, (2), 191-197.
8. Ema, T. *Current Organic Chemistry* **2004**, 8, (11), 1009-1025.
9. Malcata, F.X.; Reyes, H.R.; Garcia, H.S.; Hill, C.G.; Amundson, C.H. *Enzyme Microb. Technol.* **1992**, 14, (6), 426-446.
10. Paiva, A.L.; Balcao, V.M.; Malcata, F.X. *Enzyme Microb. Technol.* **2000**, 27, (3-5), 187-204.
11. Bendikiene, V.; Surinenaite, B.; Juodka, B.; Safarikova, M. *Enzyme Microb. Technol.* **2004**, 34, (6), 572-577.
12. Anderson, E.M.; Karin, M.; Kirk, O. *Biocatal. Biotransform.* **1998**, 16, (3), 181-204.
13. Uppenberg, J.; Öhrner, N.; Norin, M.; Hult, K.; Kleywegt, G.J.; Patkar, S.; Waagen, V.; Anthonsen, T.; Jones, T.A. *Biochemistry* **1995**, 34, (51), 16838-16851.
14. Quiros, M.; Sanchez, V.M.; Brieva, R.; Rebolledo, F.; Gotor, V. *Tetrahedron: Asymmetry* **1993**, 4, (6), 1105-1112.
15. Sinisterra, J.V.; Llama, E.F.; Delcampo, C.; Cabezas, M.J.; Moreno, J.M.; Arroyo, M. *J. Chem. Soc., Perkin Trans. 2* **1994**, (6), 1333-1336.
16. Gross, R.A.; Kumar, A.; Kalra, B. *Abstr. Pap. - Am. Chem. Soc.* **2000**, 220th, POLY-284.
17. Kobayashi, S.; Uyama, H.; Kimura, S. *Chem. Rev.* **2001**, 101, (12), 3793-3818.
18. Okumura, S.; Iwai, M.; Tsujisaka, Y. *Yukagaku* **1983**, 32, (5), 271-3.
19. Morrow, C.J.; Wallace, J.S. *Biocatalysis* **1990**, 25-62.
20. Wallace, J.S.; Morrow, C.J. *J. Polym. Sci., Part A: Polym. Chem.* **1989**, 27, (10), 3271-84.
21. Gutman, A.L.; Bravdo, T. *J. Org. Chem.* **1989**, 54, (24), 5645-6.

22. Wallace, J.S.; Morrow, C.J. *J. Polym. Sci., Part A: Polym. Chem.* **1989**, 27, (8), 2553-67.
23. Margolin, A.L.; Crenne, J.-Y.; Klibanov, Alexander M. *Tetrahedron Lett.* **1987**, 28, (15), 1607-1609.
24. Uyama, H.; Kobayashi, S. *Chem. Lett.* **1993**, (7), 1149-1150.
25. Knani, D.; Gutman, A.L.; Kohn, D.H. *J. Polym. Sci., Part A: Polym. Chem.* **1993**, 31, (5), 1221-1232.
26. van der Mee, L.; Helmich, F.; de Bruijn, R.; Vekemans, J.A.J.M.; Palmans, A.R.A.; Meijer, E.W. *Macromolecules* **2006**, 39, (15), 5021-5027.
27. Kumar, A.; Kalra, B.; Dekhterman, A.; Gross, R.A. *Macromolecules* **2000**, 33, (17), 6303-6309.
28. Bisht, K.S.; Henderson, L.A.; Gross, R.A.; Kaplan, D.L.; Swift, G. *Macromolecules* **1997**, 30, (9), 2705-2711.
29. Bisht, K.S.; Svirkin, Y.Y.; Henderson, L.A.; Gross, R.A.; Kaplan, D.L.; Swift, G. *Macromolecules* **1997**, 30, (25), 7735-7742.
30. Kobayashi, S.; Kikuchi, H.; Uyama, H. *Macromol. Rapid Commun.* **1997**, 18, (7), 575-579.
31. Deng, F.; Gross, R.A. *Int. J. Biol. Macromol.* **1999**, 25, (1-3), 153-159.
32. Kumar, A.; Garg, K.; Gross, R.A. *Macromolecules* **2001**, 34, (11), 3527-3533.
33. Tasaki, H.; Toshima, K.; Matsumura, S. *Macromol. Biosci.* **2003**, 3, (8), 436-441.
34. Binns, F.; Harffey, P.; Roberts, S.M.; Taylor, A. *J. Chem. Soc., Perkin Trans. 1* **1999**, (19), 2671-2676.
35. Binns, F.; Roberts, S.M.; Taylor, A.; Williams, C.F. *J. Chem. Soc., Perkin Trans. 1* **1993**, (8), 899-904.
36. Matsumura, S.; Harai, S.; Toshima, K. *Macromol. Chem. Phys.* **2000**, 201, (14), 1632-1639.
37. Namekawa, S.; Uyama, H.; Kobayashi, S. *Biomacromolecules* **2000**, 1, (3), 335-338.
38. Uyama, H.; Inada, K.; Kobayashi, S. *Polymer Journal (Tokyo)* **2000**, 32, (5), 440-443.
39. Mahapatro, A.; Kalra, B.; Kumar, A.; Gross, R.A. *Biomacromolecules* **2003**, 4, (3), 544-551.
40. Dong, H.; Wang, H.-D.; Cao, S.-G.; Shen, J.-C. *Biotechnol. Lett* **1998**, 20, (10), 905-908.
41. Gutman, A.L.; Oreu, D.; Boltanski, A.; Bravdo, T. *Tetrahedron Lett.* **1987**, 28, (44), 5367-8.
42. Custers, E., De Geus, M. Unpublished results. The  $M_w$  of 91 kDa was calculated based on polyethylene standards.
43. Carrea, G.; Riva, S. *Angew. Chem., Int. Ed.* **2000**, 39, (13), 2226-2254.
44. Halling, P.J. *Enzyme Microb. Technol.* **1994**, 16, (3), 178-206.
45. Valivety, R.H.; Halling, P.J.; Macrae, A.R. *Biochim. Biophys. Acta* **1992**, 1118, (3), 218-222.
46. Halling, P. *Trends Biotechnol.* **1989**, 7, (3), 50-52.
47. Halling, P.J. *Enzyme Microb. Technol.* **1984**, 6, (11), 513-16.
48. Goderis, H.L.; Ampe, G.; Feyten, M.P.; Fouwe, B.L.; Guffens, W.M.; van Cauwenbergh, S.M.; Tobback, P.P. *Biotechnol. Bioeng.* **1987**, 30, (2), 258-66.
49. Lee, C.S.; Ru, M.T.; Haake, M.; Dordick, J.S.; Reimer, J.A.; Clark, D.S. *Biotechnol. Bioeng.* **1998**, 57, (6), 686-693.
50. de Geus, M.; Peeters, J.; Wolffs, M.; Hermans, T.; Palmans, A.R.A.; Koning, C.E.; Heise, A. *Macromolecules* **2005**, 38, (10), 4220-4225.
51. Chen, C.S.; Fujimoto, Y.; Girdaukas, G.; Sih, C.J. *J. Am. Chem. Soc.* **1982**, 104, (25), 7294-9.
52. Jongejan, J.A.; van Tol, J.B.A.; Geerlof, A.; Duine, J.A. *Recl. Trav. Chim. Pays-Bas* **1991**, 110, (5), 247-254.
53. Straathof, A.J.J.; Jongejan, J.A. *Enzyme Microb. Technol.* **1997**, 21, (8), 559-571.
54. Bruggink, A.; Schoevaart, R.; Kieboom, T. *Org. Process Res. Dev.* **2003**, 7, (5), 622-640.

55. Tietze, L.F. *Chem. Rev.* **1996**, 96, (1), 115-136.
56. Leninger, A.L. *Principles of Biochemistry* **1984** Worth Publishers, New York
57. Wasilke, J.C.; Obrey, S.J.; Baker, R.T.; Bazan, G.C. *Chem. Rev.* **2005**, 105, (3), 1001-1020.
58. Denmark, S.E.; Thorarensen, A. *Chem. Rev.* **1996**, 96, (1), 137-165.
59. Fogg, D.E.; dos Santos, E.N. *Coord. Chem. Rev.* **2004**, 248, (21-24), 2365-2379.
60. Peeters, J.; Palmans, A.R.A.; Veld, M.; Scheijen, F.; Heise, A.; Meijer, E.W. *Biomacromolecules* **2004**, 5, (5), 1862-1868.
61. Verzijl, G.K.M.; De Vries, J.G.; Broxterman, Q.B. Process for the preparation of enantiomerically enriched esters and alcohols. 2001-NL383, 2001090396, 20010521., 2001.
62. de Geus, M.; Schormans, L.; Palmans, A.R.A.; Koning, C.E.; Heise, A. *J. Polym. Sci., Part A: Polym. Chem.* **2006**, 44, (14), 4290-4297.
63. Lee, J.M.; Na, Y.; Han, H.; Chang, S. *Chem. Soc. Rev.* **2004**, 33, (5), 302-312.
64. Mayer, S.F.; Kroutil, W.; Faber, K. *Chem. Soc. Rev.* **2001**, 30, (6), 332-339.
65. A. Roessner, C.; B. Spencer, J.; J. Stolowich, N.; Wang, J.; Parmesh Nayar, G.; J. Santander, P.; Pichon, C.; Min, C.; T. Holderman, M.; Ian Scott, A. *Chem. Biol. (Cambridge, MA, U. S.)* **1994**, 1, (2), 119-124.
66. Faber, K. *Chem. Eur. J.* **2001**, 7, (23), 5004.
67. Noyori, R.; Ikeda, T.; Ohkuma, T.; Widhalm, M.; Kitamura, M.; Takaya, H.; Akutagawa, S.; Sayo, N.; Saito, T.; Taketomi, T.; Kumobayashi, H. *J. Am. Chem. Soc.* **1989**, 111, (25), 9134-9135.
68. Pellissier, H. *Tetrahedron* **2003**, 59, (42), 8291-8327.
69. Persson, B.A.; Huerta, F.F.; Bäckvall, J.E. *J. Org. Chem.* **1999**, 64, (14), 5237-5240.
70. Turner, N.J. *Curr. Opin. Chem. Biol.* **2004**, 8, (2), 114-119.
71. Huerta, F.F.; Minidis, A.B.E.; Bäckvall, J.-E. *Chem. Soc. Rev.* **2001**, 30, (6), 321-331.
72. Akai, S.; Tanimoto, K.; Kanao, Y.; Egi, M.; Yanamoto, T.; Kita, Y. *Angew. Chem., Int. Ed.* **2006**, 45, (16), 2592-2595.
73. Larsson, A.L.E.; Persson, B.A.; Bäckvall, J.E. *Angew. Chem., Int. Ed. Eng.* **1997**, 36, (11), 1211-1212.
74. Kielbasinski, P.; Rachwalski, M.; Mikolajczyk, M.; Moelands, M.A.H.; Zwanenburg, B.; Rutjes, F. *Tetrahedron: Asymmetry* **2005**, 16, (12), 2157-2160.
75. Koh, J.H.; Jung, H.M.; Kim, M.-J.; Park, J. *Tetrahedron Lett.* **1999**, 40, (34), 6281-6284.
76. Lee, D.; Huh, E.A.; Kim, M.-J.; Jung, H.M.; Koh, J.H.; Park, J. *Org. Lett.* **2000**, 2, (15), 2377-2379.
77. Verzijl, G.K.M.; de Vries, J.G.; Broxterman, Q.B. *Tetrahedron: Asymmetry* **2005**, 16, (9), 1603-1610.
78. Choi, J.H.; Choi, Y.K.; Kim, Y.H.; Park, E.S.; Kim, E.J.; Kim, M.J.; Park, J.W. *J. Org. Chem.* **2004**, 69, (6), 1972-1977.
79. Martín-Matute, B.; Edin, M.; Bogár, K.; Bäckvall, J.E. *Angew. Chem., Int. Ed.* **2004**, 43, (47), 6535-6539.
80. van Nispen, S.F.G.M.; van Buijtenen, J.; Vekemans, J.A.J.M.; Meuldijk, J.; Hulshof, L.A. *Tetrahedron: Asymmetry* **2006**, 17, (15), 2299-2305.
81. Kim, N.; Ko, S.B.; Kwon, M.S.; Kim, M.J.; Park, J. *Org. Lett.* **2005**, 7, (20), 4523-4526.
82. Riermeier, T.H.; Gross, P.; Monsees, A.; Hoff, M.; Trauthwein, H. *Tetrahedron Lett.* **2005**, 46, (19), 3403-3406.

83. Casey, C.P.; Singer, S.W.; Powell, D.R.; Hayashi, R.K.; Kavana, M. *J. Am. Chem. Soc.* **2001**, 123, (6), 1090-1100.
84. Yamakawa, M.; Ito, H.; Noyori, R. *J. Am. Chem. Soc.* **2000**, 122, (7), 1466-1478.
85. Samec, J.S.M.; Bäckvall, J.E.; Andersson, P.G.; Brandt, P. *Chem. Soc. Rev.* **2006**, 35, (3), 237-248.
86. Pàmies, O.; Bäckvall, J.E. *Chem. Eur. J.* **2001**, 7, (23), 5052-5058.
87. Clapham, S.E.; Hadzovic, A.; Morris, R.H. *Coord. Chem. Rev.* **2004**, 248, (21-24), 2201-2237.
88. In metal-ligand bifunctional catalysis the metal and the surrounding ligand directly participate in the bond-forming and -breaking steps of the dehydrogenative and hydrogenative processes. This is in contrast to the mechanisms proposed for most other transition metal-catalyzed reactions.
89. Komon, Z.J.A.; Bazan, G.C. *Macromol. Rapid Commun.* **2001**, 22, (7), 467-478.
90. Komon, Z.J.A.; Bu, X.H.; Bazan, G.C. *J. Am. Chem. Soc.* **2000**, 122, (8), 1830-1831.
91. Komon, Z.J.A.; Diamond, G.M.; Leclerc, M.K.; Murphy, V.; Okazaki, M.; Bazan, G.C. *J. Am. Chem. Soc.* **2002**, 124, (51), 15280-15285.
92. Alobaidi, F.; Ye, Z.B.; Zhu, S.P. *J. Polym. Sci., Part A: Polym. Chem.* **2004**, 42, (17), 4327-4336.
93. Furlan, L.G.; Kunrath, F.A.; Mauler, R.S.; de Souza, R.F.; Casagrande, O.L. *J. Mol. Catal. A: Chem.* **2004**, 214, (2), 207-211.
94. Zhang, Z.C.; Lu, Z.X.; Chen, S.T.; Li, H.Y.; Zhang, X.F.; Lu, Y.Y.; Hu, Y.L. *J. Mol. Catal. A: Chem.* **2005**, 236, (1-2), 87-93.
95. Mecerreyes, D.; Moineau, G.; Dubois, P.; Jérôme, R.; Hedrick, J.L.; Hawker, C.J.; Malmström, E.E.; Trollsås, M. *Angew. Chem., Int. Ed.* **1998**, 37, (9), 1274-1276.
96. Bielawski, C.W.; Louie, J.; Grubbs, R.H. *J. Am. Chem. Soc.* **2000**, 122, (51), 12872-12873.
97. van As, B.A.C.; Thomassen, P.; Kalra, B.; Gross, R.A.; Meijer, E.W.; Palmans, A.R.A.; Heise, A. *Macromolecules* **2004**, 37, (24), 8973-8977.
98. Klaerner, G.; Trollsås, M.; Heise, A.; Husemann, M.; Atthoff, B.; Hawker, C.J.; Hedrick, J.L.; Miller, R.D. *Macromolecules* **1999**, 32, (24), 8227-8229.
99. Weimer, M.W.; Scherman, O.A.; Sogah, D.Y. *Macromolecules* **1998**, 31, (23), 8425-8428.
100. Villarroya, S.; Zhou, J.X.; Duxbury, C.J.; Heise, A.; Howdle, S.M. *Macromolecules* **2006**, 39, (2), 633-640.
101. Duxbury, C.J.; Wang, W.X.; de Geus, M.; Heise, A.; Howdle, S.M. *J. Am. Chem. Soc.* **2005**, 127, (8), 2384-2385.
102. Mecerreyes, D.; Trollsås, M.; Hedrick, J.L. *Macromolecules* **1999**, 32, (26), 8753-8759.
103. Drent, E.; Budzelaar, P.H.M. *Chem. Rev.* **1996**, 96, (2), 663-681.
104. Arriola, D.J.; Carnahan, E.M.; Hustad, P.D.; Kuhlman, R.L.; Wenzel, T.T. *Science* **2006**, 312, (5774), 714-719.
105. van Buijtenen, J. *Ph.D Thesis, in preparation* **2006**.
106. van As, B.A.C.; Chan, D.-K.; Kivit, P.J.J.; Palmans, A.R.A.; Meijer, E.W. *Manuscript in preparation*.
107. van As, B.A.C.; van Buijtenen, J.; Heise, A.; Broxterman, Q.B.; Verzijl, G.K.M.; Palmans, A.R.A.; Meijer, E.W. *J. Am. Chem. Soc.* **2005**, 127, (28), 9964-9965.

# 2

## Chiral block copolymers by one-pot chemoenzymatic cascade polymerization

### Abstract

A novel concept for the metal free synthesis of block copolymers combining enzymatic ring opening polymerization and nitroxide mediated living free radical polymerization from a bifunctional initiator is presented. Block copolymers comprising a poly(styrene) and a poly(caprolactone) block were obtained in two consecutive polymerization steps (macroinitiation) and in a one-pot cascade approach without intermediate transformation or work up step. By optimization of the reaction conditions a high selectivity of both transformations could be realized in the cascade polymerization resulting in high block copolymer yields. The same concept was successfully applied to enzymatic resolution polymerization of racemic 4-methyl- $\epsilon$ -caprolactone combined with the living free radical polymerization of styrene yielding block copolymers with high enantiomeric excess in the poly(4-methyl- $\epsilon$ -caprolactone) block.

Part of this chapter has been published: van As, B.A.C.; Thomassen, P.; Kalra, B.; Gross, R.A.; Meijer, E.W.; Palmans, A.R.A.; Heise, A. *Macromolecules* **2004**, 37, (24), 8973-8977.



## 2.1 Introduction

Block copolymers represent one of the most interesting classes of materials available for controlling the microstructure of materials. Their ability to self-assemble into one-, two- or three-dimensional nanostructures depending on the composition (i.e., volume fraction) has been extensively studied (Figure 2.1).<sup>1</sup> Modification of the molecular structure allows the tailoring of the superstructure, which is extremely appealing for the application of nanotechnology using a bottom-up approach. Block copolymers have found a wide variety of applications, including their use as polymeric compatibilizer,<sup>2</sup> for optical applications as photonic crystals,<sup>3</sup> as micellar structures possibly to be used for drug delivery,<sup>4</sup> and as liquid crystals.<sup>5</sup> Moreover, the use of chiral block copolymers has been explored recently, e.g. their application as chirality inducing agents in crystallizations<sup>6</sup> and as molecules for the formation of nanohelical structures.<sup>7</sup>

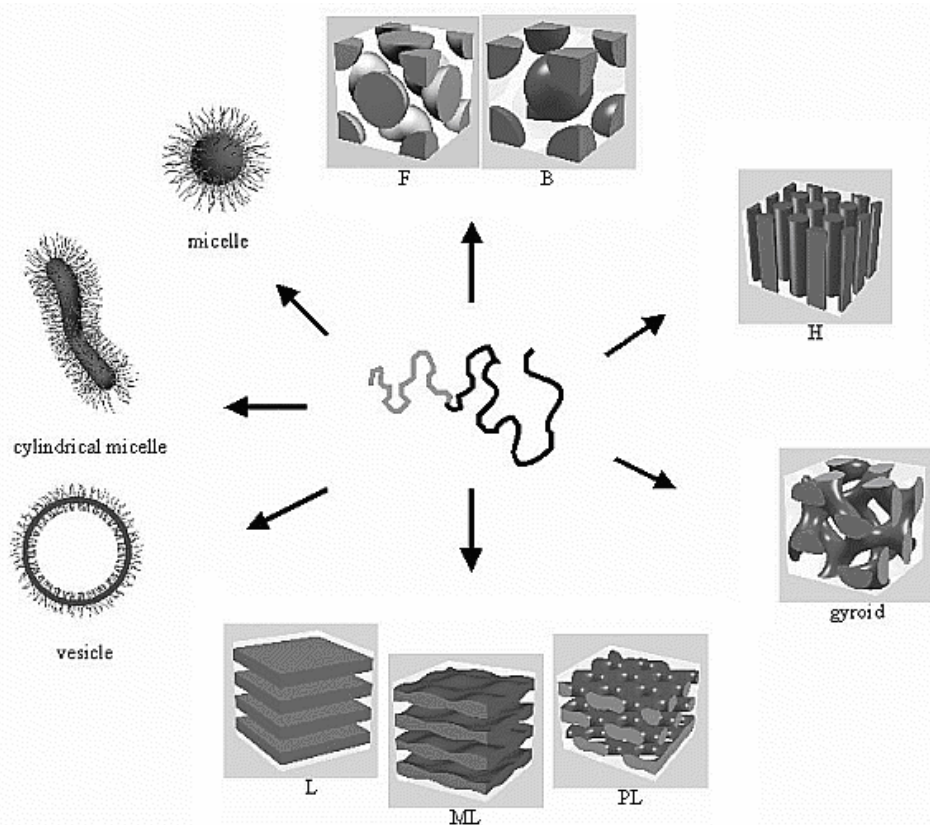


**Figure 2.1** Different morphologies through self-assembly of block copolymers.<sup>1</sup>

### 2.1.1 Synthesis of block copolymers

Until recently, frequently employed ways to procure block copolymers involved either the sequential polymerization of different monomer units using the same chemistry (i.e., two

controlled radical procedures) or the coupling of preformed homopolymers. Alternatively, a transformation of the propagating center to allow a second polymerization via a different mechanism could be employed. The recent development of bifunctional initiators enabled the synthesis of block copolymers comprising distinctly different monomers without the need for homopolymer coupling or functional group transformation. Various two-pot systems have been reported, mostly on the combination of chemical ring-opening polymerization with controlled radical polymerization techniques, such as atom transfer radical polymerization (ATRP)<sup>8-10</sup> or nitroxide-mediated controlled radical polymerization (NMP).<sup>11</sup> Exploiting the advantages of in-vitro enzyme catalysis such as mild reaction conditions, stereoselectivity and regioselectivity, also the use of enzymatic polymerization has been reported in combination with various radical polymerization techniques.<sup>12-16</sup>

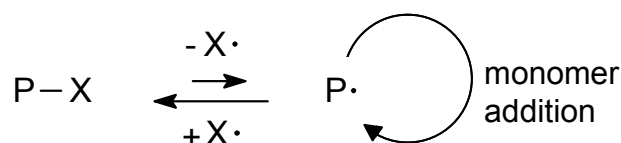
A significant disadvantage of a two-pot system, however, is that intermediate work-up is still necessary, after which the purified polymer is employed as a macroinitiator for the subsequent polymerization of the second monomer. Far more elegant is the concept of one-pot cascade conversion, i.e., combined (catalytic) reactions without intermediate recovery steps. Typically, biocatalytic processes in living cells go through a multi-step cascade approach to convert a starting material into the final product without the separation of intermediates. A number of one-pot cascade conversions yielding block copolymers have been reported, combining controlled free radical polymerization with chemical ring-opening polymerization.<sup>17-19</sup> However, attempts to realize a one-pot system combining the advantages of enzymatic catalysis with the merits of radical polymerization remained unsuccessful. At the time, the simultaneous initiation of both reaction types and the incompatibility of the ATRP catalyst with the lipase employed remained unsolved issues.<sup>13</sup> Recently, a number of reports have appeared on the chemoenzymatic one-pot synthesis of block copolymers. The combination of ATRP and enzymatic ring-opening polymerization has finally been achieved in a one-pot fashion in organic solvents and in bulk,<sup>20,21</sup> as well as in supercritical carbon dioxide.<sup>22-24</sup>

### **2.1.2 Nitroxide-mediated controlled free radical polymerization**

Approximately 50% of all polymers produced industrially are prepared using free radical processes. With free radical polymerization, a large variety of monomers can be (co)polymerized in organic solvents as well as in bulk. However, free radical processes yield materials with broad polydispersities and the control over molecular weight is limited. For most purposes this is not a problem; for sophisticated materials, however, polymers with well-defined molecular weight and low polydispersity are desirable.<sup>25</sup>

Radical polymerizations have received renewed interest during the past decade. The development of controlled free radical polymerization techniques, such as nitroxide-mediated

polymerizations (NMP), atom transfer radical polymerizations (ATRP) and reverse addition fragmentation polymerizations (RAFT) allows for the preparation of polymeric materials with well-defined molecular weight and with low polydispersities. The control of the polymerization in NMP is due to the principle of the persistent radical effect; the reversible formation of a dormant alkoxyamine from the nitroxide and a chain growing polymer radical ensures a consistently low radical concentration during the polymerization process. This results in a low occurrence of irreversible termination reactions. A key parameter for the successful control of the polymerization is the dissociation constant  $K$  (Scheme 2.1); obviously, the equilibrium must lie far on the side of the dormant species  $P-X$ .



**Scheme 2.1** Reversible activation of the dormant species in NMP.  $X$  represents the alkoxyamine moiety,  $P$  represents the growing polymer chain.

Initially, conventional free radical initiators were used in conjunction with free nitroxide radical, such as TEMPO (2,2',6,6'-tetramethylpiperidine-1-oxyl radical, **1**). The alkoxyamine is formed in situ in these systems. The use of preformed alkoxyamines, such as **2**, led to a much better control of the targeted molecular weight. Many different TEMPO-derivative structures have been employed in NMP, although with most of these cyclic structures only controlled polymerization of styrenics was possible. Non-cyclic alkoxyamines have also been found as excellent NMP initiators; these include phosphonates such as **3** and the family of TIPNO-alkoxyamines **4**, which was introduced by Hawker *et al.*<sup>26</sup> These non-cyclic alkoxyamines are excellent initiators for the polymerization of both styrenics and acrylates. Recently, Catala *et al.* introduced alkoxyamine **5**, which allowed low-temperature polymerization of styrene (60 °C) and acrylates (90 °C).<sup>27,28</sup>

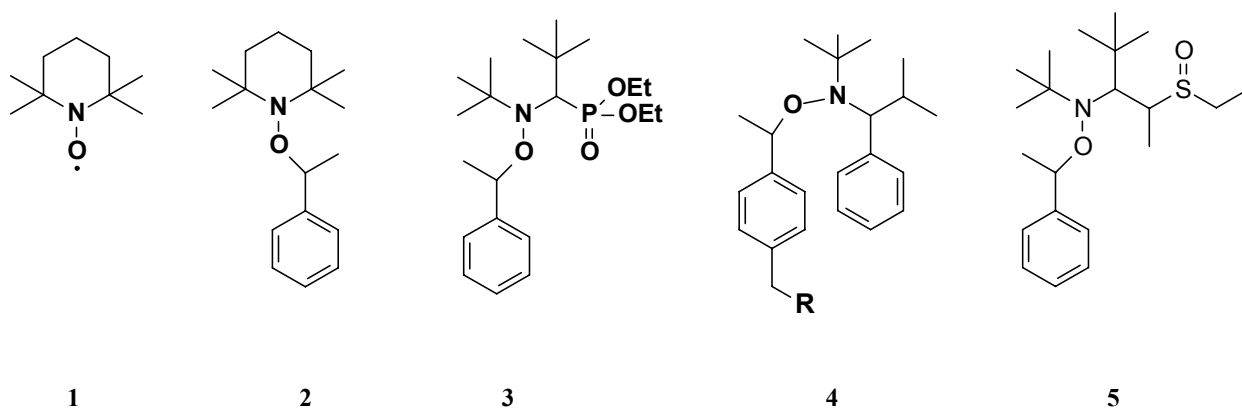


**Figure 2.2** Some alkoxyamine radicals and initiators used in NMP.

Due to the fast developments in the last decade, the prospectives of NMP have triggered much interest from industry; the first commercial applications of NMP have already seen birth.<sup>29</sup> Research on NMP initiators, however, continues to be important, since controlled polymerization of vinyl acetate and methyl methacrylate still proves to be difficult using the NMP initiators known to date.

This chapter describes the first chemoenzymatic one-pot cascade polymerization leading to well-defined block copolymers. The use of NMP results in a system where the radical polymerization is thermally activated at 90-120 °C, while lipase-catalyzed lactone ring-opening polymerizations can be performed efficiently already at 25 °C. Because nitroxide mediated free radical polymerization has a distinctive temperature window, it can be kinetically separated from the lipase-catalyzed polymerization. Moreover, NMP is a completely metal-free system, which is an important advantage for possible future biomedical applications of the block copolymers.

## **2.2 Block copolymers from a bifunctional initiator**

The bifunctional initiator **6** (Scheme 2.2) contains a nitroxide group for controlled free radical polymerization of styrene (St) and a hydroxy group for initiation of the ring-opening polymerization of  $\epsilon$ -caprolactone (CL).<sup>26</sup> Block copolymers can therefore be obtained from **6** without intermediate workup or modification steps. The initiation of styrene from this initiator and respective macroinitiators proceeds in a well-defined fashion yielding polymers with controlled molecular weight and polydispersity.<sup>30</sup> However, since **6** comprises a relatively bulky structure, the usefulness of **6** in a lipase catalyzed CL polymerization had to be investigated first at the reaction temperature of 60 °C. Inspection of Figure 2.3 shows a rapid conversion of **6** - exceeding 90 % at a CL conversion of less than 20 % - and an almost linear increase of the monomer conversion as a function of time. Moreover, the kinetics of this reaction were found to be first order with respect to monomer consumption, as evidenced by the linear relationship in the plot of  $-\ln(1 - \text{monomer conversion})$  versus time (Figure 2.4). GPC analysis of the samples revealed that the molecular weight increased over time, although not linearly with respect to conversion for the initial 20% monomer conversion (Figure 2.5). From 20% to 50% monomer conversion, an approximately linear behavior was observed. Initiation takes place from 0% to 20% monomer conversion, and CL is built into new chains as well as into existing chains. Therefore, it is expected that in this region  $M_n$  and CL conversion do not display a linear relationship. Polydispersity was found to be 1.3 in the initial stages of the reaction, and increasing to 1.9 – 2.0 at the end of reaction. Initially, initiation and propagation proceed fast, leading to a polymer with low polydispersity, while at later stages of



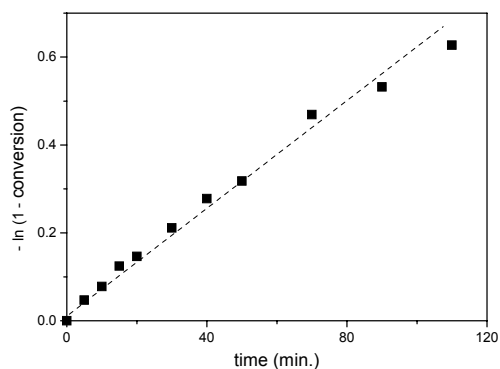


**Figure 2.4** Negative logarithmic plot of  $\ln(1 - \text{monomer conversion})$  versus time.

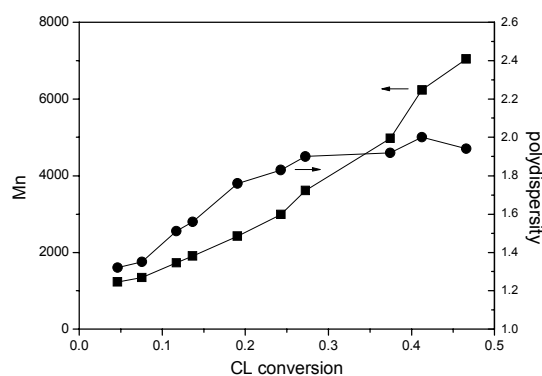


**Figure 2.5** Number-averaged molecular weight (■) and polydispersity (●) versus conversion of CL. GPC calibrated with PS standards; eluent = THF.

An example of the molecular weight and polydispersity of a polymer formed in an enzymatic ROP employing **6** at 60 °C after 3 h is given in Table 2.1, entry A1. Monomer conversions under these conditions are typically between 70 and 80 % with precipitated yields of 60 – 70 %. Initiation by water molecules leads to polymers with carboxylic acid chain ends. When the hydroxyl and carboxylic acid chain ends are derivatized with oxalyl chloride, the percentage of water initiated chains can be easily quantified by means of  $^1\text{H}$  NMR.<sup>31</sup> With carefully dried reagents and polymerization under anhydrous conditions, there were no carboxylic acid chain ends detectable in the  $^1\text{H}$ -NMR spectra. Therefore, it can be concluded that the mole percentage of polymers without the nitroxide end-group is below 5 %. Furthermore,  $^1\text{H}$  NMR analysis of the products in entries A1 and A1.2 showed a complete shift of the benzylic proton signal of **6** from 4.65 to 5.1 ppm (**h** in Figure 2.6). This is consistent with **6** linked by an ester to the PCL chain.

The precipitated macroinitiator PCL was subsequently used for nitroxide mediated St polymerization. Upon polymerization, an increase in the molecular weight relative to PCL was observed by size exclusion chromatography (Table 2.1, entry A1.2). Since any unreacted **6** was efficiently removed from PCL during the precipitation step, the initiation of chains must have exclusively occurred from the macroinitiator chains. In order to directly analyze the poly(styrene) block of the P(CL-*b*-St) block copolymers (A1.2), the PCL block was degraded according to a literature procedure (acidic degradation in dioxane / HCl).<sup>17</sup> Comparison of the SEC trace of the remaining PSt block (entry A1.3) with that of P(CL-*b*-St) reveals a shift to lower molecular weight. Moreover, the low polydispersity (PD) of the PSt is in a typical range for living free radical polymerization (LFRP). This provides further evidence of the block structure and the feasibility of the macroinitiation approach. Attempts to synthesize block

copolymers by eROP from a PSt macroinitiator in a 2-step approach failed; probably a PSt macroinitiator is too sterically hindered for enzymatic reaction with CL.

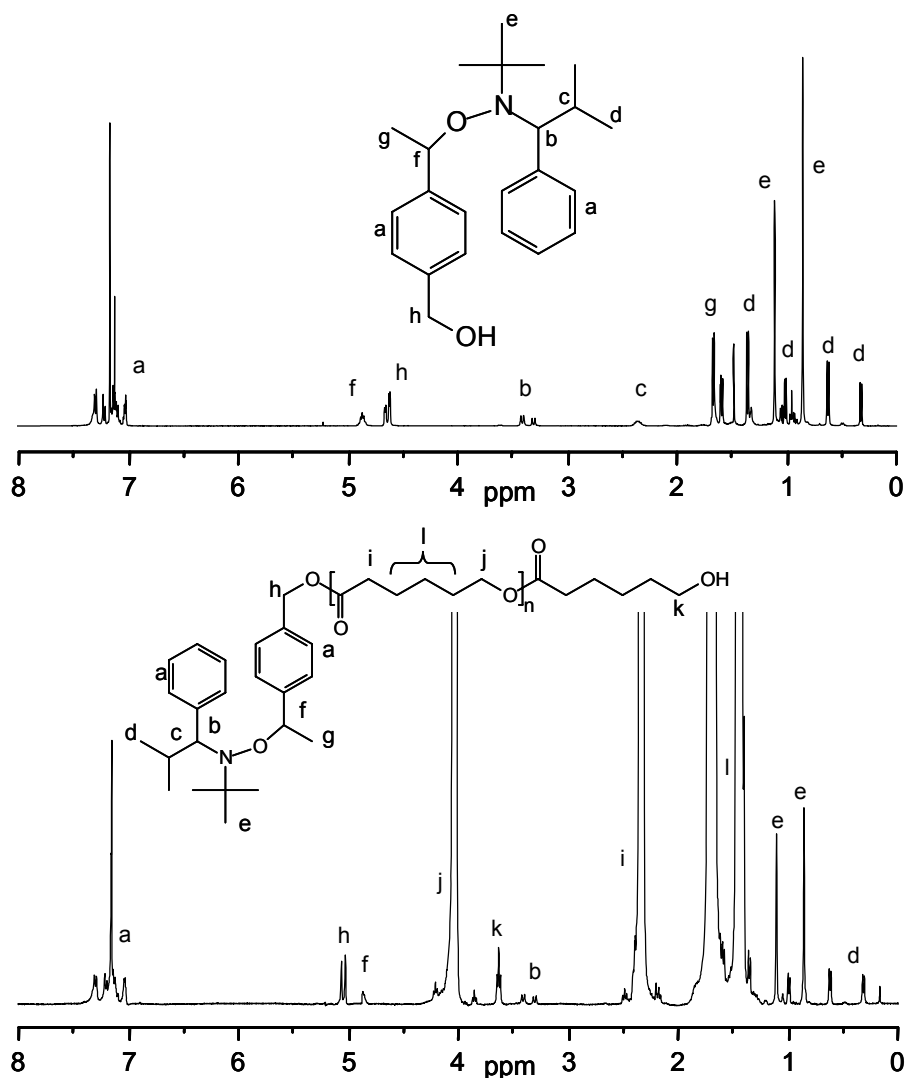


**Figure 2.6**  $^1\text{H-NMR}$  spectra of **6** and PCL initiated by **6**.

MALDI-TOF MS analysis of the polymers was attempted, but proved unsuccessful. For block copolymers, the presence of cyclic oligo( $\epsilon$ -caprolactone) species, which fly more easily than linear species, made analysis very difficult.<sup>32</sup> Analysis of a low molecular weight PS-I macroinitiator ( $M_w \sim 3$  kDa) did yield clear spectra, although fragmentation was observed. Intrapolation of the observed masses led to the conclusion that the nitroxide radical was split off during ionization (Figure 2.7); the use of different matrices and/or the addition of silver triflate did not improve this.

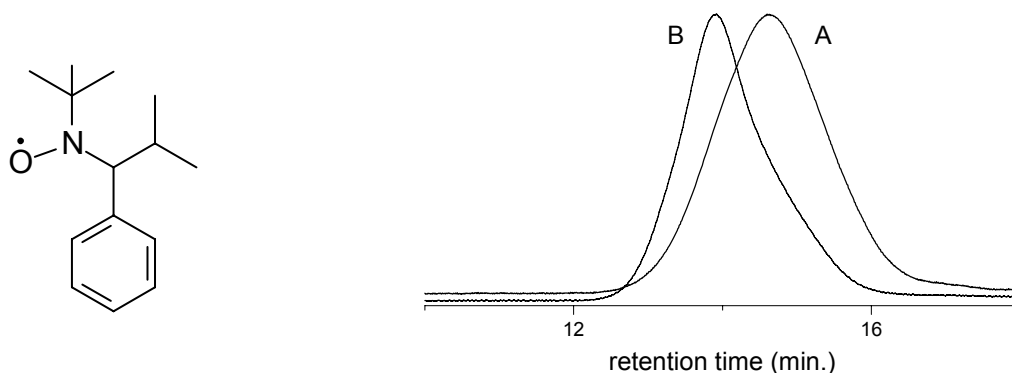


**Figure 2.7** The nitroxide radical **Figure 2.8** SEC traces of macroinitiator PCL-I (A) and splits off during ionization in block copolymer PCL-*b*-PTBA (B) (entries C1 and C1.2). MALDI-TOF MS measurements

To investigate the scope of the radical polymerization using this initiator, attempts were made to use *t*-butyl acrylate (TBA) as a monomer. In a 2-pot procedure, TBA was polymerized at 120 °C from a PCL-I macroinitiator (entries C1 and C1.2). <sup>1</sup>H NMR confirmed that indeed poly(TBA) was present in the product. A clear shift in molecular weight from 25 to 40 kDa and an accompanying lower polydispersity (from 1.7 to 1.5) indicated that indeed the acrylate monomer was built in, leading to a block copolymer. Figure 2.8 shows the shift in SEC trace from the macroinitiator PCL-I to the block copolymer PCL-*b*-PTBA.

A triblock copolymer was synthesized from the PCL-*b*-PSt block copolymer B1 by reaction with TBA at 120 °C (entry C2). <sup>1</sup>H NMR indicated that indeed poly(TBA) had been formed. A clear shift in molecular weight from 21 to 37 kDa and accompanying lowering in polydispersity from 1.4 to 1.3 provided proof that indeed a triblock copolymer had been formed. Figure 2.9 shows the shift in SEC trace from the block copolymer PCL-*b*-PSt to the triblock copolymer PCL-*b*-PSt-*b*-PTBA.

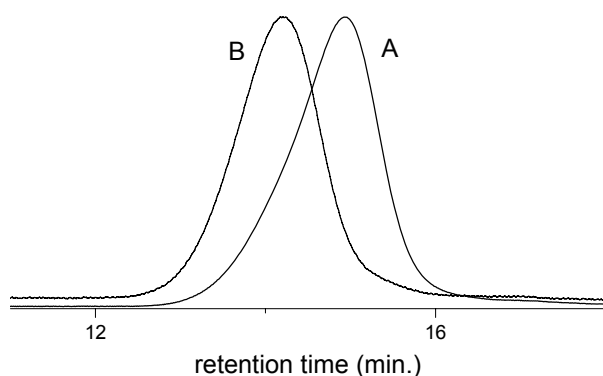


**Figure 2.9** GPC trace of block copolymer PCL-*b*-PS (A) and triblock copolymer (B) PCL-*b*-PS-*b*-PTBA (entries B1 and C2, respectively).



**Table 2.1** Characteristics of polymers obtained in enzymatic/living free radical cascade polymerization of CL. Entries A refer to two-pot, entries B to one-pot reactions, entries C to polymerizations with TBA and entries D to one-pot kinetic resolution polymerization

entry	initiator	monomer	I:CL:olefin	polymer	M <sub>w</sub> kDa <sup>a</sup>	PD <sup>a</sup>	T <sub>g</sub> °C	T <sub>m</sub> °C
A1	<b>6</b>	CL	1:150:0	PCL	24	1.7	-	56
A1.2	PCL	St	1:0:340	PCL- <i>b</i> -St	35	1.4	-	58
A1.3 <sup>b</sup>				PSt	22	1.2	n.d.	n.d.
B1	<b>6</b>	CL / St	1:80:147	PCL- <i>b</i> -St	21	1.4	-78	56
B2	<b>6</b>	CL / St	1:90:125	PCL- <i>b</i> -St	19	1.7	n.d.	n.d.
B2.1 <sup>b</sup>				PSt	3	1.2	n.d.	n.d.
C1	<b>6</b>	CL	1:100:0	PCL	25	1.7	n.d.	n.d.
C1.2	PCL	TBA	1:0:184	PCL- <i>b</i> -PTBA	40	1.5	-51 / 105	55
C2	B1	TBA	1:0:274	PCL- <i>b</i> -PS- <i>b</i> -PTBA	37	1.3	-58 / 111 / 126	-
D1 <sup>c</sup>	<b>6</b>	4-MeCL / St	1:92:76	PS-4-MeCL- <i>b</i> -St	13	1.4	-59	65 / 90
D1.1 <sup>b</sup>				PSt	5	1.2	n.d.	n.d.
D2 <sup>d</sup>	<b>6</b>	4-MeCL / St	1:92:76	PS-4-MeCL- <i>b</i> -St	12	1.4	n.d.	n.d.
D2.1 <sup>b</sup>				PSt	5	1.1	n.d.	n.d.

<sup>a</sup> data from SEC; polystyrene calibration typically overestimation of M<sub>w</sub> of PCL by about a factor 2. <sup>b</sup> after decomposition of PCL block. <sup>c</sup> method A, see Experimental Section. <sup>d</sup> method B, see Experimental Section.

### 2.3 Synthesis of block copolymers in one pot

Based on the encouraging results in the two step synthesis, i.e. high degree of initiator incorporation in the enzymatic ROP and efficient macroinitiation in the LFRP, respectively, both polymerizations were run in a one-pot cascade reaction without an intermediate precipitation step. In this case, the presence of unreacted initiator will result in unwanted PSt homopolymer formation. Furthermore, initiation of CL polymerization by water may result in PCL homopolymer. The latter can be reduced by careful drying of the starting materials as mentioned earlier. Oxygen was removed from the polymerization mixture containing only CL, St, Novozym 435 and **6** by applying five consecutive freeze-pump-thaw cycles prior to the polymerization. The reaction flask was then heated to 60 °C to initiate enzymatic ROP of CL. Nitroxide polymerization from **6** does not occur at this temperature as confirmed by a control reaction. After three hours, the temperature was raised to 95 °C for 90 h to activate and perform nitroxide mediated LFRP of St to form the PSt block. The resulting products were isolated by precipitation (B1: yield 67%, B2: 39 %). A quantitative conversion of CL was reached in both examples, while the St conversion was 72 % for B1. The SEC traces showed no evidence of radical coupling reactions. The values of M<sub>w</sub> and polydispersities from analysis of these traces are listed in Table 2.1. Their <sup>1</sup>H-NMR spectra showed signals corresponding to

both, PSt and PCL. Figure 2.10 shows the SEC trace of block copolymer B2 (Table 2.1) that was designed to have a shorter PSt block by stopping the reaction at low St conversion. This block copolymer was of particular interest since, if PSt was formed and remained in the isolated product, it would be easily separated and detected by SEC. Comparison of the SEC trace before and after degrading of the PCL block shows a significant shift of the peak to lower molecular weight (Figure 2.10). Furthermore, a peak corresponding to trace B was not observed in trace A. These results provide strong evidence that the proposed block copolymer structure was obtained in the one-pot cascade reaction.<sup>33</sup>

The successful preparation of block copolymers by the one-pot method demonstrates the compatibility of biocatalytic lactone polymerization with nitroxide mediated LFRP. The kinetic characteristics of either polymerization imply that a temperature induced kinetic separation, i.e. activation in distinct temperature windows, favors the block polymer formation by circumventing the sterically unfavorable enzymatic macroinitiation from polystyrene. To the best of our knowledge this provides the first example of a chemo-enzymatic one-pot cascade polymerization.

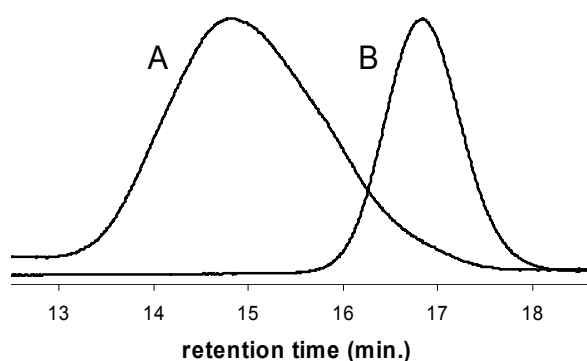


**Figure 2.10** SEC trace of block copolymer obtained in the one-pot reaction before (A) and after (B) degradation of the PCL block (Table 2.1, entries B2 and B2.1).

#### 2.4 One-pot chemo-enzymatic kinetic resolution polymerization

The concept of a one-pot chemo-enzymatic cascade polymerization allows a new route to functional polymers provided the unique features of enzyme catalysis such as enantioselectivity are retained during the process. We therefore extended our approach to a chemo-enzymatic one-pot kinetic resolution polymerization of racemic 4-methyl- $\epsilon$ -caprolactone (4-MeCL). It has been reported that CALB polymerizes (*S*)-4-MeCL at a higher rate than the *R*-enantiomer resulting in polymers with high enantiomeric excess (ee).<sup>20,34</sup> Typically, in a kinetic resolution of enantiomers, the reactivity of the less favored enantiomer is not zero, i.e., (*R*)-4-MeCL will be consumed once the conversion of (*S*)-4-MeCL approaches

100% at 50 % total monomer conversion. Therefore, the net  $ee_p$  value of the polymer depends strongly on the conversion at which the polymerization is stopped. Enantio-enriched polymers are easily achieved in homopolymerizations of racemic 4-MeCL by precipitation at the respective monomer conversion. In the case of the one-pot chemo-enzymatic synthesis of block copolymers comprising an enantio-enriched poly((*S*)-4-MeCL) block, the remaining (*R*)-4-MeCL can not be removed from the reaction mixture. Although at a lower rate, it would continuously be polymerized by the enzyme during the LFRP of St. In order to realize high  $ee$  values in a one-pot chemo-enzymatic reaction, the enzymatic polymerization of 4-MeCL has to be quenched at about 50 % total monomer conversion before the temperature is increased to initiate the LFRP. This can be accomplished by adding paraoxon (diethyl *p*-nitrophenyl phosphate), a known irreversible inhibitor for CALB.<sup>35</sup> The efficiency of this procedure was successfully tested in a control reaction, i.e., the enzymatic resolution polymerization of racemic 4-MeCL. Inspection of Figure 2.11 shows the expected fast conversion of (*S*)-4-MeCL reaching ca. 95 % within 90 minutes. A slow conversion of the *R*-enantiomer is observed at this point (10%). Upon addition of a solution of paraoxon in toluene, no further activity of the enzyme was detected.

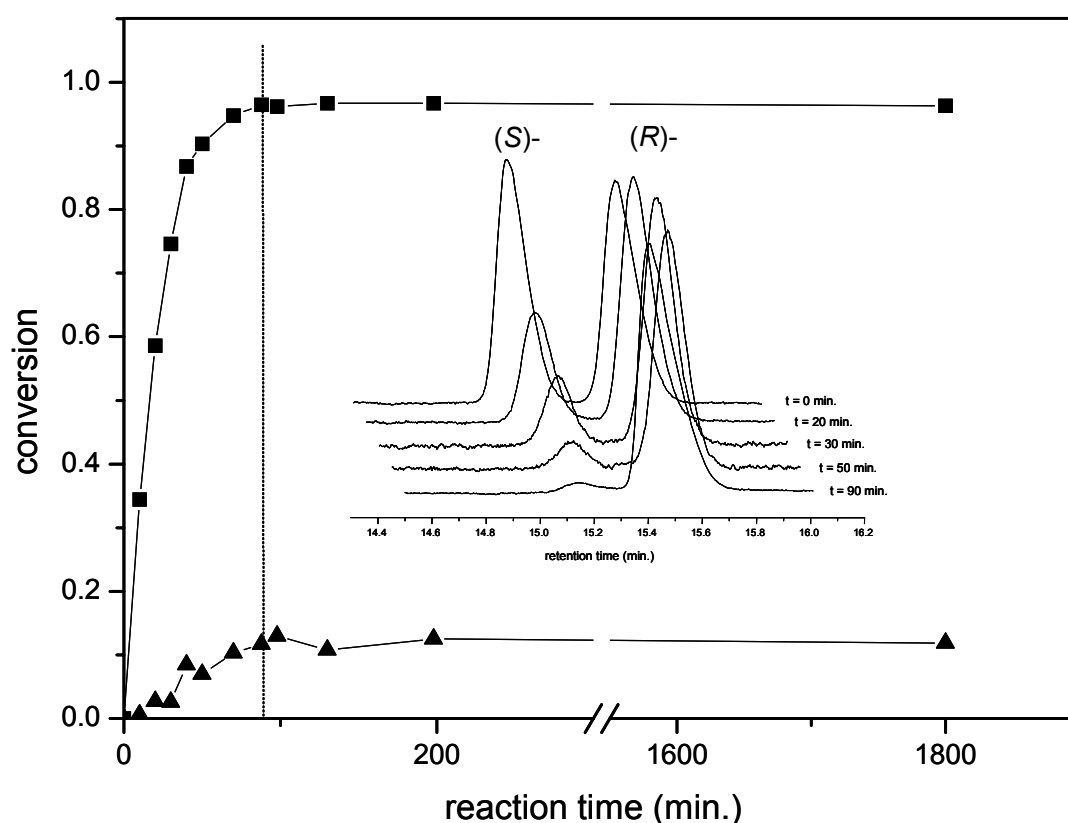


**Figure 2.11** Conversion of (*R*)- (▲) and (*S*)-4-methyl- $\epsilon$ -caprolactone (■) from a racemic mixture employing **6** and Novozym 435 in a one-pot cascade kinetic resolution polymerization. The dotted line indicates the addition of paraoxon (enzyme inhibitor). Values are obtained from chiral GC (inset).

The chemo-enzymatic one-pot synthesis of enantio-enriched block copolymers was conducted according to the synthetic protocol developed for the synthesis of P(CL-*b*-St). The reaction mixture containing 4-MeCL, St, Novozym 435 and **6** was heated to 45°C and the consumption of (*R*)- and (*S*)-4-MeCL was monitored by chiral GC and <sup>1</sup>H NMR on samples withdrawn from the reaction mixture. At a conversion of (*S*)-4-MeCL of 80 %, paraoxon was added to the reaction. Subsequently, the reaction mixture was heated to 100 °C for 90 h. A polymer with a molecular weight of 13 kDa and a polydispersity of 1.4 was recovered from this reaction (Table 2.1, entry D1). In the <sup>1</sup>H NMR spectrum all characteristic signals of the 4-MeCL- and St-blocks can be recognized (Figure 2.12). Figure 2.13 shows the corresponding GPC traces of the recovered polymer and the product obtained after degradation of the polyester block. Comparable to Figure 2.10, both traces are well separated providing strong evidence that the proposed block copolymer structure was obtained from the one-pot reaction. It has to be noted that similar results were obtained irrespective of the moment the freeze-pump-thaw cycles were conducted: prior to the reaction (D1) or immediately before the temperature was increased for the LFRP (D2).

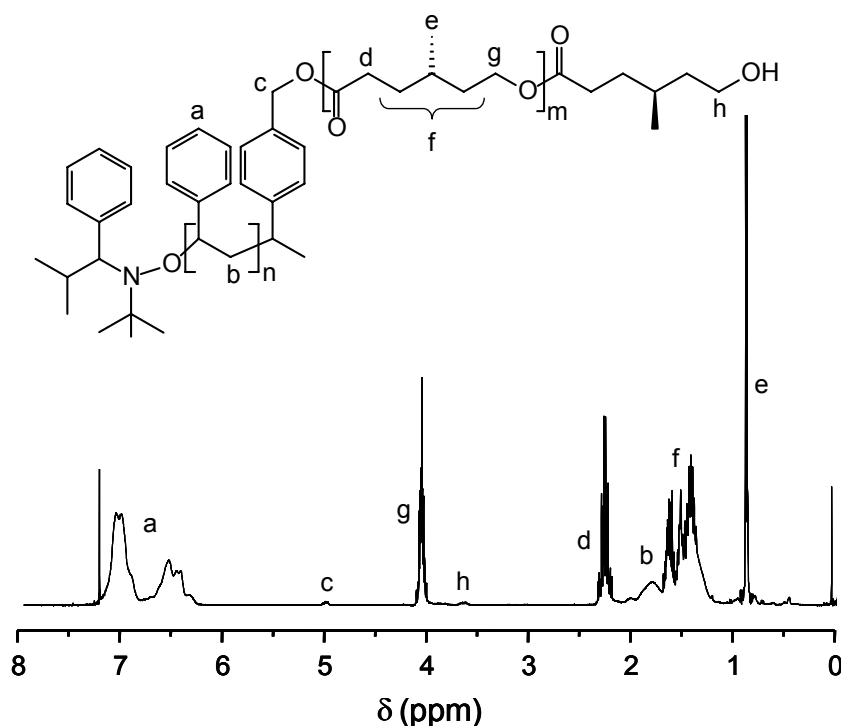


**Figure 2.12** <sup>1</sup>H NMR spectrum of poly((*S*)-4-MeCL-*b*-Sty) block copolymer (entry D1).

From the ee of the unreacted monomer ( $ee_m = 64\%$ ), an  $ee_p$  of the P(4-MeCL) block of 86 % was calculated for block copolymer D1. The specific rotation  $[\alpha]_{D^{25}}$  of the block copolymer is  $-2.6^\circ$ . This is in agreement with the optical rotation of  $-7.2^\circ$  reported by Bisht for

P((S)-4-MeCL) with an  $ee_p$  of 90% considering that the block length ratio of chiral to non-chiral block in our block copolymer is ca. 1:2.<sup>34</sup>

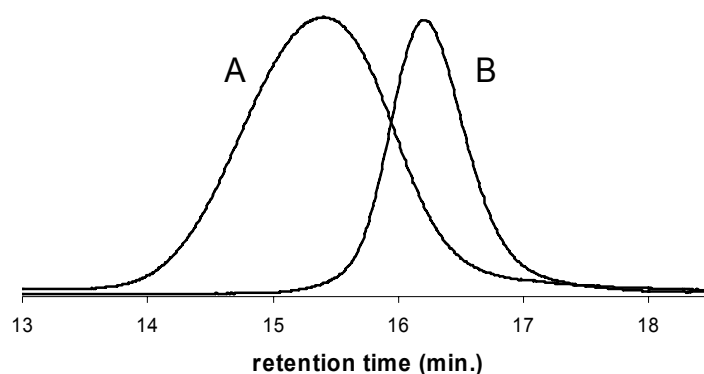


**Figure 2.13** SEC trace of block copolymer obtained in the one-pot cascade kinetic resolution polymerization before (A) and after (B) degradation of the PCL block (Table 2.1, entries D1 and D1.1).

## 2.4 Conclusions

In conclusion, we described a novel chemo-enzymatic approach towards polymeric materials by integration of metal free enzymatic ROP with nitroxide mediated LFRP from a bifunctional initiator. Block copolymers were obtained in a cascade approach without an intermediate transformation or work-up step. The results imply that the temperature induced kinetic separation favors the block polymer formation by circumventing the sterically unfavorable polystyrene macroinitiation. The unique characteristics of enzyme catalysis such as a high stereoselectivity are retained in the process as was shown in the synthesis of chiral block copolymers by this cascade approach.

## 2.5 Experimental Section

### Materials

All monomers were distilled from  $\text{CaH}_2$  under reduced pressure before use. 4-Methyl- $\epsilon$ -caprolactone (4-MeCL) was synthesized by Baeyer-Villiger oxidation of 4-methyl-cyclohexanone following a reported procedure.<sup>36</sup> Bifunctional initiator **6** was synthesized according to a literature procedure.<sup>37</sup> Novozym 435 was purchased from Novozymes A/S. All other chemicals were purchased from Aldrich and used as received unless otherwise noted.

### Analytical methods

$^1\text{H}$  and  $^{13}\text{C}$  NMR spectra were measured using a Varian Mercury Vx 400 or 300 spectrometer (400 MHz or 300 MHz) in  $\text{CDCl}_3$  with the delay time ( $d_1$ ) set at 10 s. Conversions of CL ( $C_{\text{CL}}$ ) and **6** ( $C_{\text{I}}$ ) were determined from  $^1\text{H}$ -NMR spectra: for CL by comparison of the integrated peak areas of the  $-\text{CH}_2\text{C}=\text{O}$  proton signal in the monomer at 2.65 ppm ( $I_{\delta=2.65}$ ) and in the polymer at 2.30 ppm ( $I_{\delta=2.30}$ ), i.e.,  $C_{\text{CL}} = (I_{\delta=2.30}) / [(I_{\delta=2.30}) + (I_{\delta=2.65})]$ . Similarly, the conversion of **1** was calculated as  $C_{\text{I}} = (I_{\delta=5.10}) / [(I_{\delta=5.10}) + (I_{\delta=4.65})]$  comparing the integrated peak areas of the Ph- $\text{CH}_2$ -O- protons on the reacted (5.10 ppm) and the unreacted initiator (4.65 ppm).

Chiral gas chromatography (GC) was performed on a Shimadzu 6C-17A GC equipped with an FID employing a Chrompack Chirasil-DEX CB (DF=0.12) column. Injection and detection temperatures were set at 300 and 325°C, respectively. Separations were done under isocratic conditions with the column temperature set at 125°C, which afforded in all cases baseline separation of the enantiomers of 4-MeCL. An internal standard method using either 1,3,5-tri-*t*-butylbenzene or 2-undecanone allowed for determination of the lactone conversion and enantiomeric excess ( $ee_m$ ) of the unreacted monomer. The  $ee_m$  was calculated as follows:  $ee_m = (R-S)/(R+S)$  where R and S correspond to the surfaces of the GC peaks of the *R*- and *S*-enantiomer, respectively. All samples were measured using a Shimadzu AOC-20i autosampler. The enantiomeric excess of obtained chiral block copolymers ( $ee_p$ ) was calculated from total lactone conversion and enantiomeric excess of the unreacted monomer.<sup>34</sup>

Gel permeation chromatography (GPC) was carried out on a Waters 712 WISP HPLC system with a Waters 410 Differential Refractometer detector and a PL gel guard precolumn (5 mm, 50 x 7.5 mm) followed by two PL gel mixed-C columns (10 mm, 300 x 7.5 mm, Polymer Laboratories), using THF as the eluent. Optical rotations were measured on a Jasco DIP-370 digital polarimeter.

### General procedure for a two-pot block copolymer synthesis

Novozym 435 (213.0 mg) and a magnetic stirring bar were put in a Schlenk tube. The tube was put overnight in a vacuum oven (10 mm Hg) at 50 °C in presence of  $\text{P}_2\text{O}_5$ . The oven was backfilled with nitrogen and **6** (54.0 mg; 0.15 mmol), CL (2.50 ml; 22.5 mmol) and dry molecular sieves (4 Å) were added to the tube. This mixture was stirred at 60 °C for 3 h.  $\text{CHCl}_3$  was added to the viscous reaction mixture and the immobilized enzyme was filtered off. The PCL macroinitiator was obtained by precipitation in cold methanol (yield 0.90 g). The PCL (600 mg) was then dissolved in styrene (2.00 ml; 17.3 mmol). After five consecutive freeze-pump-thaw cycles to remove the oxygen from the reaction mixture, it was heated for 68 h at 95°C, allowing the system to reach high styrene conversion as was evident by the increased viscosity of the system. The polymer was recovered by dissolving the mixture in  $\text{CHCl}_3$ , filtration and precipitation in cold methanol (yield 1.16 g). All analytical data were in agreement with literature data reported on P(CL-*b*-St).

### General procedure for a one-pot block copolymer synthesis

Novozym 435 (224.0 mg) and a magnetic stirring bar were put in a Schlenk tube. The tube was put overnight in a vacuum oven (10 mm Hg) at 50 °C in presence of  $\text{P}_2\text{O}_5$ . The oven was backfilled with nitrogen and CL (1.90 ml; 17.1 mmol), St (3.63 ml; 31.4 mmol), **6** (75.9 mg; 0.21 mmol) and molecular sieves (4Å) were added to the tube. After five consecutive freeze-pump-thaw cycles to remove the oxygen from the reaction solution, it was stirred at 60 °C for 3 h and subsequently heated to 95 °C for 114 h, allowing the system to reach high St conversion as was evident from the increased viscosity of the system. The polymer was recovered by dissolving the mixture in  $\text{CHCl}_3$ , filtration and precipitation in cold methanol. All analytical data were in agreement with literature data reported on P(CL-*b*-St).

*Synthesis of PCL-b-PTBA block copolymer*

PCL macroinitiator (590 mg), *t*-butyl acrylate (1.50 g; 15.0 mmol) and 2,2,5-trimethyl-4-phenyl-3-azahexane-3-nitroxide (TIPNO radical) (1.0 mg, 4.5  $\mu$ mol) were put in a Schlenk tube. After five consecutive freeze-pump-thaw cycles to remove the oxygen from the reaction solution, it was heated for 70 h at 120°C, allowing the system to reach high acrylate conversion as was evident from the increased viscosity of the system. The polymer was recovered by dissolving the mixture in CHCl<sub>3</sub>, filtration and precipitation in cold methanol (yield x g).

<sup>1</sup>H NMR (CDCl<sub>3</sub>)  $\delta$  5.1 (d, benzyl-CH<sub>2</sub>OCO), 4.15 (t, CH<sub>2</sub>CH<sub>2</sub>OCO), 3.68 (t, CH<sub>2</sub>CH<sub>2</sub>OH), 2.2-2.45 (m, OCOCH<sub>2</sub>CH<sub>2</sub> + CH<sub>2</sub>CHCOO), 1.2-2.2 (m, OCOCH<sub>2</sub>CH<sub>2</sub>CHCH<sub>3</sub>CH<sub>2</sub>CH<sub>2</sub>O + COOC(CH<sub>3</sub>)<sub>3</sub>).

*Synthesis of PCL-b-PSt-b-PTBA triblock copolymer*

PCL-*b*-PSt (790 mg), *t*-butyl acrylate (1.50 g; 15.0 mmol) and 2,2,5-trimethyl-4-phenyl-3-azahexane-3-nitroxide (TIPNO radical) (1.0 mg, 4.5  $\mu$ mol) were put in a Schlenk tube. After five consecutive freeze-pump-thaw cycles to remove the oxygen from the reaction solution, it was heated for 70 h at 120°C, allowing the system to reach high acrylate conversion as was evident from the increased viscosity of the system. The polymer was recovered by dissolving the mixture in CHCl<sub>3</sub>, filtration and precipitation in cold methanol (yield x g).

<sup>1</sup>H NMR (CDCl<sub>3</sub>)  $\delta$  6.8-7.4 (m, Ar-*H*), 6.3-6.8 (m, Ar-*H*), 5.1 (d, benzyl-CH<sub>2</sub>OCO), 4.15 (t, CH<sub>2</sub>CH<sub>2</sub>OCO), 3.68 (t, CH<sub>2</sub>CH<sub>2</sub>OH), 2.2-2.45 (m, OCOCH<sub>2</sub>CH<sub>2</sub> + CH<sub>2</sub>CHCOO), 1.2-2.2 (m, OCOCH<sub>2</sub>CH<sub>2</sub>CHCH<sub>3</sub>CH<sub>2</sub>CH<sub>2</sub>O + Ar-CHCH<sub>2</sub> + COOC(CH<sub>3</sub>)<sub>3</sub>).

*General procedure for a one-pot chiral block copolymer synthesis*

Method A: Novozym 435 (190 mg) and a magnetic stirring bar were put in a Schlenk tube. The tube was put in a vacuum oven (10 mm Hg) overnight at 50 °C in presence of P<sub>2</sub>O<sub>5</sub>. The oven was backfilled with nitrogen and 4-MeCL (3.00 g; 23.4 mmol), St (2.00 g; 19.2 mmol), initiator **6** (90 mg; 0.25 mmol) and molecular sieves (4Å) were added to the tube. This mixture was stirred at 45 °C for 28 h. During reaction, samples were withdrawn from the reaction mixture using a syringe and the enzyme was removed from the sample by filtration over cotton wool. The samples were analyzed by <sup>1</sup>H NMR for 4-MeCL conversion and by chiral GC for enantiomeric excess (ee<sub>m</sub>) of the unreacted monomer. At 43 % 4-MeCL conversion, the enzymatic reaction was stopped by the addition of 0.2 ml of a solution of 6.17 mM paraoxon in toluene (according to a literature procedure).<sup>35</sup> Then, the mixture was subjected to five consecutive freeze-pump-thaw cycles to remove the oxygen from the reaction solution. Subsequently, the flask was stirred at 100 °C for 90 h. The polymer was recovered by dissolving the mixture in CHCl<sub>3</sub>, filtration and precipitation in cold methanol.

<sup>1</sup>H NMR (CDCl<sub>3</sub>)  $\delta$  6.8-7.4 (m, Ar-*H*), 6.3-6.8 (m, Ar-*H*), 5.1 (d, benzyl-CH<sub>2</sub>OCO), 4.15 (t, CH<sub>2</sub>CH<sub>2</sub>OCO), 3.68 (t, CH<sub>2</sub>CH<sub>2</sub>OH), 2.2-2.45 (m, OCOCH<sub>2</sub>CH<sub>2</sub>), 1.2-2.2 (m, OCOCH<sub>2</sub>CH<sub>2</sub>CHCH<sub>3</sub>CH<sub>2</sub>CH<sub>2</sub>O + Ar-CHCH<sub>2</sub>), 0.8-1.1 (d, CH<sub>3</sub>). T<sub>g</sub> ((*S*)-4-MeCL) block: -51 °C, T<sub>g</sub> (St) block: 106 °C.

Method B: The procedure was conducted in an analogous fashion as described in Method A, except that the reaction mixture was subjected to five consecutive freeze-pump-thaw cycles prior to the start of the reaction. During the course of the reaction, the system was kept under an argon atmosphere. After the addition of inhibitor solution (which was prior to addition also subjected to five consecutive freeze-pump-thaw cycles, the system was immediately heated to 100 °C without further operations.

## 2.6 References and notes

1. Förster, S.; Plantenberg, T. *Angew. Chem., Int. Ed.* **2002**, 41, (5), 688-714.
2. Lu, Y.Y.; Hu, Y.L.; Chung, T.C.M. *Polymer* **2005**, 46, (23), 10585-10591.
3. Fink, Y.; Urbas, A.M.; Bawendi, M.G.; Joannopoulos, J.D.; Thomas, E.L. *J. Lightwave Technol.* **1999**, 17, (11), 1963-1969.
4. Riess, G. *Progr. Polym. Sci.* **2003**, 28, (7), 1107-1170.
5. Hamley, I.W.; Castelletto, V.; Lu, Z.B.; Imrie, C.T.; Itoh, T.; Al-Hussein, M. *Macromolecules* **2004**, 37, (13), 4798-4807.
6. Mastai, Y.; Sedlak, M.; Colfen, H.; Antonietti, M. *Chem. Eur. J.* **2002**, 8, (11), 2430-2437.
7. Ho, R.M.; Chiang, Y.W.; Tsai, C.C.; Lin, C.C.; Ko, B.T.; Huang, B.H. *J. Am. Chem. Soc.* **2004**, 126, (9), 2704-2705.
8. Tao, L.; Luan, B.; Pan, C.Y. *Polymer* **2003**, 44, (4), 1013-1020.
9. Hawker, C.J.; Hedrick, J.L.; Malmström, E.E.; Trollsås, M.; Mecerreyes, D.; Moineau, G.; Dubois, P.; Jérôme, R. *Macromolecules* **1998**, 31, (2), 213-219.
10. Bernaerts, K.V.; Schacht, E.H.; Goethals, E.J.; Du Prez, F.E. *J. Polym. Sci., Part A: Polym. Chem.* **2003**, 41, (21), 3206-3217.
11. Puts, R.D.; Sogah, D.Y. *Macromolecules* **1997**, 30, (23), 7050-7055.
12. de Geus, M.; Peeters, J.; Wolffs, M.; Hermans, T.; Palmans, A.R.A.; Koning, C.E.; Heise, A. *Macromolecules* **2005**, 38, (10), 4220-4225.
13. Meyer, U.; Palmans, A.R.A.; Loontjens, T.; Heise, A. *Macromolecules* **2002**, 35, (8), 2873-2875.
14. Li, D.S.; Sha, K.; Li, Y.P.; Liu, X.T.; Wang, W.; Wang, S.W.; Xu, Y.X.; Ai, P.; Wu, M.Z.; Wang, J.Y. *Polym. Bull.* **2006**, 56, (2-3), 111-117.
15. Sha, K.; Li, D.; Li, Y.; Ai, P.; Wang, W.; Xu, Y.; Liu, X.; Wu, M.; Wang, S.; Zhang, B.; Wang, J. *Polymer* **2006**, 47, (12), 4292-4299.
16. Sha, K.; Li, D.S.; Li, Y.P.; Ai, P.; Liu, X.T.; Wang, W.; Xu, Y.X.; Wang, S.W.; Wu, M.Z.; Zhang, B.; Wang, J.Y. *J. Polym. Sci., Part A: Polym. Chem.* **2006**, 44, (10), 3393-3399.
17. Mecerreyes, D.; Moineau, G.; Dubois, P.; Jérôme, R.; Hedrick, J.L.; Hawker, C.J.; Malmström, E.E.; Trollsås, M. *Angew. Chem., Int. Ed.* **1998**, 37, (9), 1274-1276.
18. Klaerner, G.; Trollsås, M.; Heise, A.; Husemann, M.; Atthoff, B.; Hawker, C.J.; Hedrick, J.L.; Miller, R.D. *Macromolecules* **1999**, 32, (24), 8227-8229.
19. Weimer, M.W.; Scherman, O.A.; Sogah, D.Y. *Macromolecules* **1998**, 31, (23), 8425-8428.
20. Peeters, J.; Palmans, A.R.A.; Veld, M.; Scheijen, F.; Heise, A.; Meijer, E.W. *Biomacromolecules* **2004**, 5, (5), 1862-1868.
21. de Geus, M.; Schormans, L.; Palmans, A.R.A.; Koning, C.E.; Heise, A. *J. Polym. Sci., Part A: Polym. Chem.* **2006**, 44, (14), 4290-4297.
22. Villarroya, S.; Zhou, J.X.; Duxbury, C.J.; Heise, A.; Howdle, S.M. *Macromolecules* **2006**, 39, (2), 633-640.
23. Duxbury, C.J.; Wang, W.X.; de Geus, M.; Heise, A.; Howdle, S.M. *J. Am. Chem. Soc.* **2005**, 127, (8), 2384-2385.
24. Zhou, J.X.; Villarroya, S.; Wang, W.X.; Wyatt, M.F.; Duxbury, C.J.; Thurecht, K.J.; Howdle, S.M. *Macromolecules* **2006**, 39, (16), 5352-5358.
25. Studer, A.; Schulte, T. *Chem. Rec.* **2005**, 5, (1), 27-35.
26. Dao, J.; Benoit, D.; Hawker, C.J. *J. Polym. Sci., Part A: Polym. Chem.* **1998**, 36, (12), 2161-2167.



27. Drockenmuller, E.; Catala, J.-M. *Polym. Prepr. (Am. Chem. Soc., Div. Polym. Chem.)* **2002**, 43, (2), 301-302.
28. Drockenmuller, E.; Catala, J.-M. *Macromolecules* **2002**, 35, (7), 2461-2466.
29. Matyjaszewski, K.; Spanswick, J. *Materials Today (Oxford, United Kingdom)* **2005**, 8, (3), 26-33.
30. Hawker, C.J.; Bosman, A.W.; Harth, E. *Chem. Rev.* **2001**, 101, (12), 3661-3688.
31. Mahapatro, A.; Kalra, B.; Kumar, A.; Gross, R.A. *Biomacromolecules* **2003**, 4, (3), 544-551.
32. Personal communication with Matthijs de Geus learned that enzymatically synthesized poly( $\epsilon$ -caprolactone) contains approximately 5% cyclic species. This was analyzed by means of SEC under critical conditions.
33. Attempts to synthesize block copolymers using TBA as the monomer in a 1-pot approach were unsuccessful; SEC traces showed multimodal distributions.
34. Al-Azemi, T.F.; Kondaveti, L.; Bisht, K.S. *Macromolecules* **2002**, 35, (9), 3380-3386.
35. Mei, Y.; Kumar, A.; Gross, R. *Macromolecules* **2003**, 36, (15), 5530-5536.
36. Trollsås, M.; Lee, V.Y.; Mecerreyes, D.; Löwenhielm, P.; Möller, M.; Miller, R.D.; Hedrick, J.L. *Macromolecules* **2000**, 33, (13), 4619-4627.
37. Benoit, D.; Chaplinski, V.; Braslau, R.; Hawker, C.J. *J. Am. Chem. Soc.* **1999**, 121, (16), 3904-3920.

# 3

## Enzymatic ring-opening of $\omega$ -substituted lactones

### Abstract

The Novozym 435-catalyzed ring-opening of several  $\omega$ -substituted  $\epsilon$ -caprolactones was investigated in detail. The ring-opening of an  $\omega$ -substituted  $\epsilon$ -caprolactone furnishes a ring-opening product bearing a secondary alcohol with the *S*-configuration, preventing propagation from taking place in an enzymatic polymerization of such a monomer. On long timescales, however, oligomers are formed due to an insertion mechanism. Lactide was shown to be an excellent substrate for CALB-catalyzed ring-opening, although oligomerization did not take place; this was shown not to be caused by the configuration of the secondary alcohol formed. Both enantiomers of 6-methyl- $\epsilon$ -caprolactone were synthesized with 99+% ee via a ring-opening/ring-closure procedure. The entropic and enthalpic contribution to enantioselectivity of the enzymatic ring-opening of 6-MeCL were determined by temperature studies.  $\Delta\Delta S^\ddagger_{(S-R)}$  was found to be 48.5 J/mol.K and  $\Delta\Delta H^\ddagger_{(S-R)}$  was found to be -23.1 kJ/mol. The racemic temperature  $T_r$  was calculated to be 476 K.

### 3.1 Introduction

Lipase-catalyzed transformations are nowadays widely recognized as useful additions to the rich repertoire of traditional organic synthesis. The biological function of lipases is the hydrolysis of fats and oils; however lipases also show catalytic activity in the areas of esterification, transesterification, amidation and transamidation. The fact that many lipases show high activity in organic solvents and under mild reaction conditions makes them extremely versatile biocatalysts. Their most appealing property, however, is enantioselectivity, since this is what distinguishes lipases from most chemical catalysts.

#### 3.1.1 Enantioselectivity of lipases towards the nucleophile

In a (trans)esterification reaction, two substrates are combined to give two products (in case of linear esters or carboxylic acids) or a single product (in case of a cyclic ester, a lactone). Lipases can display enantioselectivity towards the acyl donor as well as towards the nucleophile. Many examples have been reported of the enantioselectivity of lipases toward the nucleophile (mostly secondary alcohols).<sup>1-9</sup> Combined with ruthenium-catalyzed racemization, the dynamic kinetic resolution (DKR) process has been used for the commercial production of optically pure secondary alcohols from a racemic mixture (for a review on DKR the reader is referred to one of the extensive reviews available in literature).<sup>10-12</sup> In general, lipases display strong *R*-selectivity towards secondary alcohols. In case of *Candida antarctica* Lipase B (CALB), the active site contains a small cavity called the stereospecificity pocket, which can hold a methyl- or an ethyl-sized substituent. In this stereospecificity pocket, the smaller substituent of the secondary alcohol can be placed during reaction, while the larger substituent resides in the larger cavity. The spatial orientation of these cavities implies that *R*-secondary alcohols are highly preferred; the docking of an *S*-secondary alcohol leads to significant steric hindrance. This behavior was empirically recognized by Kazlauskas in 1991 (Figure 3.1),<sup>8</sup> and was later confirmed on a molecular level by Uppenberg *et al.*<sup>13</sup>

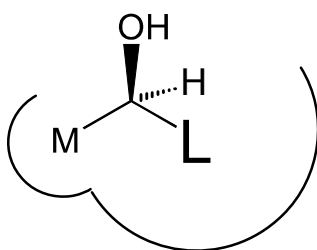
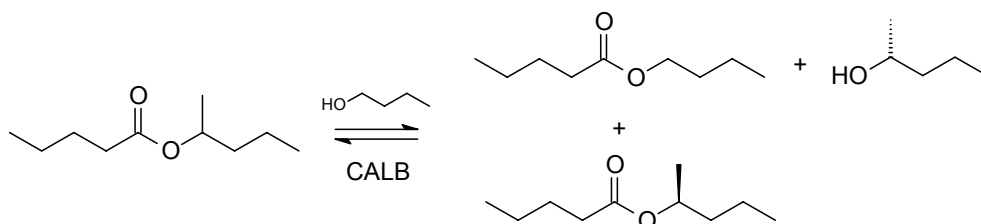


**Figure 3.1** The conformation of the large (*L*), medium (*M*) and small (*H*-atom) substituent and the hydroxyl group of the fast reacting enantiomer of secondary alcohols as predicted by Kazlauskas' rule.

### 3.1.2 Enantioselectivity of CALB toward the acyl donor

While many publications have covered the enantioselectivity of CALB towards secondary alcohols, enantioselectivity towards the acyl donor has received much less attention. Compared to the excellent enantioselectivity towards many secondary alcohols, the selectivity towards the acyl part of esters is in most cases only low to moderate. Uppenberg *et al.* suggested that the acyl side of the active site is much more spacious, thus allowing the docking of both enantiomers without much difference in steric hindrance.<sup>13</sup> Moreover, few examples can be found in literature where enantioselectivity is truly governed by the acyl donor (that is, the chiral center of the ester is situated on the side of the carbonyl).<sup>14,15</sup> Mostly, the center of chirality is located on the oxygen side of the ester.<sup>16-19</sup> The observed high enantioselectivity in the hydrolysis or transesterification of these esters can be explained by the fact that the enantioselective step in the reaction sequence is merely the reverse of the acylation of a chiral secondary alcohol; in these reactions a chiral secondary alcohol is set free as the desired optically pure reaction product (Scheme 3.1). As Chen *et al.* pointed out, in a reverse reaction the sense of chirality is the same.<sup>20</sup> In other words, the reverse reaction occurs with the same enantioselectivity and E ratio as the forward reaction, since the enantioselective step in the reaction sequence goes through the same transition state.



**Scheme 3.1** The observed enantioselectivity in an enzymatic transesterification of a chiral ester is sometimes merely the reversed acylation of a chiral secondary alcohol.

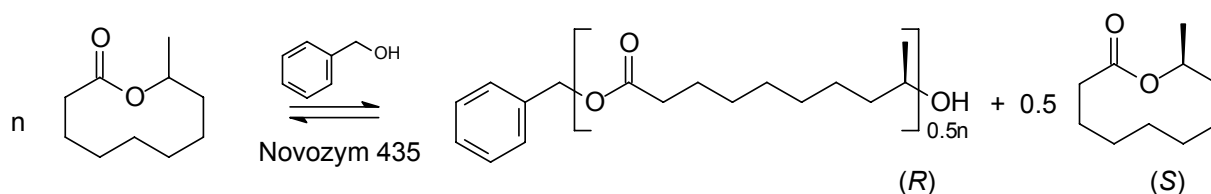
### 3.1.3 Enantioselectivity in CALB-catalyzed ring-opening of lactones

Also in the transesterification of chiral lactones enantioselectivity was reported, albeit in most cases with only moderate E-values. The hydrolysis and butanolysis of methyl- and ethyl-substituted  $\epsilon$ -caprolactones were reported, with E-values ranging from 3 to over 100,<sup>21,22</sup> as well as the enantioselective (co)polymerization of these lactones leading to enantioenriched polymers with high ee's of up to 98%.<sup>23,24</sup> However, judging from the gas chromatograms published in one paper in particular, the reliability of the enantioselectivity data is questionable.<sup>24,25</sup> Peeters *et al.* describe the enantioselective polymerization of 4-methyl- $\epsilon$ -caprolactone with reasonably high enantioselectivity (E = 93), and the subsequent formation of a chiral block copolymer.<sup>26</sup>

This chapter aims at investigating the enantioselectivity of CALB towards  $\omega$ -substituted cyclic (di)esters. The enzymatic ring-opening of 6-methyl- $\epsilon$ -caprolactone (6-MeCL) is discussed on short and long time scales. The enzymatic ring-opening of 6-EtCL, 6-PrCL and 6-BuCL is investigated, as well as the enzymatic ring-opening of lactide. In addition, the synthesis of enantiopure (*R*)- and (*S*)-6-MeCL is described. The thermodynamic contributions of entropy and enthalpy to the enantioselectivity towards 6-MeCL are determined.

### 3.2 Enzymatic ring-opening of 6-methyl- $\epsilon$ -caprolactone

Recently, we reported on the highly *R*-selective CALB-catalyzed ring-opening polymerization of  $\omega$ -substituted macrolactones.<sup>27</sup> The enzymatic ring-opening polymerization of 7-methylheptalactone proceeded with strong *R*-selectivity with a reaction rate for the *R*-enantiomer that was approximately 20,000 times greater than the reaction rate for the *S*-enantiomer. Since the ring-opening of the *R*-lactone results in an *R*-secondary alcohol (which is - in accordance to Kazlauskas' rule - the preferred enantiomer for a nucleophilic attack in the subsequent propagation),<sup>8</sup> enantioselective polymerization of these lactones proved very well possible. Similar to the enantioselective transesterification of esters, as described above, the extremely high enantioselectivity in these polymerizations can be explained by the fact that the initial ring-opening of an  $\omega$ -substituted macrolactone closely resembles the reverse reaction of the acylation of a secondary alcohol. The ester in these large lactones (with little ring strain) is expected to be in the thermodynamically favored *trans*-conformation. The transition state for the formation of the acyl-enzyme complex is, therefore, very similar to the transition state resulting from the attack of a secondary alcohol nucleophile on an enzyme-activated acyl donor (Scheme 3.2). Hence, for this type of ring-opening reaction the same model is applicable as in the esterification of secondary alcohols as described by Kazlauskas and Uppenberg.



**Scheme 3.2** The center of chirality in the highly *R*-selective Novozym 435-catalyzed polymerization of  $\omega$ -substituted macrolactones is located on the oxygen side of the cyclic ester and therefore resembles the acylation of a chiral secondary alcohol.

### 3.2.1 Enzymatic ring-opening of 6-methyl- $\epsilon$ -caprolactone on short timescales

A different case, however, arises with the enzymatic ring-opening of  $\omega$ -substituted small-ring cyclic esters. For 6-substituted  $\epsilon$ -caprolactones, such as 6-methyl- $\epsilon$ -caprolactone (6-MeCL) we discovered that Novozym 435 is *S*-selective with only low to moderate selectivity. This seven-membered ring has a considerable amount of ring strain, and the ester is forced in the *cisoid* conformation, instead of the energetically favorable *transoid* conformation (Figure 3.2). Consequently, the methyl substituent is oriented spatially into a different direction, which accounts for the deviation from the strong *R*-selectivity found for  $\omega$ -substituted macrolactones. Clearly, the resemblance with the acylation of secondary alcohols does not hold here anymore. After the *S*-selective ring-opening of such lactone, a secondary alcohol is formed with the *S*-configuration. This alcohol is not accepted as a nucleophile by CALB for the subsequent propagation, and, hence, conventional enzymatic polymerization of this type of monomers is not possible.

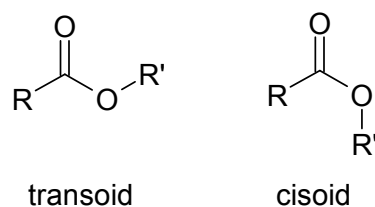
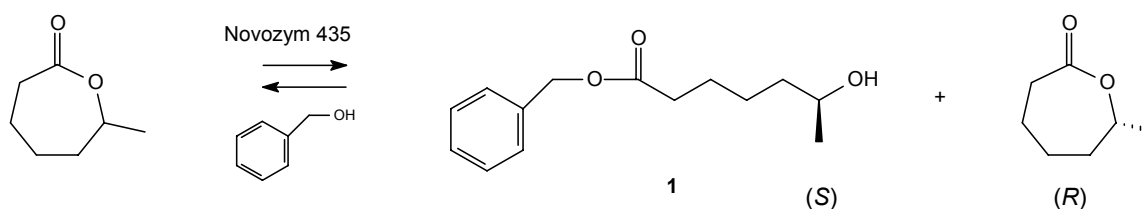


**Figure 3.2** *Cisoid and transoid conformation of the ester bond*



**Scheme 3.3** *Enzymatic ring-opening of (rac)-6-MeCL using benzyl alcohol as the nucleophile.*

Figure 3.3a shows the time-conversion plot for a typical Novozym 435-catalyzed ring-opening experiment of 6-MeCL using benzyl alcohol (BA) as the initiator with a monomer/initiator ratio of 4:1 (Scheme 3.3). Clearly, the initiator is consumed quickly in approximately 30 minutes, and exactly 1 equivalent of (*S*)-6-MeCL is consumed (4 equivalents of racemic 6-MeCL is used, hence (*S*)-6-MeCL conversion rises up to 50%). Using the Chen equation for  $ee_{\text{monomer}}$  and conversion, an *E*-value of 7.9 could be calculated (Figure 3.3b). This implies that also a significant amount of (*R*)-6-MeCL is ring-opened (approximately 0.2 equivalents with regards to initiator after 40 minutes of reaction). However, the ring-opening product of (*R*)-6-MeCL has a terminal *R*-secondary alcohol. Being a good nucleophile for the lipase, this molecule will propagate, most probably with (*S*)-6-MeCL resulting in some dimer

and trimer formation. Ultimately, all initiator molecules are “end-capped” with *S*-secondary alcohols, effectively stopping propagation.

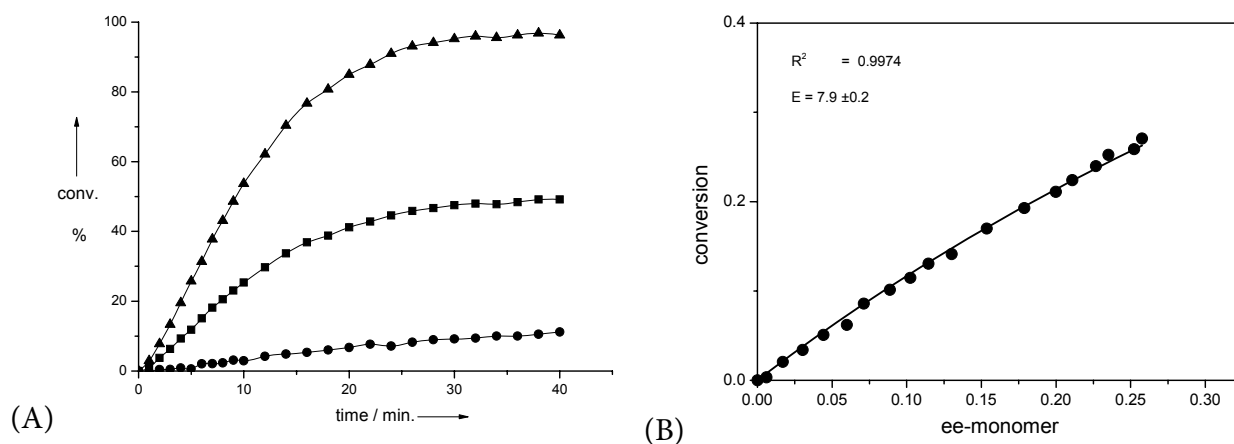
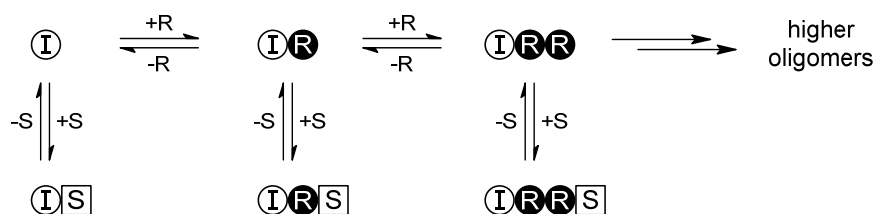


**Figure 3.3** (A) Enzymatic ring-opening of *rac*-6-MeCL by BA catalyzed by Novozym 435; (*S*)-6-MeCL (■); (*R*)-6-MeCL (●); BA (▲);  $T = 60\text{ }^{\circ}\text{C}$ ; BA/6-MeCL = 1/4; solvent: toluene (B) Linear regression fit using the Chen’ relationship of ee-monomer and conversion.

### 3.2.2 Enzymatic ring-opening of 6-methyl- $\epsilon$ -caprolactone on long time scales

If the kinetic plot in Figure 3.3a is closely investigated, a continuing consumption of (*R*)-6-MeCL can be observed, even after all initiator has been consumed. This continuing consumption of (*R*)-6-MeCL after complete conversion of the initiator can be explained by the reversibility of the ring-opening reaction in combination with the moderate enantioselectivity of the lipase towards 6-MeCL. A reverse reaction of a ring-opening product would result in the *S*-lactone and the initiator being formed again (Scheme 3.4). This initiator molecule can subsequently react enzymatically with an *S*-lactone (non-productive, reforming the original dimer), or with an *R*-lactone. The latter reaction would lead to a molecule with a reactive *R*-alcohol end-group, which would immediately lead to another ring-opening reaction, most probably with an *S*-lactone. The net effect of this sequence of reactions is the insertion of an *R*-monomer into the *S*-alcohol ‘terminated’ dimer, leading to trimers and longer oligomers.



**Scheme 3.4** Reversibility of the enzymatic ring-opening enables insertion of the *R*-lactone.

In an experiment with a monomer/initiator ratio of 1 : 4, quick consumption of the initiator and (*S*)-6-MeCL is observed, with 95+% conversion of the initiator in 40 minutes (Figure 3.4a). On a longer timescale, however, (*R*)-6-MeCL is continuously consumed and its conversion ultimately surpasses the conversion of (*S*)-6-MeCL (after approximately 1.5 days, Figure 3.4b). At  $t=6000$  minutes, (*R*)-6-MeCL consumption has reached 76%, while (*S*)-6-MeCL conversion is still below 60%. The amount of ring-opening product **1** can be quantified by chiral GC and its disappearance provides further proof that oligomerization is indeed taking place (Figure 3.5).

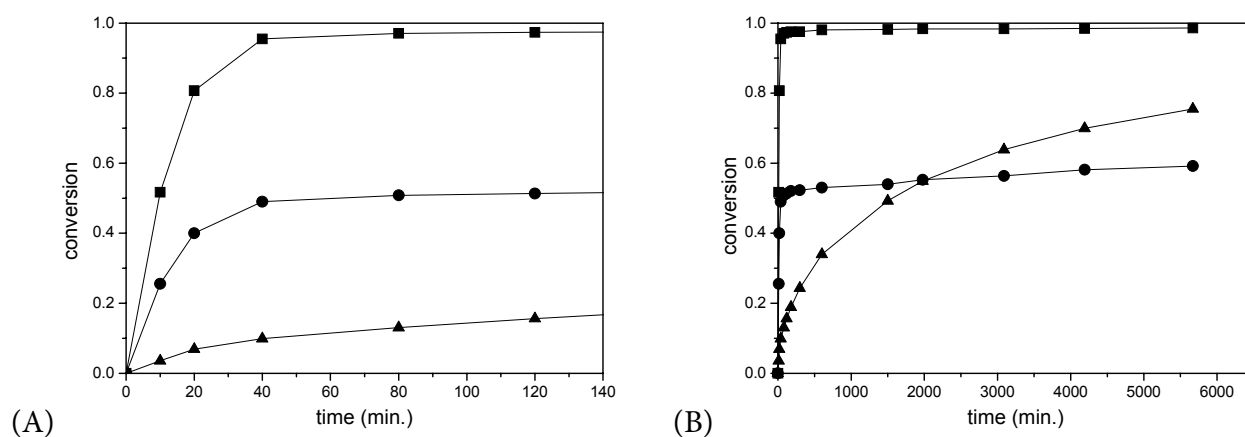


**Figure 3.4** Time-conversion plot for the ring-opening of (*rac*)-6-MeCL by BA (BA : 6-MeCL 1:4, toluene, 60 °C); BA (■), (*S*)-6-MeCL (●), (*R*)-6-MeCL (▲).

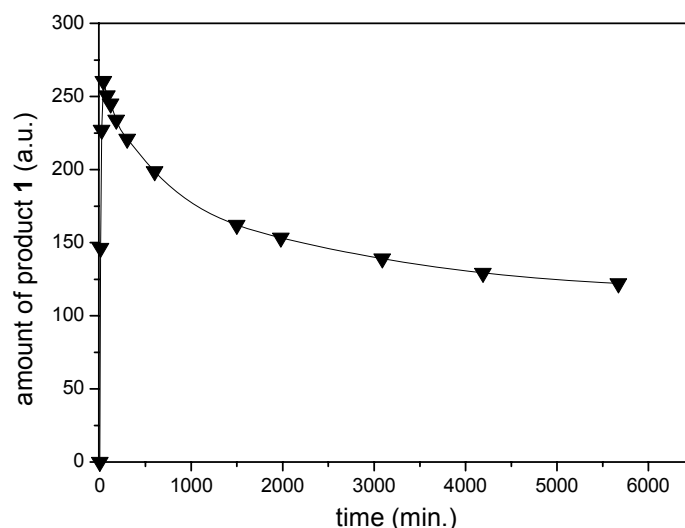


**Figure 3.5** Product **1** content of the reaction mixture versus time (Scheme 3.3).



To investigate this phenomenon, samples of the reaction mixture were analyzed by  $^{13}\text{C}$  NMR. Using  $^{13}\text{C}$  NMR, a clear distinction can be made between ring-opening product **1** and oligomeric species, by means of the intra-chain ester carbons and the benzylic carbons in the 62-72 ppm region, and by means of the aromatic carbon in the 134-136 ppm region (Figure 3.6).

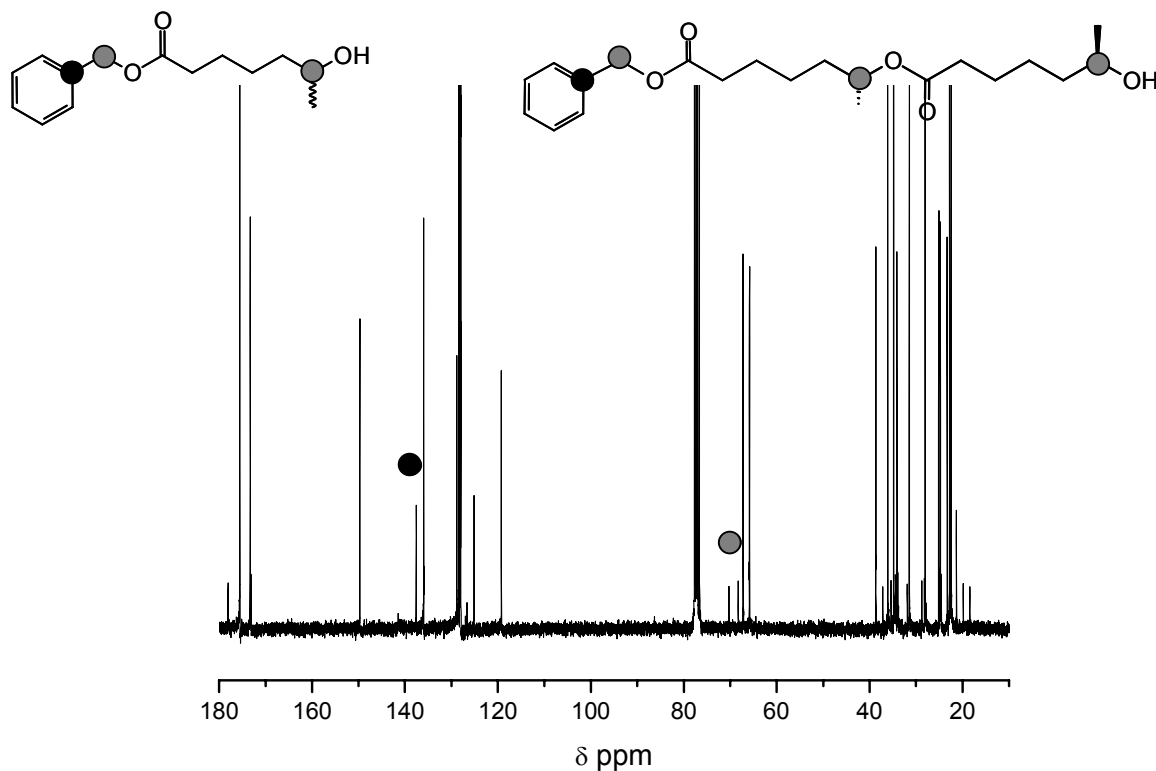


**Figure 3.6**  $^{13}\text{C}$  spectrum of crude reaction mixture with highlighted regions of interest.

In the 62-72 ppm region of the  $^{13}\text{C}$  spectrum (Figure 3.7a), the initial ring-opening by benzyl alcohol is clearly observed by the shift of the peak at 65 ppm to the peak at 66 ppm. At  $t=40$  minutes, a small peak at 71 ppm is observed with an integral area corresponding to 12% of the integral of the benzylic carbon, attributable to the carbons next to the oxygen of the in-chain esters. This value is in agreement with the expected initial formation of approximately 10% of oligomeric species, due to the E value of approximately 10 under these circumstances. After completion of the initial ring-opening reaction, the amount of oligomeric species continues to increase, with an integral area corresponding to 86% of that of the benzylic carbon at  $t=1500$  minutes, clearly indicating that oligomerization is taking place.

In the 134-136 ppm region (Figure 3.7b), the benzylic carbons of the ring-opening product and of the oligomeric species are clearly observed at 136.03 and 136.08 ppm, respectively. As expected, approximately 10% oligomeric species is observed after the initial ring-opening reaction at  $t=40$  minutes. Over time, this number increases to 48% oligomeric

species at  $t=1500$  minutes. These numbers can be correlated to the amount of ring-opening product that has reacted, as calculated from chiral GC. Using 10% oligomer at  $t=40$  as a calibration point, we see an almost linear relationship (Figure 3.8) showing that these numbers correspond with each other.

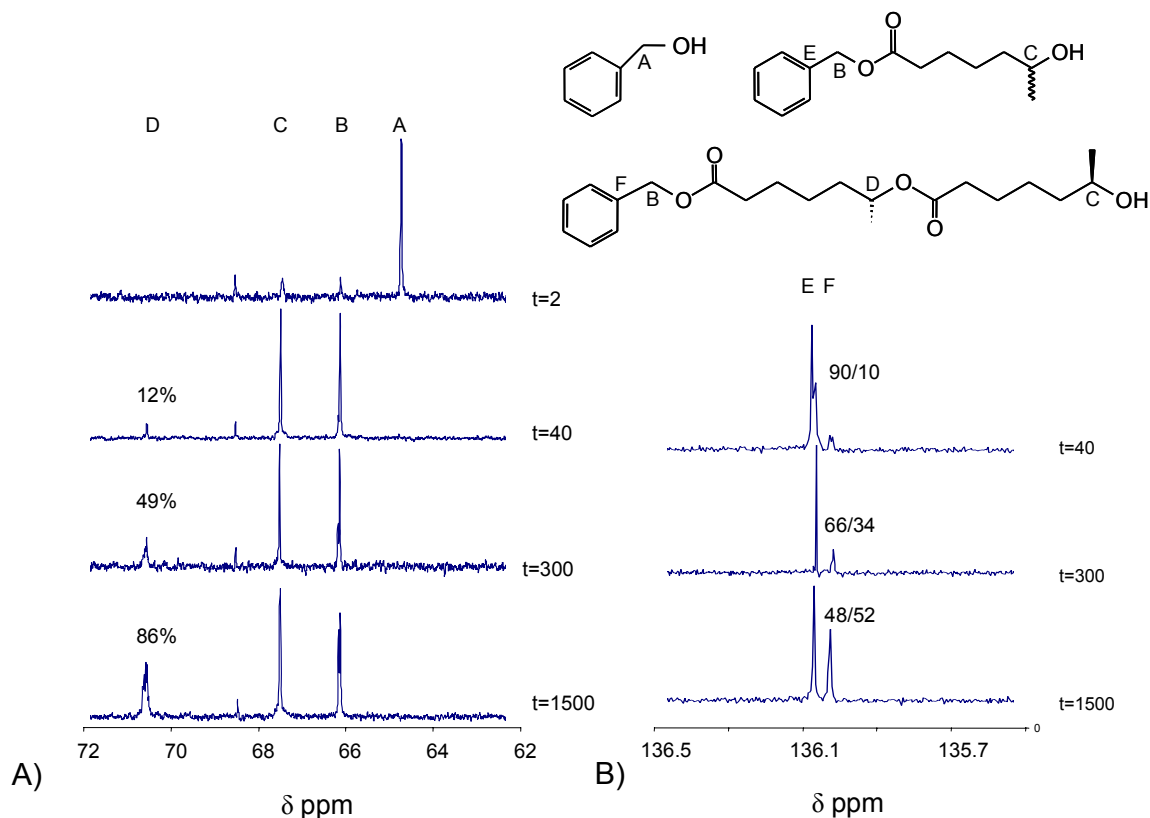


**Figure 3.7**  $^{13}\text{C}$  spectra of a) 62-72 ppm and b) 136 ppm region. The numbers in Figure 3.7b indicate the ratio of the integral areas.

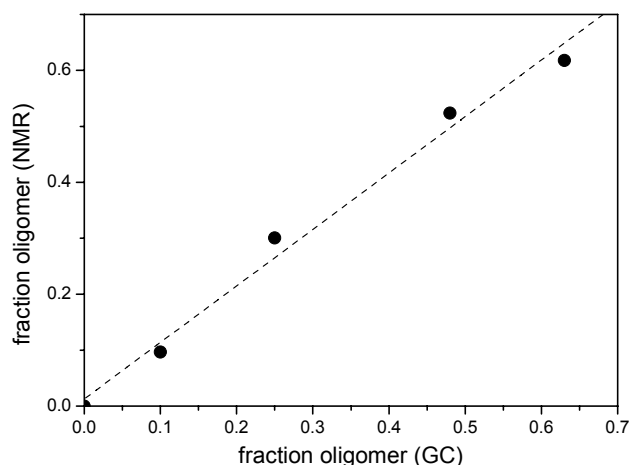


**Figure 3.8** Fraction oligomer calculated from GC data versus calculated from  $^{13}\text{C}$  NMR data. The dotted line indicates the theoretical  $y=x$  relationship.

Feringa *et al.* reported in 1985 on an easy procedure for determination of the ee of secondary alcohols by reaction with  $\text{PCl}_3$  and subsequent  $^{31}\text{P}$  NMR measurement.<sup>28</sup> To verify that the oligomers are indeed formed via the proposed insertion mechanism, we used this procedure for the sample from  $t=4190$  minutes. At this time, approximately 50% of the ring-opening product originally formed has oligomerized through reaction with (*R*)-6-MeCL. If normal propagation had taken place, half of the terminal *S*-alcohols would have reacted with (*R*)-6-MeCL and, as a result, racemic end-groups would be observed.<sup>29</sup> In contrast, insertion would leave the *S*-alcohol end-groups intact. Figure 3.9a shows that indeed a single peak is observed in  $^{31}\text{P}$  NMR at 5.4 ppm, indicating almost enantiopure *S*-endgroups, whereas in case of racemic end-groups also peaks would have been observed at 4.8 and 5.7 ppm in a 1:2:1 ratio (Figure 3.9b).

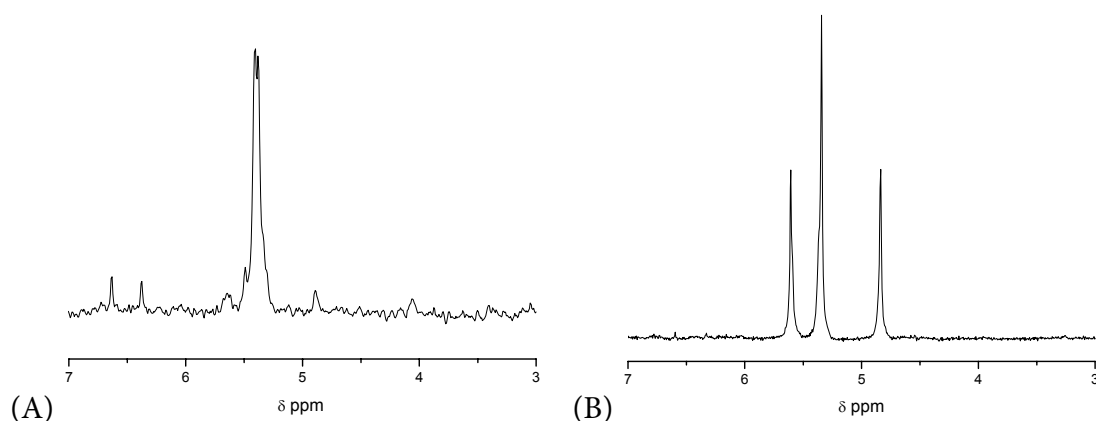


**Figure 3.9** a)  $^{31}\text{P}$  spectrum of the sample at  $t=4190$  minutes after reaction with  $\text{PCl}_3$  b)  $^{31}\text{P}$  spectrum of racemic **1** after reaction with  $\text{PCl}_3$ . Racemic **1** was obtained by ruthenium-catalyzed racemization of **1**, see Chapter 4.

### 3.2.3 Effect of solvent and temperature on the insertion of (*R*)-6-MeCL

In order to investigate the extent to which this side reaction plays a role under different circumstances, we studied the ring-opening of 6-MeCL using benzyl alcohol as the initiator ( $M/I = 4$ ) in different solvents and at different temperatures. The extent to which the side reaction takes place can be quantified from the logarithmic plot of the consumption of (*R*)-6-MeCL (Figure 3.10). Clearly, two regimes can be identified: regime I, where enzymatic ring-opening by benzyl alcohol and insertion take place, and regime II, where only the insertion of (*R*)-6-MeCL takes place. For both regimes a rate constant can be determined ( $k_{\text{RI}}$  and  $k_{\text{RII}}$ ), and the relative contribution of the side reaction can be calculated. Also, the rate constants for the ring-opening of (*S*)-6-MeCL ( $k_{\text{S}}$ ) were calculated for comparison and the  $E$ -values have been determined.<sup>30</sup> Results are shown in Table 3.1.

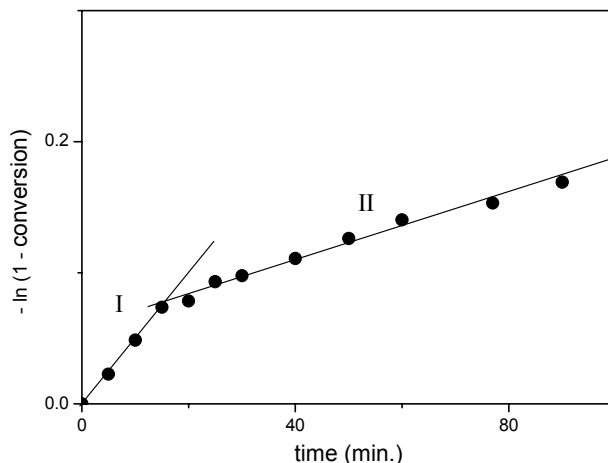


**Figure 3.10** Logarithmic plot of  $-\ln(1 - \text{conversion})$  versus time for the lipase catalyzed ring-opening of 6-MeCL by benzyl alcohol.  $M/I = 4$ , toluene,  $T = 60\text{ }^{\circ}\text{C}$ ,  $[M] = 3\text{ M}$ , 13 mmol Novozym 435 / mmol 6-MeCL.

Clearly, the solvent used and temperature do not have a significant influence on the extent to which the side reaction occurs. In all cases, the contribution of the side reaction to the total consumption of (*R*)-6-MeCL was between 12.6% and 26.8%. The use of chloroform as a solvent leads to significantly slower kinetics, while rates of reaction in diisopropyl ether, dichlorobenzene, trifluorobenzene and in bulk were comparable to those in toluene. The  $E$  values calculated are significantly lower than those calculated for the experiments with a fivefold excess of benzyl alcohol compared to the monomer (see Section 3.5). This can be explained by the occurrence of the side reaction.

**Table 3.1** Kinetic and enantioselectivity data at different temperatures and solvents.

T (°C)	solvent	E <sup>1</sup>	k <sub>S</sub> · 10 <sup>-4</sup> min <sup>-1</sup>	k <sub>R-I</sub> · 10 <sup>-4</sup> min <sup>-1</sup>	k <sub>R-II</sub> · 10 <sup>-4</sup> min <sup>-1</sup>	relative contribution (%)
2	toluene	38 +/- 4	1.9	n.d. <sup>2</sup>	n.d. <sup>2</sup>	n.d. <sup>2</sup>
22	toluene	25 +/- 2	10.5	0.44	0.08	18 %
45	toluene	12 +/- 1	26.0	1.95	0.46	24 %
63	toluene	7.5 +/- 0.2	41.9	4.87	0.82	17 %
80	toluene	6.2 +/- 0.2	56.1	8.10	1.54	19 %
100	toluene	4.9 +/- 0.2	63.9	12.32	1.55	13 %
22	chloroform	62 +/- 11	0.7	n.d. <sup>2</sup>	n.d. <sup>2</sup>	n.d. <sup>2</sup>
60	chloroform	12 +/- 1	11.6	0.88	0.24	27 %
60	diisopropyl ether	8.4 +/- 0.3	43.0	4.74	0.75	16 %
45	dichloro benzene	10 +/- 1	21.1	1.77	0.39	22 %
45	trifluoro- toluene	8.9 +/- 0.4	21.9	2.9	0.4	14 %
45	-	14 +/- 1	22.0	2.2	0.3	14 %

<sup>1</sup> Data fitted using Chen's relationship of  $ee_m$  and total monomer conversion

<sup>2</sup> n.d. = not determined

### 3.3 Enzymatic ring-opening of other cyclic esters

The stereospecificity pocket in the active site of CALB may accommodate a methyl- or an ethyl-substituent, but not a larger substituent.<sup>13</sup> Therefore, only methyl- or ethyl-secondary alcohols can react as nucleophiles in a CALB-catalyzed transesterification with reasonable rate of reaction; propyl-substituted secondary alcohols have been shown to show very little activity.<sup>1</sup> For 6-substituted  $\epsilon$ -caprolactones, the substituent determines the type of secondary alcohol that is formed after ring-opening. Therefore, it is expected that 6-methyl- $\epsilon$ -caprolactone and 6-ethyl- $\epsilon$ -caprolactone show similar behavior, while the enzymatic ring-opening of 6-propyl- $\epsilon$ -caprolactone (6-PrCL) and 6-butyl- $\epsilon$ -caprolactone (6-BuCL) shows very little oligomerization via the described insertion reaction, if any. If propagation of the secondary alcohol is possible, the conversion of the *S*-enantiomer of the lactone in experiments with M/I of 4 is expected to reach 50% conversion, since any dimeric product formed from the *R*-enantiomer will react further until the product has been end-capped with an *S*-secondary alcohol. Also, this would mean that the dimeric product content of the reaction mixture will decrease after long reaction times, due to the above-mentioned insertion mechanism. If propagation of the secondary alcohol is not possible, the combined conversion

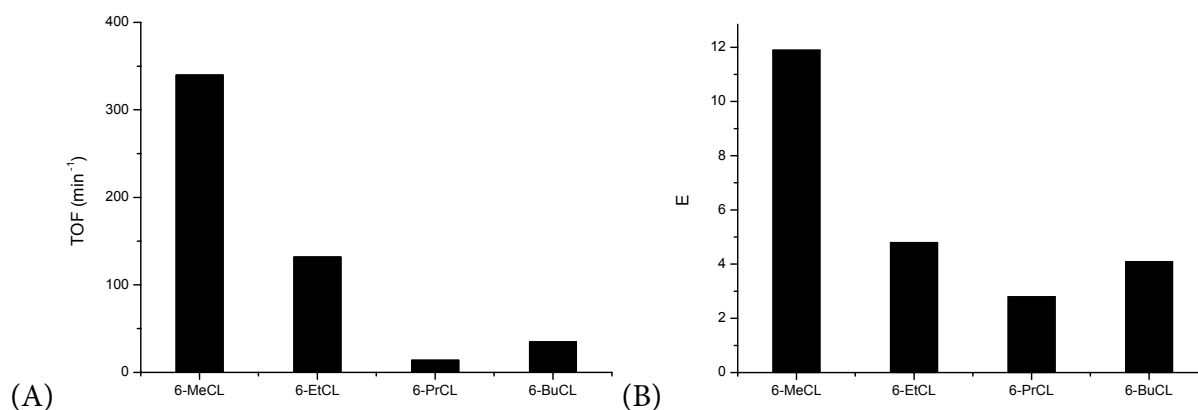
of the *R*- and *S*-enantiomer of the lactone will amount to 50%, and dimeric product content will not decrease on longer time scales.

**Table 3.2** Kinetic and enantioselectivity data for the enzymatic ring-opening of  $\omega$ -substituted  $\epsilon$ -caprolactones. BA/Lactone = 1:4;  $T=60$  °C; solvent = toluene; [lactone] = 3.4 M.

entry	substrate	TOF <sup>a</sup> min <sup>-1</sup>	E	Preferred enantiomer
1	6-MeCL	340	12 +/- 0.5	<i>S</i>
2	6-EtCL	132	4.8 +/- 0.1	<i>S</i>
3	6-PrCL	14.0	2.8 +/- 0.1	<i>S</i>
4	6-BuCL	35.0	4.1 +/- 0.3	<i>S</i>

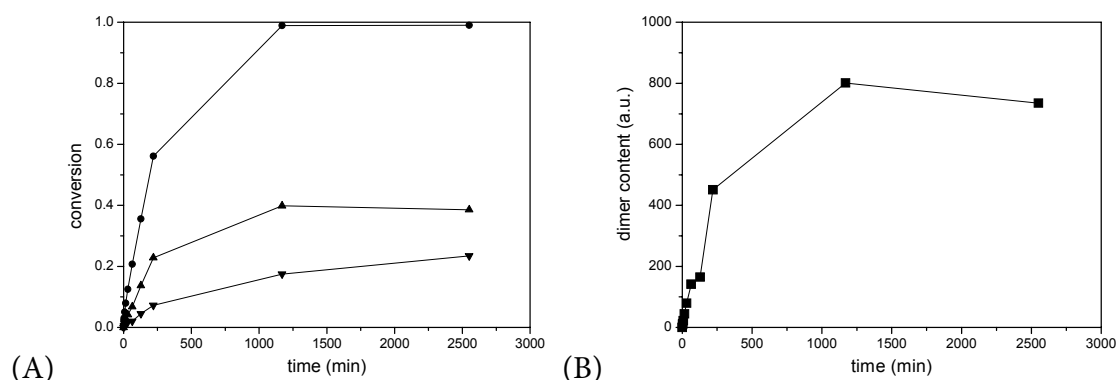
<sup>a</sup> Turn over frequency (TOF) is defined as the number of turnovers per enzyme molecule per second at the start of reaction; in order to calculate this number an active protein content of 10 wt.% of the immobilized preparation is assumed. The TOF is calculated using the formula  $TOF = k_i \cdot (\text{initial substrate concentration}) / (\text{total enzyme concentration})$ , in which  $k_i$  is the rate constant as determined by fitting a straight line to the relationship between  $-\ln(1 - \text{conversion of the lactone})$  and time.

Table 3.2 shows the kinetic and enantioselectivity data of the enzymatic ring-opening of 6-MeCL, 6-PrCL and 6-BuCL. For clarity, these data are visualized in Figure 3.11. Reactivity of 6-MeCL and 6-EtCL is in the same order of magnitude (entries 1 and 2), but drops sharply when the substituent goes from ethyl to propyl or butyl (entries 3 and 4). Only 6-MeCL shows appreciable enantioselectivity, while enantioselectivity for the lactones with ethyl to butyl substituent is significant, but low (2.8 to 4.8). Both the methyl- and ethyl-secondary alcohols are accepted as nucleophile by CALB (not shown), as evidenced by oligomer formation taking place (via the above-mentioned insertion mechanism).



**Figure 3.11** A) Rate of reaction for the different  $\omega$ -substituted  $\epsilon$ -caprolactones B) Enantiomeric ratio *E* for the different  $\omega$ -substituted  $\epsilon$ -caprolactones.

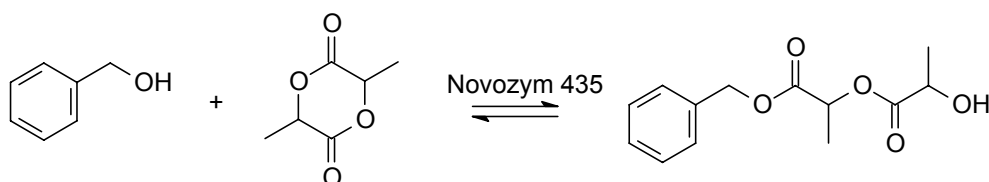
Figure 3.12a shows the time-conversion plot for the ring-opening of 6-PrCL. After all initiator has been consumed within 1200 minutes, the amount of dimeric ring-opening product of the reaction mixture only decreases slightly (Figure 3.12b). This is accompanied by a small increase in (*R*)-6-PrCL conversion, while (*S*)-6-PrCL conversion even goes down slightly (this can possibly be explained by a lower enantioselectivity under these circumstances (e.g. lower polarity of the reaction mixture)); thus, first the kinetic product is obtained, after which thermodynamics take over to form the thermodynamic product). The ring-opening of 6-BuCL showed no detectable oligomer formation (not shown).



**Figure 3.12** A) Time-conversion plot for the ring-opening of *rac*-6-PrCL by benzyl alcohol (benzyl alcohol : 6-PrCL = 1 : 4, toluene, 45 °C); BA (●); (*S*)-6-PrCL (▲); (*R*)-6-PrCL (▼). B) Dimeric product content (■) versus time.

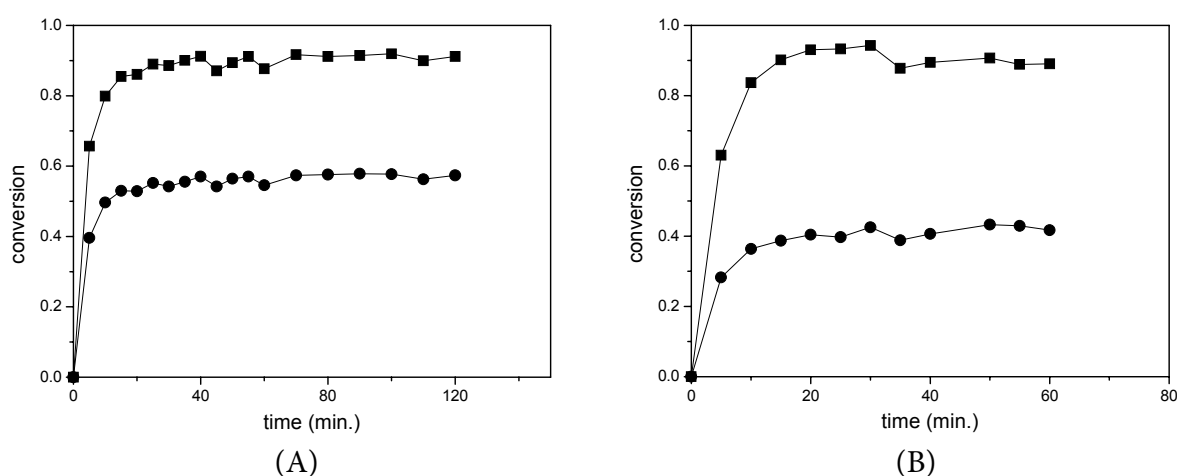
### 3.3.1 Enzymatic ring-opening of lactide

Lactide is the cyclic dimer produced by dehydration of lactic acid. Poly(L-lactide) is frequently used as a biocompatible and biodegradable polymer. However, enzymatic polymerization of lactide using CALB remains difficult if not impossible.<sup>31,32</sup> Only using porcine pancreas lipase or immobilized *Pseudomonas cepacia* species polymers were obtained, albeit at relatively high reaction temperatures and after long reaction times.<sup>33-35</sup> Since lactide resembles an  $\omega$ -substituted lactone – after ring-opening a secondary alcohol is obtained – it prompted us to investigate whether the configuration of the secondary alcohol arrests propagation, or which other factors may play a role.



**Scheme 3.5** Enzymatic ring-opening of lactide using benzyl alcohol as the nucleophile.

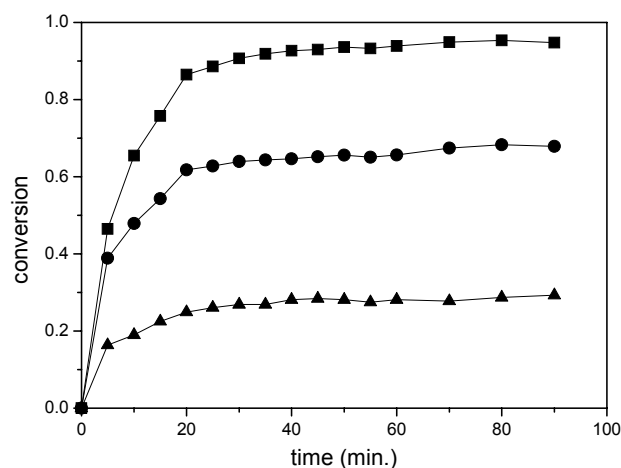
First, both D- and L-lactide were subjected to enzymatic ring-opening by benzyl alcohol using a slight excess of the alcohol (Scheme 3.5). Figure 3.13 shows that a quick reaction was observed, with calculated  $k_{\text{cat}}$  for D- and L-lactide of 1180 and 1300  $\text{min}^{-1}$ , respectively. These numbers are in the same order of magnitude as the ring-opening of  $\epsilon$ -caprolactone and 6-methyl- $\epsilon$ -caprolactone, showing that both D- and L-lactide are excellent substrates for CALB and that the enzymatic ring-opening of these lactide enantiomers proceeds smoothly at fast rates. Both D- and L-lactide, however, show no propagation on this timescale. Since the ring-opening of D- and L-lactide results in a ring-opening product with a secondary alcohol of opposite sign, the configuration of the secondary alcohol is not determining whether propagation takes place.



**Figure 3.13** Time-conversion plot for the enzymatic ring-opening of D-lactide (A) or L-lactide (B) (●) using benzyl alcohol (■) as the initiator. D-lactide / BA = 1.93; L-lactide / BA = 1.68; [BA] = 0.25 M; solvent = toluene;  $T = 45\text{ }^{\circ}\text{C}$ ; 30 mg Novozym 435 / mmol lactide.

Interestingly, when *rac*-lactide is used (a 1:1 mixture of the D- and L-enantiomer, not the *meso*-lactide), L-lactide is ring-opened significantly faster than D-lactide (Figure 3.14). This corresponds to a  $k_{\text{cat}}$  of L-lactide in this experiment that is >3 times greater than  $k_{\text{cat}}$  for D-lactide. Most likely, the  $K_{\text{M}}$ -values of both enantiomers are significantly different, leading to an uneven distribution of lactide enantiomers in the active sites of the enzyme; hence the difference in reaction rate.

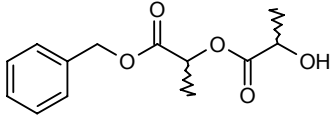
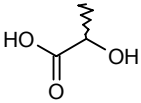
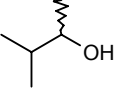
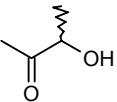




**Figure 3.14** Time-conversion plot for the enzymatic ring-opening of a 1:1 mixture of D-lactide (▲) or L-lactide (●) using benzyl alcohol (■) as the initiator. Lactide / BA = 1.94; [BA] = 0.25 M; solvent = toluene; T = 45 °C; 30 mg Novozym 435 / mmol lactide.

We then investigated whether steric hindrance or electronic effects were playing a role, by testing several nucleophiles in the enzymatic ring-opening of a good substrate. 6-Methyl- $\epsilon$ -caprolactone is a particularly good substrate, since it does not display propagation and, hence, no disturbing polymerization side reactions on short time scales are observed. Table 3.3 shows the different nucleophiles that were tested. We anticipated that the carbonyl group on the  $\beta$ -position to the alcohol could play a role, either by steric hindrance or by electronic effects. From literature it is known that lactic acid itself is a good acyl donor, but is unreactive as a nucleophile in CALB-catalyzed reactions.<sup>36</sup> 3-Methyl-2-butanol was selected as a nucleophile that is sterically hindered on the  $\beta$ -position, while 3-hydroxy-2-butanone has a carbonyl on the same position. To our surprise, both initiators were active as a nucleophile in the enzymatic ring-opening of 6-methyl- $\epsilon$ -caprolactone. As a result, the exact nature of the lack of nucleophilicity remains concealed.

**Table 3.3** Nucleophiles tested in the enzymatic ring-opening of 6-methyl- $\epsilon$ -caprolactone.

nucleophile		nucleophilic activity observed
BA-Lac		no
lactic acid		no <sup>1</sup>
3-methyl-2-butanol		yes
3-hydroxy-2-butanone		yes

<sup>1</sup> The inactivity of lactic acid as a nucleophile in CALB-catalyzed esterification was reported by From *et al.*<sup>36</sup>

### 3.4 Reversibility of enzymatic ring-opening: synthesis of both enantiomers of 6-MeCL

Enzymes are catalysts that lower the activation energy for a given reaction by providing an alternative pathway. The equilibrium composition of a reaction, however, is determined by thermodynamics and, hence, the presence of an enzyme does not change that. A catalyst only has an influence on the kinetics of a reaction, provided that the reaction is reversible. While we are mainly concerned with enzymatic ring-opening of lactones, the lipase-catalyzed synthesis of lactones via lactonization is also reported by several authors.<sup>37</sup> We observed that the enzymatic ring-opening of 6-MeCL by an equimolar amount of nucleophile is a reversible reaction that suffers from a rather unfavorable equilibrium. This is best demonstrated by the enzymatic ring-opening of (*S*)-6-MeCL by 1 equivalent of 4-*tert*-butylbenzyl alcohol (TBBA), which was synthesized as described below. Figure 3.15a shows that the conversion of TBBA only reaches 86%.<sup>38</sup> To ensure that indeed this behavior is caused by the equilibrium position, an extra 0.5 equivalent of (*S*)-6-MeCL was added at  $t=1500$  minutes. Clearly, the conversion of TBBA increased significantly to approximately 95%.

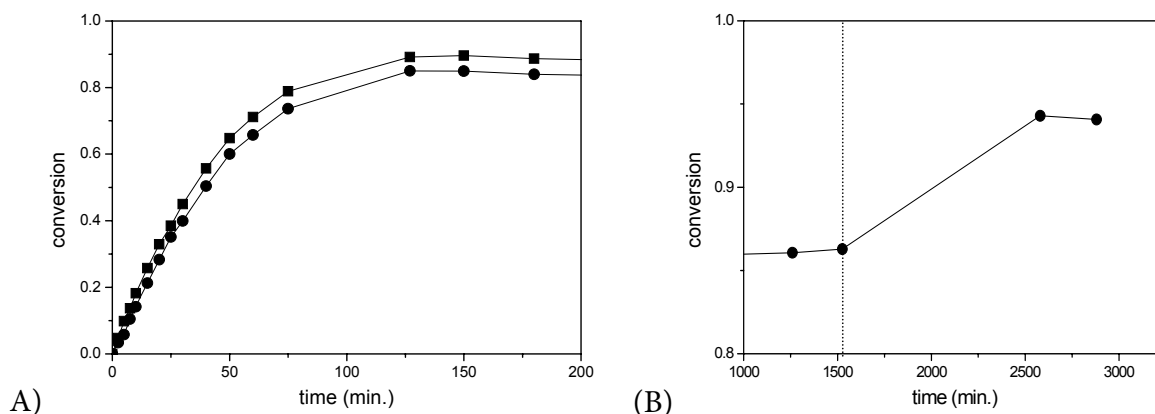
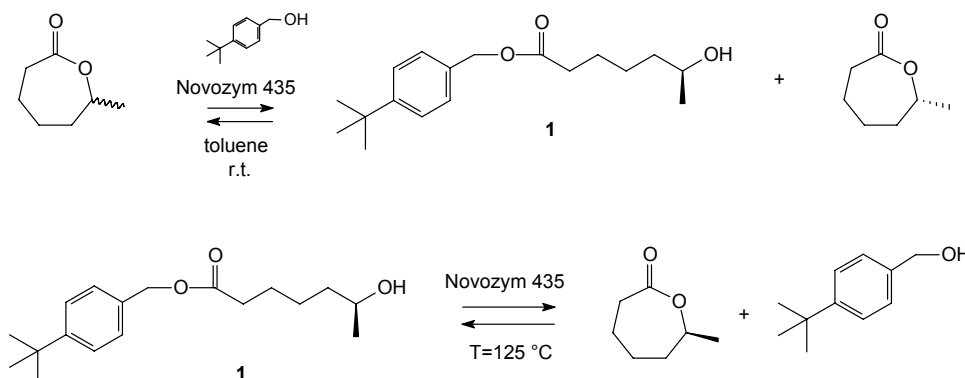


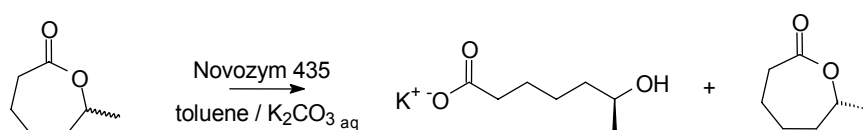
**Figure 3.15** Enzymatic ring-opening of (*S*)-6-MeCL (■) using tri-*tert*-butyl-benzyl alcohol (TBBA, ●) as the initiator; solvent = toluene;  $T = 60\text{ }^{\circ}\text{C}$ ; (*S*)-6-MeCL / TBBA = 1.05; 15 mg Novozym 435 / mmol (*S*)-6-MeCL. (B) At  $t=1500\text{ min.}$ , an extra 0.5 eq. of (*S*)-6-MeCL was added (dotted line), leading to a significant increase in TBBA conversion.

Since the equilibrium for the ring-opening of (*S*)-6-MeCL is rather unfavorable, we anticipated that it should be possible to isolate the ring-opening product and perform, quantitatively, an enzymatic ring-closure isolating the cyclic structures by distillation. Here, we report on a two step enzymatic synthesis of both enantiomers of 6-MeCL using 1) the well-established selectivity of Novozym 435 to ring-open the *S*-enantiomer and isolate the unreacted *R*-lactone and 2) enzymatic ring-closure of the resulting ring-opening product yielding the *S*-lactone. Previous research showed that (*R*)-6-MeCL can be easily obtained through kinetic resolution of 6-MeCL using lipases, since it is the slower reacting enantiomer.<sup>39-41</sup> However, to date the only way to procure (*S*)-6-MeCL is through an elaborate, multi-step procedure or by an enantioselective Bayer-Villiger oxidation using cyclohexanone monooxygenases.<sup>42,43</sup> Although the latter method affords (*S*)-6-MeCL in high enantiomeric excess ( $E > 200$ ), such biochemical oxidations require the use of whole cells of engineered *E. coli* strains which are not readily available in every chemical laboratory.



**Scheme 3.5** Enzymatic ring-opening and ring-closure of 6-MeCL.

Previous research showed that the kinetic resolution of 6-MeCL by butanolysis using Novozym 435 shows *S*-selectivity, although with low enantioselectivity (E values of 3 to 7 were reported).<sup>21</sup> We adapted this procedure and performed enzymatic ring-opening of 6-MeCL in toluene at room temperature. 4-*tert*-Butylbenzyl alcohol (TBBA) was selected as the nucleophile, providing ring-opening product **1** which has a sufficiently high boiling point for convenient removal of the remaining (*R*)-6-MeCL by distillation (Scheme 3.5). By addition of 1,2,3,4-tetramethylbenzene as an internal standard to the reaction mixture the reaction kinetics could be easily monitored by chiral GC. By fitting the enantiomeric excess (ee) of (*R*)-6-MeCL as a function of 6-MeCL conversion according to the method of Chen *et al.*, an enantiomeric ratio (E ratio) of 11 was determined.<sup>20</sup>



**Scheme 3.6** Enzymatic hydrolysis of remaining (*S*)-6-MeCL in the isolated fraction (*R*)-6-MeCL.

Using this approach, **1** was isolated with an ee of 62% (yield 94%).<sup>44</sup> Distillation and subsequent work-up of the remaining lactone afforded (*R*)-6-MeCL with an ee of 84% in a yield of 77% (see Table 3.3, entry 1). The optical purity of (*R*)-6-MeCL was further increased by enzymatic hydrolysis, which also occurs with preference for the *S*-enantiomer (Scheme 3.6).<sup>40</sup> The reaction was carried out in a toluene/water biphasic system at room temperature. Addition of  $K_2CO_3$  to the aqueous phase ensured that the hydroxyacid product **2** is extracted from the organic phase, shifting the equilibrium completely to the product side. The reaction was monitored by chiral GC, and, after complete hydrolysis of (*S*)-6-MeCL, (*R*)-6-MeCL was isolated from the organic phase with an ee of 99% in an overall yield of 50% (see Table 3.3, entry 2).

**Table 3.3** Results of the enzymatic ring opening and closing of 6-MeCL

entry	compound	$[\alpha]_D^a$	$[\alpha]_D^b$	ee (%)	yield (%) <sup>c</sup>
1	( <i>R</i> )-6MeCL	n/d <sup>d</sup>	n/d <sup>d</sup>	84.2	77
2	( <i>R</i> )-6MeCL	+24.8	+26.4	98.8	50 <sup>e</sup>
3	( <i>S</i> )-6MeCL	n/d <sup>d</sup>	n/d <sup>d</sup>	95.2	59
4	( <i>S</i> )-6MeCL	-25.9	-26.2	99.6	25 <sup>e</sup>

<sup>a</sup>  $c = 13$  g/100 mL in  $CHCl_3$ ; <sup>b</sup> Value corrected for chemical purity (see Experimental section) <sup>c</sup> Yield = 100% at 50% conversion; <sup>d</sup> Not determined; <sup>e</sup> Overall yield

Since enzymatic reactions are equilibria, **1** can be subjected to enzymatic ring-closure, yielding optically enriched 6-MeCL and the starting alcohol TBBA (Scheme 3.5). By distilling off 6-MeCL and TBBA, the equilibrium is shifted completely to the lactone side. Since the sense of chirality for both the forward reaction as well as the reverse reaction is by definition

the same, enzymatic ring-closure will also occur with enantioselectivity for the *S*-enantiomer of 6-MeCL.<sup>20</sup> Using this procedure, enzymatic ring-closure distillation was performed under reduced pressure (0.05 mm Hg) and at 125 °C. The absence of non-enzymatic ring-closure was confirmed in a blank reaction. After column chromatography to remove TBBA, (*S*)-6-MeCL was isolated with an ee of 95% and a yield of 59% (see Table 3.3, entry 3). This ring-closure demonstrates that, as expected, the reverse reaction is *S*-selective, as the ee increased from 62% in **1** to 95% in (*S*)-6-MeCL. The remaining (*R*)-6-MeCL was recovered as oligomeric species in the residual fraction after distillation. After removal of trace water by storage on molar sieves, (*S*)-6-MeCL crystallized as transparent needles (melting point 31 °C). Figure 3.16 shows the crystal structure as determined by means of X-ray crystallography.

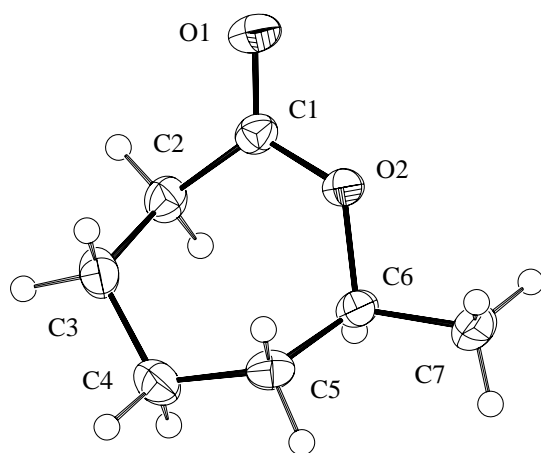


**Figure 3.16** Displacement ellipsoid plot of (*S*)-6-MeCL at 50% probability level.  $C_7H_{12}O_2$ ,  $M_r = 128.17$ , monoclinic, space group  $P2_1$  (no. 4) with  $a = 6.757(2)$ ,  $b = 7.577(2)$ ,  $c = 7.586(2)$  Å,  $\beta = 110.949(13)^\circ$ ,  $V = 362.71(17)$  Å<sup>3</sup>,  $Z = 2$ , 891 independent reflections,  $T = 150$  K, Mo  $K\alpha$  radiation,  $\lambda = 0.71073$  Å, H atom positions refined,  $wR2 = 0.0692$ ,  $R1 = 0.0260$  (for  $863 I > 2\sigma(I)$ ),  $S = 1.084$ .

To further increase the optical purity, (*S*)-6-MeCL with an ee of 95% was subjected to a second cycle of enzymatic ring-opening and ring-closure. This yielded nearly optically pure (*S*)-6-MeCL with an ee of 99.6% in an overall yield after two cycles of 25% (Table 3.3, entry 4). Characterization of the enantiomers by optical rotation showed that  $[\alpha]_D$  of (*S*)-6-MeCL was found to be  $-25.9^\circ$  (entry 4) and  $[\alpha]_D$  of (*R*)-6-MeCL to be  $+24.8^\circ$ , in accordance with previously reported literature value of  $-25.1^\circ$  and  $+25.0^\circ$ , respectively.<sup>43</sup>

### 3.5 Thermodynamic analysis of the ring-opening of 6-MeCL

The Gibbs free energy ( $G$ ) describes the balance between the enthalpy and entropy in a system. Every system seeks to achieve a minimal free energy, hence for every spontaneously proceeding reaction it holds that the change in the Gibbs free energy is negative. The Gibbs free energy consists of an enthalpy part and an entropy part, and can be described as depicted in Equation 1a. Since the entropy term of the Gibbs free energy is dependent on temperature while the enthalpic part is not, kinetic analysis of a given system at different temperatures can reveal information about the contribution of enthalpy and entropy to the chemical reaction under consideration. At constant temperature, the change in Gibbs free energy is described in Equation 1b.

$$(1a) \quad G = H - TS$$

$$(1b) \quad \Delta G = \Delta H - T\Delta S$$

A chemical reaction with a large negative value of  $\Delta G$  does not necessarily proceed at a high rate. The rate at which a reaction proceeds is dependent on the energy barrier that the system has to overcome. A low energy barrier means a fast reaction, and vice versa. This is schematically depicted in Figure 3.17. The  $\Delta G^\ddagger$  in this diagram represents the activation energy of the reaction. The activation energy of a specific reaction can be related to the rate constant  $k$  by means of Eyring's transition state theory<sup>45</sup>:

$$(2) \quad k = \kappa \frac{k_b T}{h} e^{\left(\frac{-\Delta G^\ddagger}{RT}\right)}$$

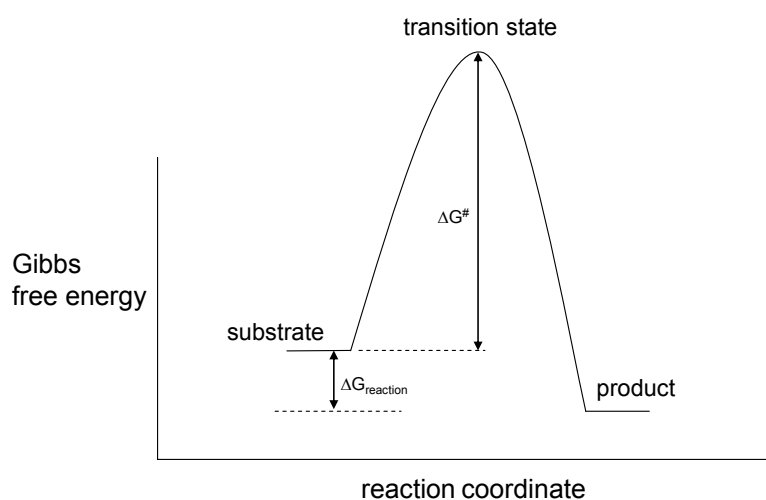


**Figure 3.17** Schematic diagram of the Gibbs free energy profile of a reaction.

Like all catalysts, enzymes work by providing an alternate pathway of lower activation energy of a reaction, thus allowing the reaction to proceed much faster than in an uncatalyzed fashion. A simple example is an irreversible single-substrate single-product reaction as shown in Equation 3 (the classic Michaelis-Menten situation):

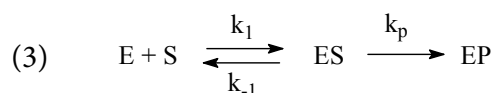
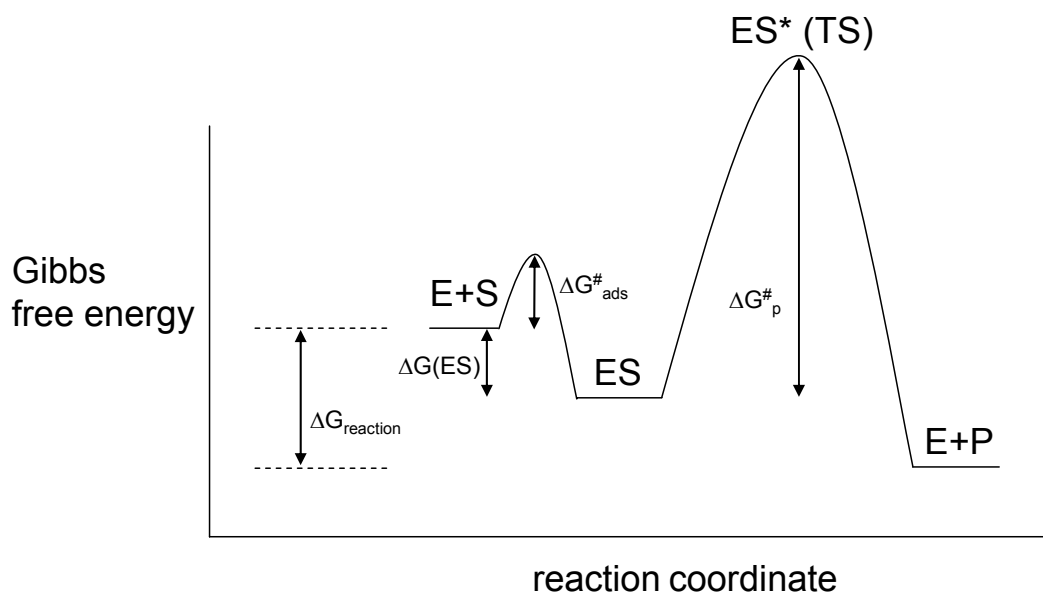


Figure 3.18 shows a simplified energy diagram for this enzyme-catalyzed reaction. The first step consists of binding the substrate S in the active site, forming the enzyme-substrate complex ES. The activation energy barrier  $\Delta G_{\text{ads}}^{\#}$  can be related to this step. To form the product P, the system has to cross the activation energy barrier via the transition state  $ES^*$ . The energy  $\Delta G(ES)$  determines the strength of the enzyme-substrate bond and is therefore related to the Michaelis constant  $K_M$ . For reaction to take place, the energy barrier  $\Delta G_p^{\#}$  has to be crossed;  $\Delta G_p^{\#}$  can be related to the catalytic constant  $k_p$ .



**Figure 3.18** Schematic diagram of the Gibbs free energy profile of an enzyme-catalyzed single-substrate single-product reaction.

### 3.5.1 Thermodynamics of enantioselectivity

Enzymes are chiral entities. Therefore in many reactions involving chiral substrates, one enantiomer reacts faster than the other, or, in other words, the enzymatic reaction is enantioselective. The origin of this enantioselectivity lies in the fact that the energy barriers  $\Delta G_{\text{ads}}^{\#}$  and/or  $\Delta G_p^{\#}$  (Figure 3.18) for reaction of the preferred enantiomer are lower than the energy barrier for the non-preferred enantiomers due to diastereomeric and hence

energetically different interactions. As described earlier (see Chapter 1), the enantioselectivity of a given reaction can be described by means of the enantiomeric ratio  $E$  (Equation 4).  $E$  is defined as the ratio of the specificity constants  $k_{sp}$  of both enantiomers.<sup>20,46</sup> At equimolar concentrations, the ratio of the initial rates (assuming no product inhibition yet) equals  $E$ . The specificity constant  $k_{sp}$  is defined as  $V_{max} / K_M$  and is a pseudo-first order rate constant.  $V_{max}$  denotes the theoretical maximum rate at which the reaction can proceed (at infinite substrate concentration) and is defined as shown in Equation 5.

$$(4) \quad E = \frac{k_{sp}^R}{k_{sp}^S} = \frac{\left(\frac{V_{max}}{K_M}\right)_R}{\left(\frac{V_{max}}{K_M}\right)_S}$$

$$(5) \quad V_{max} = k_p [E_t]$$

As we saw above,  $k_p$  can be related to activation energy  $\Delta G_p^\ddagger$  of the reaction step  $ES \rightarrow E + P$  (Figure 3.18). By applying Eyring's relationship to  $k_p$  (Equation 6) we can express the enantiomeric ratio  $E$  in terms of  $\Delta G_p^\ddagger$  for both enantiomers (Equations 7). By taking the natural logarithm of both sides Equation 8 is obtained. Under the assumption that the discrimination between the enantiomers can be ascribed to differences in  $V_{max}$  rather than  $K_M$  ( $K_M^A \sim K_M^B$  and  $\ln(K_M^A / K_M^B) \sim 0$ ), Equation 9 is obtained.<sup>47-49</sup> It should be noted that in literature this latter assumption is not fully recognized. The derivation described by Overbeeke *et al.* relates the composite value  $\Delta G_{sp}^\ddagger$  to the specificity constant  $k_{sp}$ . As Overbeeke correctly notes,  $k_{sp}$  is a lumped pseudo-rate constant, since it consists of both  $k_p$ ,  $k_1$ ,  $k_{-1}$  and the total enzyme concentration  $[E_t]$  (Equation 11). The correctness of the use of Eyring's transition state theory to relate a lumped rate constant  $k_{sp}$  to a composite thermodynamic quantity like  $\Delta G_{sp}^\ddagger$  can therefore be considered arguable. Ultimately, this inconsistency is eliminated in the mathematical derivation, since the specificity constants of both enantiomers are divided as in Equation 4. The assumption made there that the Michaelis constants for both enantiomers are taken to be equal is however not mentioned explicitly.<sup>50</sup> Close analysis of Equation 8 shows that the influence of the  $K_M$ -values on  $E$  is significant if  $E \sim K_M^S / K_M^R$ . Therefore, at high  $E$  values this term is expected to be negligible.

$$(6) \quad k_{sp} = \frac{V_{max}}{K_M} = \frac{k_p [E_t]}{K_M} = \kappa \frac{k_b T}{h} e^{\frac{-\Delta G_p^\ddagger}{RT}} \cdot \frac{[E_t]}{K_M}$$



$$(7) \quad E = \frac{k_{sp}^R}{k_{sp}^S} = \frac{\kappa \frac{k_b T}{h} e^{-\frac{\Delta G_{p(R)}^\#}{RT}} \cdot \frac{[E_t]}{K_M^R}}{\kappa \frac{k_b T}{h} e^{-\frac{\Delta G_{p(S)}^\#}{RT}} \cdot \frac{[E_t]}{K_M^S}} = e^{\frac{-\Delta G_{p(R)}^\#}{RT}} \cdot \frac{K_M^S}{K_M^R} = e^{\frac{-\Delta\Delta G_{p(R-S)}^\#}{RT}} \cdot \frac{K_M^S}{K_M^R}$$

$$(8) \quad -RT \ln E = \Delta\Delta G_{p(R-S)}^\# - RT \ln \frac{K_M^S}{K_M^R}$$

$$(9) \quad -RT \ln E = \Delta\Delta G_{(R-S)}^\#$$

$$(10) \quad -RT \ln E = \Delta\Delta H_{(R-S)}^\# - T\Delta\Delta S_{(R-S)}^\#$$

$$(11) \quad k_{sp} = \frac{V_{\max}}{K_M} = \frac{k_p [E_t]}{K_M} = \frac{k_p k_1}{k_p + k_{-1}} [E_t]$$

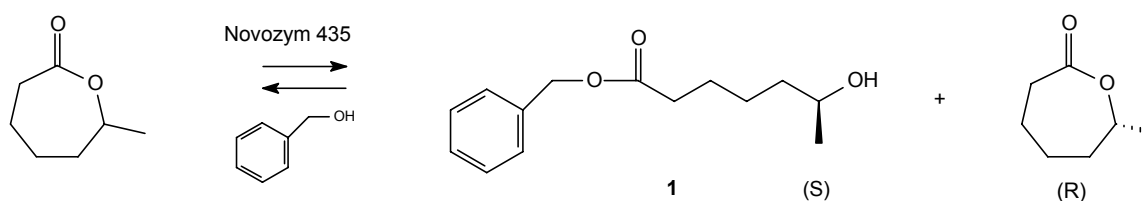
Under isothermal conditions, Equation 10 describes the enthalpy and entropy contribution to enantioselectivity,  $\Delta\Delta H_{(R-S)}^\#$  and  $\Delta\Delta S_{(R-S)}^\#$ . If the E values at different temperatures are available, one can easily determine these contributions, by plotting  $\ln E$  versus  $1/T$  and performing linear regression. The enthalpic activation energy difference between the enantiomers is easy to visualize as differences in steric hindrance during catalysis. The entropic activation energy differences, however, are more difficult to visualize. Some authors have tried to rationalize these as coming from differences in solvation of the activated complex in the transition state or from differences in freedom of certain enzyme residues between the enantiomer's transition states.<sup>51</sup>

Commonly, enantioselectivity goes down with increasing temperature. In these cases the stereochemistry of the reaction is dominated by enthalpy. If temperature is increased, the entropy contribution becomes more important, gradually decreasing enantioselectivity. This means that at some temperature, the contributions of enthalpy and entropy will become the same, resulting in similar rates of reaction of both enantiomers (and hence,  $E = 1$ ). This temperature is called the racemic temperature  $T_r$ .<sup>48,49</sup> Since there is no difference in the activation free energy for both enantiomers,  $\Delta\Delta G_{(R-S)}^\#$  must be zero, and the entropic and enthalpic contribution to enantioselectivity cancel each other out. Equation 12 can be derived to determine the racemic temperature. Above the racemic temperature, enantioselectivity is reversed and increases with increasing temperatures; in this regime the enantioselectivity is dominated by entropy. For most enzymes, the racemic temperature is well above normal operating temperature; a few exceptions have been reported, however.<sup>52-56</sup>

$$(12) \quad T_r = \frac{\Delta\Delta H_{(R-S)}^\#}{\Delta\Delta S_{(R-S)}^\#}$$

### 3.5.2 Thermodynamics of the enantioselectivity of CALB towards 6-MeCL

To investigate the underlying thermodynamical background of the enantioselectivity of immobilized CALB towards 6-methyl- $\epsilon$ -caprolactone (6-MeCL), the enzymatic ring-opening of 6-MeCL using benzyl alcohol (BA) as the initiator was carried out at five different temperatures (23, 40, 60, 80 and 100 °C, Scheme 3.7). To ensure that ring-opening is the predominant reaction, and that no significant insertion of (*R*)-6-MeCL is taking place (as described in paragraph 3.2), a fivefold excess of BA was used. A typical time-conversion plot is shown in Figure 3.19A. By fitting the data to Chen's relationship of  $ee_{\text{monomer}}$  and total monomer conversion, an E value could be determined.<sup>20</sup> For all temperatures, an excellent fit to the Chen relationship was obtained. An example of such a fit is shown in Figure 3.19B.



**Scheme 3.7** Enzymatic ring-opening of 6-MeCL using BA as the initiator.

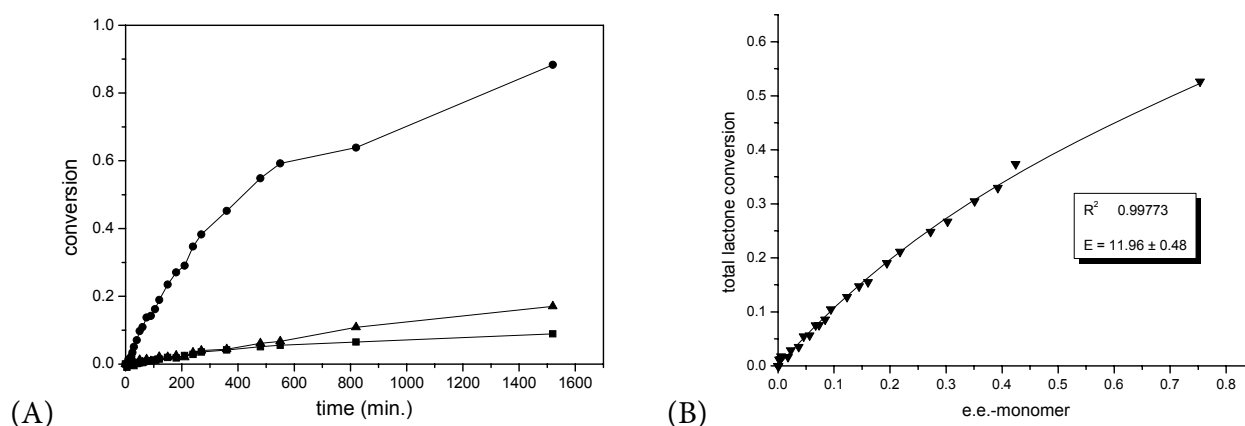


**Figure 3.19** A) Enzymatic ring-opening by Novozym 435 of (*S*)-6-MeCL (●) and (*R*)-6-MeCL (▲) using BA (■) as the initiator.  $T = 60$  °C, BA : 6-MeCL = 5 : 1, toluene, 6-MeCL = 0.75 M. B) Total lactone conversion versus  $ee_{\text{monomer}}$ , fitted using Chen's relationship.

Table 3.4 shows the E-values and rate constants for the experiments at the different temperatures. For reasons of clarity, the results are depicted graphically in Figure 3.20. At room temperature an E-value of 37 is found, and the E-value decreases with temperature, as expected. At 100 °C an E-value of only 5.2 is found. The rate of reaction increases greatly from room temperature ( $k_i = 1.9 \times 10^{-4}$ ) to 80 °C ( $k_i = 8.1 \times 10^{-4}$ ), and decreases again when temperature is increased to 100 °C. Apparently, some deactivation of the enzyme has taken place at this temperature. In our experience, reactions run with Novozym 435 at temperatures

above 80 °C give varying rates of reaction, indicating that 80 °C is approximately the upper limit for reproducible experiments. This does not mean that reactions at higher temperatures cannot be performed; we have succeeded repeatedly in Novozym 435-catalyzed ring-closure at 125 °C (see paragraph 3.4). Apparently, it is difficult to reproduce the exact circumstances at these temperatures; a slight deviation to a higher temperature or a slightly lower or higher water content of the enzyme might make a large difference in activity under these conditions.

**Table 3.4** Calculated *E* values and rate constants for the enzymatic ring-opening of 6-MeCL at different temperatures

T (°C)	<i>E</i>	$k_i$ ( $\times 10^{-4}$ )
23	37 +/- 4	1.9
40	22 +/- 1	6.2
60	12 +/- 1	7.5
80	8.1 +/- 0.2	8.1
100	5.2 +/- 0.2	6.5 *

\* The reaction rate of this reaction could not reproducibly be determined.

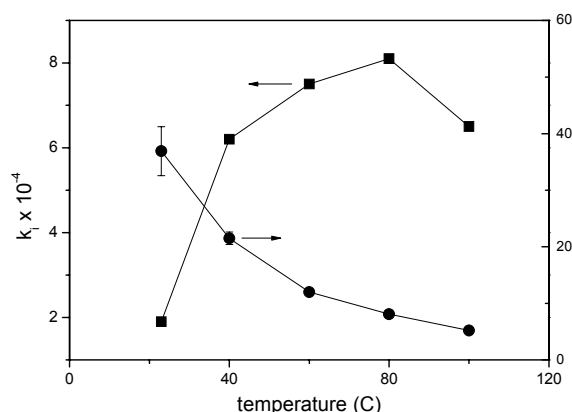


**Figure 3.20** Rate constants and *E*-values for the enzymatic ring-opening of 6-MeCL at different temperatures.

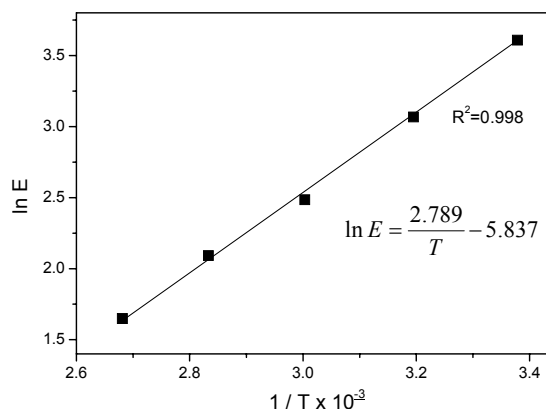


**Figure 3.21** Natural logarithm of the *E*-value versus reciprocal temperature.

According to Equation 10, a linear relationship must exist between the natural logarithm of the *E*-value and the reciprocal temperature. Figure 3.21 shows that this behavior is indeed observed. From the slope and intercept that follow from linear regression the enthalpic and entropic contribution to enantioselectivity can be calculated;  $\Delta\Delta S^\#_{(S-R)}$  was calculated to be 48.5 J/mol.K and  $\Delta\Delta H^\#_{(S-R)}$  was found to be -23.1 kJ/mol. At temperatures in the 20-100 °C range, this means that the entropic contribution to enantioselectivity is of the same order of magnitude as the enthalpic contribution; for example at 45 °C the enthalpic and

entropic contributions are -23.1 kJ/mol and 15.4 kJ/mol, respectively. These results suggest that contribution of entropy to enantioselectivity is relatively large for 6-MeCL compared to the reported values for secondary alcohols.<sup>3,57</sup> Using Equation 6, the racemic temperature was calculated to be 476 K, which is well above normal operating temperature for CALB.

### 3.6 Conclusions

The Novozym 435-catalyzed ring-opening of 6-methyl- $\epsilon$ -caprolactone (6-MeCL) results in a ring-opening product bearing a secondary alcohol. Because the enantioselectivity for 6-MeCL is moderately *S*-selective, polymerization is not possible by lipase only and results in only ring-opening product molecules with an *S*-secondary alcohol, which are not reactive as a nucleophile for propagation. Due to the reversibility of the ring-opening reaction, (*R*)-6-MeCL oligomers are formed on long time scales due to an insertion mechanism. This was proven by means of <sup>13</sup>C and <sup>31</sup>P NMR in combination with chiral GC measurements.

The equilibrium for the ring-opening of 6-MeCL was exploited for the synthesis of both enantiomers of 6-MeCL via an enzymatic ring-closure procedure. A straightforward, accessible procedure involving enzymatic ring-opening and ring-closure was developed to obtain (*S*)-6-MeCL with 95.2% ee in a yield of 59%, and after a second cycle of ring-opening / ring-closure with 99.6% ee in 25% yield. (*R*)-6-MeCL was obtained with 84.2% ee in 77% yield and, after hydrolysis of remaining *S*-enantiomer, with 99.6% ee in a yield of 25%. This convenient route provides access to both enantiomers without the need for biochemical oxidations which are not readily available in every laboratory.

The enzymatic ring-opening of 6-ethyl- $\epsilon$ -caprolactone, 6-propyl- $\epsilon$ -caprolactone and 6-butyl- $\epsilon$ -caprolactone was investigated. It was found that CALB shows *S*-selectivity for all substrates with *E* values of 3 to 4 at 60 °C. 6-Ethyl- $\epsilon$ -caprolactone shows considerable oligomer formation on long time scales, while 6-propyl- $\epsilon$ -caprolactone and 6-butyl- $\epsilon$ -caprolactone show very little and no oligomer formation, respectively.

The enzymatic ring-opening of *D*-lactide and *L*-lactide was investigated. It was shown that both lactides are excellent substrates for enzymatic ring-opening, but show no propagation in a polymerization experiment. It was shown that this is not due to the stereoconfiguration of the terminal secondary alcohol, in contrast to our findings for 6-MeCL.

The entropic and enthalpic contribution to enantioselectivity of the enzymatic ring-opening of 6-MeCL were determined by temperature dependent studies.  $\Delta\Delta S^\ddagger_{(S-R)}$  was found to be 48.5 J/mol.K and  $\Delta\Delta H^\ddagger_{(S-R)}$  was found to be -23.1 kJ/mol. The racemic temperature  $T_r$  was calculated to be 476 K.

### 3.7 Experimental section

#### *Materials*

6-Methyl- $\epsilon$ -caprolactone (6-MeCL) was synthesized by Baeyer-Villiger oxidation of 2-methylcyclohexanone following a reported procedure.<sup>58</sup> 2-Methylcyclohexanone was purchased from Fluka and used as received. Novozym 435 was obtained from Novozymes A/S. All other chemicals were purchased from Aldrich and used as received unless otherwise noted.

#### *Analytical methods*

<sup>1</sup>H NMR spectra were measured in CDCl<sub>3</sub> at 400 MHz using a Varian Mercury Vx 400 spectrometer. <sup>13</sup>C NMR spectra were measured in CDCl<sub>3</sub> at 100 MHz using a Varian Mercury Vx 400 spectrometer. For <sup>13</sup>C spectra, decoupling mode was set to “inverse gated decoupling” with a delay time (d1) of 30 s. The number of points measured (np) was set to 120000 and line broadening was set to zero to ensure maximum resolution in order to obtain baseline separation of the relevant peaks. <sup>31</sup>P NMR spectra were measured in CDCl<sub>3</sub> at 162 Mhz using a Varian Mercury Vx 400.

Chiral gas chromatography (GC) was performed on a Shimadzu 6C-17A GC equipped with an FID employing a Chrompack Chirasil-DEX CB (DF=0.12) column. Injection and detection temperatures were set at 300 and 325°C, respectively. Separations were done under using the following temperature program: column temperature isothermal at 125°C for 20 minutes; 25 °C per minute to 200 °C; isothermal at 200 °C for 25 minutes; 25 °C per minute to 225 °C. An internal standard method taking 1,3,5-tri-*t*-butylbenzene or 1,2,3,4-tetramethylbenzene as the internal standard was used to determine the lactone conversion and enantiomeric excess (*ee*<sub>m</sub>) of the unreacted monomer. The *ee*<sub>m</sub> was calculated as follows:  $ee_m = (R-S)/(R+S)$  where R and S represent the surfaces of the GC peaks of the *R*- and *S*-enantiomer, respectively. All samples were measured using a Shimadzu AOC-20i autosampler.

Optical rotations were measured on a Jasco DIP-370 digital polarimeter. TLC staining was performed with 1% *p*-methoxybenzaldehyde in a mixture of ethanol, acetic acid and H<sub>2</sub>SO<sub>4</sub> 90/5/5 v/v and subsequent heating with a heat gun.

#### *Typical procedure for the ring-opening of 6-MeCL by BA*

Benzyl alcohol (0.92 g; 8.5 mmol), 6-MeCL (4.4 g, 34 mmol), tri-*t*-butylbenzene (0.50 g, 2.0 mmol) and toluene (8.8 mL) were added to a 25 mL round-bottom flask. The mixture was stirred at 60 °C. Novozym 435 (0.36 g) was added, which represented the start of reaction. After 10, 20, 40, 80, 120, 180, 300, 600, 1500, 1980, 3090, 4190 and 5670 mins aliquots (~ 0.02 mL and ~0.1 mL) were withdrawn using a glass Pasteur pipette and diluted with dichloromethane and CDCl<sub>3</sub>, respectively. The enzyme was removed from the sample by filtration over cotton wool and the samples were analyzed by chiral GC and by <sup>13</sup>C NMR, respectively.

#### *End-group analysis by Feringa method<sup>28</sup>*

A 0.1 mL aliquot was removed from the reaction mixture using a syringe. 0.2 mL of 0.34 M PCl<sub>3</sub> in CDCl<sub>3</sub> was added and the mixture was diluted with 0.2 mL CDCl<sub>3</sub>. The mixture was stirred for 15 mins at room temperature, and directly analyzed by <sup>31</sup>P NMR.

*Typical procedure for the ring-opening of  $\omega$ -substituted  $\epsilon$ -caprolactones by BA*

Benzyl alcohol (210 mg; 1.93 mmol), 6-EtCL (1.1 g, 7.84 mmol), internal standard (50 mg; for 6-EtCL hexamethylbenzene was used, for the other lactones tri-*t*-butylbenzene was used) and toluene (1.20 mL) were added to a 5 mL screw-cap vial. The mixture was stirred at 45 °C in a carousel reactor. Novozym 435 (100 mg) was added, which represented the start of reaction. During the reaction aliquots (~ 0.02 mL) were withdrawn using a glass Pasteur pipette and diluted with dichloromethane. The enzyme was removed from the sample by filtration over cotton wool and the samples were analyzed by chiral GC.

*Typical procedure for the ring-opening of 6-methyl- $\epsilon$ -caprolactone by benzyl alcohol*

6-Methyl- $\epsilon$ -caprolactone (0.97 g, 7.6 mmol), benzyl alcohol (4.4 g, 41.1 mmol), tri-*t*-butylbenzene (0.43 g; 1.74 mmol) and 4.7 mL toluene were added to a 15 mL Schlenk tube. The mixture was prestirred for 5 minutes at the desired temperature. Novozym 435 (155 mg) was added, which indicated the start of reaction. After 0, 5, 10, 15, 20, 25, 30, 40, 50, 60, 75, 90, 105, 120, 150, 180, 210, 270, 360, 420, 480, 550, 820 and 1520 min aliquots (~ 0.02 mL) were withdrawn from the reaction mixture using a glass Pasteur pipette and diluted with dichloromethane. The enzyme was removed from the sample by filtration over cotton wool and the samples were analyzed by chiral GC.

*Synthesis of **1** and isolation of (*R*)-6-MeCL*

Novozym 435 (6.0 g) was added to a 10 mL sample vial. The vial was put overnight in a vacuum oven (10 mm Hg) at 50 °C in presence of P<sub>2</sub>O<sub>5</sub>. The oven was backfilled with nitrogen and the vial removed from the oven. 4-*tert*-Butylbenzyl alcohol (TBBA, 14.7 g; 89.6 mmol), 6-MeCL (20.2 g; 157.6 mmol), 1,2,3,4-tetramethylbenzene (0.5 g; 4.2 mmol) and toluene (25 mL) were added to a 100 mL round-bottom flask. The dried Novozym 435 was added to the flask, representing the start of reaction. The mixture was stirred at room temperature for 3 h. During reaction, samples (~ 0.02 mL) were withdrawn from the reaction mixture using a glass Pasteur pipette. The sample was diluted with dichloromethane and the enzyme was removed from the sample by filtration over cotton wool. The samples were analyzed by chiral GC for conversion of TBBA and both enantiomers of 6-MeCL. At 92% (*S*)-6-MeCL conversion, the enzymatic reaction was stopped by filtration using a class 3 glass filter. The residual enzyme was flushed 3 times with dichloromethane. The filtrate was concentrated and the remaining 6-MeCL and TBBA were removed by distillation using a Kugelrohr apparatus (115 °C, 0.05 mm Hg), yielding **1** (24.4 g; 94%). <sup>1</sup>H NMR of **1**:  $\delta$  (ppm) 7.3-7.4 (m, Ar-*H*), 5.1 (Ar-CH<sub>2</sub>-O), 3.8 (m, CH(CH<sub>3</sub>)OH), 2.4 (m, benzyl-CH<sub>2</sub>-OCOCH<sub>2</sub>), 1.70-1.35 (m, OCOCH<sub>2</sub>(CH<sub>2</sub>)<sub>3</sub>), 1.3 (Ar-C(CH<sub>3</sub>)<sub>3</sub>), 1.15 (d, CH<sub>3</sub>).

GC retention times: 1,2,3,4-tetramethylbenzene 4.6 min; (*S*)-6-MeCL 8.4 min; 2-methyl- $\epsilon$ -caprolactone 9.2 min; (*R*)-6-MeCL 9.4 min; TBBA 22.3 min; **1** 43.2 min

The mixture of TBBA, 1,2,3,4-tetramethylbenzene and (*R*)-6-MeCL was further purified by column chromatography over neutral aluminum oxide using dichloromethane / acetic acid 99/1 v/v as the eluent. Two fractions were obtained: fraction 1 ( $r_f = 0.7$ , (*R*)-6-MeCL, 7.75 g, ee 84.2%, chemical purity 94%, impurities are 2-methyl- $\epsilon$ -caprolactone (5%) and 1,2,3,4-tetramethylbenzene (1%)) and fraction 2 ( $r_f = 0.4$ , TBBA, 1.3 g).

### *Enzymatic ring-closure of 1*

Novozym 435 (2.0 g) was added to a 5 mL sample vial. The vial was put overnight in a vacuum oven (10 mm Hg) at 50 °C in presence of P<sub>2</sub>O<sub>5</sub>. The oven was backfilled with nitrogen and the vial removed from the oven.

**1** (24.4 g; 83.6 mmol) and the dried Novozym 435 were added to a Kugelrohr flask. The system was heated to 125 °C. The lactone and TBBA were distilled off under reduced pressure (0.05 mm Hg). The mixture of TBBA and (S)-6-MeCL was separated by column chromatography over neutral aluminum oxide using dichloromethane / acetic acid 99/1 v/v as the eluent. Two fractions were obtained: fraction 1 (*r<sub>f</sub>* = 0.7, (S)-6-MeCL) and fraction 2 (*r<sub>f</sub>* = 0.4, TBBA, 8.9 g). After removal of trace water by storage on 3 Å molecular sieves, 5.7 g (S)-6-MeCL (59%) was obtained as transparent needle crystals (ee 95.2%, chemical purity 99%, both determined by chiral GC).

### *Enzymatic hydrolysis of remaining (S)-6-MeCL in (R)-6-MeCL*

(R)-6-MeCL (6.6 g; 51.5 mmol) was dissolved in 6 ml toluene and transferred to a 50 ml round bottom flask. Novozym 435 (0.4 g) and 3 ml of a 1 M K<sub>2</sub>CO<sub>3</sub> solution in water were added to the mixture. The mixture was stirred vigorously at room temperature. During reaction, samples (~ 0.02 ml) were withdrawn from the reaction mixture using a glass Pasteur pipette. The sample was diluted with dichloromethane and the enzyme was removed from the sample by filtration over MgSO<sub>4</sub> on cotton wool. The samples were analyzed by chiral GC for conversion of both enantiomers of 6-MeCL. After all (S)-6-MeCL had been consumed, the enzymatic reaction was stopped by filtration using a class 3 glass filter. The residual enzyme was flushed 3 times with dichloromethane. All solvents were removed *in vacuo* and the crude product was dissolved in dichloromethane. The dissolved product was washed twice with water and once with brine. The organic layer was concentrated, yielding 4.3 g of (R)-6-MeCL (65%, ee 98.8%, chemical purity 94%, impurities are 2-methyl-ε-caprolactone (5%) and 1,2,3,4-tetramethylbenzene (1%)).

### *Enzymatic ring-opening and ring-closure of (S)-6-MeCL*

(S)-6-MeCL (4.46 g; 34.8 mmol, optical purity 95%) was subjected to enzymatic ring-opening by TBBA and subsequent enzymatic ring-closure analogous to the procedure described above, using 10.7 g TBBA (65.2 mmol) and 3.0 g Novozym 435 for the ring-opening and 2.0 g Novozym 435 for the ring-closure procedure. The mixture of TBBA and (S)-6-MeCL was separated by column chromatography over neutral aluminum oxide using dichloromethane / acetic acid 99/1 v/v as the eluent. 1.89 g (S)-6-MeCL was obtained with an optical purity of 99.6% and a chemical purity of 99% (both determined by chiral GC).

## **3.8 References**

1. Orrenius, C.; Haeffner, F.; Rotticci, D.; Ohrner, N.; Norin, T.; Hult, K. *Biocatal. Biotransform.* **1998**, 16, (1), 1-15.
2. Patel, R.N.; Banerjee, A.; Nanduri, V.; Goswami, A.; Comezoglu, F.T. *J. Am. Oil Chem. Soc.* **2000**, 77, (10), 1015-1019.
3. Ottosson, J.; Hult, K. *J. Mol. Catal. B: Enzym.* **2001**, 11, (4-6), 1025-1028.

4. Rotticci, D.; Haeffner, F.; Orrenius, C.; Norin, T.; Hult, K. *J. Mol. Catal. B: Enzym.* **1998**, 5, (1-4), 267-272.
5. Runmo, A.B.L.; Pàmies, O.; Faber, K.; Bäckvall, J.E. *Tetrahedron Lett.* **2002**, 43, (16), 2983-2986.
6. Ema, T.; Kageyama, M.; Korenaga, T.; Sakai, T. *Tetrahedron: Asymmetry* **2003**, 14, (24), 3943-3947.
7. Fransson, A.B.L.; Borén, L.; Pàmies, O.; Bäckvall, J.E. *J. Org. Chem.* **2005**, 70, (7), 2582-2587.
8. Kazlauskas, R.J.; Weissfloch, A.N.E.; Rappaport, A.T.; Cuccia, L.A. *J. Org. Chem.* **1991**, 56, (8), 2656-2665.
9. Naemura, K.; Fukuda, R.; Murata, M.; Konishi, M.; Hirose, K.; Tobe, Y. *Tetrahedron: Asymmetry* **1995**, 6, (9), 2385-2394.
10. Huerta, F.F.; Minidis, A.B.E.; Bäckvall, J.-E. *Chem. Soc. Rev.* **2001**, 30, (6), 321-331.
11. Pàmies, O.; Bäckvall, J.E. *Trends Biotechnol.* **2004**, 22, (3), 130-135.
12. Pellissier, H. *Tetrahedron* **2003**, 59, (42), 8291-8327.
13. Uppenberg, J.; Öhrner, N.; Norin, M.; Hult, K.; Kleywegt, G.J.; Patkar, S.; Waagen, V.; Anthonsen, T.; Jones, T.A. *Biochemistry* **1995**, 34, (51), 16838-16851.
14. Henke, E.; Schuster, S.; Yang, H.; Bornscheuer, U.T. *Monatsh. Chem.* **2000**, 131, (6), 633-638.
15. Yang, H.; Henke, E.; Bornscheuer, U.T. *Tetrahedron: Asymmetry* **1999**, 10, (5), 957-960.
16. Sobolev, A.; Franssen, M.C.R.; Poikans, J.; Duburs, G.; de Groot, A. *Tetrahedron: Asymmetry* **2002**, 13, (21), 2389-2397.
17. Larissegger-Schnell, B.; Glueck, S.M.; Kroutil, W.; Faber, K. *Tetrahedron* **2006**, 62, (12), 2912-2916.
18. van der Deen, H.; Cuiper, A.D.; Hof, R.P.; van Oeveren, A.; Feringa, B.L.; Kellogg, R.M. *J. Am. Chem. Soc.* **1996**, 118, (16), 3801-3803.
19. Cuiper, A.D.; Kouwijzer, M.; Grootenhuis, P.D.J.; Kellogg, R.M.; Feringa, B.L. *J. Org. Chem.* **1999**, 64, (26), 9529-9537.
20. Chen, C.S.; Fujimoto, Y.; Girdaukas, G.; Sih, C.J. *J. Am. Chem. Soc.* **1982**, 104, (25), 7294-9.
21. Kondaveti, L.; Al-Azemi, T.F.; Bisht, K.S. *Tetrahedron: Asymmetry* **2002**, 13, (2), 129-135.
22. Hedenström, E.; Nguyen, B.V.; Silks, L.A. *Tetrahedron: Asymmetry* **2002**, 13, (8), 835-844.
23. Kikuchi, H.; Uyama, H.; Kobayashi, S. *Macromolecules* **2000**, 33, (24), 8971-8975.
24. Al-Azemi, T.F.; Kondaveti, L.; Bisht, K.S. *Macromolecules* **2002**, 35, (9), 3380-3386.
25. The gas chromatogram published in this paper clearly shows that no baseline separation of the 4-methyl- $\epsilon$ -caprolactone and 4-ethyl- $\epsilon$ -caprolactone was achieved. This severely undermines the credibility of the reported optical purities of the remaining monomer and the reported optical purities of the polymer, which were calculated from these numbers. Also, the E values reported in these papers were not obtained by fitting of the data, but by single data point calculation. This severely reduces the accuracy of the reported values.
26. Peeters, J.; Palmans, A.R.A.; Veld, M.; Scheijen, F.; Heise, A.; Meijer, E.W. *Biomacromolecules* **2004**, 5, (5), 1862-1868.
27. van Buijtenen, J.; van As, B.A.C.; Palmans, A.R.A.; Vekemans, J.A.J.M.; Hilbers, P.A.J.; Roumen, L.; Pieterse, K.; Verbruggen, M.; Hulshof, L.A.; Meijer, E.W. *Manuscript in preparation*.
28. Feringa, B.L.; Smaardijk, A.; Wynberg, H. *J. Am. Chem. Soc.* **1985**, 107, (16), 4798-9.
29. If propagation had taken place, one would expect the formed *R*-secondary alcohol end-groups to be reactive nucleophiles. If these *R*-secondary alcohols would propagate, this would lead to an increased consumption of (*S*)-6-MeCL, which is not the case.
30. The enantiomeric ratio E has been determined based on the data from regime I



31. Wahlberg, J.; Persson, P.V.; Olsson, T.; Hedenström, E.; Iversen, T. *Biomacromolecules* **2003**, 4, (4), 1068-1071.
32. Kalra, B.; Kunioka, M.; Kumar, A.; Gross, R.A. *Abstr. Pap. - Am. Chem. Soc.* **2002**, 223, D7-D7.
33. Matsumura, S.; Tsukada, K.; Toshima, K. *Int. J. Biol. Macromol.* **1999**, 25, (1-3), 161-167.
34. Matsumura, S.; Mabuchi, K.; Toshima, K. *Macromol. Rapid Commun.* **1997**, 18, (6), 477-482.
35. Matsumura, S.; Mabuchi, K.; Toshima, K. *Macromol. Symp.* **1998**, 130, 285-304.
36. From, M.; Adlercreutz, P.; Mattiasson, B. *Biotechnol. Lett* **1997**, 19, (4), 315-317.
37. Theil, F. *Chem. Rev.* **1995**, 95, (6), 2203-2227.
38. Although the initiator and lactone were mixed in equimolar amounts, the conversion of (S)-6-MeCL reaches a slightly higher level due to some hydrolysis that has taken place, since undried Novozym 435 was used in this experiment.
39. Fellous, R.; Lizzanicuvelier, L.; Loiseau, M.A.; Sassy, E. *Tetrahedron: Asymmetry* **1994**, 5, (3), 343-346.
40. Shioji, K.; Matsuo, A.; Okuma, K.; Nakamura, K.; Ohno, A. *Tetrahedron Lett.* **2000**, 41, (45), 8799-8802.
41. Fouque, E.; Rousseau, G. *Synthesis* **1989**, (9), 661-666.
42. Kyte, B.G.; Rouviere, P.; Cheng, Q.; Stewart, J.D. *J. Org. Chem.* **2004**, 69, (1), 12-17.
43. Pirkle, W.H.; Adams, P.E. *J. Org. Chem.* **1979**, 44, (13), 2169-75.
44. The ee of the product was calculated based on conversions of both enantiomers of 6-MeCL. The maximum yield after work-up (on which the calculated yield is based) was calculated based on the conversion of both enantiomers of 6-MeCL.
45. Laidler, K.J.; King, M.C. *J. Phys. Chem.* **1983**, 87, (15), 2657-64.
46. *Biochem. J.* **1983**, 213, (3), 561-71.
47. Overbeeke, P.L.A.; Orrenius, S.C.; Jongejan, J.A.; Duine, J.A. *Chem. Phys. Lipids* **1998**, 93, (1-2), 81-93.
48. Phillips, R.S. *Trends Biotechnol.* **1996**, 14, (1), 13-16.
49. Phillips, R.S. *Enzyme Microb. Technol.* **1992**, 14, (5), 417-419.
50. Overbeeke *et al.* also derive an expression for E that shows that the enantioselectivity is governed by the energy differences of the energies of the transition states towards adsorption and reaction compared to the ground state energy of enzyme and substrate. If these energies of the transition states towards adsorption and reaction become comparable in magnitude, Equation 9 would not hold anymore. This corresponds to our conditions for the use of Equation 9, since in that situation  $k_p$  would be of comparable magnitude as  $k_{-1}$ .  $K_M$  then is truly a lumped constant that represents both adsorption and reaction of the substrate. If this is the case, then the  $K_M$  values for an enantioselective reaction will not be the same.
51. Ottosson, J.; Fransson, L.; King, J.W.; Hult, K. *Biochim. Biophys. Acta* **2002**, 1594, (2), 325-334.
52. Magnusson, A.O.; Takwa, M.; Harnberg, A.; Hult, K. *Angew. Chem., Int. Ed.* **2005**, 44, (29), 4582-4585.
53. Zheng, C.S.; Pham, V.T.; Phillips, R.S. *Catal. Today* **1994**, 22, (3), 607-620.
54. Pham, V.T.; Phillips, R.S. *J. Am. Chem. Soc.* **1990**, 112, (9), 3629-3632.
55. Yasufuku, Y.; Ueji, S. *Bioorg. Chem.* **1997**, 25, (2), 88-99.
56. Yasufuku, Y.; Ueji, S. *Biotechnol. Lett* **1995**, 17, (12), 1311-1316.
57. Ottosson, J.; Fransson, L.; Hult, K. *Protein Sci.* **2002**, 11, (6), 1462-1471.
58. Tietze, L.F.; Rackelmann, N. *Pure Appl. Chem.* **2004**, 76, (11), 1967-1983.

# 4

## Iterative Tandem Catalysis

### Abstract

Iterative tandem catalysis (ITC) is introduced as a novel polymerization technique for the synthesis of well-defined materials. In ITC, multiple catalysts are operating simultaneously in one pot and iterative action of each of the catalysts is required for chain growth. Proof of principle is provided by the synthesis of enantioenriched *R*-oligomers from (*S*)-6-methyl- $\epsilon$ -caprolactone (6-MeCL) in a two-pot system, employing *Candida antarctica* Lipase B as the transesterification catalyst and a Ru complex with *p*-cymene and (*rac*)-2-phenyl-2-amino-propionamide ligands as the racemization catalyst. Hydrogenation of 6-MeCL and dehydrogenation of the alcohol end-groups were identified as important side reactions that severely reduce the molecular weight.

Experiments in a one-pot system afford short oligomers only. This is caused by insufficient compatibility of the two catalysts. The presence of  $K_2CO_3$  as a heterogeneous base in the polymerization of highly polar, small lactones dramatically reduces the enzymatic activity, while the racemization activity is also severely impacted by the presence of these highly polar small lactones. Modification of the tandem catalytic system by using a different racemization catalyst ultimately enabled the one-pot ITC of 6-MeCL. These results are described in the thesis of Jeroen van Buijtenen.

Part of this chapter has been published: van As, B.A.C.; van Buijtenen, J.; Heise, A.; Broxterman, Q.B.; Verzijl, G.K.M.; Palmans, A.R.A.; Meijer, E.W. *J. Am. Chem. Soc.* **2005**, *127*, (28), 9964-9965.

## 4.1 Introduction

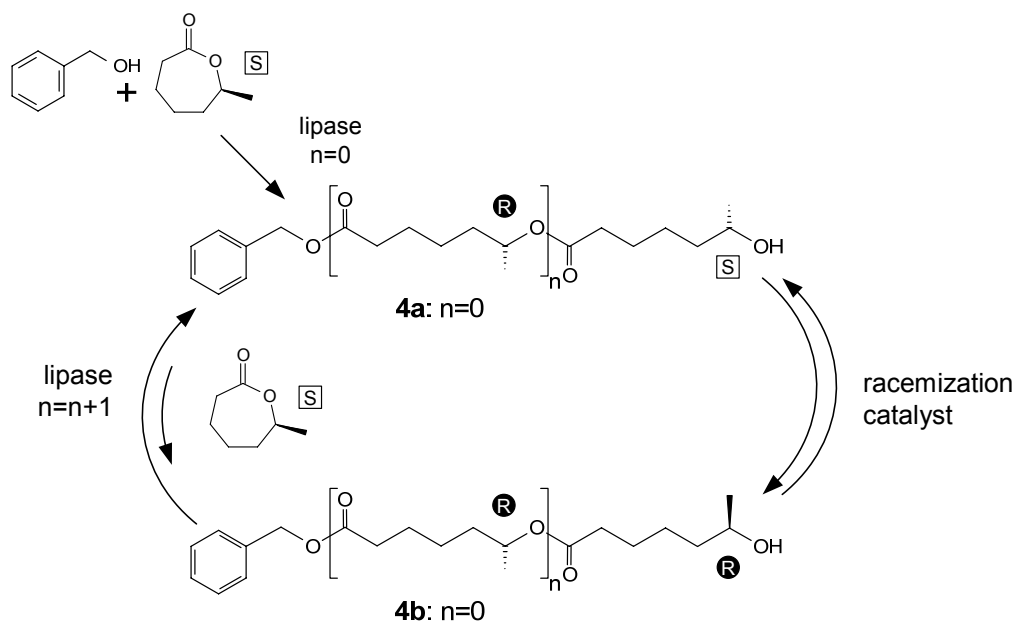
Tandem catalysis, being defined as a combination of catalytic reactions without intermediate product recovery, attracts increasing interest from academia and industry as an alternative to multi-step synthetic procedures.<sup>1,2</sup> Evidently, by carrying out multiple transformations in one pot, a substantial improvement in both the economics and the environmental acceptability of the process can be achieved. In concurrent tandem catalysis, multiple catalysts are operating simultaneously in a cooperative fashion. A prominent example is the dynamic kinetic resolution (DKR) of secondary alcohols.<sup>3-9</sup> In this process, a racemic alcohol is completely converted into the corresponding *R*-ester by coupling enzyme-catalyzed kinetic resolution to Ru-catalyzed racemization. The *S*-esters could be obtained when using *Subtilisin Carlsberg* instead of a lipase, and with the appropriate Ru catalyst, even chiral primary amines were selectively transformed into the corresponding *R*-amide via DKR.<sup>10-12</sup>

In contrast to its increasingly successful applications in the transformation of single molecules, tandem catalysis is still rarely employed in the field of polymer chemistry.<sup>1</sup> Examples include the synthesis of linear low-density polyethylene (LLDPE) via concurrent tandem catalysis.<sup>13-18</sup> Here, one catalyst oligomerizes ethylene to  $\alpha$ -olefins, while the second catalyst polymerizes these  $\alpha$ -olefins as well as the remaining ethylene. Furthermore, block copolymers were synthesized in one pot by combining ring-opening polymerization (ROP) with radical polymerization using an unsymmetrical bifunctional initiator.<sup>19-28</sup> Analogously, graft copolymers can be synthesized in a one-pot procedure by using a suitable monomer.<sup>29</sup>

In these polymerizations, however, the catalytic processes are not necessarily performed in one pot – if the two catalytic steps are carried out separately, a similar polymer would still result after two steps. In literature, few examples can be found where the catalytic processes involved in a polymerization are truly complementary and cannot be separated. Drent *et al.* described a copolymerization of ethylene and carbon monoxide where one palladium complex alternatively builds in both monomers via distinctively different catalytic mechanisms.<sup>30</sup> In addition, a concept called *chain shuttling polymerization* was recently introduced, where a growing chain is transferred repeatedly from one catalyst to another to achieve “multiblock” copolymer formation.<sup>31</sup>

Here, we introduce the concept of *iterative tandem catalysis* as a novel polymerization method.<sup>32</sup> We define iterative tandem catalysis (ITC) as a polymerization process in which chain growth is effectuated by a combination of two (or more) intrinsically different catalytic processes that are both compatible and complementary. This implies that the catalytic processes must operate concurrently for propagation to occur. The major advantage of such

ITC systems is that a higher degree of control over the chemical structure of the material can be achieved, since the cooperative action of two catalytic processes is exploited.



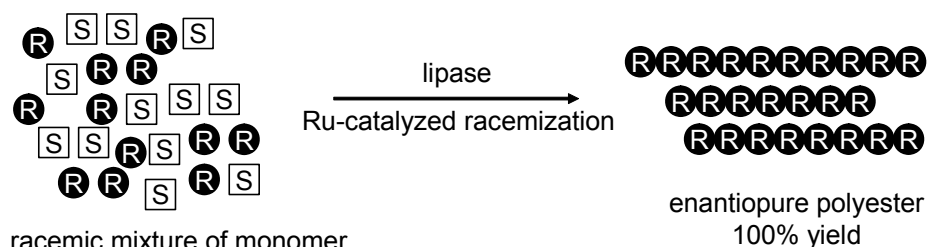
**Scheme 4.1** Synthesis of oligo-(*R*)-6-MeCL from (*S*)-6-MeCL by ITC.

This chapter focuses on the application of ITC for the synthesis of enantiopure polyesters from racemic  $\omega$ -substituted lactones. As a model system, the ITC of (*S*)-6-methyl- $\epsilon$ -caprolactone ((*S*)-6-MeCL) is selected (Scheme 4.1). We described in Chapter 3 that lipase-catalyzed ring-opening of 6-MeCL is *S*-selective, resulting in a molecule with an *S*-secondary alcohol (**4a** in Scheme 4.1,  $n=0$ ). Since lipases are highly enantioselective towards secondary alcohols (typically  $E > 100$ ), only *R*-secondary alcohols are accepted as the nucleophile. Therefore, **4a** is virtually unreactive and propagation cannot occur. To enable polymerization of (*S*)-6-MeCL, racemization of the *S*-alcohols that are formed upon ring-opening is required, which affords reactive *R*-chain ends (**4b** in Scheme 4.1). Racemisation can be achieved with a variety of homogeneous catalysts.

As a result of the complications that may arise from the concurrent use of 2 fundamentally different catalysts – a lipase and a metal-based racemization catalyst – this chapter deals with three major issues:

1. Selection of the catalysts: selectivity and complementarity.
2. Compatibility of the catalysts.
3. Proof of principle of ITC.

Theoretically, if a racemic mixture of monomer is used an enantiopure polyester can be obtained with full monomer conversion (Scheme 4.2). This will be addressed in detail in the Ph.D thesis of Jeroen van Buijtenen.<sup>33</sup>



**Scheme 4.2** Iterative tandem catalysis of 6-MeCL.

## 4.2 Selection of the catalysts: selectivity and complementarity

In the ITC of 6-MeCL, a transesterification catalyst and a racemization catalyst (to change the configuration of unreactive *S*-secondary alcohols) must act simultaneously. A number of requirements must be met by both catalysts:

1. They must be active in a nearly anhydrous environment, since water limits the molecular weight achievable.
2. The temperature window in which the catalysts operate must overlap.
3. The kinetics of both catalytic processes must be in the same order of magnitude under the required conditions.

Below a short description is given of the available transesterification and racemization catalysts (the available catalysts are discussed elaborately in Chapter 1). Based on this, a suitable catalytic system is selected for the ITC of (*S*)-6-MeCL.

### 4.2.1 The transesterification catalyst

Although many excellent organic and metal based catalysts are available to catalyze transesterification reactions, none rivals lipases in terms of enantioselectivity. High enantioselectivity is of paramount importance in ITC to prevent build-in of “wrong” configuration. Lipases are excellent enantioselective transesterification catalysts and many lipases have been reported to catalyze the ring-opening of lactones in organic solvents.<sup>34,35</sup> Moreover, they are the enzymes of choice to polymerize lactones by enzymatic ring-opening polymerization.

Not all lipases can be applied in ITC, however. Next to the required compatibility with the racemization catalyst, sufficiently high activity under anhydrous conditions is highly important. Water is a competitive nucleophile in the transesterification reaction (the hydrolysis of ester bonds is the natural role of a lipase). When lactones are used as the monomer, this results in the initiation of extra chains, reducing the molecular weight of the product.

Novozym 435 is one of the few lipase preparations that shows activity at very low water activities.<sup>22,23,36</sup> Novozym 435 is a preparation of *Candida antarctica* Lipase B (CALB) immobilized on an acrylic resin and is described in more detail in Chapter 1. It is widely used in ring-opening polymerization of lactones.<sup>37</sup> In a typical polymerization of  $\epsilon$ -caprolactone using this lipase, de Geus *et al.* were able to synthesize benzyl alcohol-initiated poly( $\epsilon$ -caprolactone) with no detectable carboxylic acid headgroups originating from competing water initiation.<sup>38,23</sup> Additionally, the thermal stability can be described as exceptional, with prolonged activity even at temperatures of 150 °C.<sup>39-41</sup> Typically, toluene is used as the reaction medium, but numerous publications exist describing the use and stability of this lipase in bulk, in ionic liquids, in supercritical CO<sub>2</sub> and in various conventional solvents including THF, chloroform and diethyl ether.<sup>42-44</sup> It is therefore not surprising that Novozym 435 is the most frequently used lipase in DKR.<sup>4</sup> Although not a lipase but a peptidase (EC 3.4.21), *Subtilisin Carlsberg* is sometimes employed in DKR, since it also displays transesterification activity.<sup>10,11</sup> Its activity, selectivity and stability are inferior to that of lipases – at 70 °C within 35 minutes all its activity is lost.<sup>11</sup> Its selectivity for *S*-secondary alcohols, however, in contrast to the *R*-selectivity that is commonly observed for lipases, renders it a very useful enzyme in DKR.

For the ITC of (*S*)-6-MeCL, Novozym 435 is by far the most suitable transesterification catalyst, since it fulfills the requirement for activity under anhydrous conditions, at high temperature, showing high activity and selectivity in organic solvent, and has an excellent track record in DKR.

#### 4.2.2 The racemization catalyst

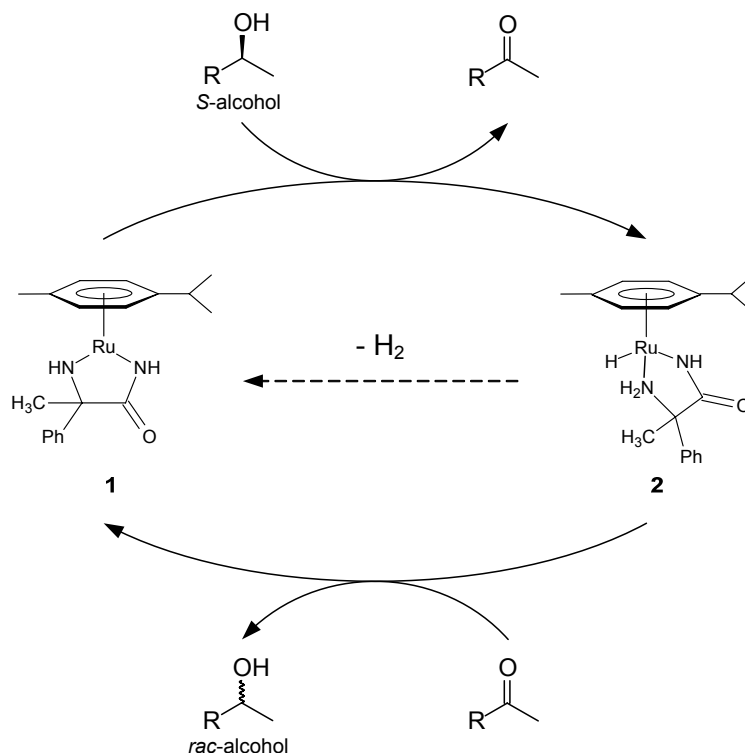
Many types of metal-based catalysts have been used for racemization purposes. In DKR, by far the most employed are ruthenium-based catalysts.<sup>3-9</sup> They have appeared as highly successful catalysts as a result of their compatibility with lipases. Chapter 1 gives an overview of Ru-based complexes typically used in DKR. For the ITC of (*S*)-6-MeCL we selected complex **1** (Scheme 4.3) as the most suitable because of its high activity and excellent results in the DKR of secondary alcohols, even on industrial scale, and easy accessibility (see Chapter 1 for synthesis and details). In a typical DKR experiment, a racemic secondary alcohol can be

completely converted into the corresponding *R*-butyrate (*ee* > 99%) within 24 h, employing only 0.1 mol% of catalyst **1** at 70 °C.<sup>45,46</sup>

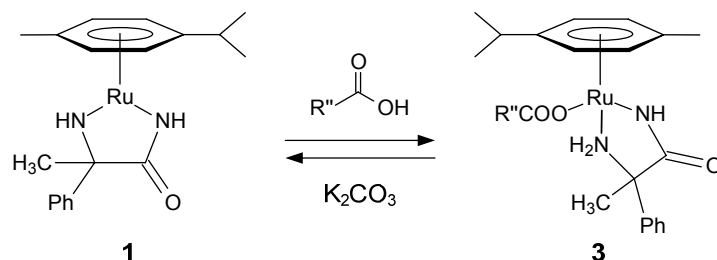
Regarding the compatibility with reaction conditions, the situation in ITC is considerably more complicated than in DKR. In ITC, there is a very low concentration of the alcohol available, which severely suppresses the reaction rate. Moreover, a well-known side reaction such as dehydrogenation has major implications in ITC. In a polymerization, non-reactive terminal ketone groups act as a chain-stoppers, reducing the molecular weight that can be achieved. Therefore, suppression of dehydrogenation is crucial. Scheme 4.3 shows that the mechanism of racemization by complex **1** proceeds via dehydrogenation of the *S*-secondary alcohol, resulting in the formation of the corresponding ketone and the hydride complex **2**. Conversely, hydrogenation of a ketone by complex **2** gives the corresponding alcohol with the overall transfer hydrogenation process resulting in racemization. Alternatively, hydride complex **2** can eliminate molecular hydrogen to reform complex **1**, resulting in the build-up of ketone. In DKR, this side reaction is only minor, and no significant ketone formation is observed. To compensate for dehydrogenation by the Ru catalyst, a hydrogen donor can be added to the system. This results in the formation of additional complex **2**, that can subsequently reduce the unwanted ketones formed. For this purpose, 2,4-dimethyl-3-pentanol (DMP) is a suitable choice, a secondary alcohol which is known to suppress net dehydrogenation of the substrate, while steric hindrance renders it virtually unreactive in

Reaction of the active catalyst **1** with a carboxylic acid gives inactive complex **3** (Scheme 4.4). Small amounts of carboxylic acid are inevitably formed in the enzymatic transesterification as trace water in the lipase induces ester hydrolysis and, therefore, significant deactivation of the catalyst will occur. However, in the presence of K<sub>2</sub>CO<sub>3</sub> the equilibrium of this reaction shifts to the side of the active catalyst **1**. Therefore, all DKR reactions employing catalyst **1** use an excess of K<sub>2</sub>CO<sub>3</sub> in the reaction mixture.

the enzymatic transesterification.<sup>47,48</sup>



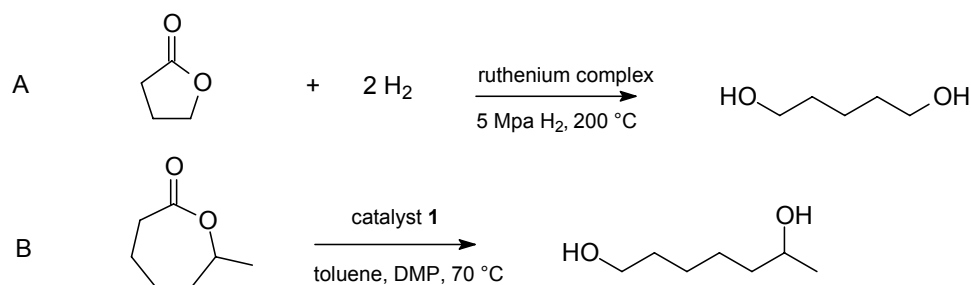
**Scheme 4.3** Racemization of secondary alcohols by catalyst **1**; for reasons of clarity, reversibility of the reactions is not shown.



**Scheme 4.4** Carboxylic acids deactivate catalyst **1** by forming acetato complex **3**; in the presence of  $K_2CO_3$  the equilibrium is shifted to active complex **1**.

Several Ru complexes are known to catalyze the hydrogenation of lactones, resulting in the formation of diol (an example is shown in Scheme 4.5A).<sup>49-51</sup> In case of 6-MeCL, this would result in formation of 1,6-heptanediol (Scheme 4.5B). If this occurs during the ITC of 6-MeCL, the formed diol would act as a nucleophile in the lipase-catalyzed ring-opening of 6-MeCL and initiate additional polymer chains. Since high temperature and high hydrogen pressure are normally necessary for this reaction to proceed, we do not expect that hydrogenation of 6-MeCL plays a significant role in ITC.





**Scheme 4.5** Ru-catalyzed hydrogenation of butyrolactone to 1,5-pentanediol;<sup>50</sup> (B) Ru-catalyzed hydrogenation of 6-MeCL would lead to the formation of 1,6-heptanediol.

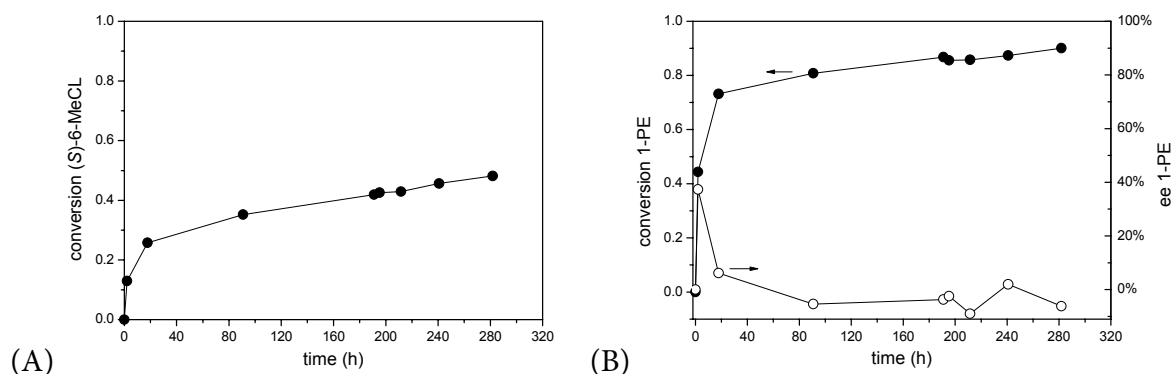
Based on the requirements described above, the most promising catalytic system for the ITC of (*S*)-6-MeCL consists of the combination of Novozym 435 as the transesterification catalyst and complex **1** as the racemization catalyst.

### 4.3 ITC of (*S*)-6-MeCL in a one-pot system

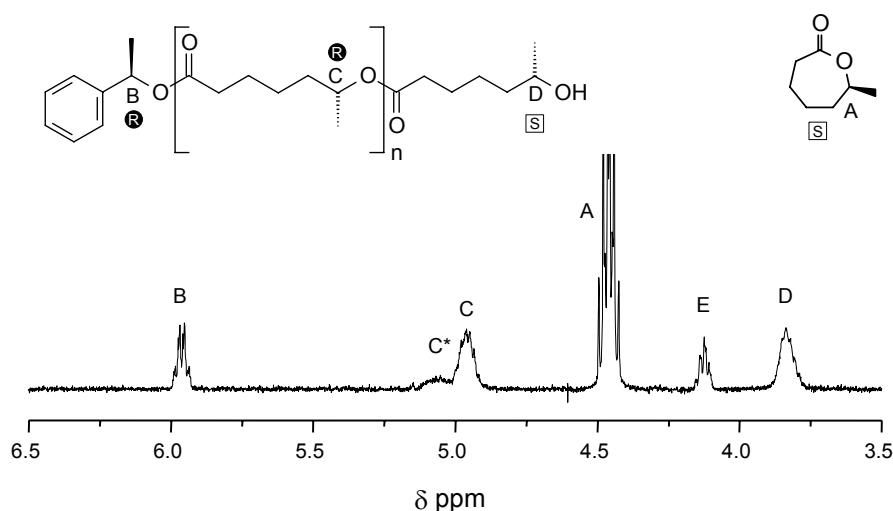
We performed an ITC experiment of (*S*)-6-MeCL in one pot, employing complex **1** and Novozym 435 as the catalysts.<sup>52</sup> The experiment was carried out with (*S*)-6-MeCL, synthesized with ee of 95% (see Chapter 3). Here, racemic 1-phenylethanol (1-PE) was used as the initiator – a secondary alcohol that is frequently used as a model substrate in DKR and that is known to be a good substrate for both the lipase and the racemization catalyst. CALB exhibits extremely high enantioselectivity towards (*R*)-1-PE (an E-value in excess of 1 million was recently reported).<sup>53</sup> Therefore, conversion of (*S*)-1-PE can only occur if the racemization catalyst is active. As a result, the conversion of (*R*)-1-PE gives immediate information whether the enzyme is active, while conversion of (*S*)-1-PE confirms that the racemization catalyst is active. To avoid the deactivation of catalyst **1** an excess of K<sub>2</sub>CO<sub>3</sub> was employed and DMP was added to suppress dehydrogenation of alcohol end-groups. The reaction was carried out in toluene at 70 °C under an argon atmosphere and was monitored by chiral GC.

Figure 4.1 shows the time-conversion plots of (*S*)-6-MeCL and 1-PE. Unfortunately, oligomerization proved to be very slow: a lactone conversion of 50% is only reached after 280 h (Figure 4.1A). Although the Ru loading is 12 mol% with respect to 1-PE (1.3 mol% with respect to (*S*)-6-MeCL), it takes 18 hours to reach a 1-PE conversion of 72% with a low ee (Figure 4.1B). Since the lactone conversion ultimately reaches 50%, oligomers should have been formed. To confirm this, the reaction mixture after 190 hours reaction time was analyzed by <sup>1</sup>H NMR (Figure 4.2). The signal at 4.9 ppm (C) is attributed to the CH<sub>2</sub> next to intra-chain esters, suggesting that propagation did indeed take place and that oligomers were formed. From the integral values of the various peaks, a degree of polymerization (DP) of only 2.5 was

calculated.<sup>54</sup> Signal C\* was found to belong to cyclic 6-MeCL dimers, which are always formed as a byproduct. Signal E was attributed to 1,6-heptanediol-initiated oligomers. Apparently, the hydrogenation of lactones under these relatively mild conditions does play a significant role. From <sup>1</sup>H NMR, it was calculated that 26% of the chains were initiated by 1,6-heptanediol instead of 1-phenylethanol.<sup>55</sup>



**Figure 4.1** Conversion time history of a 1-PE-initiated one-pot ITC experiment. (A) Conversion of (S)-6-MeCL as a function of time (B) Conversion (●) and ee (○) of 1-PE as function of time. Reaction conditions: catalyst **1** (0.049 mmol), Novozym 435 (56 mg), (S)-6-MeCL (3.8 mmol), (rac)-1-PE (0.42 mmol, M/I = 9), K<sub>2</sub>CO<sub>3</sub> (330 mg), 1,3,5-tri-tert-butylbenzene (0.25 mmol) and DMP (10 mmol) in toluene (5 mL) at 70 °C.



**Figure 4.2** <sup>1</sup>H NMR spectrum of the product mixture after 190 hours of reaction for the one-pot ITC experiment. For reasons of clarity, only the relevant part of the spectrum is shown (3.5-6.5 ppm). Signal E originates from 1,6-heptanediol-initiated oligomers.

Several attempts were then made to improve the catalyst activity in the one-pot system, including the use of an alternative base and the use of a large concentration of preformed

catalyst (without additional base), but without success. In all experiments, reaction rates were very low at best and short oligomers were only formed after long reaction times (typically > 200 h).

#### 4.4 Compatibility of the catalysts

While oligomerization undeniably takes place in a one-pot system, the reaction was very slow and catalytic activity was dramatically lower than in DKR. The combination of Novozym 435 and complex **1** was successfully employed in the DKR of secondary alcohols.<sup>45</sup> In this system, the compatibility of the two catalysts is excellent. However, in the one-pot ITC of (*S*)-6-MeCL a number of additional challenges are present, such as the use of a polar cyclic ester as the monomer and the low concentration of alcohol. In an attempt to rationalize the observed inhibition, we analyzed the catalytic activity of both catalysts in one-pot ITC experiments of (*S*)-6-MeCL.

##### 4.4.1 Activity of the racemization catalyst in one-pot ITC

Figure 4.3 shows the time-conversion plot of a typical one-pot ITC experiment of (*S*)-6-MeCL. Oligomerization again proved to be very slow; a lactone conversion of 34% is only reached after 145 h (Figure 4.3A). At this time, the initiator (*rac*)-1-PE has largely been consumed (conversion after 145h was 82%) and the ee of the remaining 1-PE was close to 0% (Figure 4.3B). To analyze the activity of the racemization catalyst at this stage of the reaction, 1 mmol of (*S*)-1-PE was added to the reaction mixture. This resulted in an increase of the ee to 94%. If the racemization catalyst is still active, the ee should decrease over time. Indeed, the ee decreases to 22% after 185h total reaction time (Figure 4.3B). A TOF of 1.4 h<sup>-1</sup> was calculated for the reaction, which is dramatically lower than the activity in a separate racemization experiment in the absence of 6-MeCL (a TOF of 200 h<sup>-1</sup> was calculated for the racemization of (*S*)-1-PE from a reference experiment). The racemization of the (*S*)-1-PE results in the formation of reactive (*R*)-1-PE. This should lead to a further increase of the conversion of (*S*)-6-MeCL, which is indeed observed (Figure 4.3A).

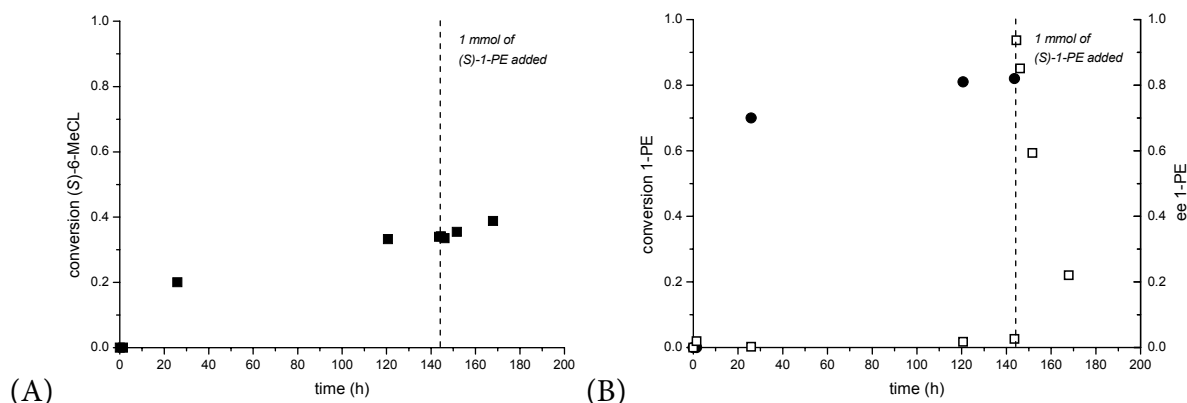


**Figure 4.3** (A) Conversion of (S)-6-MeCL (■, left axis) in an ITC experiment with catalyst **1**. (B) Conversion (●, left axis) and ee of 1-PE (□, right axis). Conditions: catalyst **1** (0.044 mmol), Novozym 435 (57 mg), (S)-6-MeCL (3.9 mmol), (rac)-1-PE (0.41 mmol), 1,3,5-tri-tert-butylbenzene (0.33 mmol) and DMP (9 mmol) in toluene (4 mL) at 70 °C. After 90 min,  $K_2CO_3$  (330 mg) was added to the reaction mixture. After 145 h, (S)-1-PE (1 mmol, ee > 99%) is added to the reaction to determine the racemization activity.

#### 4.4.2 Activity of the lipase catalyst in one-pot ITC

Figure 4.4 shows the time-conversion plot of a typical one-pot ITC experiment of (S)-6-MeCL. After 164h, a lactone conversion of 52% was observed. To analyze the transesterification activity of the lipase at this stage of the reaction, 0.8 mmol benzyl alcohol (BA) was added to the reaction mixture. If the lipase is still active, this should lead to an increased rate of conversion of (S)-6-MeCL as extra initiator is introduced. Indeed, an increase in the conversion of (S)-6-MeCL was observed; after 188h the conversion had risen to 65%. However, the calculated TOF was only  $155\text{ h}^{-1}$ , compared to  $4.0 \cdot 10^4\text{ h}^{-1}$  in a reference experiment with 6-MeCL/BA = 4 at 70 °C.

In conclusion, we observed that both the lipase catalyst and the racemization catalyst show very low activity in the one-pot ITC of (S)-6-MeCL; far less activity than observed in reference experiments. To investigate the cause of the observed deactivation, we decided to examine the compatibility of the catalysts under the reaction conditions of ITC. A typical ITC experiment would be run under the following conditions: toluene as the solvent with DMP as a cosolvent, a suitable initiator such as benzyl alcohol, (S)-6-MeCL, Novozym 435,  $RuCl_2(\text{cymene})_2$ , (rac)-2-phenyl-2-amino-propionamide, and an excess of  $K_2CO_3$ , stirred at 70 °C under an argon atmosphere.

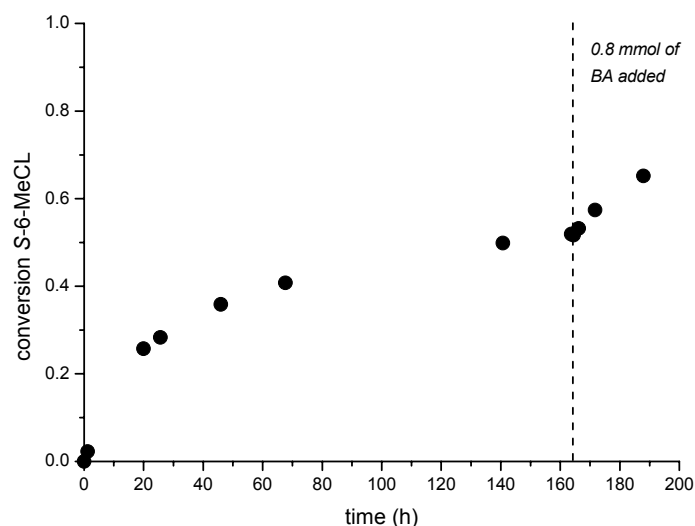


**Figure 4.4** ITC of (S)-6-MeCL. Conditions: catalyst **1** (0.046 mmol), Novozym 435 (57 mg), (S)-6-MeCL (3.9 mmol), BA (0.42 mmol), 1,3,5-tri-*tert*-butylbenzene (0.33 mmol) and DMP (13 mmol) in toluene (4 mL) at 70 °C. After 90 min,  $K_2CO_3$  (330 mg) was added to the reaction mixture. After 164 h, BA (0.8 mmol) is added to determine the enzymatic activity.

#### 4.4.3 Deactivation of the lipase under ITC conditions

The effect of the presence of the different reactants required for ITC on the enzymatic activity was investigated. As a model reaction, the benzyl alcohol-initiated enzymatic ring-opening polymerization of  $\epsilon$ -caprolactone was selected. Screening of the various components present in ITC except for  $K_2CO_3$  showed no significant effect on lipase activity (data not shown). However, the presence of  $K_2CO_3$  did play a crucial role; the polymerization activity of the lipase was severely decreased in the presence of  $K_2CO_3$ . Therefore, we concentrated on the effect of the presence of a solid base on lipase activity.

Enzymatic ring-opening polymerizations display first-order kinetic behavior. Therefore, a first-order rate constant and the turnover frequency (TOF) can be calculated.  $\epsilon$ -Caprolactone (CL) and  $\omega$ -pentadecalactone (PDL) were polymerized in the presence of several solid bases. Table 4.1 summarizes the results obtained from these experiments.

**Table 4.1** Activity of Novozym 435 in polymerization of CL and PDL using benzyl alcohol (BA) as the initiator in presence of various solid bases.

entry	substrate	[M]/[I]	additive	TOF (s <sup>-1</sup> ) <sup>a</sup>
1	CL	14	-	233
2	CL	14	5 mg K <sub>2</sub> CO <sub>3</sub> <sup>b</sup>	15
3	CL	14	80 mg K <sub>2</sub> CO <sub>3</sub> <sup>b</sup>	7.0
4	CL	14	80 mg K <sub>2</sub> CO <sub>3</sub> <sup>c</sup>	73
5	CL	14	80 mg K <sub>2</sub> CO <sub>3</sub> <sup>d</sup>	12
6	CL	14	160 mg Cs <sub>2</sub> CO <sub>3</sub>	23
7	CL	1	-	18
8	CL	1	80 mg K <sub>2</sub> CO <sub>3</sub> <sup>b</sup>	12
9	CL	1	350 mg K <sub>2</sub> CO <sub>3</sub> <sup>b</sup>	23
10	PDL	14	-	429
11	PDL	14	80 mg K <sub>2</sub> CO <sub>3</sub> <sup>b</sup>	384

Conditions: Novozym 435 (25 mg), solid base, BA and 1.3 M of lactone in toluene (2.25 mL) at 70 °C. <sup>a</sup> Turnover frequency; defined as the number of turnovers per active site per second at the start of reaction; in order to calculate this number an active protein content of 2 % (w/w) of the immobilized preparation is assumed.<sup>56</sup> The TOF is calculated according to the formula  $TOF = k_i \times (\text{initial substrate concentration}) / (\text{total active enzyme concentration})$ , in which  $k_i$  is the rate constant as determined by fitting a straight line to the relationship between  $-\ln(1 - \text{conversion of the lactone})$  and time. <sup>b</sup> K<sub>2</sub>CO<sub>3</sub> used from Sigma-Aldrich (347825,-325 mesh). <sup>c</sup> K<sub>2</sub>CO<sub>3</sub> used from Fluka (60108, Biochemika, extra pure with low non-potassium cation content). <sup>d</sup> K<sub>2</sub>CO<sub>3</sub> used from Fluka, ground (60108, Biochemika, extra pure with low non-potassium cation content).

In a typical CL polymerization using benzyl alcohol (BA) as the initiator in the absence of a solid base, a TOF of 233 s<sup>-1</sup> was calculated (Table 4.1, entry 1). The addition of only a small amount of K<sub>2</sub>CO<sub>3</sub> (entry 2, 5 mg K<sub>2</sub>CO<sub>3</sub>, source: Sigma-Aldrich, fine powder, -325 mesh) resulted in a 94% decrease in activity. Addition of 80 mg of K<sub>2</sub>CO<sub>3</sub> led to a further decrease in activity (entry 3).

Experiments with an extra pure batch of K<sub>2</sub>CO<sub>3</sub> that was obtained from Fluka also resulted in a large decrease in activity (BioChemika Ultra grade, entries 4 and 5). Since this preparation consists of a rather coarse granulate, it was used both as such and after grinding. Using the coarse granulate a relatively high TOF of 73 s<sup>-1</sup> was found (entry 4). However, after grinding the activity of the lipase was much lower and a TOF of only 12 s<sup>-1</sup> was calculated (entry 5). For Cs<sub>2</sub>CO<sub>3</sub> a similar detrimental effect on the activity of Novozym 435 was observed, with a measured TOF of only 23 s<sup>-1</sup> (entry 6).<sup>57</sup>

Surprisingly, the deactivation was not observed when BA and CL were reacted in equimolar amounts. Reaction rates were much lower (TOF = 18 s<sup>-1</sup>, entry 7), but the presence of K<sub>2</sub>CO<sub>3</sub> in this system, even in larger amounts, did not lead to significant deactivation

(entries 8 and 9). Also in the polymerization of PDL no significant effect was observed of the presence of  $K_2CO_3$  (entries 10 and 11).

In conclusion, the presence of  $K_2CO_3$  leads to a large decrease in lipase activity in the polymerization of CL. Since the use of extra pure  $K_2CO_3$  results in the same decrease in the rate of reaction, the deactivation should be attributed to the  $K_2CO_3$  itself and not to the presence of impurities (anionic or cationic). The experiments with the coarse and ground granulate indicate that the particle size of the solid base is a determining factor in the degree of deactivation.

Lipase deactivation is not observed in the polymerization of PDL in presence of  $K_2CO_3$ . This suggests that the polarity of the system might play an important role here. PDL is a large-ring lactone with little ring strain, and, therefore, much less polar than CL. The dipole moment of CL is 4.45 D while the dipole moment of PDL is only 1.86 D.<sup>58,59</sup>

When BA and CL are reacted in equimolar amounts, the activity is much lower compared to a CL polymerization. This might be attributed to the increased polarity of the system (the concentration of BA is much higher) or to the described inhibitory effect of the alcohol on CALB.<sup>60</sup> In this system  $K_2CO_3$  was not found to significantly deactivate the lipase. This suggests that both  $K_2CO_3$  and the presence of oligomers are important factors. The exact nature of the deactivation of the lipase remains concealed.

#### 4.4.4 Deactivation of the racemization catalyst under ITC conditions

In order to investigate the activity of catalyst **1** under ITC conditions, the racemization of (*S*)-1-PE was studied in the presence of various lactones.<sup>61</sup> The results are summarized in Table 4.2. The effect of the addition of 6-MeCL and PDL on the racemization activity is also displayed graphically in Figure 4.5.

As can be seen from entries 1 and 2 in Table 4.2, the addition of 1 eq of 6-MeCL with respect to (*S*)-1-PE resulted in the rate of racemization being reduced by ~ 80 %. With 5 eq of 6-MeCL the effect is even more pronounced and almost no racemization activity was observed (entry 11). For other small-ring lactones such as  $\epsilon$ -caprolactone (CL),  $\delta$ -valerolactone (VL) and 5-methylvalerolactone (5-MeVL) a similar reduction of the racemization activity was observed (entries 3, 6 and 7, respectively). In contrast, the presence of  $\omega$ -pentadecalactone (PDL), an apolar macrolactone, did not significantly reduce the rate of racemization (entry 4), even not in high concentration (entry 8).

**Table 4.2** Racemization of (S)-1-PE in the presence of various lactones.<sup>a</sup>

entry	[Ru] (mol%)	lactone	equivalents of lactone <sup>b</sup>	TOF (h <sup>-1</sup> ) <sup>c</sup>	normalized activity <sup>d</sup>
1	0.4	none	-	179	100
2	0.4	6-MeCL	1	38	21
3	0.4	CL	1	97	54
4	0.4	PDL	1	178	99
5	0.4	none	-	113	100
6	0.4	VL	1	34	30
7	0.4	5-MeVL	1	28	25
8	0.4	PDL	3	116	103
9 <sup>e</sup>	0.2	none	-	232	100
10 <sup>e</sup>	0.2	6-MeCL	1	26	11
11 <sup>e</sup>	0.2	6-MeCL	5	2	1

<sup>a</sup> Unless otherwise noted, Ru catalyst **1** was performed for 2 h at 70 °C under an argon atmosphere in toluene/2-propanol (2:1) in the presence of K<sub>2</sub>CO<sub>3</sub>. This catalyst solution was filtered and 0.20 mol% of the catalyst was added to a mixture of (S)-1-PE (ee = 99%, 2 mmol), the lactone and K<sub>2</sub>CO<sub>3</sub> (50 mg). <sup>b</sup> Equivalents of lactone added with regard to (S)-1-PE. <sup>c</sup> Turnover frequency; the TOF can be calculated according to:  $TOF = k_i \times (\text{initial substrate concentration}) / (\text{total Ru concentration})$  in which  $k_i$  is the rate constant as determined by fitting a straight line to the relationship between  $-\ln(1 - \text{conversion})$  and time where conversion is defined as  $(1 - ee/ee_0)$ . <sup>d</sup> Racemization activity relative to an experiment without lactone. <sup>e</sup> No catalyst preformation; reaction performed in a 6 mL vial.

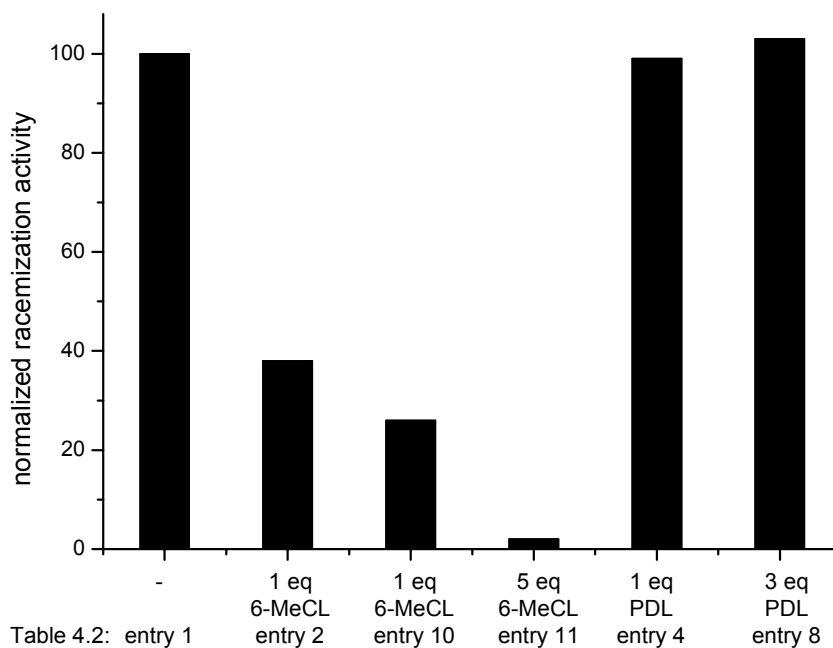


**Figure 4.5** Racemization activity of catalyst **1** at 70 °C in the presence of 1 eq of 6-MeCL (Table 4.2, entry 2), 1 eq of 6-MeCL (entry 10), 5 eq of 6-MeCL (entry 11), 1 eq of PDL (entry 4), 3 eq of PDL (entry 8), relative to an experiment in the absence of lactone (A).



Judging from these results, racemization catalyst **1** is incompatible with small-ring lactones, which renders it an unsuitable catalyst for the one-pot ITC of 6-MeCL. The exact nature of this incompatibility remains unclear. The high polarity of these small-ring lactones might play an important role, since the racemization activity is retained in presence of the (apolar) macrolactone PDL. An alternative explanation would be that CL and PDL act as competitive substrates for the ruthenium complex. Since the hydrogenation of 6-MeCL occurs under the conditions of ITC (as shown in section 4.3), it is conceivable that lactones occupy the catalytic centers of the ruthenium complexes, reducing racemization activity. The *cisoid* and *transoid* conformation of the ester groups in CL and PDL, respectively, might then explain the observed difference in deactivation, assuming the *cisoid* conformation of CL allows easier coordination of the lactone to the ruthenium.

In conclusion, in the one-pot ITC of (*S*)-6-MeCL the activity of both the racemization catalyst and the lipase is very low. This can be attributed to the presence of small, polar lactones in case of the racemization catalyst, and to the presence of the solid base  $K_2CO_3$  in case of the lipase. Compared to the activity of the catalysts in reference experiments, under one-pot ITC conditions only 0.7% and 0.4% residual activity for the ruthenium and for the lipase was observed, respectively. This implies that using this catalytic system, one-pot ITC of (*S*)-6-MeCL is not feasible.

The observation that the catalytic activity of the lipase and the racemization catalyst is retained in presence of large, apolar macrolactones, such as PDL, suggests that ITC of  $\omega$ -substituted macrolactones should be possible using this catalytic system. However, we recently found that the CALB-catalyzed ring-opening of  $\omega$ -substituted lactones with a ring size larger than 7 (7-methylheptalactone, 8-methyloctalactone and 12-methyldodecalactone) turned out to be highly *R*-selective, in contrast to the observed *S*-selectivity for 6-MeCL. This renders these monomers of no use for ITC. The details of this study are described in Jeroen van Buijtenens thesis.

#### 4.5 Proof of principle: ITC of (*S*)-6-MeCL in a two-pot system

The difficulties encountered in the one-pot ITC experiments prompted us to investigate the process in a two-pot system. Therefore, ring-opening product **4a** was isolated (Scheme 4.1; the  $^1H$  NMR spectrum of **4a** is shown in Figure 4.6). **4a** was subsequently racemized by catalyst **1**; isopropanol was added as a hydrogen donor to compensate for dehydrogenation.<sup>62</sup> To prevent base-catalyzed transesterification, the catalyst was preformed from  $[RuCl_2(cymene)]_2$  and (*rac*)-2-phenyl-2-amino-propionamide in the presence of  $K_2CO_3$ . The solid base was removed by filtration before adding the catalyst solution to the reaction

mixture. Racemization of **4a** resulted in 50% of disfavored substrate **4a** and 50% of favored substrate **4b**, which was confirmed by  $^{31}\text{P}$  NMR spectroscopy of the diastereomers formed upon addition of  $\text{PCl}_3$  to the alcohol.<sup>63</sup> When the racemized product was reacted with (*S*)-6-MeCL, a fast reaction was observed (with comparable kinetics to reaction of BA with 6-MeCL), with an ultimate conversion of racemized **4** of 50% and consumption of an additional 0.5 equivalent of (*S*)-6-MeCL (Figure 4.7).  $^1\text{H}$  NMR confirmed the formation of oligomers and indicated that indeed 50% of the molecules had propagated, hence, leading to an increase of the average degree of polymerization with 0.5.

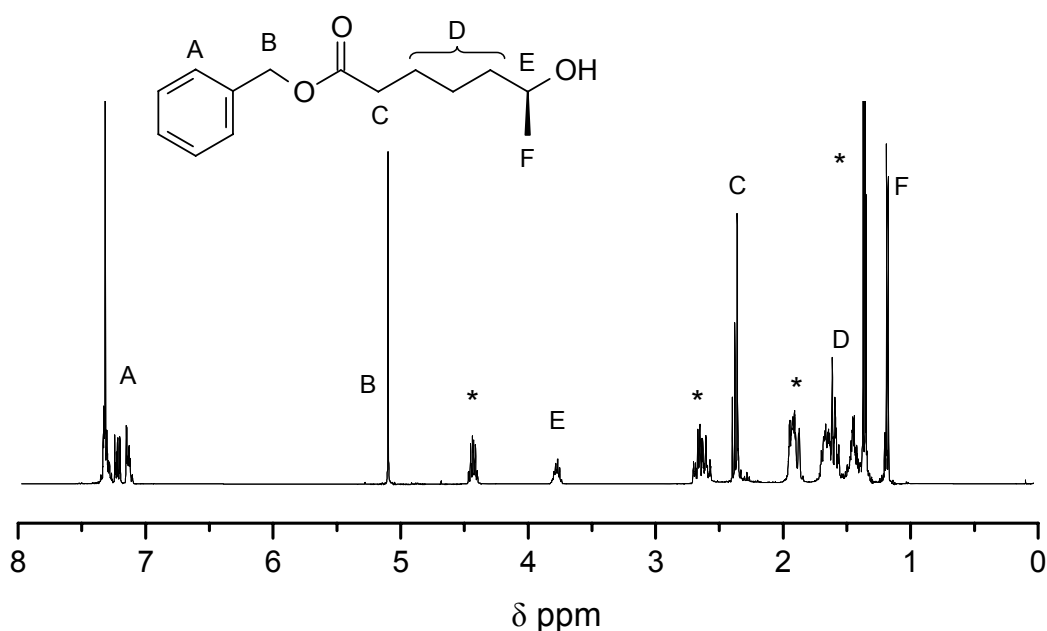


**Figure 4.6**  $^1\text{H}$  NMR spectrum of the ring-opening product of BA and 6-MeCL (generation 1). Signals with \* are attributed to 6-MeCL monomer which was added in excess.

After this first successful racemization/ring-opening cycle, the procedure was repeated until the 5<sup>th</sup> generation of the oligomer was obtained.<sup>64</sup> The resulting products from generations 1 to 5 were analyzed by  $^1\text{H}$  NMR. The obtained spectra revealed that, as expected, with every generation, the average degree of polymerization increased by 0.5 (Table 4.3). Figure 4.8 shows the  $^1\text{H}$  NMR spectrum obtained from generation 5. The signal at 4.9 ppm (G) is attributed to the  $\text{CH}_2$  next to intra-chain esters, indicating that indeed oligomers were formed. From the integral values of the various peaks, a degree of polymerization (DP) of 3.2 was calculated. Signal I at 4.1 ppm is in the typical range for primary esters; it was attributed to 1,6-heptanediol-initiated oligomers.

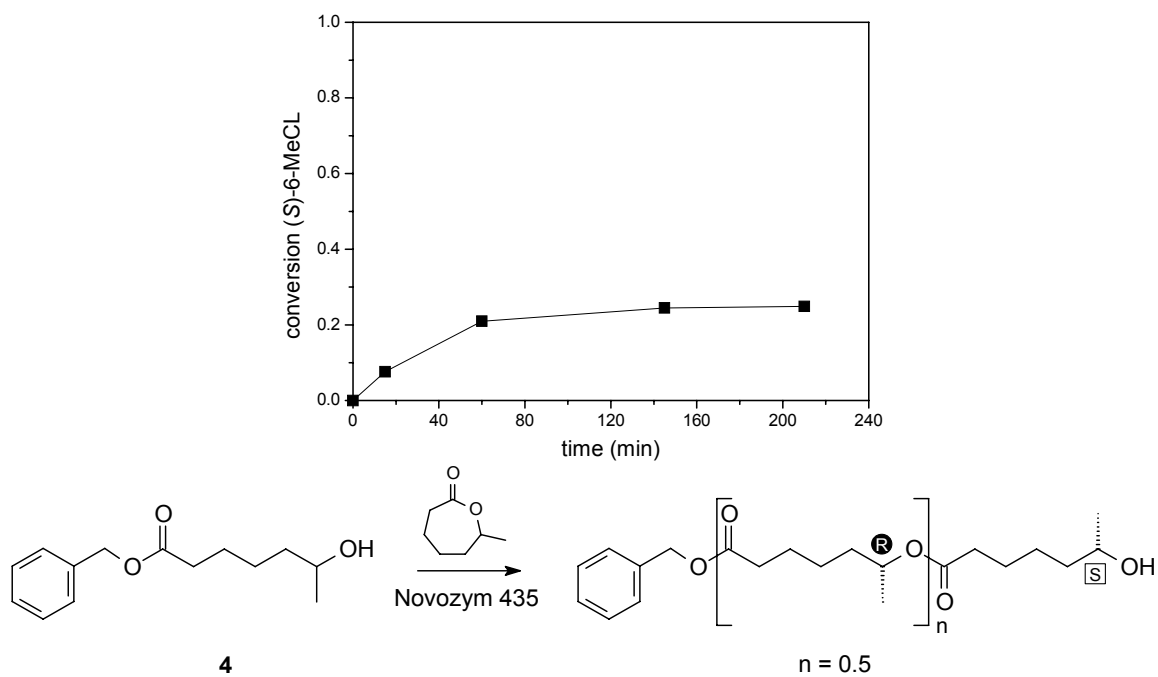


**Figure 4.7** Enzymatic ring-opening of 6-MeCL by racemized **4** with (S)-6-MeCL : **4** = 2.

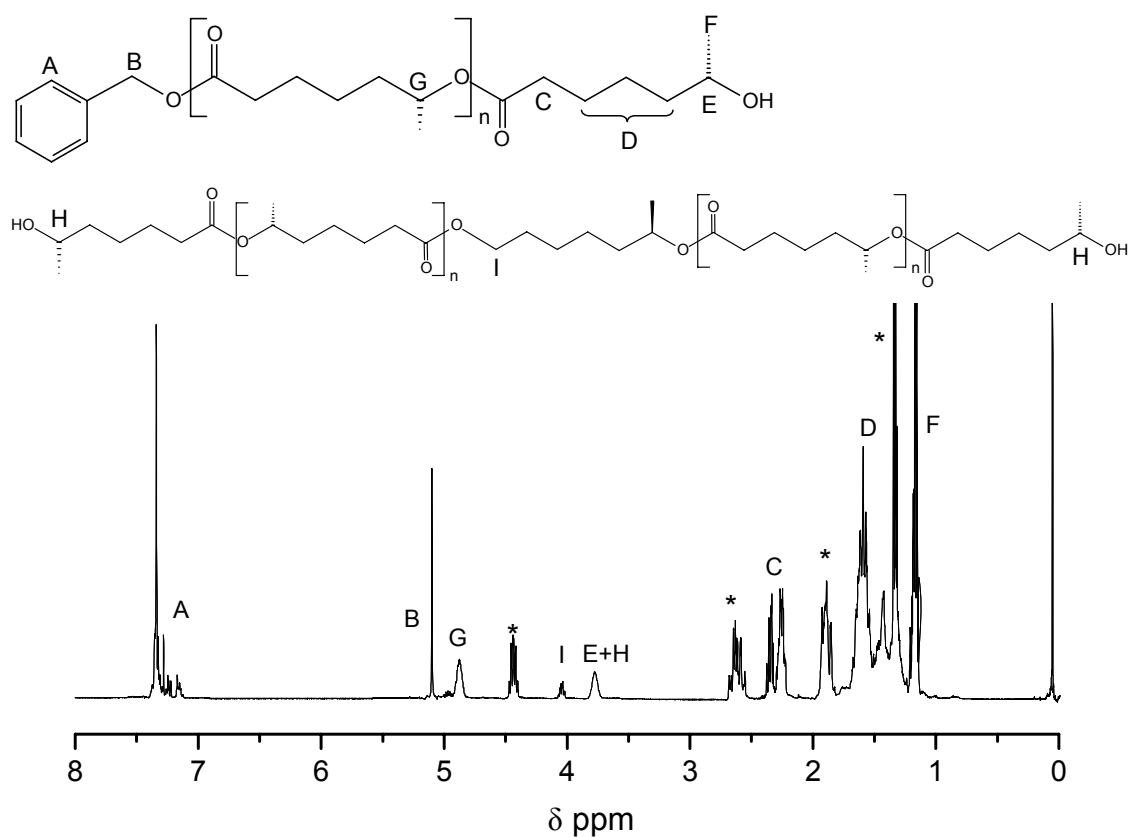


**Figure 4.8** <sup>1</sup>H NMR spectrum of the oligomeric species obtained from generation 5. Both BA and 1,6-heptanediol-initiated oligomers are present. Signals with \* are attributed to 6-MeCL monomer which was added in excess.

To analyze this in more detail, a MALDI-ToF MS spectrum was measured of generations 3 to 5 (Figure 4.11). Benzyl alcohol-initiated oligomers of 6-MeCL have clearly been formed (distributions A and B;  $\text{Na}^+$  and  $\text{K}^+$  ionized oligomers of 6-MeCL). It is clear that the molecular weight of the oligomers increases with every generation; in addition, the maximum of the distribution shifts to a higher mass.<sup>65</sup>

Next to distributions A and B, two different sets of distributions were observed. Distribution E is a MALDI-ToF MS artifact.<sup>66</sup> Distributions C and D correspond to  $\text{Na}^+$  and  $\text{K}^+$  ionized oligomers of 6-MeCL which are initiated by 1,6-heptanediol instead of BA.  $^1\text{H}$  NMR confirms the presence of 25% of 1,6-heptanediol-initiated 6-MeCL oligomers in the 5<sup>th</sup> generation oligomer.<sup>67</sup>

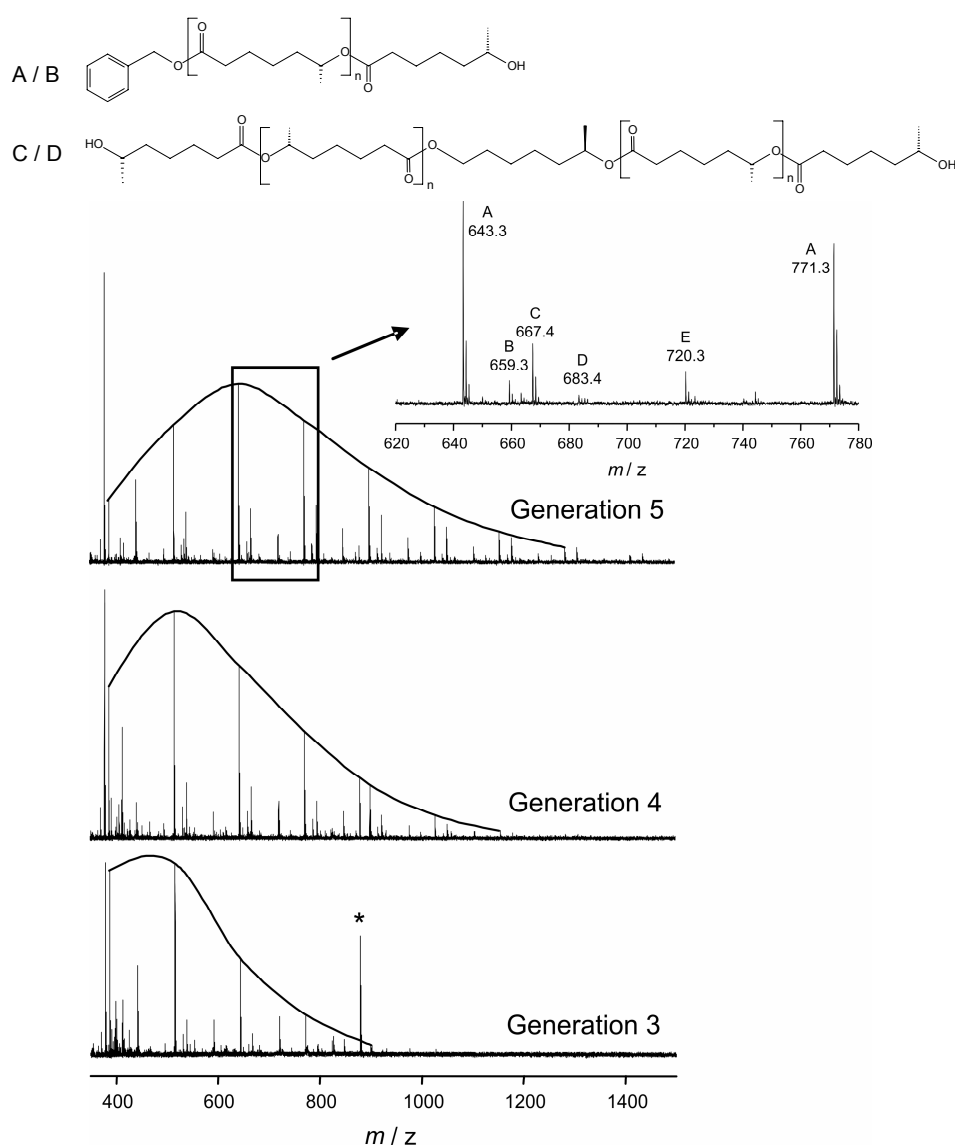


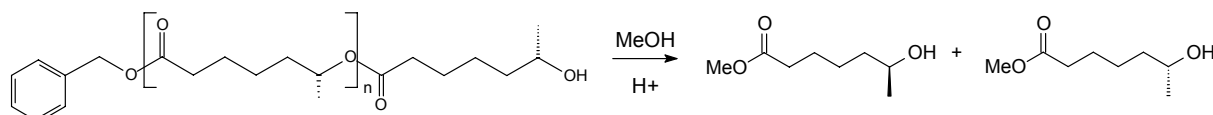
**Figure 4.9** MALDI-ToF MS spectra of generations 3, 4 and 5; A and B correspond to  $\text{Na}^+$  and  $\text{K}^+$  ionized BA-initiated oligomers of 6-MeCL; C and D to  $\text{Na}^+$  and  $\text{K}^+$  ionized 1,6-heptanediol-initiated oligomers of 6-MeCL; E and \* to MALDI-ToF MS related artifacts.

**Table 4.3** Chiral 6-MeCL oligomers by iterative tandem catalysis.

generation	DP <sup>a</sup>	DP <sub>th</sub> <sup>b</sup>	% diol-initiated chains <sup>a</sup>
1	1.0	1.0	0
2	1.5	1.5	0
3	2.0	2.0	9
4	2.5	2.5	15
5	3.2	3.0	25

<sup>a</sup> Determined by <sup>1</sup>H NMR; <sup>b</sup> Theoretical DP; with every generation, 50% of the chains have propagated leading to an increase in the DP of 0.5.

To prove that *R*-esters have indeed been formed in the process, generation 5 was degraded by acid-catalyzed methanolysis to afford methyl 6-hydroxyheptanoate (Scheme 4.6). Analysis of the methyl ester by chiral GC revealed that 92% of the ester groups in the oligomer chains were in the *R*-configuration.<sup>68</sup> Evidently, the conversion of (*S*)-6-MeCL into *R*-esters was successful.

**Scheme 4.6** Methanolysis of the generation 5 oligomer.

## 4.6 Conclusions

Iterative tandem catalysis (ITC) was introduced as a novel polymerization technique for the synthesis of well-defined materials. In ITC, multiple catalysts are operating simultaneously in one pot and iterative action of each of the catalysts is required for chain growth. Proof of principle was provided by the synthesis of enantioenriched *R*-oligomers from (*S*)-6-MeCL in a two-pot system, employing *Candida antarctica* Lipase B as the transesterification catalyst and a Ru complex with *p*-cymene and (*rac*)-2-phenyl-2-amino-propionamide ligands as the racemization catalyst. Hydrogenation of 6-MeCL, leading to the formation of 1,6-heptanediol, and dehydrogenation of end-groups were identified as important side reactions that severely reduce molecular weight.

Experiments in a one-pot system only afforded short oligomers. It was shown that this was caused by insufficient compatibility of the two catalysts. The presence of K<sub>2</sub>CO<sub>3</sub> as a heterogeneous base in the polymerization of highly polar small lactones dramatically reduced the enzymatic activity, while the racemization activity was severely reduced by the presence of these highly polar small lactones. Modification of the tandem catalytic system by using a different racemization catalyst ultimately enabled the one-pot ITC of 6-MeCL. These results are described in Jeroen van Buijtenens thesis. The successful tandem catalytic system was also

extended to the polycondensation of diols and diesters, a process called dynamic kinetic resolution polymerization (DKRP). This work is described in Chapter 5 of this thesis.

## 4.7 Experimental section

### Materials

6-Methyl- $\epsilon$ -caprolactone (6-MeCL) was synthesized by Baeyer-Villiger oxidation of 2-methylcyclohexanone following a reported procedure.<sup>69</sup> (S)-6-MeCL was synthesized by a double enzymatic ring-opening/ring-closure procedure.<sup>41</sup> Benzyl alcohol (BA) was purchased from Aldrich and distilled from CaH<sub>2</sub> before use. Novozym 435 was purchased from Novozymes A/S. All solvents were stored on dry molecular sieves (3 Å) to remove traces of water. All other chemicals were purchased from Aldrich and used as received unless otherwise noted.

### Analytical methods

<sup>1</sup>H NMR spectra were measured in CDCl<sub>3</sub> at 400, 300 or 200 MHz using a Varian Mercury Vx 400, 300 or 200 spectrometer. <sup>31</sup>P NMR spectra were measured in CDCl<sub>3</sub> at 162 Mhz using a Varian Mercury Vx 400. <sup>13</sup>C NMR spectra were measured in CDCl<sub>3</sub> at 100 MHz using a Varian Mercury Vx 400 spectrometer. Chiral gas chromatography (GC) was performed on a Shimadzu 6C-17A GC equipped with a Chrompack Chirasil-DEX CB (DF=0.25) column and an FID. Samples were injected using a Shimadzu AOC-20i autosampler. Injection temperature was set at 250 °C and detection temperature was set at 300 °C. Separations were performed under isothermal conditions with the column temperature set at 125 °C, which afforded in all cases baseline separation of the enantiomers of 6-MeCL. Lactone conversions were determined by the internal standard method using 1,3,5-tri-*tert*-butylbenzene as the internal standard. The ee<sub>monomer</sub> was calculated as follows: ee<sub>monomer</sub> = (R-S)/(R+S) where R and S represent the area of the GC peaks of the *R*- and *S*-enantiomer, respectively. MALDI-TOF MS spectra were recorded on a PerSeptive Biosystems Voyager DE PRO spectrometer using a 50:50 mixture of  $\alpha$ -cyano-4-hydroxycinnamic acid (CHCA) and trans-2-[3-(4-*t*-butylphenyl)-2-methyl-2-propenylidene]malononitrile (DCTB) as a matrix. The ee of the end-groups of the oligomers was determined according to a published method.<sup>63</sup> The terminal alcohols were reacted with 0.5 eq of PCl<sub>3</sub> and <sup>31</sup>P NMR spectroscopy revealed different signals for the possible diastereomers, making discrimination between racemic and high ee end-groups possible.

### One-pot synthesis of 6-MeCL oligomers

A 5 mL vial was charged with Novozym 435 (56 mg) and put overnight in a vacuum oven (10 mm Hg) at 50 °C in presence of P<sub>2</sub>O<sub>5</sub>. The oven was backfilled with nitrogen and the vial was removed from the oven. A Schlenk tube was charged with [RuCl<sub>2</sub>(cymene)]<sub>2</sub> (15 mg, 0.024 mmol), *rac*-2-phenyl-2-amino-propionamide (9.5 mg, 0.058 mmol), K<sub>2</sub>CO<sub>3</sub> (0.33 g, 2.4 mmol), 1-PE (52 mg, 0.42 mmol), (S)-6-MeCL (0.48 g, 3.8 mmol), 1,3,5-tri-*tert*-butylbenzene (62 mg, 0.25 mmol), toluene (4.9 mL), 2,4-dimethyl-3-pentanol (1.4 mL, 10 mmol) and dry molecular sieves (3 Å). Five vacuum-argon cycles were performed to remove oxygen. The mixture was stirred at 70 °C for 2.5 h to allow preformation of the catalyst. The dried enzyme was then added, indicating the start of the reaction. The reaction mixture was stirred at 70 °C for 282 h. The reaction was stopped by filtration using a class 3 glass filter. The filtrate was concentrated *in vacuo* and the catalyst was removed by column chromatography over

silica using dichloromethane and subsequently ethyl acetate as the eluent. Evaporation of the solvent yielded the product.

*Typical procedure for an enzymatic polymerization of CL in presence of a solid base*

Novozym 435 (25 mg),  $K_2CO_3$  (80 mg) and toluene (2.25 mL) were added to a 5 mL vial. The mixture was stirred and heated to 70 °C in a carousel reactor. A mixture of BA (25 mg, 0.20 mmol) and  $\epsilon$ -caprolactone (320 mg, 2.96 mmol) was added to the vial, which indicated the start of the reaction. After 0, 5, 10, 20, 40, 80 and 160 min, aliquots (~ 0.02 mL) were taken from the reaction mixture using a glass Pasteur pipette. The samples were diluted with dichloromethane and the enzyme was removed by filtration over cotton wool. The samples were analyzed by chiral GC.

*Typical procedure for the racemization of (S)-1-PE in the presence of lactones*

A Schlenk tube was charged with  $[RuCl_2(cymene)]_2$  (17 mg, 0.03 mmol), *rac*-2-phenyl-2-amino-propionamide (10 mg, 0.06 mmol),  $K_2CO_3$  (0.6 g, 4.3 mmol), 5 mL 2-propanol (65 mmol) and 10 mL toluene. The system was subjected to five vacuum-argon cycles to remove oxygen and stirred at 70 °C for 2 h. (S)-1-PE (0.25 g, 2.0 mmol), *rac*-6-MeCL (0.25 g, 2.0 mmol) and  $K_2CO_3$  (25 mg, 0.18 mmol) were added to a Schlenk tube and the reaction mixture was subjected to five vacuum-argon cycles to remove oxygen. 2.3 mL of the catalyst solution was filtered through a 1  $\mu$ m PTFE syringe filter and added to the reaction mixture. The mixture was subjected to five vacuum-argon cycles to remove oxygen and stirred at 70 °C for 4 h. Small aliquots of reaction mixture were taken for GC analysis.

*Synthesis of 4a using (S)-6-MeCL*

Novozym 435 (0.10 g) and a magnetic stirring bar were added to a Schlenk tube. The tube was put overnight in a vacuum oven (10 mm Hg) at 50 °C in presence of  $P_2O_5$ . The oven was backfilled with nitrogen and the tube was removed from the oven. BA (0.78 g, 7.2 mmol), 6-MeCL (3.0 g, 23 mmol), 1,3,5-tri-*tert*-butylbenzene (0.05 g, 0.20 mmol) and toluene (8 mL) were added to the tube. The mixture was stirred at 80 °C for 16 hours. After completion of the reaction, which was confirmed by  $^1H$  NMR, the enzymatic reaction was stopped by filtration using a class 3 glass filter and the filter was flushed with dichloromethane. The filtrate was concentrated and the product was used without further purification. Yield: 3.49 g (93%).

$^1H$  NMR  $\delta$  (ppm) 7.3-7.4 (m, Ar-H), 5.1 (Ar- $CH_2$ -O), 3.8 (m,  $CH(CH_3)OH$ ), 2.4 (m, benzyl- $CH_2$ - $OCOCH_2$ ), 1.65-1.35 (m,  $OCOCH_2(CH_2)_3$ ), 1.15 (d,  $CH_3$ )

*Typical procedure for the racemization of 6-MeCL oligomers*

$[RuCl_2(cymene)]_2$  (38 mg, 0.06 mmol), *rac*- $\alpha$ -methyl-phenylglycinamide (22 mg, 0.14 mmol),  $K_2CO_3$  (0.50 g, 3.6 mmol), 5 mL 2-propanol (65 mmol) and 5 mL toluene were added to a 25 mL Schlenk tube. To remove oxygen, five consecutive vacuum-argon cycles were performed. The system was stirred at 80 °C for 1 h. 6-MeCL oligomer (1.0 g, 1.3 mmol) was dissolved in a mixture of 0.5 mL toluene and 0.5 mL 2-propanol. The mixture was transferred into a 15 mL Schlenk tube. Five vacuum-argon cycles were performed to remove oxygen. 5 mL of the catalyst solution was filtered through a 1  $\mu$ m PTFE syringe filter and added to the reaction mixture. The mixture was subjected to 3 vacuum-argon cycles and stirred at 70 °C for 16 h. The reaction mixture was concentrated and the catalyst was removed by column chromatography over silica using dichloromethane and subsequently ethyl acetate as the eluent. Evaporation of the solvent yielded the racemized product. Yield: 0.97 g (97 %).

*Typical procedure for the addition of (S)-6-MeCL to racemized 4*

Novozym 435 (50 mg) was added to a 10 mL sample vial. The vial was put overnight in a vacuum oven (10 mm Hg) at 50 °C in presence of P<sub>2</sub>O<sub>5</sub>. The oven was backfilled with nitrogen and the vial was removed from the oven. The racemized product mixture (1.1 g; containing 2.1 mmol **4**, 4.7 mmol (S)-6-MeCL and 1,3,5-tri-*tert*-butylbenzene), (S)-6-MeCL (1.0 g, 7.8 mmol), toluene (4 mL) and dry molecular sieves (3 Å) were added to a 50 mL round-bottom flask. The mixture was stirred at 45 °C for 16 h to remove traces of water. The dried Novozym 435 was added, which represented the start of the reaction. The mixture was stirred at 80 °C for 16 h. After completion of the reaction, which was confirmed by <sup>1</sup>H NMR, the enzymatic reaction was stopped by filtration using a class 3 glass filter and the filter was flushed with dichloromethane. The filtrate was concentrated. The product was quantitatively obtained and used without further purification.

*Hydrolysis of Generation 5 6-MeCL oligomers*

Oligomer of generation 5 (0.40 g) was dissolved in 7 mL toluene in a 50 mL round-bottom flask. 1 mL MeOH and 2 drops of 37% v/v HCl<sub>aq</sub> were added to the mixture. The mixture was stirred at reflux for 21 h. After completion of the reaction, which was confirmed by <sup>1</sup>H NMR, an aliquot of the reaction mixture was diluted with dichloromethane and 2 drops of trifluoroacetic anhydride were added. The mixture was analyzed on chiral GC (90 °C isothermal, r.t. = 26.34 and 26.99 min.).

By performing the same procedure with (S)-6-MeCL, the peak at r.t. = 26.99 min. was identified as the S-enantiomer of the secondary alcohol formed.

#### 4.8 References and notes

1. Wasilke, J.C.; Obrey, S.J.; Baker, R.T.; Bazan, G.C. *Chem. Rev.* **2005**, 105, (3), 1001-1020.
2. Bruggink, A.; Schoevaart, R.; Kieboom, T. *Org. Process Res. Dev.* **2003**, 7, (5), 622-640.
3. Larsson, A.L.E.; Persson, B.A.; Bäckvall, J.E. *Angew. Chem., Int. Ed. Eng.* **1997**, 36, (11), 1211-1212.
4. Pàmies, O.; Bäckvall, J.E. *Chem. Rev.* **2003**, 103, (8), 3247-3261.
5. Pàmies, O.; Bäckvall, J.E. *Trends Biotechnol.* **2004**, 22, (3), 130-135.
6. Choi, J.H.; Choi, Y.K.; Kim, Y.H.; Park, E.S.; Kim, E.J.; Kim, M.J.; Park, J.W. *J. Org. Chem.* **2004**, 69, (6), 1972-1977.
7. Martín-Matute, B.; Edin, M.; Bogár, K.; Bäckvall, J.E. *Angew. Chem., Int. Ed.* **2004**, 43, (47), 6535-6539.
8. Martín-Matute, B.; Edin, M.; Bogár, K.; Kaynak, F.B.; Bäckvall, J.E. *J. Am. Chem. Soc.* **2005**, 127, (24), 8817-8825.
9. Verzijl, G.K.M.; de Vries, J.G.; Broxterman, Q.B. *Tetrahedron: Asymmetry* **2005**, 16, (9), 1603-1610.
10. Kim, M.J.; Chung, Y.I.; Choi, Y.K.; Lee, H.K.; Kim, D.; Park, J. *J. Am. Chem. Soc.* **2003**, 125, (38), 11494-11495.
11. Borén, L.; Martín-Matute, B.; Xu, Y.M.; Córdova, A.; Bäckvall, J.E. *Chem. Eur. J.* **2005**, 12, (1), 225-232.
12. Paetzold, J.; Bäckvall, J.E. *J. Am. Chem. Soc.* **2005**, 127, (50), 17620-17621.
13. Komon, Z.J.A.; Bazan, G.C. *Macromol. Rapid Commun.* **2001**, 22, (7), 467-478.



14. Komon, Z.J.A.; Bu, X.H.; Bazan, G.C. *J. Am. Chem. Soc.* **2000**, 122, (8), 1830-1831.
15. Komon, Z.J.A.; Diamond, G.M.; Leclerc, M.K.; Murphy, V.; Okazaki, M.; Bazan, G.C. *J. Am. Chem. Soc.* **2002**, 124, (51), 15280-15285.
16. Alobaidi, F.; Ye, Z.B.; Zhu, S.P. *J. Polym. Sci., Part A: Polym. Chem.* **2004**, 42, (17), 4327-4336.
17. Furlan, L.G.; Kunrath, F.A.; Mauler, R.S.; de Souza, R.F.; Casagrande, O.L. *J. Mol. Catal. A: Chem.* **2004**, 214, (2), 207-211.
18. Zhang, Z.C.; Lu, Z.X.; Chen, S.T.; Li, H.Y.; Zhang, X.F.; Lu, Y.Y.; Hu, Y.L. *J. Mol. Catal. A: Chem.* **2005**, 236, (1-2), 87-93.
19. Mecerreyes, D.; Moineau, G.; Dubois, P.; Jérôme, R.; Hedrick, J.L.; Hawker, C.J.; Malmström, E.E.; Trollsås, M. *Angew. Chem., Int. Ed.* **1998**, 37, (9), 1274-1276.
20. Bielawski, C.W.; Louie, J.; Grubbs, R.H. *J. Am. Chem. Soc.* **2000**, 122, (51), 12872-12873.
21. Peeters, J.; Palmans, A.R.A.; Veld, M.; Scheijen, F.; Heise, A.; Meijer, E.W. *Biomacromolecules* **2004**, 5, (5), 1862-1868.
22. van As, B.A.C.; Thomassen, P.; Kalra, B.; Gross, R.A.; Meijer, E.W.; Palmans, A.R.A.; Heise, A. *Macromolecules* **2004**, 37, (24), 8973-8977.
23. de Geus, M.; Peeters, J.; Wolffs, M.; Hermans, T.; Palmans, A.R.A.; Koning, C.E.; Heise, A. *Macromolecules* **2005**, 38, (10), 4220-4225.
24. Klaerner, G.; Trollsås, M.; Heise, A.; Husemann, M.; Atthoff, B.; Hawker, C.J.; Hedrick, J.L.; Miller, R.D. *Macromolecules* **1999**, 32, (24), 8227-8229.
25. Weimer, M.W.; Scherman, O.A.; Sogah, D.Y. *Macromolecules* **1998**, 31, (23), 8425-8428.
26. de Geus, M.; Schormans, L.; Palmans, A.R.A.; Koning, C.E.; Heise, A. *J. Polym. Sci., Part A: Polym. Chem.* **2006**, 44, (14), 4290-4297.
27. Villarroya, S.; Zhou, J.X.; Duxbury, C.J.; Heise, A.; Howdle, S.M. *Macromolecules* **2006**, 39, (2), 633-640.
28. Duxbury, C.J.; Wang, W.X.; de Geus, M.; Heise, A.; Howdle, S.M. *J. Am. Chem. Soc.* **2005**, 127, (8), 2384-2385.
29. Mecerreyes, D.; Trollsås, M.; Hedrick, J.L. *Macromolecules* **1999**, 32, (26), 8753-8759.
30. Drent, E.; Budzelaar, P.H.M. *Chem. Rev.* **1996**, 96, (2), 663-681.
31. Arriola, D.J.; Carnahan, E.M.; Hustad, P.D.; Kuhlman, R.L.; Wenzel, T.T. *Science* **2006**, 312, (5774), 714-719.
32. van As, B.A.C.; van Buijtenen, J.; Heise, A.; Broxterman, Q.B.; Verzijl, G.K.M.; Palmans, A.R.A.; Meijer, E.W. *J. Am. Chem. Soc.* **2005**, 127, (28), 9964-9965.
33. Buijtenen, J. van. Thesis, in press, Eindhoven University of Technology, 2006.
34. Reetz, M.T. *Curr. Opin. Chem. Biol.* **2002**, 6, (2), 145-150.
35. Varma, I.K.; Albertsson, A.C.; Rajkhowa, R.; Srivastava, R.K. *Progr. Polym. Sci.* **2005**, 30, (10), 949-981.
36. Dolman, M.; Halling, P.J.; Moore, B.D.; Waldron, S. *Biopolymers* **1997**, 41, (3), 313-321.
37. Gross, R.A.; Kumar, A.; Kalra, B. *Chem. Rev.* **2001**, 101, (7), 2097-2124.
38. The method used for end-group detection has an estimated detection limit of 5%. Therefore, we concluded that water initiation occurred to less than 5% of the polymer chains.
39. Lozano, P.; de Diego, T.; Carrie, D.; Vaultier, M.; Iborra, J.L. *Chem. Commun.* **2002**, (7), 692-693.
40. Lozano, P.; De Diego, T.; Carrie, D.; Vaultier, M.; Iborra, J.L. *Biotechnol. Progr.* **2003**, 19, (2), 380-382.

41. van As, B.A.C.; Chan, D.-K.; Kivit, P.J.J.; Palmans, A.R.A.; Meijer, E.W. *Manuscript in preparation*.
42. Kumar, A.; Gross, R.A. *Biomacromolecules* **2000**, 1, (1), 133-138.
43. Loeker, F.C.; Duxbury, C.J.; Kumar, R.; Gao, W.; Gross, R.A.; Howdle, S.M. *Macromolecules* **2004**, 37, (7), 2450-2453.
44. Mahapatro, A.; Kalra, B.; Kumar, A.; Gross, R.A. *Biomacromolecules* **2003**, 4, (3), 544-551.
45. Verzijl, G.K.M.; De Vries, J.G.; Broxterman, Q.B. Process for the preparation of enantiomerically enriched esters and alcohols. 2001-NL383, 2001090396, 20010521., 2001.
46. Krämer, R.; Maurus, M.; Bergs, R.; Polborn, K.; Sünkel, K.; Wagner, B.; Beck, W. *Chem. Ber.* **1993**, 126, (9), 1969-1980.
47. Pàmies, O.; Bäckvall, J.E. *J. Org. Chem.* **2002**, 67, (4), 1261-1265.
48. The absence of reactivity of DMP in enzymatic transesterification was confirmed by a control experiment.
49. Grey, R.A.; Pez, G.P.; Wallo, A. *J. Am. Chem. Soc.* **1981**, 103, 7536.
50. Hara, Y.; Inagaki, H.; Nishimura, S.; Wada, K. *Chem. Lett.* **1992**, (10), 1983-1986.
51. Zhang, J.; Leitus, G.; Ben-David, Y.; Milstein, D. *Angew. Chem., Int. Ed.* **2006**, 45, (7), 1113-1115.
52. An experiment in which ring-opening product **4a** was racemized and an additional unit of 6-MeCL was subsequently added, confirmed our hypothesis regarding the requirement of racemization for the propagation of the ring-opening product.
53. Magnusson, A.O.; Takwa, M.; Harnberg, A.; Hult, K. *Angew. Chem., Int. Ed.* **2005**, 44, (29), 4582-4585.
54. The degree of polymerization (DP) can be calculated from the <sup>1</sup>H NMR spectrum in Figure 4.2 using the following formula:  $DP = 1 + ( \text{integral area peak C} / ( \text{integral area peak D} - 0.5 * \text{integral area peak E} ) )$ . The diol-initiated oligomers have two secondary alcohol end-groups, hence the correction using the integral area of peak E. The DP calculated was not corrected for the presence of dimeric cycles.
55. The amount of diol-initiated oligomer can be quantified by means of the characteristic CH<sub>2</sub>OH-signal at  $\delta=4.1$  ppm.
56. Secundo, F.; Carrea, G.; Soregaroli, C.; Varinelli, D.; Morrone, R. *Biotechnol. Bioeng.* **2001**, 73, (2), 157-163.
57. The effect of the addition of Na<sub>2</sub>CO<sub>3</sub> was also investigated. It was found that Na<sub>2</sub>CO<sub>3</sub> did not show such a dramatic effect and almost full activity of the lipase was retained. However, Na<sub>2</sub>CO<sub>3</sub> is not suitable as a base for activation of the Ru complex, and therefore not applicable in one-pot ITC.
58. Huisgen, R.; Ott, H. *Tetrahedron* **1959**, 6, 253-67.
59. It is assumed that the dipole moment of 6-MeCL is similar to that of CL.
60. Garcia-Alles, L.F.; Gotor, V. *Biotechnol. Bioeng.* **1998**, 59, (2), 163-170.
61. Catalyst **1** was preformed in the presence of 2-propanol and K<sub>2</sub>CO<sub>3</sub>. After preformation approximately 2 mL of the catalyst solution was filtered through a 1  $\mu$ m PTFE syringe filter and added to the reaction mixture. Judging from the different values obtained for the TOF for the reference experiments without lactone, there is some variation between the different sets of experiments (Table 4.2, entries 1-4 and entries 5-8). In the experiments described in Table 4.2, entries 9-11, the catalyst was formed in-situ.

62. Since the racemization is now performed in the absence of lipase, isopropanol can be used to compensate for dehydrogenation. Isopropanol (and the acetone that is formed due to dehydrogenation) can be easily removed *in vacuo* after racemization has completed.
63. Feringa, B.L.; Smaardijk, A.; Wynberg, H. *J. Am. Chem. Soc.* **1985**, 107, (16), 4798-9.
64. The generation of the oligomer equals the number of enzymatic ring-opening reactions performed in its synthesis. The term generation was inspired by dendrimer nomenclature.
65. In the ideal case, a narrow molecular weight distribution is obtained. Since with every generation 50% of the chains propagate, the distribution is based on Pascal's triangle. However, transesterification is responsible for the observed relatively broad distribution.
66. Upon the use of different matrices distribution E disappears or shifts to different masses. Since the CHCA/DCTB matrix yields by far the clearest spectra, the spectra obtained using this matrix are displayed.
67. The amount of diol-initiated oligomer can be quantified by means of the characteristic CH<sub>2</sub>OH-signal at  $\delta=4.1$  ppm.
68. The percentage of intrachain esters in the R-configuration can be calculated using the following formula: fraction R-esters =  $\frac{1}{2} I^{-1} \times (I + E) \times (ee + 1)$  where I and E represent, respectively, the integrals in <sup>1</sup>H NMR for the intrachain esters and the end-groups, and ee is the measured enantiomeric excess of the methyl ester.
69. Trollsås, M.; Lee, V.; Mecerreyes, D.; Löwenhielm, P.; Möller, M.; Miller, R.; Hedrick, J. *Abstr. Pap. - Am. Chem. Soc.* **2000**, 219, U371-U371.

# 5

## Dynamic kinetic resolution polymerization of diols and diesters

### Abstract

Iterative tandem catalysis was extended to a polycondensation of a diol and a diester, dynamic kinetic resolution polymerization (DKRP). As a model system, the DKRP of 1,1'-(1,3-phenylene)diethanol (1,3-diol) and diisopropyl adipate was chosen. While the dynamic kinetic resolution (DKR) of 1,3-diol with isopropyl hexanoate as the acyl donor shows faster kinetics using catalyst **1**, we did not succeed in obtaining polymers by DKRP using this particular catalyst; severe deactivation of the lipase was observed. It was demonstrated that the solid base  $K_2CO_3$  – which is necessary for (re)activation of the catalyst – plays a crucial role herein.

With Shvo's catalyst **2**, chiral polymers were obtained from 1,3-diol and diisopropyl adipate. An optimization study was performed, which lead to the optimal conditions of 2 mol. % **2**, 12 mg Novozym 435 per mmol alcohol group in the presence of 0.5 M 2,4-dimethyl-3-pentanol (DMP) as the hydrogen donor. With these conditions, chiral polymers were obtained with peak molecular weights up to 15 kDa, ee's up to 99% and with 1-3% ketone functionalities. Also with the structural isomer 1,4-diol a chiral polyester was obtained, albeit with lower molecular weight and slightly lower ee. This can probably be attributed to the lack of optimization for this particular monomer.

The DKRP using aliphatic diols also succeeded, but did not lead to enantiopure polymers. At most, an ee of 46% was obtained with low molecular weights in the range of 3.3-3.7 kDa. A kinetic resolution experiment using vinyl acetate as the acyl donor showed that the selectivity of CALB towards the secondary alcohol groups of aliphatic diols is only moderate, explaining the low ee's obtained. The observations made clear that DKRP of these aliphatic diols is only possible if (1) a faster racemization catalyst becomes available that is compatible with this process or (2) a more enantioselective lipase is used, possibly to be obtained by modification of CALB.

## 5.1 Introduction

In Chapter 4, we introduced the concept of iterative tandem catalysis (ITC) as a polymerization strategy by which chain growth is effectuated by a combination of two (or more) intrinsically different catalytic processes that are both compatible and complementary. Proof of principle was provided by the ITC of 6-methyl- $\epsilon$ -caprolactone (6-MeCL). We showed that the lipase-catalyzed ring-opening of  $\omega$ -substituted lactones, such as 6-MeCL, results in a ring-opening product bearing a secondary alcohol. Since lipases generally only accept the *R*-enantiomer of a secondary alcohol as the nucleophile, propagation halts after the ring-opening of an (*S*)-6-MeCL molecule. Combining ruthenium-catalyzed racemization with lipase-catalyzed ring-opening enabled the two-pot oligomerization of (*S*)-6-MeCL (Scheme 5.1, type A).<sup>1</sup> An efficient one-pot polymerization proved difficult using catalyst **1** (Figure 5.1). It was shown that lipase activity was severely affected by the presence of the solid base  $K_2CO_3$ , which is necessary for (re)activation of catalyst **1**. Moreover, the racemization activity of catalyst **1** was shown to be severely affected by the presence of small-ring highly polar lactones, such as 6-MeCL. Recently, we achieved the synthesis of well-defined chiral 6-MeCL polymers in one pot, with ee's up to 96% and  $M_n$  up to 25 kDa.<sup>2</sup> This was realized by replacing racemization catalyst **1** by Shvo's catalyst, **2**, which does not require an additional base (Figure 5.1).<sup>3</sup> Details of this study are presented in the thesis of Jeroen van Buijtenen.<sup>4</sup>

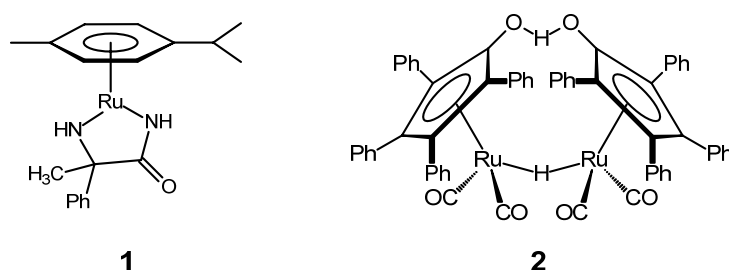
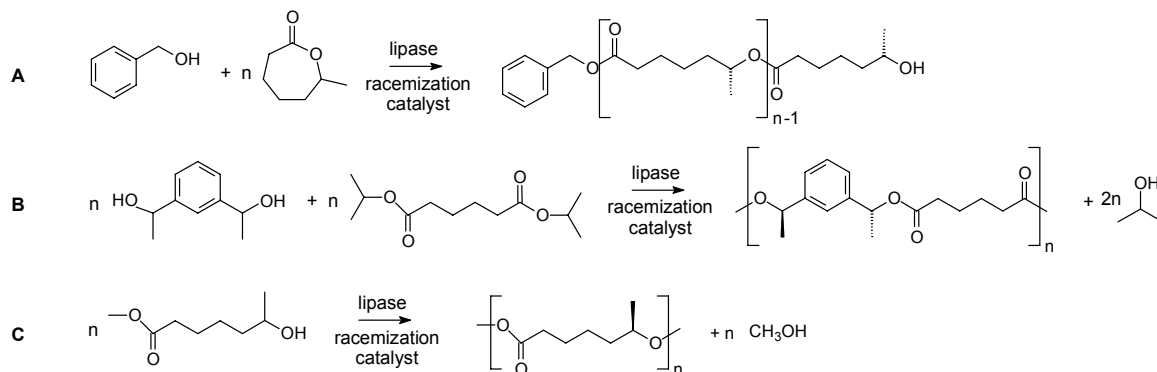


**Figure 5.1** Racemization catalysts employed in ITC.

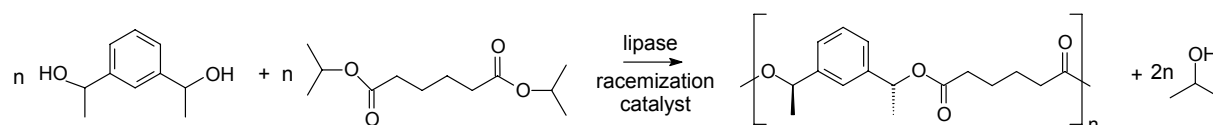
Using  $\omega$ -substituted lactones, the scope of ITC is limited to small-ring lactones only, such as 6-methyl- $\epsilon$ -caprolactone and 6-ethyl- $\epsilon$ -caprolactone. We recently found that the Novozym 435-catalyzed ring-opening of  $\omega$ -substituted lactones with a ring size larger than  $\epsilon$ -caprolactone displays strong *R*-selectivity, rendering these monomers useless for ITC.<sup>5</sup> To broaden the applicability of ITC in the synthesis of chiral polyesters, we aimed at performing a polycondensation with the same catalytic system. Two approaches can be envisioned: a copolymerization of a diol and a diester (AA/BB, Scheme 5.1, type B) or a homopolymerization of a hydroxyester (AB-monomer, Scheme 5.1, type C).<sup>6</sup> The use of diols and diesters is the most flexible approach, since a wide range of monomers can be used.

Moreover, a large variety of diesters is commercially available. The use of hydroxyesters, however, eliminates the need for exact stoichiometry of the diol and the diester, which is crucial in a polycondensation in order to achieve high molecular weights.<sup>7</sup>



**Scheme 5.1** Different variants of ITC based on the combination of enantioselective esterification and racemization.

Recently, initial efforts on achieving a DKR polycondensation (DKRP) were reported comprising a diol and a diester as the monomers and using complex **1** as the racemization catalyst.<sup>8</sup> Until now, only low molecular weight materials were obtained despite rather high lipase catalyst loadings (600 mg Novozym 435 per mmol diol). Here, we report on our efforts to improve the catalytic performance of DKRP. As model compounds, 1,1'-(1,3-phenylene)diethanol (1,3-diol) and diisopropyl adipate (DIA) were selected as the chiral diol and the diester, respectively (Scheme 5.2).<sup>9</sup> In order to explore the generality of DKRP, the 1,4-substituted structural isomer 1,4-diol and aliphatic diols were tested as well.



**Scheme 5.2** DKRP of 1,1'-(1,3-phenylene)diethanol (1,3-diol) and diisopropyl adipate (DIA).

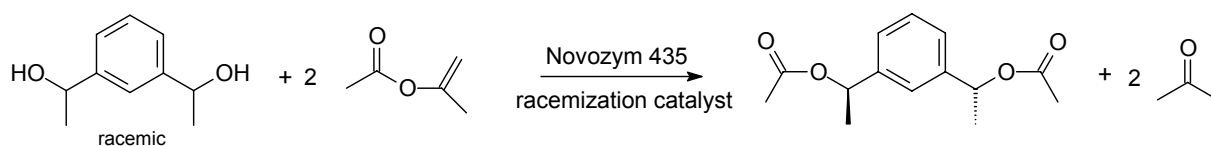
## 5.2 Selection of the racemization catalyst

The conditions required for a successful ITC (see Chapter 4) and for DKRP are quite similar. In both cases, a transesterification catalyst is required for the acylation of the *R*-alcohol and a racemization catalyst for providing reactive *R*-chain ends. However, the substrates used in DKRP and ITC are quite different. Moreover, the concentration of alcohol groups constantly decreases as alcohol functionalities gradually become acylated. Furthermore, in a polycondensation, significant oligomerization only occurs at appreciable conversion; at 50% conversion mainly dimers and trimers are present.

For ITC, the combination of Novozym 435 and catalyst **2** proved highly successful.<sup>2</sup> However, catalyst **2** shows much slower racemization activity than catalyst **1**. Therefore, we investigated the compatibility of both catalyst **1** and catalyst **2** with Novozym 435 under the required reaction conditions for DKRP. The catalysts **1** and **2** are described in more detail in Chapter 1.

### 5.2.1 Reference experiments with catalysts **1** and **2**

Firstly, we performed a kinetic resolution of 1,3-diol with isopropenyl acetate as the acyl donor (Scheme 5.3). The reaction was carried out without racemization catalyst and with racemization complexes **1** and **2** present. Since isopropenyl acetate is an activated ester, the enzymatic reaction is very fast and the racemization activity is assumed to be negligible compared to the rate of enzymatic acylation. This way, it is possible to compare the enzymatic activity with and without ruthenium catalyst present. As an objective measure of activity, the production rate of the *RR*-diester was taken. Figure 5.2 shows the normalized enzymatic activity as calculated from these experiments. As is clear from these data, the presence of either ruthenium catalyst does not have a large influence on the enzymatic activity.



**Scheme 5.3** Kinetic resolution of 1,3-diol using vinyl acetate as the acyl donor.

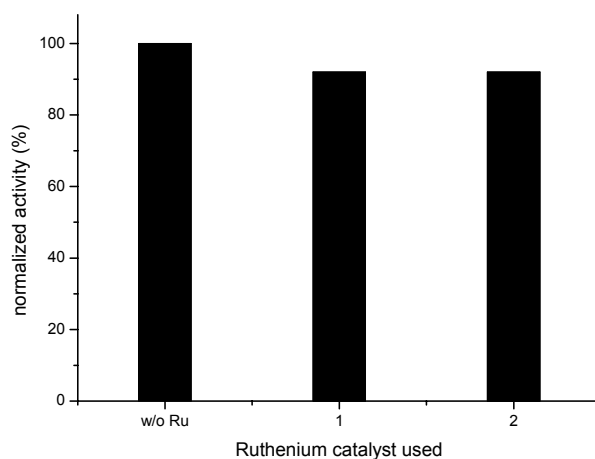
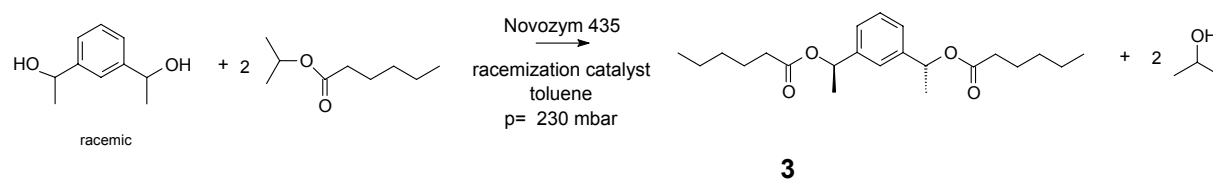


**Figure 5.2** Lipase activity in the kinetic resolution of 1,3-diol using isopropenyl acetate as the acyl donor without and in presence of ruthenium racemization catalysts. The activity was determined by measuring the initial production rate of the *RR*-diester and was normalized to 100% for the experiment without ruthenium.

Secondly, a DKR experiment was carried out using 1,3-diol as the alcohol and isopropyl hexanoate as the acyl donor in a 1 : 2 ratio, yielding chiral product **3** (Scheme 5.4). In this experiment, we followed the kinetics of the racemization catalysts **1** and **2** by probing the overall alcohol conversion as a function of time. Only *R*-alcohols are accepted by the lipase, so the conversion can only increase above 50% if racemization occurs. To remove isopropanol, the reaction was performed under reduced pressure (230 mbar).<sup>10</sup>

The results are shown in Figure 5.3. Clearly, both racemization catalysts are active, since all secondary alcohol groups are being acylated.<sup>11</sup> Moreover, using complex **1**, 94 % conversion is reached in less than 48 h, while the catalytic system employing catalyst **2** needs 80-100 hours to reach this conversion level. This indicates the faster racemization kinetics of complex **1**. Although the kinetics using 1,3-diol are slower than in a DKR experiment employing 1-phenylethanol as the chiral alcohol and DIA as the acyl donor (conversion of both enantiomers reached 95+% within 24h using 1 mol.% of complex **1** or **2** with respect to 1-phenylethanol; data not shown), both catalysts are very promising for the DKRP of 1,3-diol and diester.



**Scheme 5.4** Dynamic kinetic resolution of 1,3-diol using isopropyl hexanoate as the acyl donor.

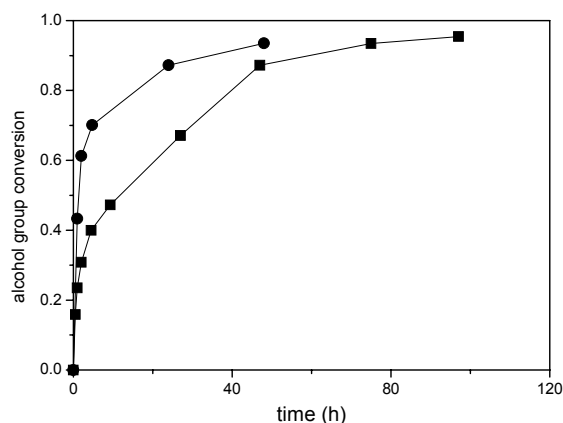


**Figure 5.3** Time-conversion plot for the dynamic kinetic resolution of 1,3-diol using isopropyl hexanoate as the acyl donor and **1** (●) or **2** (■) as the racemization catalyst. Conditions: 0.87 mmol 1,3-diol, 17.5 mmol isopropyl hexanoate, toluene (2 mL), DMP (120 mg); 2 mol.% Ru; 37 mg Novozym 435 / mmol alcohol functionality. The reaction was performed at 70 °C under reduced pressure (230 mbar).



From these results shown above, it is clear that the addition of either ruthenium catalyst has no significant effect on the activity of the lipase. The DKR experiment shows that complex **1** displays significantly faster kinetics than complex **2**. Therefore, complex **1** was selected as the racemization catalyst for DKRP.

### 5.2.2 DKRP using racemization catalyst **1**

DKRP is in essence the same reaction as DKR, but then performed with equimolar amounts of 1,3-diol and DIA (Scheme 5.2). A DKRP was performed using the more active complex **1** as the racemization catalyst. The reaction was performed in toluene at 70 °C and under an argon atmosphere. In order to shift the equilibrium to polymers, a reduced pressure of 280 mbar was applied to remove isopropanol. Figure 5.4 shows the conversion of alcohol groups versus time. An initially fast reaction was observed with a conversion level of 52% after 7 hours. This corresponds with fast acylation of the *R*-secondary alcohol groups in the reaction mixture. The rate of reaction then slows down severely. After reaching the 80% conversion level, the reaction does not proceed anymore. Addition of another batch of Novozym 435 at 120 h did not significantly increase the conversion level. This can be attributed either to a severe deactivation of the lipase, or to the presence of only *S*-alcohols, which are not accepted as a substrate, thereby preventing further consumption of the alcohol groups. At 145 h, a 2 mL aliquot was withdrawn from the reaction mixture and was tested separately on racemization activity by addition of (*S*)-1-phenylethanol. A turnover frequency (TOF) of 192 h<sup>-1</sup> for the racemization catalyst was calculated, which is in the normal range observed for this catalyst, indicating that the racemization catalyst is still fully active.<sup>12</sup> This suggests that deactivation of the lipase is the main cause of the slowing down of the reaction.

To improve the system, we tried several modifications, such as the addition of 2,4-dimethyl-3-pentanol (DMP) as a hydrogen donor, the use of dimethyl adipate instead of DIA as the acyl donor, the use of an aliphatic diol (2,5-hexanediol) instead of an aromatic diol, higher and lower concentration of monomer, different ruthenium loadings and the addition of molar sieves. Unfortunately, in all attempts, severe lipase deactivation was observed and no polymeric species were obtained. In conclusion, these results suggest that the residual activity of the lipase in this system, once oligomers have been formed, is very limited.

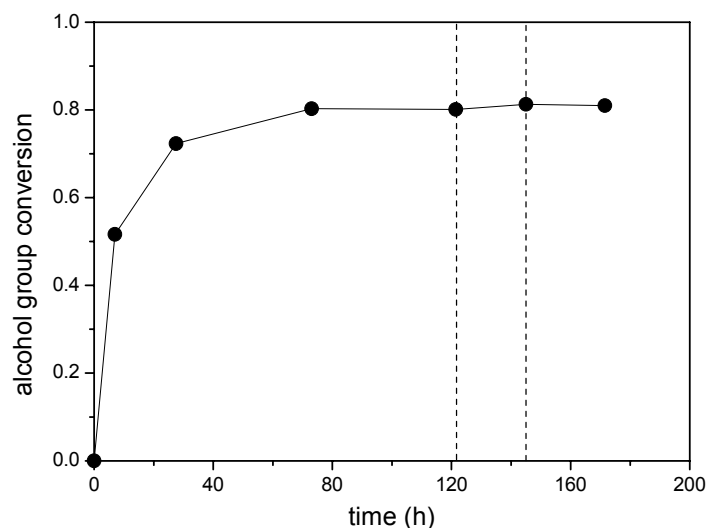


**Figure 5.4** Time-conversion plot for the DKRP of 1,3-diol and DIA using complex **1** as the racemization catalyst. The conversion was determined by  $^1\text{H}$  NMR. At 120 h (indicated with dotted line), 450 mg dried Novozym 435 was added. At 145 h (indicated with dotted line), a 2 mL aliquot was withdrawn from the reaction mixture to verify the racemization activity. Conditions: 6 mmol 1,3-diol, 6 mmol DIA, 50 mL toluene, 450 mg Novozym 435, 2 mol.% complex **1**, 500 mg  $\text{K}_2\text{CO}_3$ ,  $T=70^\circ\text{C}$ ,  $p=280$  mbar.

To investigate the deactivation of the lipase in more detail, an experiment was carried out using a 2:1 stoichiometry of 1,3-diol:DIA. In this way, the number of ester functionalities equals the number of *R*-secondary alcohols present in the system. Hence, racemization activity is not required in order to achieve full conversion of ester groups. The reaction was performed at reduced pressure to remove isopropanol. Figure 5.5 shows the conversion of ester groups versus time, as determined by  $^1\text{H}$  NMR. With only lipase present, the reaction proceeds smoothly to 94% conversion of ester groups in approximately 220 hours. The addition of Shvo's catalyst **2** is clearly beneficial to the rate of ester conversion; full conversion is observed in only 120 h. This can be attributed to the increased concentration of *R*-secondary alcohols due to the racemization activity. On the other hand, the addition of  $\text{K}_2\text{CO}_3$  leads to significant reduction in the rate of ester group conversion; the system does not even proceed beyond the 60% conversion level. Introduction of racemization catalyst **1** (consisting of  $[\text{RuCl}_2(\text{cymene})]_2$  precursor, (*rac*)-2-phenyl-2-amino-propionamide ligand and  $\text{K}_2\text{CO}_3$ ) leads to an even greater reduction in reaction rate and to similar deactivation behavior. Clearly, the presence of  $\text{K}_2\text{CO}_3$  and oligomeric species together leads in this system to deactivation of the lipase.

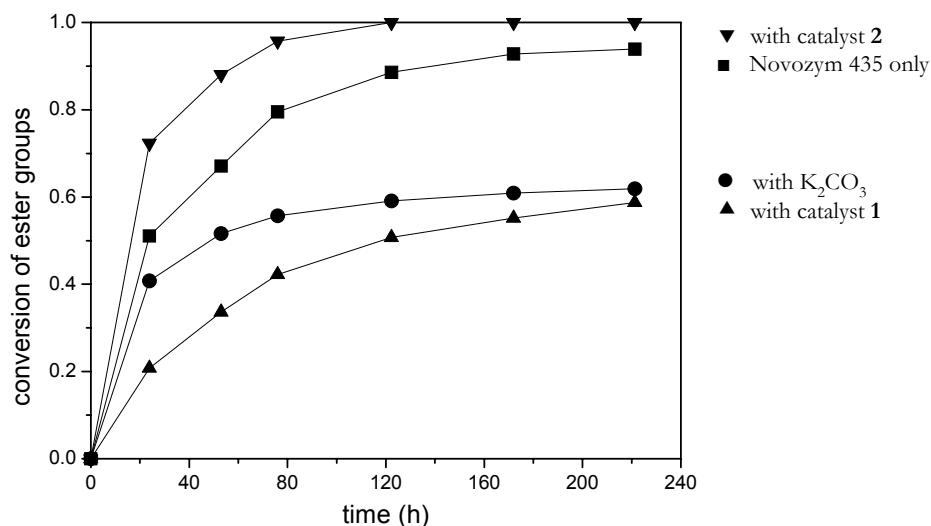


**Figure 5.5** Time-conversion plot for the transesterification of DIA by 2.05 equivalents of 1,3-diol using Novozym 435 only (■), with K<sub>2</sub>CO<sub>3</sub> (●), with catalyst 1 (▲) and with catalyst 2 (▼). The conversion was determined by <sup>1</sup>H NMR. Conditions: 1.8 mmol 1,3-diol; 0.9 mmol DIA; 40 mg Novozym 435; T=70 °C; 2 mL toluene; 100 mg K<sub>2</sub>CO<sub>3</sub>; 2 mol.% Ru with respect to alcohol groups; p=280 mbar.

Deactivation of Novozym 435 in the presence of K<sub>2</sub>CO<sub>3</sub> has been observed by us before in the polymerization of ε-caprolactone (see section 4.3.2). Also in those experiments, deactivation was only observed when oligomeric material was formed. Lipase deactivation was not observed in experiments with equimolar amounts of lactone and nucleophile. Moreover, DKR experiments using complex 1 never showed lipase deactivation.

Further evidence that the presence of oligomers enhances lipase deactivation is found in the DKRP experiments using complex 1. In these experiments, the initial lipase activity is high, but drops sharply when the conversion reaches 60-80% (Figure 5.4). In a polycondensation, significant oligomerization only occurs at appreciable conversion; at 50% conversion mainly dimers and trimers are present. In addition, we can rule out the hypothesis that the high polarity of the system in combination with K<sub>2</sub>CO<sub>3</sub> causes the deactivation; since the alcohol groups are acylated in the polymerization process, polarity drops as the reaction proceeds.

This leads us to the hypothesis that the deactivation of Novozym 435 may be caused by a combination of the presence of K<sub>2</sub>CO<sub>3</sub> and the formation of oligomeric or polymeric species (Figure 5.6). Further research on this subject is necessary in order to discover the exact nature of the observed deactivation.

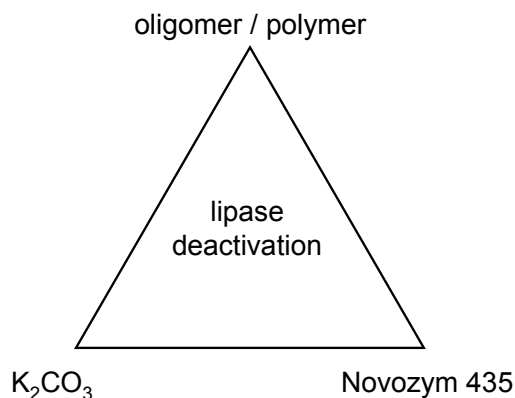


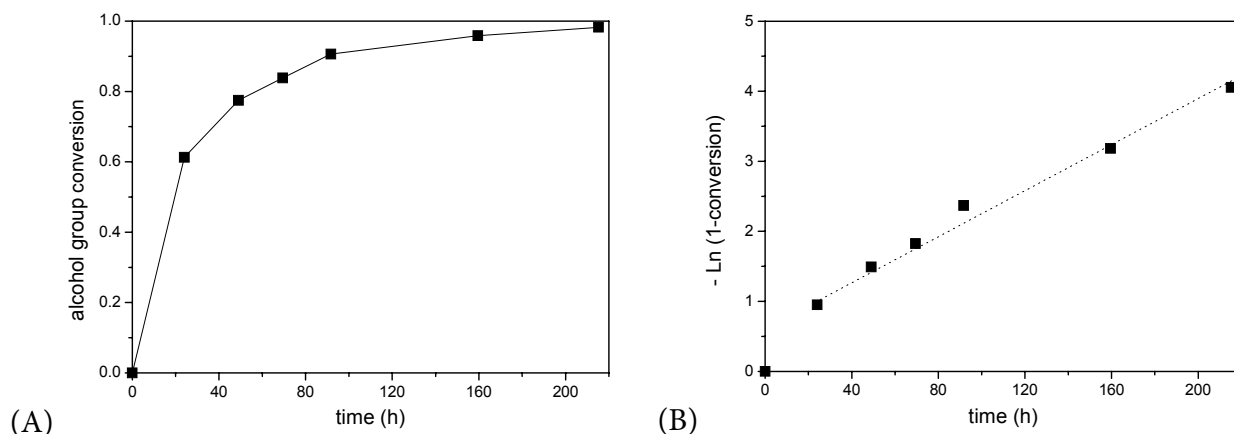
**Figure 5.6** Deactivation of Novozym 435 is only observed if both  $K_2CO_3$  and oligomeric or polymeric species are present.

### 5.2.3 DKRP using racemization catalyst 2

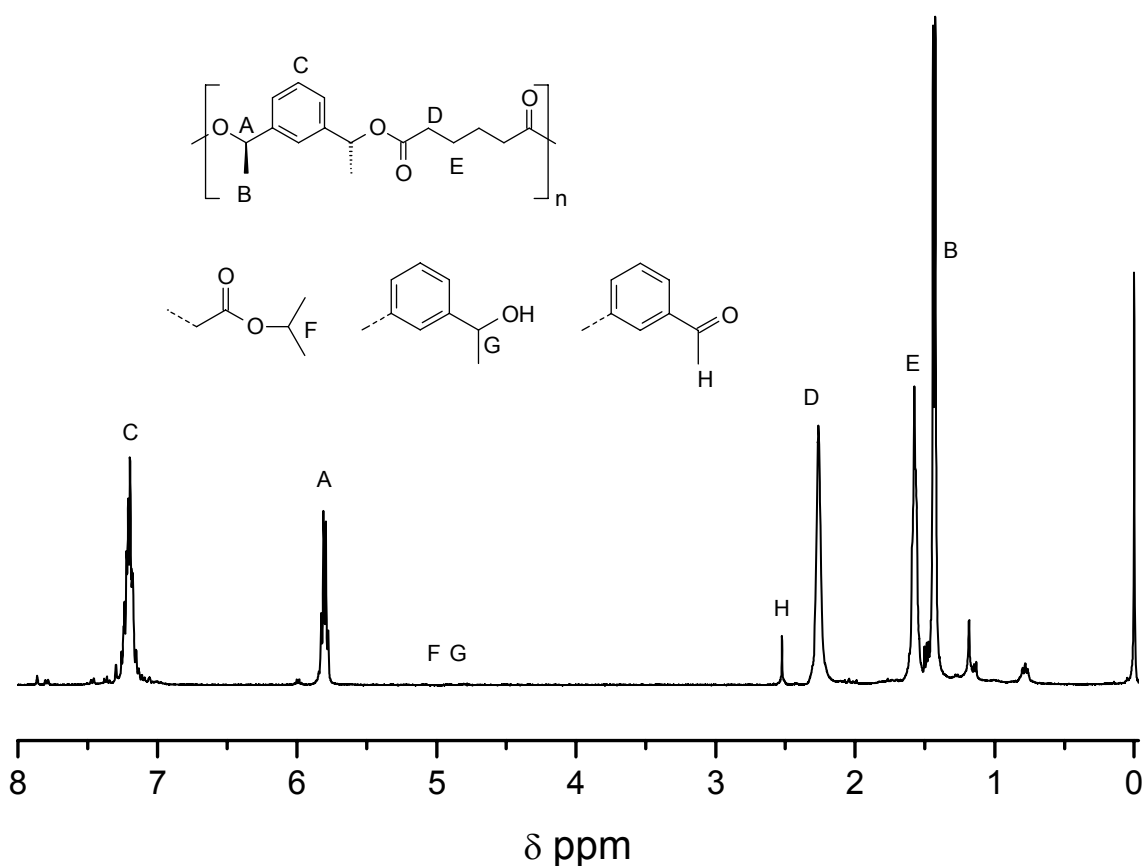
Since the  $K_2CO_3$  is needed to activate racemization complex **1**, we performed the DKRP of 1,3-diol and DIA using Shvo's catalyst **2** as the racemization catalyst. This racemization complex does not require an additional base. The reaction was performed in toluene at 70 °C. In order to shift the equilibrium to polymers, a vacuum of 280 mbar was applied to remove isopropanol. 2,4-Dimethyl-3-pentanol (DMP) was added here as a hydrogen donor to suppress dehydrogenation of end-groups, a strategy successfully employed by us previously (see section 4.3). Figure 5.7A shows the time-conversion plot for the acylation of the alcohol groups. The polymerization now proceeded smoothly; in 215 h, a conversion level of 98% was observed. Initially, the reaction proceeds quickly, with a conversion level of 61% reached within 24 hours. At this point, all *R*-secondary alcohol functionalities have been acylated and the racemization reaction has now become rate-limiting. Figure 5.7B shows that, once the 50% conversion threshold has been passed, an approximately linear relationship between the natural logarithm of (1 – conversion of alcohol groups) and time is observed, indicating first order kinetic behavior.<sup>13</sup> This linear relationship allows the calculation of a pseudo first order rate constant, in this case  $k_i = 15.8 \cdot 10^{-3} \text{ h}^{-1}$ .

Figure 5.8 shows the  $^1\text{H}$  NMR spectrum obtained from this polymer. The end-groups that appear at 4.9 and 5.0 ppm (designated with F and G in Figure 5.8) have almost fully disappeared and the intrachain  $\beta$ -hydrogens are observed 5.8 ppm (designated with A in Figure 5.8). Analysis of the polymer by GPC indicated that indeed polymeric material had been formed; a peak molecular weight  $M_p$  of 10.7 kDa was calculated (Figure 5.9). To confirm the formation of an enantiomerically enriched polyester, the polymer was degraded under basic conditions (overnight stirring at room temperature in 0.5 M NaOH in ethanol), restoring the 1,3-diol. Analysis by chiral GC indicated an ee of 92% for the alcohol groups in the polymer. A total amount of 0.5% of ketone functionalities was calculated from the chiral GC trace, which is surprisingly low considering the dehydrogenation potential of the Shvo-

catalyst.<sup>14</sup> Based on these results, we concluded that the DKRP of 1,3-diol and DIA using Novozym 435 and racemization catalyst **2** was successful and an enantioenriched polyester has been formed.



**Figure 5.7** (A) Time-conversion plot for the DKRP of 1,3-diol and DIA using Novozym 435 and Shvo's catalyst **2**; 1 mol.% Ru; 23 mg Novozym 435 per mmol alcohol functionality; 0.7 M DMP;  $T=70\text{ }^{\circ}\text{C}$ ; solvent: toluene;  $p=280\text{ mbar}$ . The conversion was determined by  $^1\text{H}$  NMR. (B) Logarithmic plot of (1-conversion of alcohol groups) versus time.



**Figure 5.8**  $^1\text{H}$  NMR spectrum of the polymer obtained from the DKRP of 1,3-diol with DIA.

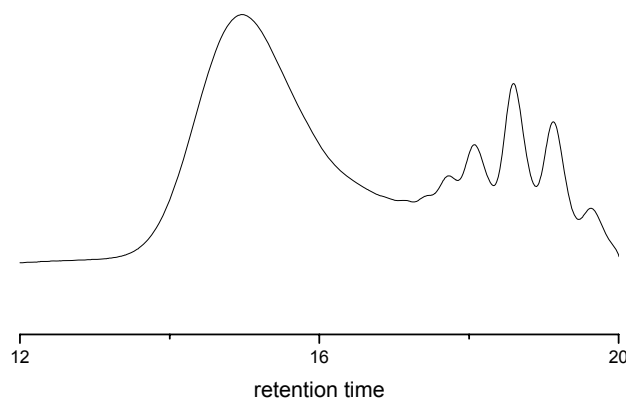


**Figure 5.9** GPC trace of the polymer obtained from the DKRP of 1,3-diol with DIA.

### 5.3 DKRP of other substrates

In order to investigate the scope of DKRP, we investigated the use of several other diols as monomers (Figure 5.10). Table 5.1 summarizes the results obtained. In all polymerizations, DIA was used as the diester. The reactions were performed in toluene at 70 °C with 2 mol.% of catalyst **2** and 23 mg Novozym 435 per mmol alcohol group. 0.5 M DMP was added as a hydrogen donor. In order to shift the equilibrium to polymers, a vacuum of 280 mbar was applied to remove isopropanol.

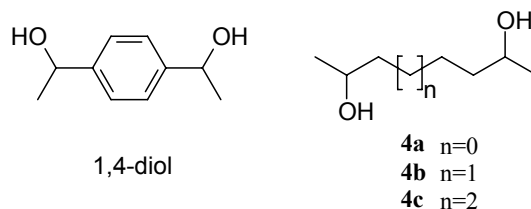


**Figure 5.10** 1,4-Diol and aliphatic diols employed in DKRP.

Entry 1 shows that 1,4-diol could be successfully subjected to DKRP. The polymerization proceeded smoothly to 97% conversion, and in 171 h a polymer was obtained with a peak molecular weight of 8.3 kDa (Table 5.1, entry 1). The amount of ketone functionalities was found to be 2.4%, while the enantiomeric excess of this polymer was 94%.

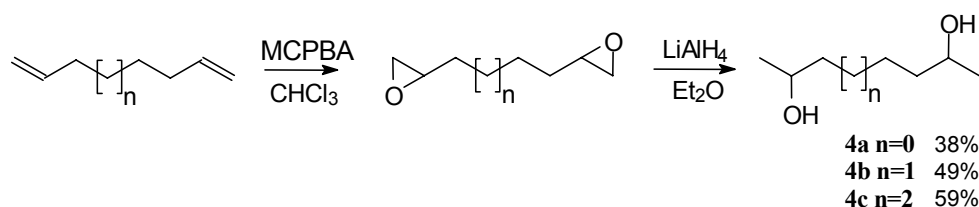
**Table 5.1** Results of the DKRP of 1,4-diol and aliphatic diols using DIA as the diester

Entry <sup>a</sup>	Monomer <sup>b</sup>	Time (h)	Conv. (%) <sup>d</sup>	$k_i \cdot 10^3$ (h <sup>-1</sup> ) <sup>e</sup>	ee <sub>p</sub> (%)	M <sub>p</sub> (kDa)	ketone (%)
1	1,4-diol	171	97	20.9	94%	8.3	2.4%
2	<b>4a</b>	390	98	6.5	43%	3.3	n.d.
3	<b>4b</b>	390	94	4.6	41%	3.7	n.d.
4	<b>4c</b>	310	98	9.1	46%	3.7	n.d.

<sup>a</sup> Conditions: 0.87 mmol diol, 0.87 mmol DIA, 0.034 mmol catalyst **2**, 40 mg Novozym 435, 3 Å m.s., 0.5 M DMP, 2 mL dry toluene; T = 70 °C; p=280 mbar. <sup>b</sup> The synthesis of monomers **4a-c** is described in Scheme 5.5 <sup>c</sup> The catalyst loadings are calculated with respect to the total amount of alcohol groups. <sup>d</sup> Conversion is based on the total conversion of alcohol groups. <sup>e</sup> The initial rate constant  $k_i$  was determined by linear regression from the logarithmic plot of (1 – conversion of alcohol groups) versus time.

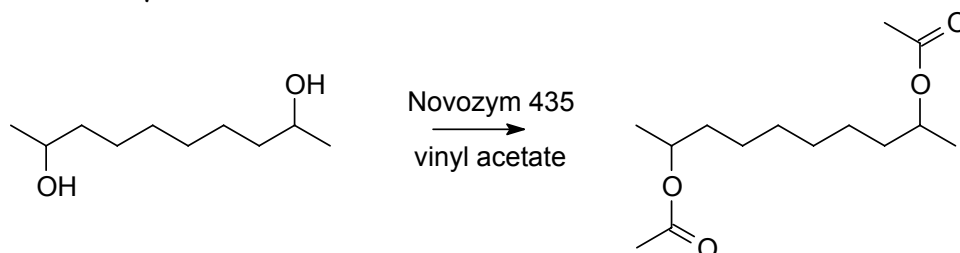
Extending on these results, we sought to polymerize aliphatic diols. It has been reported that the enantioselective CALB-catalyzed esterification of short-chain aliphatic diols such as 2,4-pentanediol and 2,5-hexanediol is problematic and leads to significant formation of the *meso*-diester. In case of 2,4-pentanediol this was attributed to intramolecular acyl transfer. In case of 2,5-hexanediol the formation of the *meso*-diester was caused by reduced specificity of CALB towards the second alcohol moiety once the first *R*-secondary alcohol group was acylated due to a neighboring group effect.<sup>19</sup> Hence, we chose to investigate the use of longer aliphatic diols.

Since these substrates are not commercially available, they were synthesized from the appropriate dienes by first converting the latter to the diepoxide by treatment with *m*-chloroperbenzoic acid (MCPBA). Reduction with LiAlH<sub>4</sub> furnished selectively the aliphatic secondary diols **4a-c** in yields of 38 to 59% (Scheme 5.5). By careful reduction (ice-cooled), the amount of primary alcohol groups could be limited to 2-3%. Since primary alcohols are readily acylated by the lipase, this impurity does not pose a problem in DKRP.

**Scheme 5.5** Synthesis of aliphatic secondary diols from the corresponding dienes.

Although the enantioselectivity of CALB towards linear secondary alcohols is very high (for 2-octanol an E value of 340 was reported<sup>20</sup>), this is not necessarily also the case for

aliphatic diols. Therefore, we first investigated the enantioselectivity of CALB towards aliphatic diols in a kinetic resolution experiment. **4c** was subjected to enzymatic acylation as depicted in Scheme 5.6. To ensure a fast reaction, vinyl acetate was selected as the acyl donor, a substrate that is frequently used in kinetic resolution experiments.<sup>21</sup> The reaction was performed in toluene at 70 °C. If the enantioselectivity of CALB in the acylation of the first secondary alcohol group is sufficiently high, then a negligible amount of the *SS*-diastereomer would react away.



**Scheme 5.6** Lipase-catalyzed acylation of **4c** with vinyl acetate as the acyl donor.

The time-conversion plot of this reaction is shown in Figure 5.11. The *RR*- and *RS*-diastereomers quickly react away, with – as expected – the highest reaction rate for the *RR*-diastereomer. However, the *SS*-diastereomer also shows considerable reactivity.<sup>22</sup> Figure 5.12 shows the composition of the reaction mixture as determined by chiral GC. Within 40 minutes, all of the *RR*-diastereomer is converted into the *RR*-diester, while it takes considerably more time before significant amounts of the *RS*- and *SS*-diesters are observed.<sup>23</sup> Comparison of the logarithmic plots (not shown) indicated that the *RR*-enantiomer reacted approximately 30 times faster than the *SS*-enantiomer. This indicates that the enantioselectivity for CALB is considerably lower for **4c** than for regular secondary alcohols, such as 2-octanol.



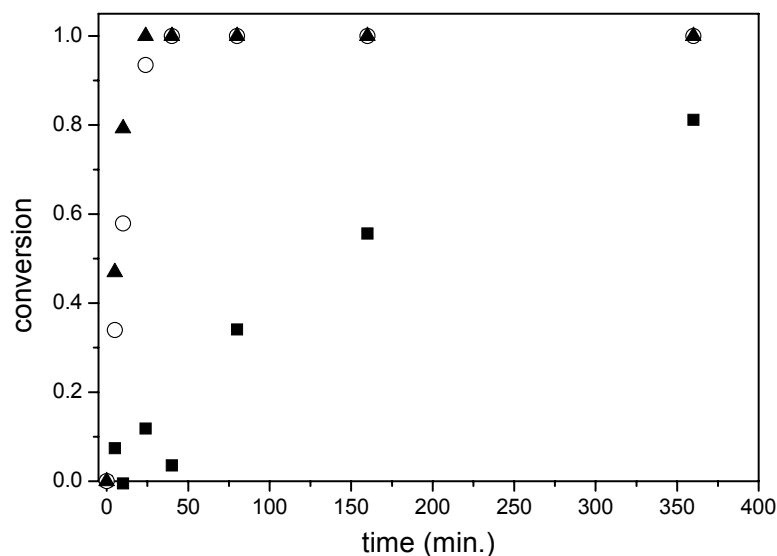


**Figure 5.11** Time-conversion plot for the lipase-catalyzed acylation of **4c** using vinyl acetate as the acyl donor; SS-diol (■), RS-diol (○), RR-diol (▲). Conditions: 25 mg Novozym 435, 1.15 mmol **4c**, 4.64 mmol vinyl acetate, 5 mL toluene,  $T=70\text{ }^{\circ}\text{C}$ .

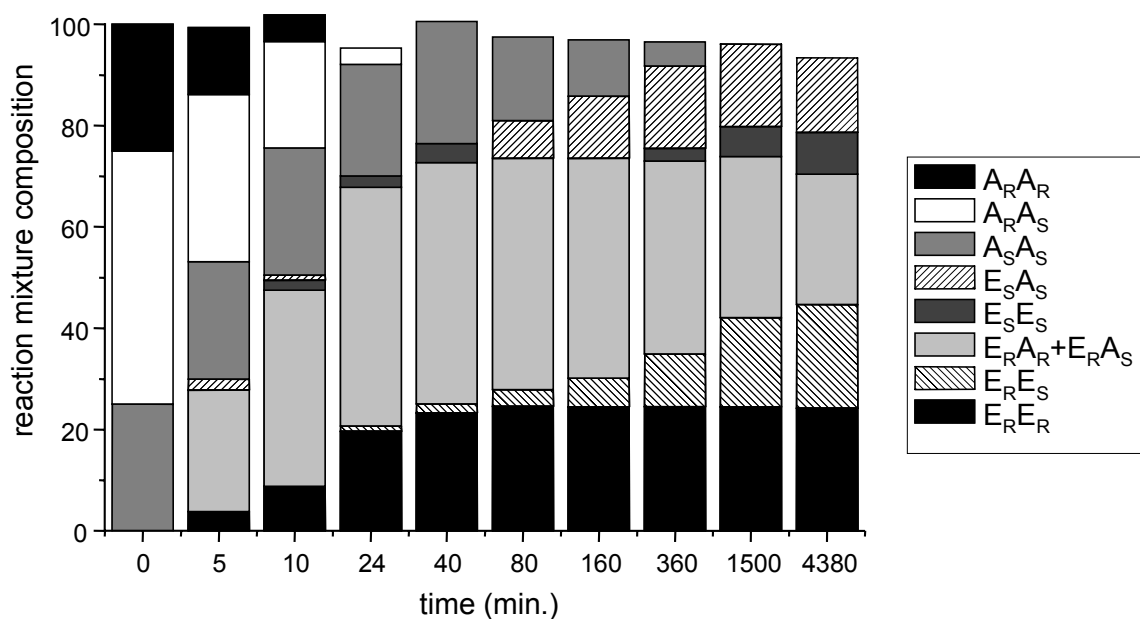


**Figure 5.12** Composition of the reaction mixture of the lipase-catalyzed acylation of **4c** with vinyl acetate as the acyl donor. A: alcohol group; E: ester group; the subscripts denote the configuration of the alcohol or ester.

Although the kinetic resolution of **4c** did not proceed with high enantioselectivity, we performed a one-pot DKRP using aliphatic diols **4a-c** and DIA (Table 5.1, entries 2 to 4). Gratefully, we concluded that for all monomers indeed polymerization took place and conversions of 94-98 % were reached, although long reaction times were necessary to reach this conversion level (310 to 390 h). The ee's of these polymers were low with values ranging

from 41 to 46 %. As expected, considerable acylation of the S-secondary alcohol groups has taken place. The peak molecular weights of these polymers were in the range of 3.3-3.7 kDa; considerably lower than using aromatic diols. Presumably, these relatively low molecular weights can be attributed to a relatively high extent of dehydrogenation of end-groups.

#### 5.4 Optimization study of the DKRP of 1,3-diol and DIA using catalyst 2

Encouraged by the promising result of the DKRP of 1,3-diol and DIA, we started to optimize this polymerization. We focused on obtaining high molecular weight polymers with high optical purity, while minimizing reaction time. Since the molecular weight in a polycondensation is highly dependent on stoichiometry, the percentage of ketone end-groups is the only reasonable parameter to consider, since ketone end-groups act as chain stoppers. As DMP is used as a hydrogen donor in order to suppress dehydrogenation, the concentration of DMP is thought to be of importance. Naturally, the catalyst loadings may have an effect on the rate of reaction observed. Therefore, we evaluated the effect of DMP concentration and the catalyst loadings employed on the kinetics, the optical purity and the percentage of end-groups in the isolated polymers. In all experiments, first order kinetic behavior was observed after 50% of the alcohol groups were acylated. The calculated rate constants are related to this stage of the reaction. The results of this study are given in Table 5.2.

**Table 5.2** Results of the dynamic kinetic resolution polymerization of 1,3-diol and DIA.

Entry <sup>a</sup>	Ru mol % <sup>b</sup>	Nov435 mg/mmol <sup>b</sup>	DMP (M)	Time (h)	Conv. (%) <sup>c</sup>	$k_i \cdot 10^3$ (h <sup>-1</sup> ) <sup>d</sup>	ee <sub>p</sub> (%)	M <sub>p</sub> (kDa)	ketone (%)
1	0.5	23	0.5	121	97	18.3	93%	7.2	2.2%
2	1	12	0.5	121	98	25.8	98%	5.2	2.2%
3	1	46	0.5	121	98	26.9	92%	7.7	2.3%
4	2	23	0.5	121	99	48.5	95%	12.3	1.9%
5	2	23	0.1	118	95	33.0	99%	8.4	2.2%
6	4	23	0.1	118	99	26.9	99%	15.4	3.1%
7	2	23	0.2	118	98	38.3	98%	14.0	1.8%
8	1	23	0.7	223	96	12.0	95%	4.5	0.8%
9	1	23	3.9	168	57	1.7	n.a.	n.a.	n.a.
10 <sup>e</sup>	2	23	0.5	98	78	12.5	n.a.	n.a.	n.a.
11 <sup>e</sup>	6	23	0.5	98	86	13.9	n.a.	n.a.	n.a.

<sup>a</sup> Condition: 0.87 mmol diol, 0.87 mmol DIA, 3Å m.s., 2 mL toluene, T=70 °C; p=280 mbar.

<sup>b</sup> The catalyst loadings are calculated with respect to the total amount of alcohol groups.

<sup>c</sup> Conversion is based on the total conversion of alcohol groups. <sup>d</sup> The initial rate constant  $k_i$  was determined by linear regression from the logarithmic plot of (1 – conversion of alcohol groups) versus time. <sup>e</sup> 6 mL toluene was used instead of 2 mL.

*Effect of the lipase loading*

The amount of lipase that is used in DKRP might have an influence on the kinetics, as well as on the optical purity of the polymer obtained. In DKR experiments using racemization catalyst **2**, usually racemization is the rate-limiting process, since the racemization activity of catalyst **2** is much lower than the acylation activity of the lipase. If this is also the case in DKRP, the observed kinetics would not change when increasing or decreasing the lipase catalyst loading. The optical purity might decrease if the amount of lipase is increased. The rate of acylation of *S*-secondary alcohols is very low, and insignificant with respect to overall rate of acylation; however, the effect of more lipase can have a significant negative effect on the ee of the polymer. By performing the DKRP at lipase catalyst loadings of 12 and 46 mg per mmol alcohol functionality, the effect on these parameters was investigated. The results are visualized in Figure 5.13.

Entries 2 and 3 show that indeed, as expected, the lipase loading does not have an influence on the net rate of reaction; the calculated reaction rate constants for the experiments with 12 and 46 mg Novozym 435 per mmol alcohol functionality were  $25.8$  and  $26.9 \cdot 10^{-3} \text{ h}^{-1}$ , respectively (Figure 5.13A). Apparently, the racemization is rate-limiting even when using only 12 mg Novozym 435 per mmol alcohol functionality.

The optical purity of the polymer, however, is dependent on the amount of lipase used. Entries 2 and 3 clearly show that an increase in the amount of enzyme from 12 to 46 mg/mmol alcohol functionality leads to a decrease in the ee of the polymer from 98% to 92% (Figure 5.13B).

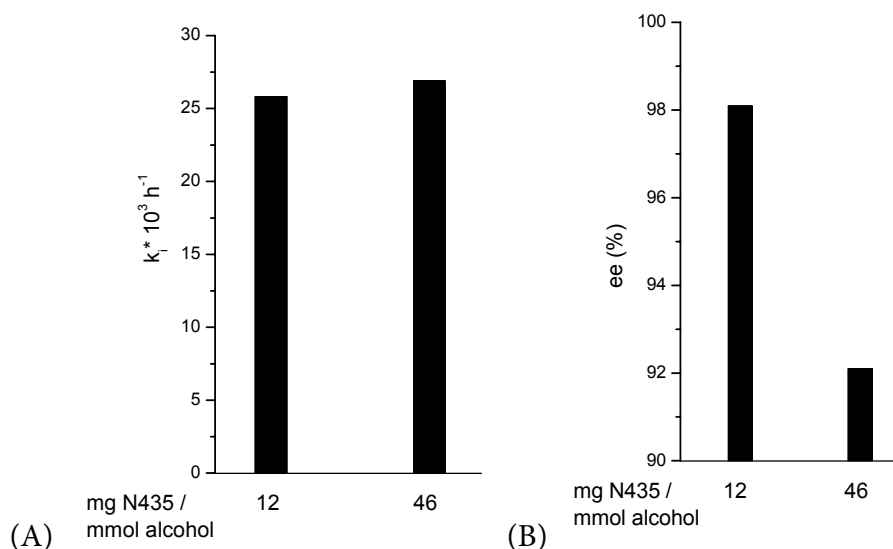


**Figure 5.13** Effect of the enzyme concentration on the rate of reaction (A) and ee (B) of the polymer obtained (Table 5.1, entries 2 and 3).

*Effect of the ruthenium loading*

Since the racemization is rate-limiting after 50% conversion, it is expected that the kinetics are dependent on the ruthenium loading. To investigate this, the DKRP was carried out with ruthenium loadings of 0.5 mol.% to 4 mol.% (entries 1 and 3 to 6). Also, the effect of the concentration of ruthenium was investigated by diluting the system (entries 10 and 11). The results are visualized in Figure 5.14.

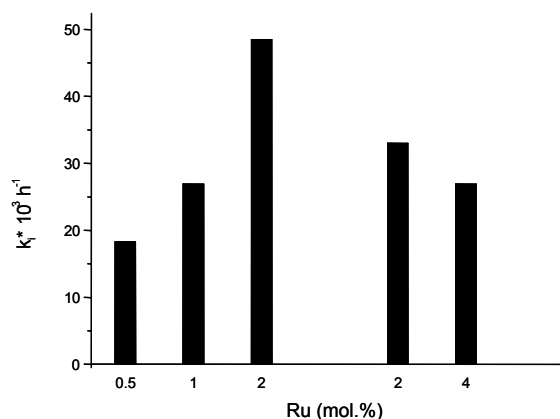


**Figure 5.14** Effect of the ruthenium loading on the kinetics of the polymerization (Table 5.1, entries 1, 3, 4, 5 and 6). The two experiments with 2 mol.% Ru are at different DMP concentration and, therefore, display different reaction rates.

Entries 1, 3 and 4 show that an increase from 0.5 mol.% to 2 mol.% results in a faster rate of reaction (left part of Figure 5.14): the calculated rate constants were  $18.3$ ,  $26.9$  and  $48.5 \cdot 10^{-3} \text{ h}^{-1}$ , respectively. As shown by entries 5 and 6, surprisingly, a further increase to 4 mol.% leads to slightly slower kinetics (right part of Figure 5.14): the calculated rate constants were  $33.0$  and  $26.9 \cdot 10^{-3} \text{ h}^{-1}$ , respectively.<sup>15,16</sup>

A threefold dilution of the system by using more solvent resulted in a sharp decrease in reaction rate (entry 10); a rate constant of only  $12.5 \cdot 10^{-3} \text{ h}^{-1}$  was calculated. This is attributed to slower racemization kinetics due to the lower alcohol concentration.<sup>17</sup> An alternative explanation would be that the equilibrium between the inactive dimeric ruthenium-precursor and the active 16-electron Ru(0)- and 18-electron Ru(II)-complexes (see section 1.4.2) is affected by the dilution. However, the experiment with a threefold dilution while keeping the ruthenium concentration constant with respect to the undiluted experiments with 2 mol.% (thus effectively increasing the ruthenium loading to 6 mol.%) shows that this is not the case, as the kinetics of this experiment are equally slow with a  $k_i$  of  $13.9 \cdot 10^{-3} \text{ h}^{-1}$  (entry 11).

*Effect of the DMP concentration*

DMP is added to the DKRP system to suppress dehydrogenation of alcohols group. Therefore, it is of interest to investigate the effect of different concentrations of DMP on the

amount of ketone end-groups in the isolated polymers. Although DMP is a sterically hindered hydrogen donor, it acts a competitive substrate for the racemization catalyst. Thus, it is expected that DMP has an influence on the racemization kinetics. By changing the DMP concentration from 0.1 M to 3.9 M, these effects were investigated (entries 3 to 5 and 7 to 9).

Increasing the DMP concentration from 0.1 to 0.5 M lead to significantly faster kinetics with  $k_i$ -values of 33.0, 38.3 and  $48.5 \cdot 10^{-3} \text{ h}^{-1}$ , respectively (entries 5, 7 and 4; left part of Figure 5.15). A further increase from 0.5 M to 3.9 M resulted in a sharp decrease in reaction rate (entries 3, 8 and 9; right part of Figure 5.15); the calculated  $k_i$ -values were 26.9, 12.0 and  $1.7 \cdot 10^{-3} \text{ h}^{-1}$ , respectively.<sup>18</sup> Apparently, the addition of a limited amount of DMP results in faster kinetics; possibly the change in polarity affects the equilibrium between inactive dimeric ruthenium precursor and the active monomeric complexes (see section 1.4.2), or in higher activity of these active complexes. At higher concentrations, substrate competition by DMP prevails, and net kinetics slow down severely. Finally, the amount of ketone functionalities appeared to be independent of the DMP concentration; percentages of ketone always were in the 0.5-3.1% range and no clear trend could be observed.

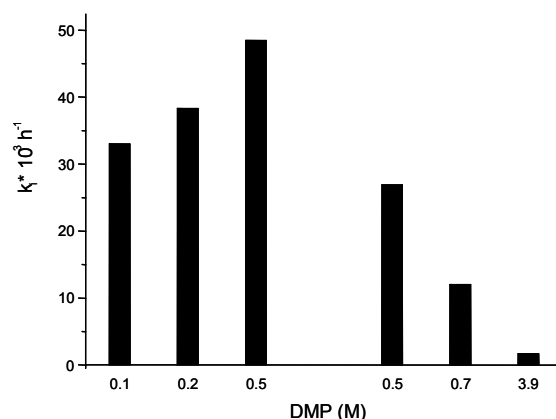


**Figure 5.15** Effect of the amount of hydrogen donor DMP on the kinetics of the polymerization (Table 1, entries 6, 8, 5, 4, 9 and 10). The two experiments with 0.5 M DMP are at different catalyst loadings and, therefore, display different reaction rates.

In conclusion, we showed that the amount of lipase has no significant influence on the overall kinetics of DKRP. The optical purity of the polymer, however, was optimal at 12 mg lipase per mmol alcohol functionality. The overall kinetics were fastest when using 2 mol% ruthenium catalyst. The DMP concentration had no influence on the amount of ketone functionalities in the isolated polymers; the overall kinetics of DKRP, however, were fastest at 0.5 M. From these results, we concluded that the optimal conditions for the DKRP of 1,3-diol and DIA are 2 mol.% ruthenium catalyst, 12 mg Novozym 435 per mmol alcohol functionality and 0.5 M DMP.

## 5.5 Conclusions

Iterative tandem catalysis was extended to a polycondensation of a diol and a diester, dynamic kinetic resolution polymerization (DKRP). As a model system, the DKRP of 1,1'-(1,3-phenylene)diethanol (1,3-diol) and DIA was chosen. While the dynamic kinetic resolution (DKR) of 1,3-diol with isopropyl hexanoate as the acyl donor shows faster kinetics using catalyst **1**, we did not succeed in obtaining polymers by DKRP using this particular catalyst; severe deactivation of the lipase was observed. It was demonstrated that the solid base  $K_2CO_3$  – which is necessary for (re)activation of the catalyst – plays a crucial role herein.

With Shvo's catalyst **2**, chiral polymers were obtained from 1,3-diol and DIA. An optimization study was performed, which led to the optimal conditions of 2 mol. % **2**, 12 mg Novozym 435 per mmol alcohol group in the presence of 0.5 M 2,4-dimethyl-3-pentanol (DMP) as the hydrogen donor. With these conditions, chiral polymers were obtained with peak molecular weights up to 15 kDa, ee's up to 99% and with 1-3% ketone functionalities. Also with the structural isomer 1,4-diol a chiral polyester was obtained, albeit with lower molecular weight and slightly lower ee. This can probably be attributed to the lack of optimization for this particular monomer.

The DKRP using aliphatic diols also succeeded, but did not lead to enantiopure polymers. At most, an ee of 46% was obtained with low molecular weights in the range of 3.3-3.7 kDa. A kinetic resolution experiment using vinyl acetate as the acyl donor showed that the selectivity of CALB towards the secondary alcohol groups of aliphatic diols is only moderate, explaining the low ee's obtained. The observations made clear that DKRP of these aliphatic diols is only possible if (1) a faster racemization catalyst becomes available that is compatible with this process or (2) a more enantioselective lipase is used, possibly to be obtained by modification of CALB.

## 5.6 Experimental section

### Materials

1,1'-(1,3-Phenylene)diethanol (1,3-diol) and 1,1'-(1,4-phenylene)diethanol (1,4-diol) were synthesized by reduction of the corresponding ketone with  $NaBH_4$  according to a literature procedure.<sup>24</sup> Diisopropyl adipate (DIA) was purchased from TCI Europe. Novozym 435 was purchased from Novozymes A/S. All solvents were purchased from Biosolve and stored on dry molecular sieves (4 Å) prior to use to remove traces of water. (*rac*)-2-Phenyl-2-amino-propionamide was a gift from DSM Research. Shvo's catalyst **2** was purchased from Strem Chemicals. All other chemicals were purchased from Aldrich and used as received unless otherwise noted.

*Analytical methods*

$^1\text{H}$  and  $^{13}\text{C}$  NMR spectra were measured in  $\text{CDCl}_3$  at 400, 300 or 200 MHz ( $^1\text{H}$  NMR) and 100, 75 or 50 MHz ( $^{13}\text{C}$  NMR) using a Varian Mercury Vx 400, 300 or 200 spectrometer. Chiral gas chromatography (GC) was performed on a Shimadzu 6C-17A GC equipped with a Chrompack Chirasil-DEX CB (DF=0.25) column and an FID. Samples were injected using a Shimadzu AOC-20i autosampler. Injection and detection temperatures were set at 250 °C and 300 °C, respectively. Conversions were determined by the internal standard method using 1,3,5-tri-*tert*-butylbenzene as the internal standard. The  $ee_m$  was calculated as follows:  $ee_m = (R-S)/(R+S)$  where R and S represent the area of the GC peaks of the *R*- and *S*-enantiomer, respectively. Samples containing 1,4-diol were - prior to analysis - derivatized with butyric anhydride for 16 h at 80 °C in toluene. GC-MS spectra were taken with a Shimadzu GC-17A employing a Zebron-ZB-5 column (DF ) 0.25 mm). Injector and detector temperatures were set at 300 °C. Gel permeation chromatography (GPC) was carried out on a Shimadzu HPLC system equipped with a Shimadzu LC-10AD VP pump, a Shimadzu RID-10A differential refractometer detector and two PL gel columns (mixed C and mixed D, 10  $\mu\text{m}$ , 300  $\times$  7.5 mm, Polymer Laboratories), using THF as the eluent. All molecular weights are given relative to polystyrene standards.

*Kinetic resolution of 1,3-diol using isopropenyl acetate as the acyl donor*

Novozym 435 (10 mg), 1,3-diol (100 mg, 0.60 mmol), isopropenyl acetate (150 mg, 1.50 mmol), tri-*t*-butylbenzene (38 mg, 0.15 mmol), dry toluene (2 mL) and a magnetic stirring bar were put in a 5 mL vial. In the experiments with racemization catalyst present, either **2** (20 mg, 0.019 mmol) or the catalytic system of **1** (consisting of  $[\text{RuCl}_2(\text{cymene})]_2$  (14.6 mg; 0.024 mmol), (*rac*)-2-phenyl-2-propionamide (9.5 mg; 0.058 mmol) and  $\text{K}_2\text{CO}_3$  (200 mg; 1.45 mmol)) was also added. The reaction mixture was degassed by five consecutive vacuum/argon cycles and stirred at 70 °C. During reaction, samples (~ 0.02 mL) were withdrawn from the reaction mixture using a syringe, which was flushed with argon prior to use. The sample was diluted with dichloromethane and the enzyme was removed from the sample by filtration over cotton wool. The samples were analyzed by chiral GC (temperature program 150 °C isothermal for 45 min, temperature gradient 50 °C per min to 200 °C, isothermal at 200 °C for 40 min, temperature gradient 25 °C to 225 °C). GC retention times: diketone 8.1 min, ketone-monoester 11.7 min, *RR*-diester 15.06 min, *R*-alcohol-*R*-monoester 19.8 min, *S*-alcohol-*R*-monoester 20.8 min, *SS*-diol 32.5 min, *RS*-diol 33.3 min, *RR*-diol 35.2 min.

*Dynamic kinetic resolution of 1,3-diol using isopropyl hexanoate and Shvo's catalyst 2*

Novozym 435 (40 mg), **2** (18 mg, 0.017 mmol), 3 Å molar sieves and a magnetic stirring bar were put in a 15 mL Schlenk tube. The tube was put overnight in a vacuum oven (10 mm Hg) at 50 °C in presence of  $\text{P}_2\text{O}_5$ . The oven was backfilled with nitrogen and the tube was removed from the oven. 1,3-Diol (144 mg, 0.87 mmol), isopropyl hexanoate (276 mg, 1.75 mmol), tri-*t*-butylbenzene (44 mg, 0.18 mmol), dry toluene (2 mL) and 2,4-dimethyl-3-pentanol (120 mg) were added to a 5 mL round bottom flask and were stirred at 45 °C for 16 h in presence of 3 Å molar sieves to remove traces of water. The mixture was allowed to cool to room temperature and subsequently transferred to the Schlenk tube. Five vacuum-argon cycles were performed to remove oxygen. The mixture was stirred at 70 °C at reduced pressure (230 mbar). During reaction, samples (~ 0.02 mL) were withdrawn from the reaction mixture using a syringe, which was flushed with argon prior to use. The sample was diluted with dichloromethane and the enzyme was removed from the sample by filtration over cotton wool. The samples were analyzed by chiral GC (temperature program 150 °C isothermal for 45 min, temperature

gradient 50 °C per min to 200 °C, isothermal at 200 °C for 40 min, temperature gradient 25 °C to 225 °C). GC retention times: diketone 7.76 min, R-alcohol-ketone 19.44 min, S-alcohol-ketone 20.06 min, SS-diol 32.1 min, RS-diol 32.8 min, RR-diol 34.9 min, ketone-monoester 47.1 min, S-alcohol-R-monoester 50.3 min, R-alcohol-R-monoester 50.6 min, RR-diester 66.3 min.

#### *Dynamic kinetic resolution of 1,3-diol using isopropyl hexanoate and catalyst 1*

The procedure is the same as for the DKR using **2**, but instead of **2** the Schlenk tube is charged with [RuCl<sub>2</sub>(cymene)]<sub>2</sub> (7.3 mg; 0.012 mmol), (*rac*)-2-phenyl-2-propionamide (6.0 mg; 0.037 mmol) and K<sub>2</sub>CO<sub>3</sub> (50 mg; 0.36 mmol).

#### *Typical procedure for DKRP using catalyst 1*

Novozym 435 (447 mg), [RuCl<sub>2</sub>(cymene)]<sub>2</sub> (68.7 mg; 0.112 mmol), (*rac*)-2-phenyl-2-propionamide (60.2 mg; 0.367 mmol) and K<sub>2</sub>CO<sub>3</sub> (510 mg; 3.69 mmol), 3 Å molar sieves and a magnetic stirring bar were put in 50 mL 3-neck round bottom flask. The tube was put overnight in a vacuum oven (10 mm Hg) at 50 °C in presence of P<sub>2</sub>O<sub>5</sub>. The oven was backfilled with nitrogen and the tube was removed from the oven. 1,3-Diol (1.01 g, 6.09 mmol), DIA (1.40 g, 6.09 mmol) and dry toluene (50 mL) were put in a 100 mL round bottom flask and were stirred at 45 °C for 16 h in presence of 3 Å molar sieves to remove traces of water. The mixture was allowed to cool to room temperature and subsequently transferred to the 3-neck flask. Five vacuum-argon cycles were performed to remove oxygen. The mixture was stirred at 70 °C for 172 h at reduced pressure (280 mbar). During reaction, samples (~ 0.1 mL) were withdrawn from the reaction mixture using a syringe, which was flushed with argon prior to use. The sample was diluted with CDCl<sub>3</sub> and analyzed by <sup>1</sup>H NMR. At 120 h reaction time, dried Novozym 435 (450 mg) was added to the reaction mixture. At 145 h reaction time, a 2 mL aliquot was withdrawn from the reaction mixture using a syringe, and added to a sample vial. (*S*)-1-phenylethanol (1.13 g, 9.28 mmol) and K<sub>2</sub>CO<sub>3</sub> (50 mg, 0.37 mmol) were added and the mixture was subjected to five consecutive vacuum/argon cycles. The mixture was stirred at 70 °C for 2 h. A sample (~ 0.02 mL) was withdrawn from the reaction mixture, diluted with dichloromethane and analyzed by chiral GC (ee 1-phenylethanol 38%).

#### *Typical procedure for DKRP using Shvo's catalyst 2*

Novozym 435 (40 mg), **2** (18 mg, 0.017 mmol), 3 Å molar sieves and a magnetic stirring bar were put in a 15 mL Schlenk tube. The tube was put overnight in a vacuum oven (10 mm Hg) at 50 °C in presence of P<sub>2</sub>O<sub>5</sub>. The oven was backfilled with nitrogen and the tube was removed from the oven. 1,3-Diol (144 mg, 0.87 mmol), DIA (199 mg, 0.87 mmol), dry toluene (2 mL) and 2,4-dimethyl-3-pentanol (120 mg) were added to a 5 mL round bottom flask and were stirred at 45 °C for 16 h in presence of 3 Å molar sieves to remove traces of water. The mixture was allowed to cool to room temperature and subsequently transferred to the Schlenk tube. Five vacuum-argon cycles were performed to remove oxygen. The mixture was stirred at 70 °C for 120 h at reduced pressure (280 mbar). During reaction, aliquots (~ 0.05 mL) were drawn from the reaction mixture using a syringe, which was flushed with argon prior to use. The sample was diluted with CDCl<sub>3</sub> analyzed by <sup>1</sup>H NMR. After reaction, the enzyme was removed by filtration over a class 3 glass filter. The filter was flushed with dichloromethane. The crude product was obtained after removal of the organics by rotary evaporation as a brownish oil (120 mg).

<sup>1</sup>H NMR δ (ppm) 7.21 (m, Ar-H), 5.80 (m, CH(CH<sub>3</sub>)(OCO)), 2.53 (bs, Ar-CO-CH<sub>2</sub>), 2.30 (bs, OCOCH<sub>2</sub>), 1.55 (bs, OCOCH<sub>2</sub>CH<sub>2</sub>), 1.45 (CH<sub>3</sub>)



*Typical procedure for the hydrolysis of chiral polymers*

Chiral polymer (40 mg) was dissolved in EtOH (2 mL). NaOH (42 mg, 1.0 mmol) was added, and the mixture was stirred for 16 h at room temperature. The mixture was poured into a solution of 300 mg NH<sub>4</sub>Cl in 10 mL H<sub>2</sub>O. A few drops of concentrated hydrochloric acid were added, until pH ~ 7 as evidenced by the use of pH paper. The EtOH was removed by concentration *in vacuo* and the mixture was extracted with ethyl acetate (3 x 20 mL). The organics were combined, washed with brine and dried over MgSO<sub>4</sub>. After concentration, the resulting mixture (40 mg) was analyzed by <sup>1</sup>H NMR to confirm full degradation of the polymeric material and subsequently analyzed by chiral GC for determination of the enantiomeric excess of the monomer.

*1,2,9,10-Diepoxydecane*

1,9-Decadiene (10.6 g; 77 mmol) was dissolved in chloroform (100 ml) and added dropwise in 1 h using a dropping funnel to a suspension of 77% *m*-chloroperbenzoic acid (34 g; 197 mmol) in chloroform (150 mL). The mixture was stirred overnight at room temperature. Then, the solution was filtered over celite and the filtrate was washed with Na<sub>2</sub>S<sub>2</sub>O<sub>3</sub> solution (150 mL, 10 %), Na<sub>2</sub>CO<sub>3</sub> solution (3 x 150 mL, saturated) and brine (150 mL). The organic layer was dried with MgSO<sub>4</sub>, filtered and concentrated *in vacuo*. The resulting clear liquid (12.4 g, 98 %) was characterized by <sup>1</sup>H NMR and used in the second step without further purification.

<sup>1</sup>H NMR δ (ppm) 2.90 (m, CH<sub>2</sub>-O-CH), 2.75 (dd CH<sub>2</sub>-O-CH), 2.45 (dd CH<sub>2</sub>-O-CH), 1.2-1.8 (CH<sub>2</sub>-R).

*1,2,7,8-Diepoxyoctane*

<sup>1</sup>H NMR δ (ppm) 2.90 (m, CH<sub>2</sub>-O-CH), 2.75 (dd CH<sub>2</sub>-O-CH), 2.45 (dd CH<sub>2</sub>-O-CH), 1.2-1.8 (CH<sub>2</sub>-R)

*1,2,8,9-Diepoxyonane*

<sup>1</sup>H NMR δ (ppm) 2.90 (m, CH<sub>2</sub>-O-CH), 2.75 (dd CH<sub>2</sub>-O-CH), 2.45 (dd CH<sub>2</sub>-O-CH), 1.2-1.8 (CH<sub>2</sub>-R)

*2,9-Decanediol (4c)*

1,2,9,10-Diepoxydecane (12.4 g; 76 mmol) was dissolved in diethyl ether (300 mL) and added dropwise in 1 h using a dropping funnel to an ice cooled suspension of LiAlH<sub>4</sub> (2.22 g; 59.25 mmol) in diethyl ether (300 mL). The reaction was performed under a nitrogen atmosphere. The resulting suspension was stirred overnight. After completion of the reaction (as confirmed by <sup>1</sup>H NMR), the mixture was quenched with water and aqueous hydrochloric acid was added (200 mL, 1M). The organic layer was separated and the aqueous layer was washed with dichloromethane (2 x 200 mL). The organic layers were combined and concentrated *in vacuo*. The resulting liquid was distilled (b.p. 100 °C, T<sub>oil</sub> = 160 °C, p=0.03 mbar). The product was characterized by <sup>1</sup>H NMR, <sup>13</sup>C NMR and GC/MS. According to <sup>1</sup>H NMR, the product contained 97 % secondary alcohol groups and 3% primary alcohol groups (7.5 g, 60 %). Prior to GC analysis, the sample was derivatized using trifluoroacetic anhydride.

<sup>1</sup>H NMR δ (ppm) 3.78 (m, CH<sub>3</sub>CH(OH)), 3.63 (t, CH<sub>2</sub>CH<sub>2</sub>OH), 1.2-1.6 (m, CH(CH<sub>2</sub>)<sub>6</sub>), 1.18 (d, CH<sub>3</sub>CH(OH)); <sup>13</sup>C NMR δ (ppm) 67 (CH<sub>3</sub>CH(OH)), 39 (CH<sub>2</sub>CH(OH)CH<sub>3</sub>), 30 (CH<sub>3</sub>CH(OH)CH<sub>2</sub>CH<sub>2</sub>CH<sub>2</sub>), 26 (CH<sub>3</sub>CH(OH)CH<sub>2</sub>CH<sub>2</sub>), 24 (CH<sub>3</sub>CH(OH)); GC/MS (FW=174.28): m/z 155 (<1% abundance); GC retention times (temperature program: 105 °C isothermal for 30 min, temperature gradient 50 °C per min to 200 °C, isothermal at 200 °C for 10 min, temperature gradient 25 °C to 225 °C): SS-diol 23.74 min, RS-diol 24.15 min, RR-diol 24.96 min.

<sup>1</sup>H NMR of the polymer obtained from the DKRP of 2,9-decanediol and DIA:  $\delta$  (ppm) 4.98 (m, COOCH(CH<sub>3</sub>)<sub>2</sub>), 4.89 (m, CH(CH<sub>3</sub>)(OCO)), 4.05 (t, CH<sub>2</sub>(OCO)), 3.79 CH(CH<sub>3</sub>)OH), 2.30 (bs, OCOCH<sub>2</sub>), 2.10 (s, COCH<sub>3</sub>), 1.78-1.22 (m, OCOCH<sub>2</sub>CH<sub>2</sub> and COOCH(CH<sub>3</sub>)CH<sub>2</sub>CH<sub>2</sub>CH<sub>2</sub>), 1.19 (d, CH<sub>3</sub>)

#### 2,7-Octanediol (**4a**)

Yield: 2.55 g (38 %). B.p. 82 °C, T<sub>oil</sub> = 130 °C, p=0.03 mbar. According to <sup>1</sup>H NMR, the product contained 98 % secondary alcohol groups and 2% primary alcohol groups. Prior to GC analysis, the sample was derivatized using trifluoroacetic anhydride.

<sup>1</sup>H NMR  $\delta$  (ppm) 3.78 (m, CH<sub>3</sub>CH(OH)), 3.63 (t, CH<sub>2</sub>CH<sub>2</sub>OH), 1.2-1.6 (m, CH(CH<sub>2</sub>)<sub>6</sub>), 1.18 (d, CH<sub>3</sub>CH(OH)); <sup>13</sup>C NMR  $\delta$  (ppm) 68 (CH<sub>3</sub>CH(OH)), 39 (CH<sub>3</sub>CH(OH)CH<sub>2</sub>), 26 (CH<sub>3</sub>CH(OH)CH<sub>2</sub>CH<sub>2</sub>), 24 (CH<sub>3</sub>CH(OH)); GC/MS (FW=146.23): m/z 126 (<1% abundance); GC retention times (temperature program: 95 °C isothermal for 20 min, temperature gradient 50 °C per min to 200 °C, isothermal at 200 °C for 10 min, temperature gradient 25 °C to 225 °C): SS-diol 12.1 min, RS-diol 12.4 min, RR-diol 13.0 min.

<sup>1</sup>H NMR of the polymer obtained from the DKRP of 2,7-octanediol and DIA:  $\delta$  (ppm) 4.98 (m, COOCH(CH<sub>3</sub>)<sub>2</sub>), 4.89 (m, CH(CH<sub>3</sub>)(OCO)), 4.05 (t, CH<sub>2</sub>(OCO)), 3.79 CH(CH<sub>3</sub>)OH), 2.30 (bs, OCOCH<sub>2</sub>), 2.10 (s, COCH<sub>3</sub>), 1.78-1.22 (m, OCOCH<sub>2</sub>CH<sub>2</sub> and COOCH(CH<sub>3</sub>)CH<sub>2</sub>CH<sub>2</sub>), 1.19 (d, CH<sub>3</sub>)

#### 2,8-Nonanediol (**4b**)

Yield: 3.14 g (49 %). B.p. 95 °C, T<sub>oil</sub> = 130 °C, p=0.03 mbar. According to <sup>1</sup>H NMR, the product contained 98 % secondary alcohol groups and 2% primary alcohol groups. Prior to GC analysis, the sample was derivatized using trifluoroacetic anhydride.

<sup>1</sup>H NMR  $\delta$  (ppm) 3.78 (m, CH<sub>3</sub>CH(OH)), 3.63 (t, CH<sub>2</sub>CH<sub>2</sub>OH), 1.2-1.6 (m, CH(CH<sub>2</sub>)<sub>6</sub>), 1.18 (d, CH<sub>3</sub>CH(OH)); <sup>13</sup>C NMR  $\delta$  (ppm) 68 (CH<sub>3</sub>CH(OH)), 39 (CH<sub>3</sub>CH(OH)CH<sub>2</sub>), 30 (CH<sub>3</sub>CH(OH)CH<sub>2</sub>CH<sub>2</sub>CH<sub>2</sub>), 26 (CH<sub>3</sub>CH(OH)CH<sub>2</sub>CH<sub>2</sub>), 23 (CH<sub>3</sub>CH(OH)); GC/MS (FW=160.25): m/z 141 (<1% abundance); GC retention times (temperature program: 95 °C isothermal for 20 min, temperature gradient 50 °C per min to 200 °C, isothermal at 200 °C for 10 min, temperature gradient 25 °C to 225 °C): SS-diol 21.5 min, RS-diol 22.5 min, RR-diol 23.1 min.

<sup>1</sup>H NMR of the polymer obtained from the DKRP of 2,8-nonanediol and DIA:  $\delta$  (ppm) 4.98 (m, COOCH(CH<sub>3</sub>)<sub>2</sub>), 4.89 (m, CH(CH<sub>3</sub>)(OCO)), 4.05 (t, CH<sub>2</sub>(OCO)), 3.79 CH(CH<sub>3</sub>)OH), 2.30 (bs, OCOCH<sub>2</sub>), 2.10 (s, COCH<sub>3</sub>), 1.78-1.22 (m, OCOCH<sub>2</sub>CH<sub>2</sub> and COOCH(CH<sub>3</sub>)CH<sub>2</sub>CH<sub>2</sub>CH<sub>2</sub>), 1.19 (d, CH<sub>3</sub>)

#### Kinetic resolution of 2,9-decanediol using vinyl acetate as the acyl donor

Novozym 435 (25 mg), 2,9-decanediol (**4c**) (200 mg, 1.15 mmol), vinyl acetate (400 mg, 4.64 mmol), tri-*t*-butylbenzene (40 mg, 0.16 mmol), dry toluene (5 mL), dry 2,4-dimethyl-3-pentanol (1 mL) and a magnetic stirring bar were put in a 10 mL vial. The mixture was stirred at 70 °C. At 5, 10, 24, 40, 80, 160, 360 and 1500 min samples (~ 0.02 mL) were withdrawn from the reaction mixture using a syringe, which was flushed with argon prior to use. The sample was diluted with dichloromethane and the enzyme was removed from the sample by filtration over cotton wool. The samples were analyzed by chiral GC. For determination of the conversions of the separate enantiomers, the samples were derivatized using trifluoroacetic anhydride prior to analysis. Temperature program underivatized

samples: 125 °C isothermal for 20 min, temperature gradient 20 °C per min to 200 °C, isothermal at 200 °C for 25 min, temperature gradient 25 °C to 225 °C). GC retention times: diol 23.50 min, *S*-ester-*S*-alcohol 23.80 min, *SS*-diester 23.97 min, *R*-ester-*R*-alcohol + *R*-ester-*S*-alcohol 24.01 min, *RS*-diester 24.24 min, *RR*-diester 24.49 min. The peaks were tentatively assigned based on deduction and mass balance consistency. Temperature program derivatized samples: 105 °C isothermal for 30 min, temperature gradient 50 °C per min to 200 °C, isothermal at 200 °C for 10 min, temperature gradient 25 °C to 225 °C). GC retention times: *SS*-diol 23.74 min, *RS*-diol 24.15 min, *RR*-diol 24.96 min.

## 5.7 References and notes

1. van As, B. A. C.; van Buijtenen, J.; Heise, A.; Broxterman, Q. B.; Verzijl, G. K. M.; Palmans, A. R. A.; Meijer, E. W. *J. Am. Chem. Soc.* **2005**, 127, (28), 9964-9965.
2. van Buijtenen, J.; van As, B. A. C.; Meuldijk, J.; Palmans, A. R. A.; Vekemans, J.; Hulshof, L. A.; Meijer, E. W. *Chem. Commun.* **2006**, (30), 3169-3171.
3. Karvembu, R.; Prabhakaran, R.; Natarajan, K. *Coord. Chem. Rev.* **2005**, 249, (9-10), 911-918.
4. Buijtenen, J. van *Thesis*, **2006**
5. Buijtenen, J. van. *Manuscript in preparation*
6. Kanca, U., van As, B.A.C., van Buijtenen, J., Palmans, A.R.A., Meijer, E.W. *Manuscript in preparation* **2006**.
7. When dehydrogenation of alcohol groups takes place to a significant extent, the use of an excess of diol results in a higher theoretically achievable molecular weight than equimolar stoichiometry. Therefore, when dehydrogenation cannot be sufficiently suppressed, the diol/diester system is expected to yield higher molecular weight polymers than the hydroxyester approach.
8. Hilker, I.; Rabani, G.; Verzijl, G. K. M.; Palmans, A. R. A.; Heise, A. *Angew. Chem., Int. Ed.* **2006**, 45, (13), 2130-2132.
9. Hilker *et al.* use the 1,4-substituted analogue as a model compound.<sup>8</sup> Because of its much higher solubility in toluene, we chose to use the 1,3-diol as our model compound.
10. All reference experiments were performed in duplo; similar results were obtained. In addition, the experiments described using 1,3-diol were also performed using the 1,4-diol; again, similar results were obtained.
11. In a blank reaction (without racemization catalyst) no acylation of *S*-secondary alcohols was observed, indicating that the observed acylation of these *S*-secondary alcohols ensures that the racemization catalyst is active.
12. Turnover frequency; defined as the number of turnovers per catalyst molecule per second at the start of reaction; The TOF is calculated according to the formula  $TOF = k_i \times (\text{initial substrate concentration}) / (\text{total catalyst concentration})$ , in which  $k_i$  is the rate constant as determined by fitting a straight line to the relationship between  $-\ln(1 - \text{conversion})$  and time.
13. The rate of racemization (which equals the rate of production of *R*-secondary alcohols if racemization is rate-limiting) is assumed to be first order in the concentration of the *S*-alcohol. If indeed racemization is rate-limiting and all alcohols groups are in the *S*-configuration, (and assuming that the changing polarity of the system plays no significant role) the total rate of reaction (which equals the production of *R*-secondary alcohols) will be first order in

- concentration of the S-alcohol. Therefore, once the 50% conversion threshold has been crossed, a linear relationship should hold between  $\ln(1 - \text{conversion})$  and time and a pseudo first order rate constant can be calculated.
14. Choi, J. H.; Kim, N.; Shin, Y. J.; Park, J. H.; Park, J. *Tetrahedron Lett.* **2004**, 45, (24), 4607-4610.
  15. The two experiments with 2 mol.% Ru are at different DMP concentration and, therefore, display different reaction rates
  16. Entries 3 and 4 show that use of 12 mg Novozym 435/mmol leads to the same rate of reaction as 23 mg/mmol. Therefore, we do not expect that lipase activity has become rate-limiting at 4 mol.% Ru, since 23 mg Novozym 435/mmol is used and the observed rate constant is similar to entries 3 and 4.
  17. The kinetics of racemization are assumed to be first order in alcohol concentration.
  18. The two experiments with 0.5 M DMP are at different catalyst loadings and, therefore, display different reaction rates.
  19. Edin, M.; Bäckvall, J. E. *J. Org. Chem.* **2003**, 68, (6), 2216-2222.
  20. Orrenius, C.; Haeffner, F.; Rotticci, D.; Ohrner, N.; Norin, T.; Hult, K. *Biocatal. Biotransform.* **1998**, 16, (1), 1-15.
  21. Gotor-Fernandez, V.; Brieva, R.; Gotor, V. *J. Mol. Catal. B: Enzym.* **2006**, 40, (3-4), 111-120.
  22. Since a diol consists of diastereomers (SS, RS and RR), an E-value can not be calculated.
  23. The data displayed are not normalized; due to the error of measurement the total mass balance does not add up to 100%, but fluctuates between 94 and 101%
  24. Wallace, J. S.; Baldwin, B. W.; Morrow, C. J. *J. Org. Chem.* **1992**, 57, (19), 5231-5239.



# 6

## Kinetics of enzymatic ROP and ITC - Theory and practice

### Abstract

Enzymatic ring-opening polymerizations generally obey Michaelis-Menten kinetics. Assuming that the dissociation constants from the active site for polyester and lactone are similar, net pseudo first order kinetics are expected. However, if this is not the case, deviation from first order kinetics will occur. This deviation is indeed observed experimentally in the enzymatic ring-opening polymerization of  $\epsilon$ -caprolactone. The calculated dissociation constants for poly( $\epsilon$ -caprolactone) and poly( $\omega$ -pentadecalactone) were 0.24 M and 0.19 M, respectively, compared to 0.72 M and 0.31 M for  $\epsilon$ -caprolactone and  $\omega$ -pentadecalactone. This suggests that the affinity of the lipase for esters in the *transoid*-conformation generally is higher than for esters in the *cisoid*-conformation.

A kinetic analysis based on the Langmuir-Hinshelwood (LH) mechanism was introduced as an efficient method for the derivation of rate equations for enzymatic reactions. Although based on the same principles as Michaelis-Menten kinetics, the LH mechanism allows description of the kinetics of complex processes. Based on the LH mechanism, a model was developed that describes the kinetics of the iterative tandem catalysis of (S)-6-methyl- $\epsilon$ -caprolactone. It was shown that the predicted conversion-time history accurately matches the experimental observations.

## 6.1 Introduction

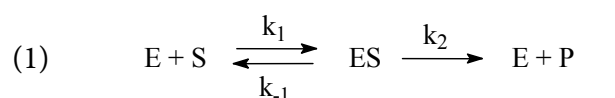
By analyzing the kinetics of an enzymatic reaction, it is possible to obtain a detailed insight into the mechanism of reaction. When the enzyme itself is the object of study, often only initial rate studies are considered, and standard Michaelis-Menten kinetics suffice. However, in the case of lipase-catalyzed polymerizations, the kinetics up to a considerable conversion are analyzed (in the optimal case up to complete conversion). This yields a more complex situation, and a proper understanding of the kinetics is crucial in order to draw justified conclusions. This chapter aims to give a general overview of Michaelis-Menten kinetics, its application to lipase-catalyzed ring-opening polymerization and the effect of product inhibition on the observed rate of reaction. In addition, using Langmuir-Hinshelwood kinetics, a rate equation is derived for iterative tandem catalysis (ITC). The developed model is compared to the experimental data.

## 6.2 Kinetics of lipase-catalyzed polymerizations

If an enzymatic ring-opening polymerization (eROP) is monitored up to a considerable conversion, product molecules will occupy available active sites and, consequently, the reaction rate goes down. This phenomenon is commonly described by the term “product inhibition”. In this section, we first describe standard Michaelis-Menten kinetics for a single-substrate single-product reaction, neglecting product inhibition. Then, the complexities that arise analyzing the kinetics of eROP are discussed. The effect of product inhibition on the rate of reaction is described, and the effect of different affinities towards the substrate and the polyester product is investigated. Finally, the described kinetic models are applied to experimental results obtained in the eROP of  $\epsilon$ -caprolactone and  $\omega$ -pentadecalactone.

### 6.2.1 Michaelis-Menten kinetics

Equation 1 describes a simple single-substrate single-product reaction. Many enzymatic systems display similar behavior in two limiting cases of substrate concentration. At very low substrate concentration, the reaction rate  $\nu$  is first order in substrate concentration (Equation 2), and at very high (infinite) substrate concentration reaction rate is zero order in substrate concentration, and  $\nu = V_{\max}$  (Equation 3).<sup>1</sup>



$$(2) \quad \nu = k[S] \qquad (3) \quad \nu = V_{\max}$$

To describe the rates of enzymatic reactions at intermediate concentrations, the Michaelis-Menten (MM) model has proven to be very useful.<sup>2</sup> Equations 4 and 5 show the well-known Michaelis-Menten equations, which are applicable to many enzymatic systems.

$$(4) \quad v = \frac{V_{\max}[S]}{K_M + [S]} \quad (5) \quad K_M = \frac{k_2 + k_{-1}}{k_1}$$

Under the assumption of a rapid adsorption of substrate ( $E + S \rightleftharpoons ES$  is at equilibrium) and slow formation of product ( $ES \rightarrow E + P$  is rate-limiting, thus  $k_2 \ll k_{-1}$ ), the Michaelis concentration  $K_M$  has the physical meaning of an adsorption constant  $K_S$  and can be defined as  $K_M = K_S = k_{-1} / k_1$ . In all other cases, it holds that  $K_M > K_S$ .<sup>3</sup> Only in the simplest case (the classic Michaelis-Menten situation as described above, where  $E$ ,  $S$  and  $ES$  are in equilibrium) the meaning of  $K_M$  is truly a dissociation constant. In all other cases,  $K_M$  – although often termed the Michaelis constant – is only “that substrate concentration where  $v = 0.5 * V_{\max}$ ”.<sup>1,4</sup>

#### Applicability of the MM-equation

Although Equations 4 and 5 formally only hold for single-substrate single-product reactions, many enzymatic systems behave as if they obey MM-kinetics. In these situations, the calculated  $K_M$  and  $V_{\max}$  have no physical or kinetic meaning, but rather are apparent values of  $K_M$  and  $V_{\max}$ :  $K_M^{app}$  and  $V_{\max}^{app}$  (Equation 6). Many systems have been described; an example is shown in Equation 7, where inhibition by a competitive inhibitor  $I$  is taken into account ( $K_S$  here denotes the dissociation constant  $k_{-1}/k_1$ ).<sup>2,5</sup>

$$(6) \quad v = \frac{V_{\max}^{app}[S]}{K_M^{app} + [S]} \quad (7) \quad K_M^{app} = K_S \left( 1 + \frac{[I]}{K_i} \right)$$

#### 6.2.2 Michaelis-Menten kinetics in an enzymatic ring-opening polymerization

A more complex situation arises when we consider an enzymatic ring-opening polymerization. Figure 6.1 shows the Cleland plot for the initiation step in the enzymatic ring-opening of  $\epsilon$ -caprolactone. First the lactone (A) adsorbs in the active site (resulting in EA). The nucleophilic attack of the hydroxy of the serine residue provides the acyl enzyme complex F. A nucleophile (in this case benzyl alcohol) then performs a nucleophilic attack resulting in the adsorbed product P in the active site (EP). Desorption of the product reforms the free enzyme E. In the subsequent propagation steps, the alcohol end-group of P acts as the nucleophile and the same mechanism applies. Since the reactants must adsorb in this specific order for product formation to occur, this mechanism can be described according to Cleland





$$(9) \quad [E_0] = [E] + [EP] + [ES]$$

$$(10) \quad \frac{d[ES]}{dt} = 0 = k_1[E][S] - (k_{-1} + k_2)[ES]$$

$$(11) \quad \frac{d[EP]}{dt} = 0 = k_{-3}[E][P] - k_3[EP] + k_2[ES]$$

$$(12) \quad v = -\frac{d[S]}{dt} = k_2[ES]$$

$$(13) \quad [E] = \frac{k_2 + k_{-1}}{k_1} \frac{[ES]}{[S]} = K_S \frac{[ES]}{[S]} \quad \text{with } K_S = \frac{k_2 + k_{-1}}{k_1}$$

$$(14) \quad [EP] = \frac{k_{-3}}{k_3} [E][P] + \frac{k_2}{k_3} [ES] = K_P \frac{[ES]}{[S]} + \frac{k_2}{k_3} [ES] \quad \text{with } K_P = \frac{k_{-3}}{k_3}$$

$$(15) \quad [ES] = \frac{[E_0][S]}{[S] + K_S + \frac{K_S}{K_P}[P] + [S]\frac{k_2}{k_3}} = \frac{[E_0][S]}{[S] + K_S + \frac{K_S}{K_P}[P]} \quad \text{with } \frac{k_2}{k_3} \ll 1$$

$$(16) \quad v = -\frac{d[S]}{dt} = \frac{k_2[E_0][S]}{[S] + K_S + \frac{K_S}{K_P}[P]} = V_{\max} \frac{[S]}{[S] + K_S + \frac{K_S}{K_P}[P]}$$

Equation 16 shows the relationship between the reaction rate  $v$  and substrate ( $[S]$ ) and product concentration ( $[P]$ ). If we assume equal affinity of the enzyme towards an ester group in a lactone and in the polyester chain ( $K_S = K_P$ ), Equation 17 is obtained. Since  $[S] + [P]$  is constant, Equation 17 is of the form  $v = (\text{constant}) \times [S]$  and thus obeys pseudo first order kinetics. Therefore, the natural logarithm of  $(1 - \text{conversion})$  versus time is expected to yield a linear relationship, which allows the calculation of a pseudo first order rate constant.

$$(17) \quad v = -\frac{d[S]}{dt} = V_{\max} \frac{[S]}{[S] + K_S + [P]}$$

#### *Product inhibition with unequal affinity for substrate and product*

The assumption of equal affinity of the enzyme towards lactone and polyester may not in all cases be a valid one; the ester groups in  $\epsilon$ -caprolactone and poly( $\epsilon$ -caprolactone) for example exist in the *cisoid* and the *transoid* conformation, respectively. One would expect the enzyme to distinguish between these types of ester groups. This might lead to considerably different dissociation constants for substrate and product ( $K_S$  and  $K_P$ ). If  $K_P$  is smaller than  $K_S$  (i.e. the enzyme has more affinity for the product than for the substrate), the rate of reaction will slow down more than expected based on pseudo first order kinetics. As a consequence, the relationship between  $\ln(1 - \text{conversion})$  and time will deviate from linearity.

The derivation is based on Equation 16. First, [S], d[S] and [P] are replaced by expressions using only the variable X for conversion. The constant [S]<sub>0</sub> is the initial substrate concentration [S].

$$(16) \quad v = -\frac{d[S]}{dt} = V_{\max} \frac{[S]}{[S] + K_s + \frac{K_s}{K_p}[P]}$$

$$(18) \quad [S] = [S]_0(1 - X) \quad d[S] = -[S]_0 dX \quad [P] = [S]_0 X$$

$$(19) \quad -\frac{d[S]}{dt} = [S]_0 \frac{dX}{dt} = V_{\max} \frac{[S]_0(1 - X)}{[S]_0(1 - X) + K_s + \frac{K_s}{K_p}[S]_0 X}$$

$$(20) \quad [S]_0 \frac{dX}{dt} = V_{\max} \frac{1 - X}{1 + \frac{K_s}{[S]_0} + \left(\frac{K_s}{K_p} - 1\right)X}$$

Separating variables and integration from t=0 to t=t and X=0 to X=X gives:

$$(21) \quad \int_0^X \frac{1 + \frac{K_s}{[S]_0} + \left(\frac{K_s}{K_p} - 1\right)X}{1 - X} dX = \frac{V_{\max}}{[S]_0} \int_0^t dt$$

$$(22) \quad \left(1 + \frac{K_s}{[S]_0}\right) \int_0^X \frac{1}{1 - X} dX + \left(\frac{K_s}{K_p} - 1\right) \int_0^X \frac{X}{1 - X} dX = \frac{V_{\max}}{[S]_0} t$$

Using the standard integral 23 Equation 24 is obtained:

$$(23) \quad \int \frac{x}{ax + b} dx = \frac{x}{a} - \frac{b}{a^2} \ln(ax + b)$$

$$(24) \quad -\left(\frac{[S]_0 + K_s}{[S]_0}\right) \ln(1 - X) - \left(\frac{K_s}{K_p} - 1\right) [\ln(1 - X) + X] = \frac{V_{\max}}{[S]_0} t$$

This latter equation is of the form:

$$(24a) \quad -A \ln(1 - X) - B [\ln(1 - X) + X] = Ct$$

$$(24b) \quad A = \frac{[S]_0 + K_S}{[S]_0} \quad B = \frac{K_S}{K_P} - 1 \quad C = \frac{V_{\max}}{[S]_0}$$

If  $K_S = K_P$  then  $B = 0$  and Equation 24a reduces to Equation 17, i.e. first order kinetics. If  $K_S \neq K_P$ , the term  $[B(\ln(1 - X) + X)]$  represents the deviation from linearity. To investigate the effect of different dissociation constants on the linearity of  $\ln(1 - X)$  versus time plots, a specific example is discussed. Assuming  $K_S = K_P = 0.1$  M,  $[S]_0 = 2$  M and  $V_{\max} = 0.01$  mol/[m<sup>3</sup>.s], Figure 6.2a is obtained and from linear regression a slope of 0.00476 s<sup>-1</sup> is calculated. Indeed, multiplication of  $k$  with  $[S]_0$  now yields  $v_0$ , 0.00952 mol/m<sup>3</sup>.s.<sup>8</sup> If  $K_P$  is considerably smaller, e.g. 0.02 M (Figure 6.2b), the obtained plot is no longer linear. In the initial stages of the reaction this plot is pseudo-linear, and from the first 5 data points (conversion up to 25%), linear regression yields a seemingly acceptable result with  $R^2 = 0.984$  (Figure 6.2c). However, the calculated slope now is 0.00336 s<sup>-1</sup>. In this example, the true rate constant  $k$  is 42% larger than the calculated value. Consequently, one should be very cautious when calculating rate constants from non-linear plots based on expected pseudo-first order kinetics.

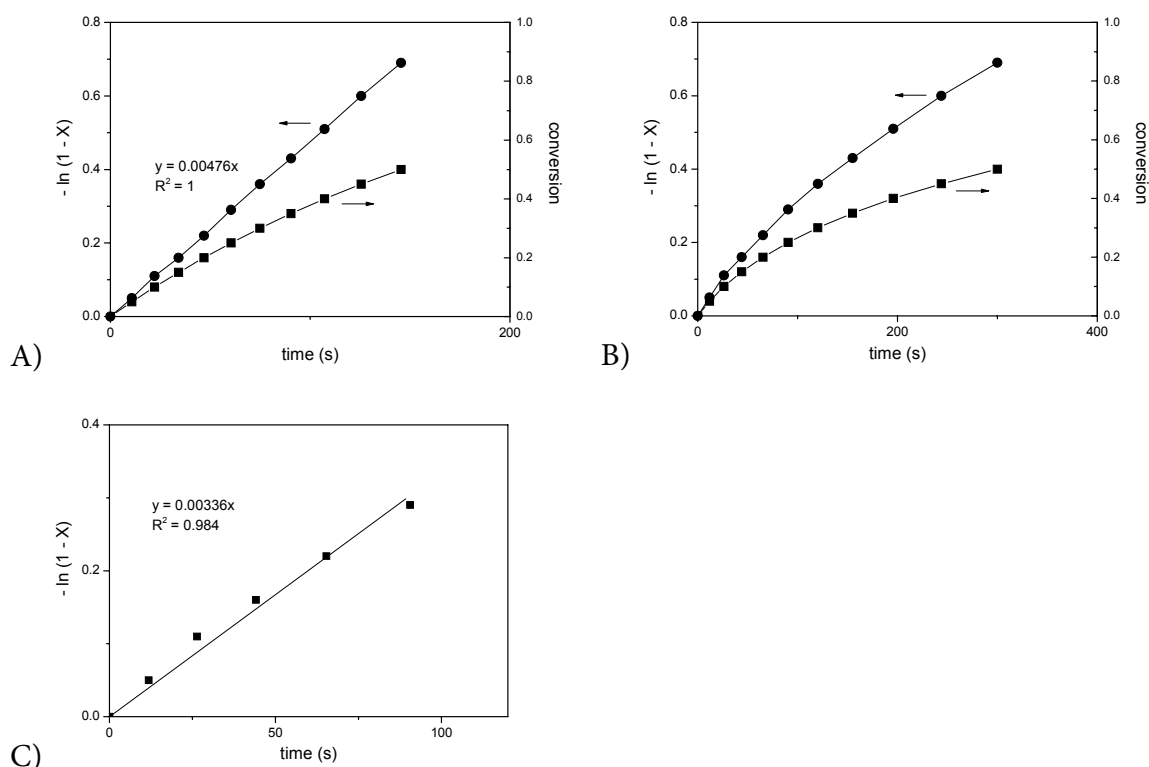


**Figure 6.2** –  $\ln(1 - X)$  and conversion versus time; (A)  $K_S = K_P = 0.1$  M,  $[S]_0 = 2$  M and  $V_{\max} = 0.01$  mol/m<sup>3</sup>.s (B)  $K_S = 0.1$  M,  $K_P = 0.02$  M (C) Linear regression performed on the data points of figure B ( $K_P = 0.02$  M) with conversion up to 25%.

### 6.2.3 Experimental results

The developed model was tested on experimental data obtained from enzymatic polymerizations of  $\epsilon$ -caprolactone (CL) and  $\omega$ -pentadecalactone (PDL). The data were analyzed by linear regression on the  $\ln(1 - X)$  versus time plot, as well as by fitting the data to the model. The initial rates of reaction  $v_i$  at  $t=0$  were calculated. Using linear regression,  $v_i$  is obtained by multiplication of the first order rate constant  $k_i$  with the initial substrate concentration (Equation 25). Using the developed model,  $v_i$  can be calculated according to Equation 26 (A and C correspond to the constants as defined by Equation 24b).

$$(25) \quad \begin{aligned} v &= k_i[S] \\ v_i &= k_i[S]_0 \end{aligned} \quad (26) \quad v_i = A^{-1}C[S]_0$$

Figure 6.3A shows the time-conversion history for a typical polymerization of CL. The  $\ln(1 - X)$  versus time plot in Figure 6.3B does not yield a straight line; the reaction slows down more than expected based on first order kinetics. Still, linear regression can be performed with an  $R^2$  value of 0.9806 (dotted line in Figure 6.3B). A value for the initial rate  $v_i$  of  $5.4 \cdot 10^{-2} \text{ mol.L}^{-1}.\text{min}^{-1}$  was calculated from these data.

Using the proposed model, non-linear curve fitting was performed (the solid line in Figure 6.3B; see also Table 6.1).<sup>9</sup> The calculated initial rate of reaction  $v_i$  now is  $7.43 \cdot 10^{-2} \text{ mol.L}^{-1}.\text{min}^{-1}$ , or 38% higher than using linear regression. Moreover, a  $K_p$ -value of 0.24 M was calculated, compared to 0.72 M for CL.<sup>10</sup> This suggests that the affinity of the enzyme for the ester groups in poly( $\epsilon$ -caprolactone) is approximately 3 times greater than for CL itself. This difference can be rationalized by the change in conformational preference going from a cyclic ester to the linear polyester.

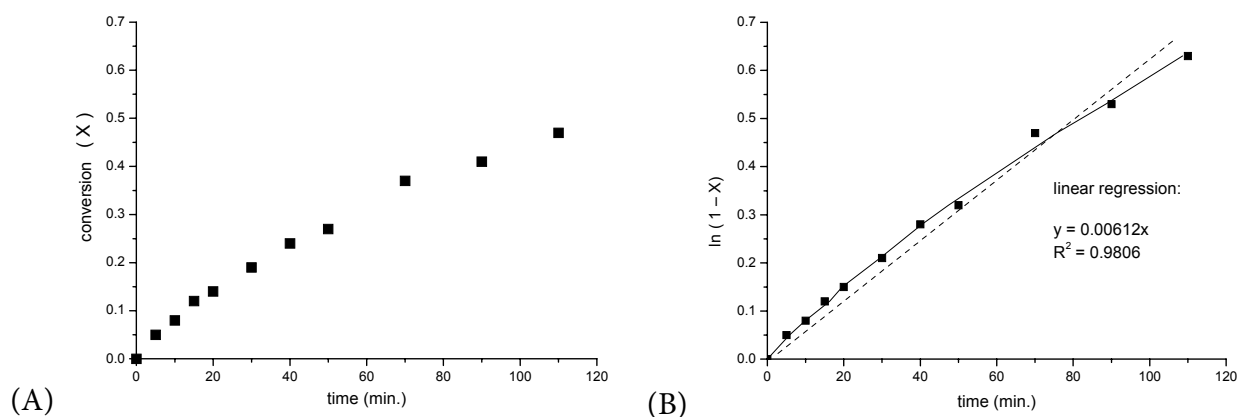


**Figure 6.3** Enzymatic ring-opening polymerization of  $\epsilon$ -caprolactone. (A) Time-conversion history (B) Plot of logarithmic  $(1 - X)$  versus time; (■)  $\epsilon$ -caprolactone; dotted line: relationship obtained by linear regression; solid line: relationship obtained by the proposed model;  $M/I = 90$ ; polymerization performed in bulk ( $[S]_0 = 8.8 \text{ M}$ );  $T = 60 \text{ }^\circ\text{C}$ ; 8.0 mg Novozym 435 / mmol lactone; as the initiator the bifunctional initiator **6** as described in Chapter 3 was used.

**Table 6.1** Initial rate and dissociation constants for CL polymerization as obtained by linear regression and by the proposed model

	$v_i$ $\text{mol}\cdot\text{L}^{-1}\cdot\text{min}^{-1} \cdot 10^{-2}$	$K_S / K_P$	$K_P$ (M)
Linear regression	5.4	1 <sup>a</sup>	0.72 (=K <sub>M-CL</sub> )
Modeled	7.43 +/- 0.32	3.0	0.24 +/- 0.43

<sup>a</sup> Assuming a linear relationship implies the assumption that  $K_S=K_P$ , thus  $K_S/K_P = 1$ .

Figure 6.4A shows the time-conversion plot for a typical polymerization of PDL. The ester in this macrolactone is completely in the *transoid*-conformation. PDL is a very good substrate for CALB;  $V_{\max}$  for PDL is almost 3 times higher than for CL, as was recently reported by our laboratory; an intriguing observation in view of the absence of ring strain and, hence, the absence of enthalpic driving force.<sup>10</sup> Linear regression on these data yields a reasonably good fit, with an  $R^2$  value of 0.9963 (dotted line in Figure 6.4B). Using the obtained  $k_i$  and  $[S]_0$ , an initial rate  $v_i$  of  $4.79 \cdot 10^{-2} \text{ mol}\cdot\text{L}^{-1}\cdot\text{min}^{-1}$  was calculated.

Application of the proposed model by means of non-linear curve fitting also yields a good fit (solid line in Figure 6.4B; see also Table 6.2). An initial rate  $v_i$  of  $5.92 \cdot 10^{-2} \text{ mol}\cdot\text{L}^{-1}\cdot\text{min}^{-1}$  was calculated, which is 24% higher than the value calculated from linear regression results. A slightly lower  $K_P$  was calculated, with 0.19 M versus 0.31 M for the lactone. This suggests that the affinity the poly( $\omega$ -pentadecalactone) is slightly higher than for the lactone, although the difference is less dramatic than for CL.

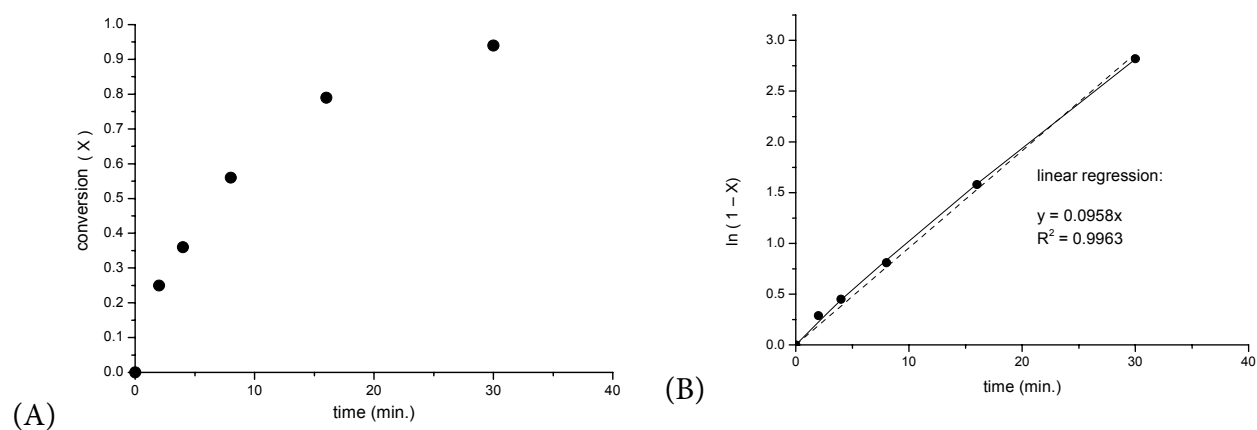


**Figure 6.4** Enzymatic ring-opening polymerization of  $\omega$ -pentadecalactone. (A) Time-conversion history (B) Plot of logarithmic (1 - conversion) versus time; (●)  $\omega$ -pentadecalactone; dotted line: relationship obtained by linear regression; solid line: relationship obtained by the proposed model;  $M/I = 50$ ; polymerization performed in toluene;  $[S]_0 = 0.5 \text{ M}$ ;  $T = 45 \text{ }^\circ\text{C}$ ; 10 mg Novozym 435 / mmol lactone; as the initiator benzyl alcohol was used.

**Table 6.2** Initial rate and dissociation constants for PDL polymerization as obtained by linear regression and by the proposed model

	$v_i$ $\text{mol}\cdot\text{L}^{-1}\cdot\text{min}^{-1} \cdot 10^{-2}$	$K_S / K_P$	$K_P$ (M)
Linear regression	4.79	1 <sup>a</sup>	0.31 (=K <sub>M-PDL</sub> )
Modeled	5.92 +/- 0.26	1.63	0.19 +/- 0.024

<sup>a</sup> Assuming a linear relationship implies the assumption that  $K_S=K_P$ , thus  $K_S/K_P = 1$ .

Although other factors that do not directly involve substrate-enzyme interaction might play a role – such as increased viscosity during the course of reaction, and the concomitant limitation in diffusion of molecules – it appears that the model can accurately describe the time-conversion history of enzymatic ring-opening polymerization. Using this model, the initial velocity of the enzymatic reaction can be estimated more accurately.

### 6.3 Application of the LH model to enzyme kinetics

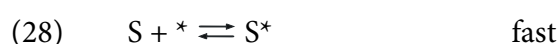
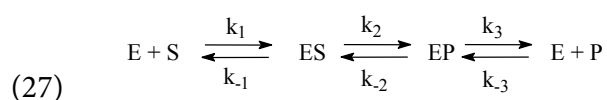
Many enzymatic reactions can be described using Michaelis-Menten (MM) kinetics. A wide variety of systems have been described with MM- or MM-like rate equations.<sup>2</sup> For more complex situations (e.g. multiple substrate, multiple products) where no suitable Michaelis-Menten-type equation is available, the King-Altman method was developed, which allows the (partly graphical) construction of a custom rate equation for virtually every enzymatic system.<sup>2</sup> In situations where the King-Altman method is considered too complex, the application of Langmuir-Hinshelwood (LH) kinetics might be considered. We believe this can be a valuable addition to the general MM-approach. Derivation of rate equations for e.g. iterative tandem catalysis (multiple substrates, product inhibition, and, in addition, coupled racemization kinetics) is extremely complex if not impossible using MM kinetics, but can readily be done adopting this approach.

The LH mechanism was developed for description of surface catalysis, originating from heterogeneous catalysis in which reaction occurs between species that are both adsorbed on

the surface.<sup>11</sup> The adsorption of substrate on the surface is described by Langmuir isotherms. Reaction kinetics are then derived based on the assumption that reaction occurs between adsorbed species, and that the rate of reaction can be described using the fractions of the catalytic sites occupied by substrates, rather than concentrations. The similarity between enzymatic and heterogeneous catalysis is striking; both share the general concept of adsorption – reaction – desorption. This was recognized as early as in 1972 by Chaplain, although very few authors, if any, have followed his approach.<sup>12</sup> The use of LH kinetics constitutes a more general approach towards enzyme kinetics than MM kinetics or the King-Altman Method. First, we show that LH kinetics results in the same rate equation as MM by analyzing a single-substrate single-product reaction (the classic MM case). Then, in section 6.4, a rate equation is derived for an ITC polymerization and calculation with the resulting model is compared with the experimental data.

### 6.3.1 Langmuir-Hinshelwood applied to a MM single substrate single product reaction

Equation 27 shows the classic single-substrate single-product batch reaction on which the Michaelis-Menten kinetic model is based. Using the LH mechanism, Equations 28 to 30 can be developed, describing the reaction mechanism. In these equations, \* denotes a free active site and S\* denotes an active site occupied by a substrate molecule. As in MM-kinetics, it is assumed that the conversion of substrate to product is rate-determining. Based on these reaction steps, the kinetic equations 28a-30a are derived. In these equations,  $\Theta_s$  denotes the fraction of catalytic sites occupied by a substrate molecule; [S] represents the substrate concentration.  $K_s$  and  $K_p$  are the association constants for substrate and product, respectively. Since the formation of product ( $ES \rightarrow EP$ ) is assumed to be the rate-determining step, the rate of reaction  $\nu$  is based on the kinetics of this step (Equation 29a). Since fractions of the active sites are used, the rate equation includes  $[E]_t$  which represents the total concentration of enzyme active sites in the system. Naturally, the sum of fractions of catalytic sites must equal unity (Equation 31). Solving Equation 31 for  $\Theta^*$  results in Equation 32, and subsequently the rate equation 33 can be derived by replacing  $\Theta_s$  and  $\Theta_p$  accordingly in Equation 29a.





$$(28a) \quad \Theta_S = \frac{k_{-1}}{k_1} [S] \Theta^* = K_S [S] \Theta^*$$

$$(29a) \quad v = -\frac{d[S]}{dt} = [E]_t (k_2 \Theta_S - k_{-2} \Theta_P)$$

$$(30a) \quad \Theta_P = \frac{k_{-3}}{k_3} [P] \Theta^* = K_P [P] \Theta^*$$

$$(31) \quad \Theta^* + \Theta_S + \Theta_P = 1$$

$$(32) \quad \Theta^* = \frac{1}{1 + K_S [S] + K_P [P]}$$

$$(33) \quad v = [E]_t \frac{k_2 K_S [S] - k_{-2} [P] K_P}{1 + K_S [S] + K_P [P]}$$

### Analysis of limiting cases

In case of very high substrate concentration ( $[S] \rightarrow \infty$ ), the rate equation simplifies to Equation 34. In MM-kinetics, we know that at saturating substrate concentration, reaction rate equals  $V_{\max}$ . Therefore, in this model  $k_2[E]_t$  is equivalent to  $V_{\max}$ .

$$(34) \quad v = k_2 [E]_t$$

$$(35) \quad k_2 [E]_t = V_{\max}$$

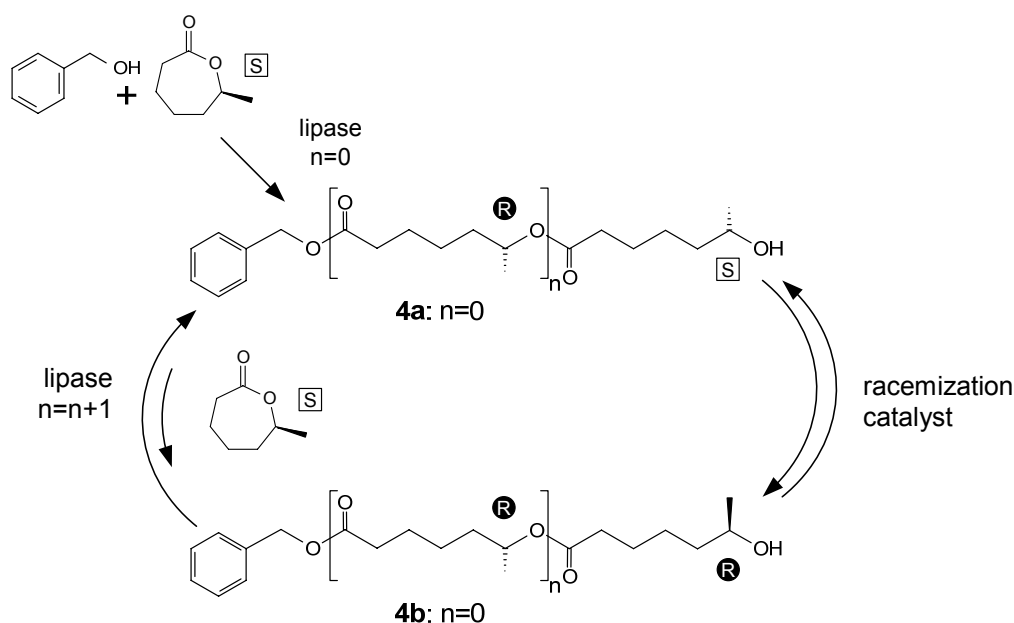
When  $[S] = K_S^{-1}$  (and neglecting reverse reaction and product inhibition, so  $k_{-2} = K_P = 0$ ), Equation 36 is obtained. The reaction now runs at half of  $V_{\max}$ . In the MM model, this occurs when  $[S] = K_M$ . Therefore, Equation 37 shows the relationship between the association constant  $K_S$  and the Michaelis-Menten concentration  $K_M$ . Note that  $K_S$  is a true association constant, and is only directly related to  $K_M$  if  $ES \rightarrow EP$  is indeed significantly slower than adsorption of substrate on the catalytic site ( $k_2 \ll k_{-1}$ ). Briggs and Haldane showed this very elegantly already in 1925 by deriving Equation 38.<sup>2</sup>

$$(36) \quad v = \frac{1}{2} k_2 [E]_t \quad (37) \quad K_M = \frac{1}{K_S} \quad (38) \quad K_M = \frac{k_{-1} + k_2}{k_1}$$

From Equation 33, the MM-equation (Equation 6) is easily obtained by replacing  $k_2[E]_t$  and  $K_S$  by  $V_{\max}$  and  $K_M$  and by neglecting product inhibition and reverse reaction ( $k_{-2} = K_P = 0$ ). For an enzymatic ring-opening polymerization and for a two-substrate reaction, rate equations have also been derived using the LH-mechanism. The details thereof can be found in Appendix A.

## 6.4 Kinetic evaluation of iterative tandem catalysis of (*S*)-6-MeCL

In Chapter 4, we introduced the concept of iterative tandem catalysis (ITC) as a polymerization strategy by which chain growth is effectuated by a combination of two (or more) intrinsically different catalytic processes that are both compatible and complementary. Proof of principle was provided by the ITC of (*S*)-6-methyl- $\epsilon$ -caprolactone ((*S*)-6-MeCL). The lipase-catalyzed ring-opening of  $\omega$ -substituted lactones, such as 6-MeCL, results in a ring-opening product bearing a secondary alcohol (Scheme 6.1). Since lipases generally only accept the *R*-enantiomer of a secondary alcohol as the nucleophile, propagation halts after the ring-opening of a (*S*)-6-MeCL molecule. Combining ruthenium-catalyzed racemization with lipase-catalyzed ring-opening enabled the two-pot oligomerization of (*S*)-6-MeCL.<sup>13</sup>



**Scheme 6.1** Synthesis of oligo-*R*-6-MeCL from (*S*)-6-MeCL by ITC.

### 6.4.1 Kinetic behavior of one-pot ITC of (*S*)-6-MeCL

In an ITC polymerization of (*S*)-6-MeCL two simultaneous catalytic reactions are taking place: enzymatic ring-opening polymerization (eROP) and Ru-catalyzed racemization of secondary alcohols. A typical one-pot ITC experiment using (*S*)-6-MeCL shows three different kinetic regimes in the conversion-time history (Figure 6.6).<sup>14</sup> In the early stages of the reaction, initiation takes place and consumption of lactone is fast (regime A). Now, all initiator molecules have started a polymer chain and the alcohol end-groups are in the *S*-configuration. Racemization is rate-limiting, and zero order kinetics are observed (regime B). At the final stages of reaction, competition by the polyester product results in a large decrease

of net enzymatic activity, and the reaction is slowed down; formation of the acyl enzyme complex is now rate-limiting (regime C).

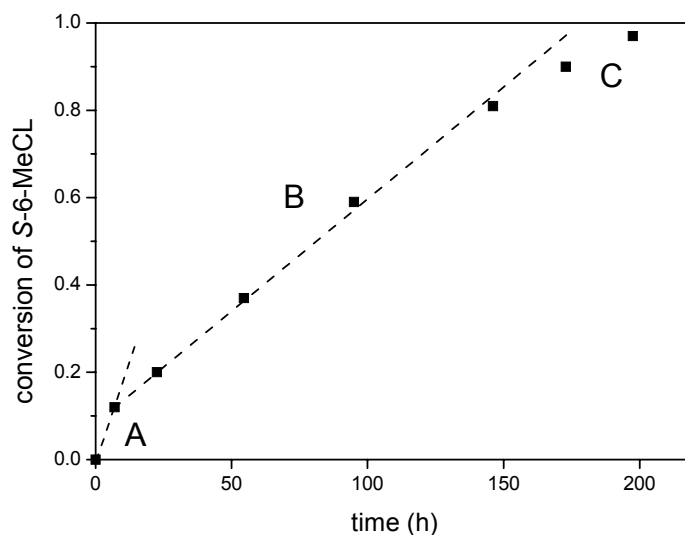


**Figure 6.6** Regimes in the conversion-time history of a typical ITC experiment: (A) high rate of consumption during the initial stages of the reaction as a result of initiation; (B) zero-order in substrate concentration due to rate-limiting racemization; (C) deviation from zero-order kinetics at high conversion due to rate-limiting formation of the acyl enzyme EM. Experimental conditions: 0.06 mmol Ru catalyst **2** (Shvo's catalyst; see Chapter 5), 35 mg Novozym 435, 0.125 mmol BA, 2.5 mmol (S)-6-MeCL, 0.20 mmol 2.5 mL toluene (2.5 mL), 0.24 mmol 2,4-dimethyl-3-pentanol, 1,3,5-tri-tert-butylbenzene (internal standard),  $T = 70\text{ }^{\circ}\text{C}$  under an argon atmosphere.

The zero-order behavior of the ITC experiments can be explained by the kinetics of the tandem catalytic system. The mechanism of eROP is proposed to proceed via an acyl enzyme complex (EM) at a Ser-OH residue in the active site of the lipase.<sup>15,16</sup> Figure 6.7 shows the Cleland plot for enzymatic ring-opening of (S)-6-MeCL (**A**). This mechanism can be described as a “bi uni sequential ordered” mechanism. In a typical eROP of a lactone, the formation of EM is the rate-determining step.<sup>6</sup> In some cases, nucleophilic attack by the hydroxyl chain ends (**B**) can become rate-limiting (e.g. sterically hindered nucleophiles, or in the case of a very low nucleophile concentration).<sup>17</sup> The kinetics of such systems are often described by Michaelis Menten (MM) kinetics.

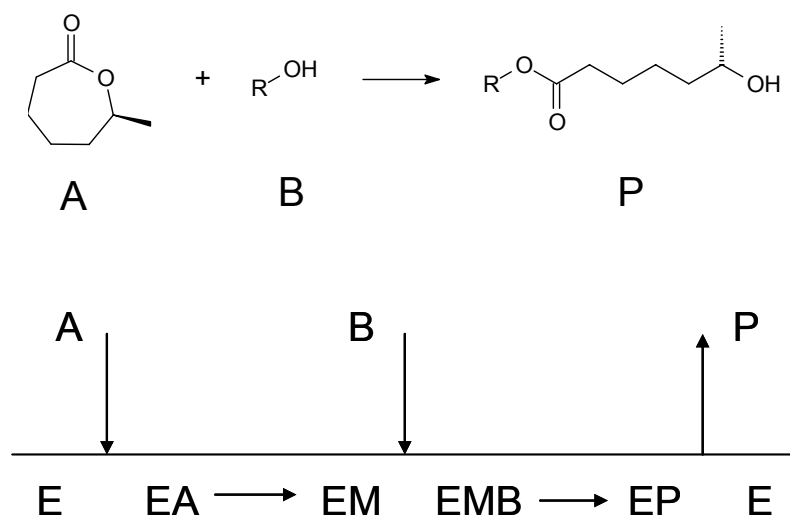


**Figure 6.7** Cleland plot for enzymatic ring-opening polymerization of (S)-6-MeCL.

As ring-opening of (S)-6-MeCL furnishes an *S*-secondary alcohol whereas lipase-catalyzed transesterification of secondary alcohols is *R*-selective, Ru-catalyzed racemization is required for a polymerization on a realistic time-scale. The racemization is assumed to obey first-order kinetics with respect to the *S*-secondary alcohol concentration. During the polymerization, the total concentration of alcohol end-groups ( $R + S$ ) will be constant. To analyze the kinetic behavior of such system, it is instructive to take a closer look at two extreme cases.

1. When the time constant of racemization is (much) lower than that of the enzymatic reaction, approximately half of the alcohol groups will be in the *R*-configuration ( $ee = 0\%$ ). The enzymatic reaction is rate-limiting; more specifically, the *formation of EM* is now rate determining, and pseudo MM kinetics will be observed. Thus, rate of reaction will be first order in (S)-6-MeCL concentration.

2. When the time constant of the enzymatic reaction is (much) lower than that of the racemization, the *ee* of the end-groups will be high (near 100%). The rate of reaction is now proportional to the 'production' of *R*-alcohol by the racemization catalyst. If the *ee* is near 100%, then the production of *R*-alcohol is first order in *S*-alcohol concentration. The concentration of *S*-alcohol end-groups remains constant during most of the reaction, and, therefore, the rate of production of reactive *R*-alcohol is approximately constant during reaction. Therefore, zero order kinetics will be observed for the reaction.



$$(45) \quad \Theta_A = K_A[A]\Theta^*$$

$$(46) \quad \Theta_M = K_{AM}\Theta_A = K_A K_{AM}[A]\Theta^*$$

$$(47) \quad v = \Theta_M[R][E]_t$$

$$(48) \quad \Theta_{MR} = K_{MR}\Theta_P = K_{MR}K_P[A]\Theta^*$$

$$(49) \quad \Theta_P = K_P[P]\Theta^*$$

Together with Equation 50, which states that the sum of these fractions should equal unity, an expression for  $\Theta^*$  can be derived (Equation 51):

$$(50) \quad \Theta^* + \Theta_A + \Theta_M + \Theta_{MR} + \Theta_P = 1$$

$$(51) \quad \Theta^* = \frac{1}{1 + K_A[A] + K_A K_{AM}[A] + K_{MR}K_P[P] + K_P[P]}$$

Using Equations 45, 46, 47 and 51, differential equations 52 and 53 can be derived which describe the consumption of A, R and S and the formation of P.<sup>19</sup> As can be seen, the rate of reaction (i.e. monomer (A) consumption) is dependent on lactone concentration ([A]) as well as R-alcohol concentration ([R]). This is, at first sight, somewhat counterintuitive, since we observe zero order kinetics in the ITC of (S)-6-MeCL in regime B. During the course of reaction, however, the concentration of (S)-6-MeCL goes down, while the concentration of polyester (P) goes up. Therefore, less active sites are available to perform a productive reaction, i.e. the ring-opening of (S)-6-MeCL. If the rate of reaction would drop only slightly, the concentration of R-alcohol [R] would immediately increase, as the production of R-alcohols by the racemization catalyst is related to the concentration of S-alcohols [S]; this concentration barely changes since ee is close to 100%, so the production of R-alcohol stays constant. Consequently, the product [A]·[R] apparently stays approximately constant in ITC while in regime B.

$$(52) \quad \frac{d[A]}{dt} = -\frac{d[P]}{dt} = -k_3\Theta_M[R][E]_t = -[E]_t \frac{k_3 K_A K_{AM}[A][R]}{1 + K_A[A] + K_A K_{AM}[A] + K_{MR}K_P[P] + K_P[P]}$$

$$(53) \quad \frac{d[R]}{dt} = -\frac{d[S]}{dt} = k_{-6}[S] - k_6[R] - [E]_t \frac{k_3 K_A K_{AM}[A][R]}{1 + K_A[A] + K_A K_{AM}[A] + K_{MR}K_P[P] + K_P[P]}$$

### 6.4.3 Simulation of ITC based on the LH model

Equations 52 and 53 have been solved numerically using Matlab software (the scripts applied can be found in the Experimental section). Table 6.3 shows the values that were used for the constants and initial concentrations. A M/I ratio of 20 was chosen. The racemization constant was set 3 orders of magnitude smaller than the enzymatic rate constant. The values of these constants were chosen so that the timescale of the simulation corresponds to the timescale of the actual experiment of Figure 6.6.  $K_A$  was set at  $1 \text{ M}^{-1}$  and  $K_P$  at  $2 \text{ M}^{-1}$ , which are credible values considering the  $K_M$  of  $0.73 \text{ M}$  for  $\epsilon$ -caprolactone.<sup>10,20</sup> In a typical ring-opening of  $\epsilon$ -caprolactone the formation of the acyl enzyme complex is known to be rate-limiting.<sup>6</sup> Therefore, the constant  $K_{AM}$  is expected to be significantly smaller than  $K_{MR}^{-1}$  (see Equations 46 and 48). To correspond to the data of Figure 6.6, the parameters were set at 0.1 and 0.01, respectively.

**Table 6.3** Values for constants and initial concentrations used in simulation of the ITC of (S)-6-MeCL.

parameter	value
initial (S)-6-MeCL concentration $[A]_0$	2 M
initial initiator concentration $[R]_0$	0.1 M <i>R</i> -1-phenylethanol <sup>21</sup>
racemization rate constant $k_6 = k_{-6}$	$0.0019 \text{ min}^{-1}$
enzymatic rate constant $k_3$	$2.8 \text{ min}^{-1}$
$K_A$	$1 \text{ M}^{-1}$
$K_P$	$2 \text{ M}^{-1}$
$K_{AM}$	0.1
$K_{MR}$	0.01

With these parameters, the simulation was performed and Figures 6.8 to 6.10 show the conversion-time history, the concentration of R and S, the ee of the alcohol groups and the product of [R] and [A], respectively. In Figure 6.8 the simulated lactone conversion is placed as an overlay on the obtained experimental data, indicating that the model matches the observed conversion-time history quite accurately. Regimes A, B (zero order) and C can be recognized clearly. Figure 6.9 shows the concentration and ee of the terminal secondary alcohol groups versus time. As expected, the concentration of R ([R]) gradually increases over time, as the lactone concentration goes down. Figure 6.10 shows that indeed the product of [A] and [R] is approximately constant in the time span during which zero order kinetics were observed experimentally.<sup>22</sup>

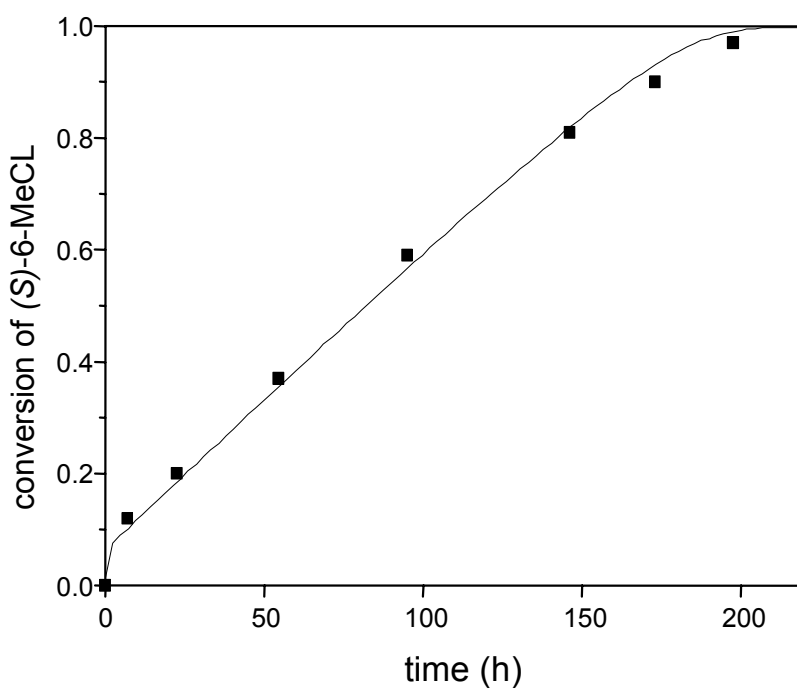


**Figure 6.8** Experimental data (■) and simulated data (straight line) of (S)-6-MeCL during the course of ITC.

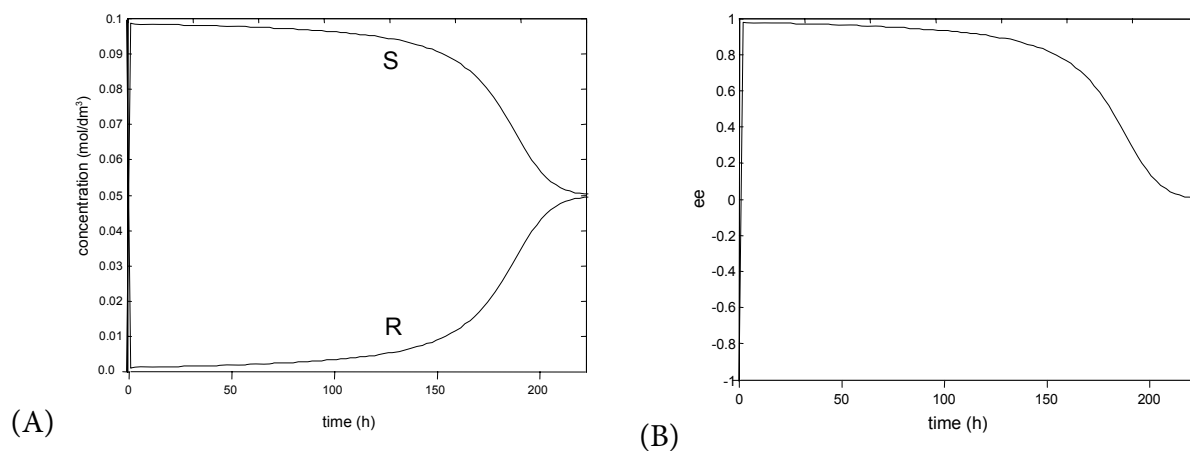


**Figure 6.9** (A) Concentration of R and S during the course of ITC of (S)-6-MeCL (simulated) (B) ee of the secondary alcohol groups.



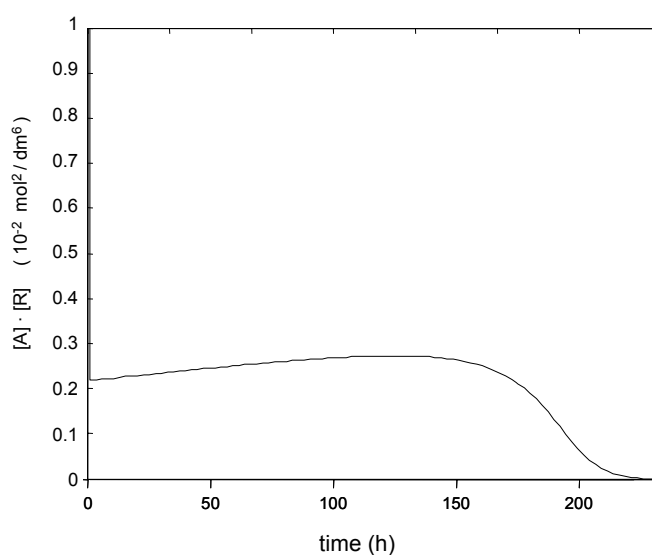


**Figure 6.10** Value obtained for the product of  $[A]$  and  $[R]$  during the course of ITC of (S)-6-MeCL (simulated).

#### 6.4 Conclusions

Enzymatic ring-opening polymerizations generally follow a Michaelis-Menten kinetic profile. Competition by the polyester product (product inhibition) has to play an important role. Assuming that the dissociation constants for polyester and lactone are similar, net pseudo first order kinetics are expected. However, if this is not the case, deviation from first order kinetics will occur. This deviation is indeed observed experimentally in the enzymatic ring-opening polymerization of  $\epsilon$ -caprolactone. The calculated dissociation constants for poly( $\epsilon$ -caprolactone) and poly( $\omega$ -pentadecalactone) were 0.24 M and 0.19 M, respectively. This suggests that the affinity of the lipase for esters in the *transoid*-conformation generally is higher than for esters in the *cisoid*-conformation.

A kinetic analysis based on the Langmuir-Hinshelwood (LH) mechanism was introduced as an efficient method for the derivation of rate equations for enzymatic reactions. Although based on the same principles as Michaelis-Menten kinetics, the LH mechanism allows description of the kinetics of more complex processes. Based on the LH mechanism, a model was developed that describes the kinetics of the ITC of (S)-6-MeCL. It was shown that the predicted conversion-time plot accurately matches the experimental observations.

## 6.5 Experimental

### *Matlab scripts used for ITC simulation*

#### **ITC.m**

```
% This script calculates and plots time-conversion/concentration for the 0th order region
% of ITC. The underlying kinetic analysis is described in Chapter 6 of the
% thesis of B.A.C. van As, Eindhoven University of Technology. The
% accompanying differential equations are described in deITC.m
```

```
% definition of variables
```

```
global k6f k6b KAM KA KP k3f KMR R0 S0 A0 P0
```

```
% the different components in the reaction mixture are numbered as follows:
```

```
% 1 = R-alcohol
```

```
% 2 = S-alcohol
```

```
% 3 = Lactone (A)
```

```
% 4 = Polyester (P)
```

```
% definition of all constants
```

```
k6f=0.0019;
```

```
k6b=k6f;
```

```
KA=1;
```

```
KAM=.1;
```

```
KP=2*KA;
```

```
KMR=.01;
```

```
k3f=2.8;
```

```
% runtime of the simulation
```

```
endtime=14000;
```

```
% initial conditions
```

```
R0=.1;
```

```
S0=0;
```

```
L0=2;
```

```
P0=0;
```

```
%initial condition matrix
```

```
y0=[R0 S0 L0 P0]';
```

```
% defining the stepsize for the iterative calculation
```

```
n=100;
```

```
step=endtime/n;
```

```
% creating empty matrices for data storage
```

```
R=[];
S=[];
P=[];
L=[];
t=[];
XL=[];
ee=[];
cRcA=[];

% calling ODE45 for solving the set of DE
[t,y]=ode45('deITC', [0:step:endtime], y0);

% calculating the conversion, ee and product of cR and cL
sizey=size(y);
XL=zeros(sizey(1),1);
XL=1-(y(:,3)/(L0+P0));
ee=zeros(sizey(1),1);
ee=(y(:,2)-y(:,1))./(y(:,1)+y(:,2));
cRcA=zeros(sizey(1),1);
cRcA=y(:,1).*y(:,3);

%drawing figures to display simulation results
figure(1);
plot(t,[XL]);
legend('Conversion Lactone');
xlabel('time (min.)');
ylabel('Conversion');

figure(2);
plot(t,[y(:,1),y(:,2)]);
legend('R','S');
xlabel('time (min.)');
ylabel('concentration');

figure(3);
plot(t,ee);
legend('ee');
xlabel('time (min.)');
ylabel('ee');

figure(4);
plot(t,cRcA);
legend('cR*cA');
xlabel('time (min.)');
ylabel('cR*cA');
```

### **deITC.m**

% This function describes the differential equations belonging to

% ITC.m The underlying kinetic analysis is described in Chapter 6 of the  
% thesis of B.A.C. van As, Eindhoven University of Technology.

```
function dy=dv(t,y)
global k6f k6b KAM KA KP k3f KMR R0 S0 A0 P0

% 1 = R-alcohol
% 2 = S-alcohol
% 3 = Lactone (A)
% 4 = Polyester (P)

dy=zeros(4,1);
dy(1)=k6f*y(2)-k6b*y(1)-((k3f*y(1)*KAM*KA*y(3))/(1+KA*y(3)+KAM*KA*y(3)+KP*y(4)+KMR*KP*y(4)));
dy(2)=-dy(1);
dy(3)=-((k3f*y(1)*KAM*KA*y(3))/(1+KA*y(3)+KAM*KA*y(3)+KP*y(4)+KMR*KP*y(4)));
dy(4)=-dy(3);
```

## 6.6 References and notes

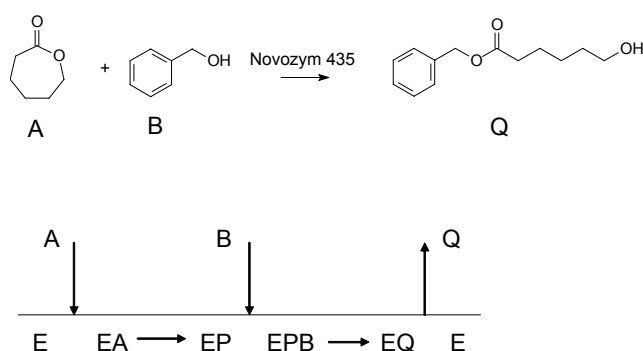
1. *Biochem. J.* **1983**, 213, (3), 561-71.
2. Segel, I. *Enzyme Kinetics* **1993** Wiley Classics Library
3. The latter statement only holds in situations where no intermediate enzyme species exist after ES, i.e. when the reaction scheme is not more complex than presented in Equation 1.
4. Regardless of the values of  $k_2$  and  $k_{-1}$ ,  $K_M$  can be regarded as a pseudo-dissociation constant, since it always holds that  $K_M = [ES]/[E].[S]$ . Only if the adsorption of substrate on the enzyme is at equilibrium during reaction (which is the case if  $k_2 \ll k_{-1}$ ),  $K_M$  truly is a dissociation constant.
5. Fersht, A. *Enzyme structure and mechanism* **1977**.
6. Martinelle, M.; Hult, K. *Biochim. Biophys. Acta* **1995**, 1251, (2), 191-197.
7. If the nucleophile concentration is very low (e.g. in an attempt to synthesize very high molecular weight polyester by using very little or no initiator), this assumption does not hold anymore and the attack of the nucleophile may become rate-limiting.
8. At  $S_0 = 2$  M,  $V_{max} = 0.01$  mol/m<sup>3</sup>.s and  $K_S = 0.1$  M,  $v_0 = 0.952 \cdot V_{max}$ , which is exactly the result of the calculation.
9. Microcal OriginPro 7.5 SR1 was used to perform the non-linear curve fitting. The data were fitted to the relationship between time and conversion as described by Equation 22.
10. van der Mee, L.; Helmich, F.; de Bruijn, R.; Vekemans, J.A.J.M.; Palmans, A.R.A.; Meijer, E.W. *Macromolecules* **2006**, 39, (15), 5021-5027.
11. Chorkendorff, I.; Niemantsverdriet, J.W. *Concepts of Modern Catalysis and Kinetics* **2003** Wiley-VCH, Weinheim
12. Chaplain, R.A. *Chemische Technik (Leipzig, Germany)* **1972**, 24, (1), 4-10.
13. van As, B.A.C.; van Buijtenen, J.; Heise, A.; Broxterman, Q.B.; Verzijl, G.K.M.; Palmans, A.R.A.; Meijer, E.W. *J. Am. Chem. Soc.* **2005**, 127, (28), 9964-9965.
14. van Buijtenen, J. *Ph.D Thesis, in preparation* **2006**.
15. Uyama, H.; Namekawa, S.; Kobayash, S. *Polymer Journal* **1997**, 29, (3), 299-301.

16. Macdonald, R.T.; Pulapura, S.K.; Svirkin, Y.Y.; Gross, R.A.; Kaplan, D.L.; Akkara, J.; Swift, G.; Wolk, S. *Macromolecules* **1995**, 28, (1), 73-78.
17. Peeters, J.W.; van Leeuwen, O.; Palmans, A.R.A.; Meijer, E.W. *Macromolecules* **2005**, 38, (13), 5587-5592.
18. Reactions on esters in the growing polymer chain, such as transesterification and formation of cyclic species, are neglected. These reactions will take place, but are not productive in terms of monomer conversion as the concentration of (*S*)-6-MeCL and the concentration of *R*-alcohol are not altered. Furthermore, the initiation is not explicitly taken into account. Also, nucleophilic attack by *S* is neglected.
19. It is assumed that the reverse reaction of Equation 41 can be neglected.
20. Note that  $K_A$  and  $K_P$  are defined association constants, whereas  $K_M$  is a dissociation constant. Therefore  $K_P$  is larger than  $K_A$ , since the affinity of the enzyme for polyester is assumed to be higher.
21. In the experiment described in Figure 6.6 benzyl alcohol is used as the initiator. In the simulation, only secondary alcohols are considered, therefore (*R*)-1-phenylethanol was set to be the initiator; the initiation behavior of these molecules is supposed to be similar.
22. The association constant for the polyester ester groups ( $K_P$ ) is set higher than for the lactone ( $K_A$ ), in accordance with the observations described in section 6.2. Therefore, the reaction rate will slow down more than anticipated based on first order kinetics. Thus, the denominator in Equations 51 and 52 is not constant, but grows during the course of the reaction. Thus, the product of  $[A]$  and  $[R]$  is not constant, but increases slightly over time. The rate of reaction then is approximately constant, and pseudo first order kinetics are observed.

## Appendix A. Application of the LH mechanism on enzymatic ring-opening polymerization and an enzymatic two-substrate reaction

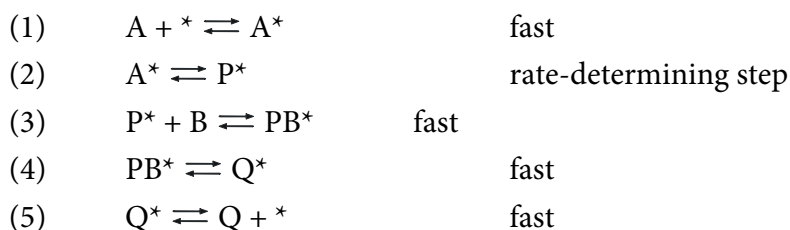
### A.1 Application of the LH mechanism on an enzymatic ring-opening polymerization

Figure A.1 shows the Cleland plot for an enzymatic ring-opening polymerization of  $\epsilon$ -caprolactone. First the lactone (A) adsorbs in the active site (resulting in EA). The nucleophilic attack of the Ser-OH results in formation of the acyl-enzymcomplex EP. A nucleophile (the alcohol) performs a nucleophilic attack resulting in EPB which transforms in the adsorbed product Q in the active site (EQ). Desorption of the product Q reforms the free enzyme E. In Cleland nomenclature this mechanism can be described as a “bi mono sequential ordered” mechanism, since the reactants must adsorb in this specific order for product formation to occur. It is generally accepted that under most circumstances  $EA \rightarrow EP$  is the rate-determining step.<sup>1</sup>



**Figure A.1** Cleland plot for the ring-opening polymerization of  $\epsilon$ -caprolactone

Equations 1 to 5 describe the adsorption and reactions in this system. The kinetic equations 1a-5a can then be derived, and together with Equation 6 rate equation 8 is derived.



$$(1a) \quad \Theta_A = K_A \Theta^* [A]$$

$$(2a) \quad v = k_f \Theta_A - k_b \Theta_P$$

$$(3a) \quad \Theta_P = \frac{\Theta_{PB}}{K_B [B]}$$

$$(4a) \quad \Theta_{PB} = \frac{\Theta_Q}{K_{PBQ}}$$

$$(5a) \quad \Theta_Q = K_Q[Q]\Theta^*$$

$$(6) \quad \Theta^* + \Theta_A + \Theta_P + \Theta_{PB} + \Theta_Q = 1$$

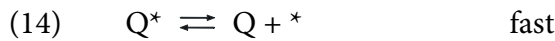
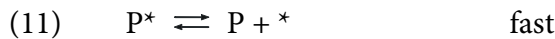
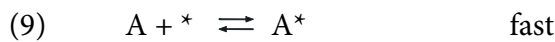
$$(7) \quad \Theta^* = \frac{1}{1 + K_A[A] + \frac{K_Q}{K_{PBQ}K_B} \frac{[Q]}{[B]} + \frac{K_Q}{K_{PBQ}} [Q] + K_Q[Q]}$$

$$(8) \quad r = \frac{k_f K_A [A]}{1 + K_A [A] + \frac{K_Q}{K_{PBQ}K_B} \frac{[Q]}{[B]} + \frac{K_Q}{K_{PBQ}} [Q] + K_Q [Q]} - \frac{k_b K_Q \frac{[Q]}{[B]}}{K_{PBQ}K_B \frac{[Q]}{[B]} + \frac{1}{1 + K_A [A] + \frac{K_Q}{K_{PBQ}K_B} \frac{[Q]}{[B]} + \frac{K_Q}{K_{PBQ}} [Q] + K_Q [Q]}}$$

Analogous to the single-substrate single-product case, the limiting cases  $[A] \rightarrow \infty$  with no reverse reaction, and  $K_A[A] = 1$  yield the Michaelis-Menten constants  $V_{\max} = k_f$  and  $K_M = K_A^{-1}$ .

#### Langmuir-Hinshelwood model applied to a two substrate enzymatic reaction

A more complex situation arises when two substrates compete for the enzyme's active site. Examples include an enantioselective reaction or a copolymerization of two monomers in an enzymatic ring-opening polymerization (assuming the nucleophilic attack of the alcohol is not rate-limiting). Equations 9-14 describe this system, resulting in rate equations 9a-14a. Solving Equations 10a and 13a yields the differential equations 19 and 20.



$$(9a) \quad \Theta_A = K_A \Theta^* [A]$$

$$(10a) \quad v_A = k_A^f \Theta_A - k_A^b \Theta_P$$

$$(11a) \quad \Theta_P = K_P \Theta^* [P]$$

$$(12a) \quad \Theta_B = K_B \Theta^* [B]$$

$$(13a) \quad v_B = k_B^f \Theta_B - k_B^b \Theta_Q$$

$$(14a) \quad \Theta_Q = K_Q \Theta^* [Q]$$

$$(15) \quad \Theta^* + \Theta_A + \Theta_P + \Theta_{PB} + \Theta_Q = 1$$

$$(16) \quad [P] = [A]_0 - [A]$$

$$(17) \quad [Q] = [B]_0 - [B]$$

$$(18) \quad \Theta^* = \frac{1}{1 + K_A[A] + K_B[B] + K_P[A]_0 + K_Q[B]_0 - K_P[A] - K_Q[B]}$$

$$(19) \quad v_A = -\frac{d[A]}{dt} = \frac{k_A^f K_A[A] - k_A^b K_P[A]_0 + k_A^b K_P[A]}{1 + K_A[A] + K_B[B] + K_P[A]_0 + K_Q[B]_0 - K_P[A] - K_Q[B]}$$

$$(20) \quad v_B = -\frac{d[B]}{dt} = \frac{k_A^f K_A[B] - k_A^b K_P[B]_0 + k_A^b K_P[B]}{1 + K_A[A] + K_B[B] + K_P[A]_0 + K_Q[B]_0 - K_P[A] - K_Q[B]}$$

To solve these differential equations, the backward rate constants  $k_b^A$  and  $k_b^B$  need to be estimated. We can relate these kinetic constants to the equilibrium constants, when  $v_A = v_B = 0$  (analogous to the Haldane equations). This yields Equations 21 and 22. Assuming a one-substrate one-product equilibrium, they can be defined as in Equations 23 and 24 and be determined experimentally.

$$(21) \quad k_A^b = k_A^f \frac{K_A}{K_P K_A^{EQ}}$$

$$(22) \quad k_B^b = k_B^f \frac{K_B}{K_Q K_B^{EQ}}$$

$$(23) \quad K_A^{EQ} = \frac{[P]}{[A]}$$

$$(24) \quad K_B^{EQ} = \frac{[Q]}{[B]}$$

## A.2 Scripts used for simulation using Matlab

### **de\_twosubstrate.m**

```
% This function describes the differential equations belonging to
% twosubstrateLH.m The underlying kinetic analysis is described in Appendix A of the
% thesis of B.A.C. van As, Eindhoven University of Technology.
```

```
function dy=dv(t,y)
global k1f k1b k2f k2b KS1 KS2 KP1 KP2 KEQ CS10 CS20
```

```
% 1 = substrate 1
```



% 2 = substrate 2

dy=zeros(2,1);

dy(1)=-((k1f\*KS1\*y(1)-k1b\*KP1\*CS10+k1b\*KP1\*y(1))/(1+KS2\*y(2)+KS1\*y(1)+KP2\*CS20+KP1\*CS10-  
KP2\*y(2)-KP1\*y(1)));

dy(2)=-((k2f\*KS2\*y(2)-k2b\*KP2\*CS20+k2b\*KP2\*y(2))/(1+KS2\*y(2)+KS1\*y(1)+KP2\*CS20+KP1\*CS10-  
KP2\*y(2)-KP1\*y(1)));

### **twosubstrateLH.m**

% This script calculates and plots time-conversion/concentration for a two-substrate reaction

% The underlying kinetic analysis is described in Appendix A of the

% thesis of B.A.C. van As, Eindhoven University of Technology. The

% accompanying differential equations are described in de\_twosubstrate.m

% y1 = substrate 1

% y2 = substrate 2

global k1f k1b k2f k2b KS1 KS2 KP1 KP2 KEQ CS10 CS20 CS1eind CS2eind CP1eind CP2eind CP1 CP2 CS1  
CS2

% definition of all constants

k1f=.5;

k2f=.1;

KS1=1;

KS2=1;

KP1=1 ;

KP2=1;

KEQ=2;

XEQ=1/(1+(1/KEQ));

% runtime of the simulation

endtime=15;

% calculating the backward rate constants using the derived Haldane equations

k1b=k1f/(KS1\*KEQ);

k2b=k2f/(KS2\*KEQ);

% initial conditions

CS10=.1;

CS20=.1;

%initial condition matrix

y0=[CS10 CS20]';

% defining the stepsize for the iterative calculation

n=100;

step=endtime/n;

```
% creating empty matrices for data storage
CS1=[];
CS2=[];
t=[];
XS1=[];
XS2=[];
Xtot=[];
LNX=[];
XXEQ=[];
LNXXEQ=[];

% calling ODE45 for solving the set of DE
[t,y]=ode45('DE', [0 endtime], y0);

% calculating the conversions and ln (1 - conversion)
sizey=size(y);

XS1=zeros(sizey(1),1);
XS2=zeros(sizey(1),1);
XS1=zeros(sizey(1),1);
XS1=1-y(:,1)/CS10;
XS2=1-y(:,2)/CS20;
Xtot=(0.5*(1-y(:,1)/CS10)+0.5*(1-y(:,2)/CS20));
LNX=-log(1-Xtot(:,1));
XXEQ=1-(Xtot(:,1)/XEQ);
LNXXEQ=-log(XXEQ);

%drawing figures to display simulation results
figure(1);
plot(t,[XS1,XS2,Xtot]);
legend('Conversion-S1','Conversion-S2','Conversion-tot');
xlabel('time (min.)');
ylabel('Conversion');
figure(2);
plot(t,[LNX,LNXXEQ]);
legend('-ln(1-X)', '-ln(1-X/Xeq)');
xlabel('time (min.)');
ylabel('-ln(1-X); -ln(1-X/Xeq)');
```

### A.3 References

1. Martinelle, M.; Hult, K. *Biochimica Et Biophysica Acta-Protein Structure And Molecular Enzymology* **1995**, 1251, (2), 191-197.

## Summary of the thesis

### Tandem catalysis in polymer chemistry

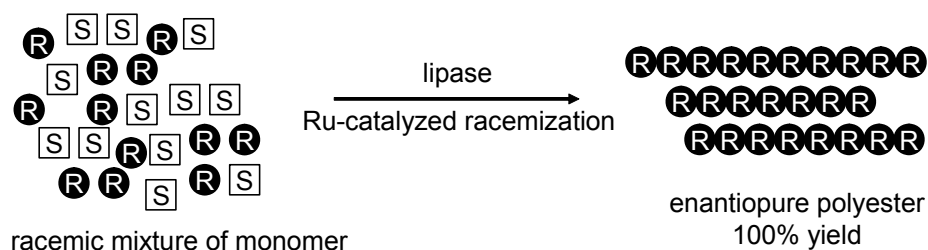
Catalysis is of paramount importance in the chemical industry; the production of most industrially relevant chemicals involves catalysis. One distinguishes between homogeneous catalysis (a molecularly dissolved catalyst), heterogeneous catalysis (a solid catalyst in a liquid or gaseous phase) and biocatalysis (the use of nature's catalysts, enzymes). Each of these has its distinct features, applications and advantages. In the past decade, the concurrent use of multiple catalysts in a single system, known as tandem catalysis, has gained considerable interest. The reasons for this are clear: a decrease in waste, energy use and costs can be achieved by eliminating intermediate work-up. Moreover, the interplay of the catalysts may allow for the synthesis of materials of higher structural complexity.

In organic synthetic chemistry, this integration of different catalytic processes has become commonplace. Many different synthetic schemes have been developed that make use of multiple catalysts in a single system. Often the merits of different catalytic disciplines (i.e. heterogeneous, homogeneous and/or biocatalysis) are simultaneously exploited. Surprisingly, in synthetic polymer chemistry tandem catalysis is hardly ever employed. A reason for this may lie in the complexity of tandem catalytic polymerizations: all concurrent reactions must occur with almost perfect selectivity and conversion in order to reach high molecular weight materials. Even fewer examples of tandem catalysis in polymer synthesis exist where both catalytic processes are truly complementary, and cannot be separated. In this thesis, we introduce *iterative tandem catalysis* (ITC) as a process in which multiple catalytic processes are operating simultaneously in one pot and iterative action of each of the catalysts is required for chain growth to occur.

The thesis is dedicated to the synthesis of well-defined polymeric materials by combining lipase catalysis with either nitroxide mediated radical polymerization or ruthenium-catalyzed racemization. Mechanistic and kinetic studies of lipase catalysis are performed, since a thorough understanding of the chemistry and kinetics is crucial in order to design a balanced, well-working system.

Chapter 1 starts with an overview of lipase catalysis. The mechanism of lipase-catalyzed transesterification is discussed. The application of lipases in polymer chemistry is reviewed, as well as the role of water in lipase-catalyzed polymerizations. Subsequently, tandem catalysis is discussed; the nomenclature and its applications in organic and polymer chemistry are described. A short review of ruthenium-catalyzed racemization is given, and the principle of iterative tandem catalysis (ITC) is laid out.

The synthesis of block copolymers by lipase catalysis in combination with nitroxide mediated living free radical polymerization is described in Chapter 2. This was achieved with a bifunctional initiator molecule bearing a hydroxyl group for initiation of enzymatic ring-opening polymerization of lactones and a nitroxide moiety for the radical polymerization of olefins. Block copolymers comprising a poly(styrene) and a poly( $\epsilon$ -caprolactone) block were obtained in two consecutive polymerization steps (by macroinitiation) and in a one-pot approach without intermediate transformation or work up step. The same concept was successfully applied to enzymatic resolution polymerization of racemic 4-methyl- $\epsilon$ -caprolactone combined with the radical polymerization of styrene yielding chiral block copolymers with high enantiomeric excess in the poly(4-methyl- $\epsilon$ -caprolactone) block. The lipase-catalyzed ring-opening of  $\omega$ -substituted  $\epsilon$ -caprolactones is covered in depth in Chapter 3. It is shown that the Novozym 435-catalyzed ring-opening of 6-methyl- $\epsilon$ -caprolactone (6-MeCL) is fast and *S*-selective. This results in a ring-opening product bearing a secondary alcohol with the *S*-configuration. Since lipases are strongly *R*-selective towards the nucleophile, propagation does not occur and polymerization is not possible on a realistic timescale by lipase only. Due to the reversibility of the ring-opening reaction, *R*-6-MeCL oligomers are formed on long time scales via an insertion mechanism. This unfavorable equilibrium was exploited for the development of a straightforward, accessible, ring-opening – ring-closure procedure, yielding both enantiomers of 6-MeCL with high optical purity. Iterative tandem catalysis (ITC) is introduced in Chapter 4 as a novel polymerization technique for the synthesis of well-defined materials. ITC allows the synthesis of optically pure polyesters from the racemic mixture with full conversion (see Scheme). Proof of principle is provided by the synthesis of enantioenriched *R*-oligomers from *S*-6-methyl- $\epsilon$ -caprolactone (6-MeCL) in a two-pot system. We showed that hydrogenation of 6-MeCL and dehydrogenation of the alcohol end-groups were important side reactions that severely reduce the molecular weight. Experiments in a one-pot system afforded short oligomers only. This is caused by insufficient compatibility of the two catalysts. Modification of the tandem catalytic system by using a different racemization catalyst ultimately enabled the one-pot ITC of 6-MeCL. These results are described in the thesis of Jeroen van Buijtenen.



In Chapter 5, we extended ITC to the polycondensation of a diol and a diester; dynamic kinetic resolution polymerization (DKRP). Chiral polymers were obtained from 1,1'-(1,3-

phenylene)diethanol and diisopropyl adipate. An optimization study was performed, which lead to reasonably high molecular weight polymers with high enantiomeric excess. Also with the structural isomer 1,1'-(1,4-phenylene)diethanol a chiral polyester was obtained. The DKRP using aliphatic diols also succeeded, but did not lead to enantiopure polymers. We showed that this was due to the low enantioselectivity of CALB towards the secondary alcohol groups of aliphatic diols.

The kinetics of tandem catalytic systems involving lipase catalysis are complex. In Chapter 6, we evaluate the kinetics of enzymatic ring-opening polymerizations of lactones. Special consideration is given to the dissociation constants from the active site for lactone and polyester; if these are unequal, deviation from first order kinetics will occur, as is observed experimentally. Using the Langmuir-Hinshelwood mechanism we derived rate equations for the ITC of 6-MeCL. The predicted conversion-time history accurately matches the experimental observations.

## Samenvatting van het proefschrift Tandemkatalyse in polymeerchemie

Katalyse is van groot belang voor de chemische industrie en vrijwel alle industrieel relevante chemicaliën worden geproduceerd met behulp van een katalytisch proces. Binnen de katalyse wordt onderscheid gemaakt tussen homogene katalyse (waarbij de katalysator moleculair opgelost is), heterogene katalyse (het gebruik van een vaste katalysator in een gas of vloeistof) en biokatalyse (het gebruik van enzymen, de katalysatoren van de natuur). Elk van deze drie heeft zo zijn eigen karakteristieken, toepassingen en voordelen. In de afgelopen tien jaar is er in toenemende mate onderzoek gedaan naar het simultaan toepassen van meerdere katalysatoren in één systeem, oftewel 'tandemkatalyse'. De redenering hierachter is duidelijk: het elimineren van tussentijdse opwerking resulteert in minder afvalproductie, minder energieverbruik en lagere kosten. Daarnaast biedt de wisselwerking tussen de katalysatoren de mogelijkheid tot de selectieve synthese van meer complexe moleculen.

In de synthetisch-organische chemie is de integratie van verschillende katalytische processen inmiddels gemeengoed geworden. Er is een grote variëteit aan synthetische routes ontwikkeld die simultaan gebruik maken van verschillende katalysatoren. Vaak worden daarbij de verschillende katalytische disciplines gecombineerd (homogene, heterogene en biokatalyse). Het mag daarom verrassend genoemd worden dat tandemkatalyse zelden toegepast wordt in de synthese van polymeren. Mogelijk heeft dit te maken met de complexiteit van tandemkatalytische polymerisaties: alle simultane reacties moeten verlopen met haast perfecte selectiviteit en conversie om materialen met hoog molecuulgewicht te verkrijgen. Nog zeldzamer is de toepassing van tandemkatalyse in de synthese van polymeren waarbij de katalytische processen complementair zijn en niet gescheiden kunnen worden. In dit proefschrift wordt *iteratieve tandemkatalyse* (ITC) geïntroduceerd als een proces waarbij meerdere katalytische processen tegelijkertijd actief zijn in één systeem en waarbij iteratieve werking van elke katalysator nodig is voor propagatie.

In dit proefschrift wordt de synthese van goed gedefinieerde polymeren met behulp van lipases in combinatie met nitroxide radicaalpolymerisatie of ruthenium-gekatalyseerde racemisatie beschreven. Er is mechanistisch en kinetisch onderzoek uitgevoerd, aangezien een diepgaand begrip van de chemie en de kinetiek cruciaal is voor het ontwerpen van een goedwerkend systeem.

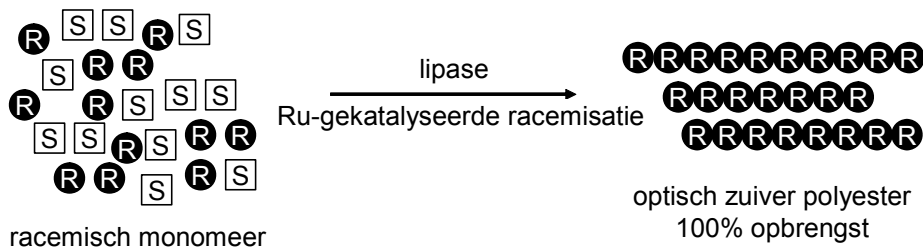
Hoofdstuk 1 geeft een overzicht van katalyse door lipases. Het mechanisme van lipase-gekatalyseerde omestering wordt beschreven en er wordt ingegaan op de toepassingen van lipases in polymeersynthese en op de rol van water hierin. Vervolgens wordt tandemkatalyse beschreven; de nomenclatuur en toepassingen in organische en polymeerchemie worden

behandeld. Verder wordt een kort overzicht van ruthenium-gekatalyseerde racemisatie gegeven en wordt het principe van ITC uitgelegd.

In Hoofdstuk 2 wordt de synthese van blokcopolymeren door middel van de combinatie van lipases met nitroxide radicaalpolymerisatie beschreven. Hiervoor is een bifunctioneel initiatormolecuul gebruikt met een hydroxylgroep voor de initiatie van de enzymatische ringopeningpolymerisatie en een nitroxidegroep voor de radicaalpolymerisatie van alkenen. Er zijn blokcopolymeren verkregen met een poly(styreen)- en een poly( $\epsilon$ -caprolacton)blok. De polymeren zijn gesynthetiseerd in een tweestapsprocedure (via macro-initiatie), maar ook in één pot zonder tussentijdse omzetting of opwerking. Dezelfde procedure is toegepast op de combinatie van een enzymatische resolutiepolymerisatie van racemisch 4-methyl- $\epsilon$ -caprolacton met de radicaalpolymerisatie van styreen, resulterend in chirale blokcopolymeren met een hoge enantiomere zuiverheid in het poly(4-methyl- $\epsilon$ -caprolacton)blok.

In hoofdstuk 3 wordt ingegaan op de lipase-gekatalyseerde ringopening van  $\omega$ -gesubstitueerde lactonen. Ringopening van 6-methyl- $\epsilon$ -caprolacton (6-MeCL) met Novozym 435 is snel en *S*-selectief. Het ringopeningsproduct bevat een secundaire alcoholfunctie met de *S*-configuratie. Omdat lipases een hoge selectiviteit vertonen ten opzichte van *R*-alcoholen als nucleofiel, is propagatie niet mogelijk; polymerisatie vindt op deze tijdschaal niet plaats met alleen lipase. Aangezien de ringopening reversibel is, worden op de lange duur wel *R*-6-MeCL oligomeren gevormd via een insertiemechanisme. Op basis van dit evenwicht is vervolgens een eenvoudige, toegankelijke procedure ontwikkeld op basis van ringopening en ringsluiting voor de synthese van beide enantiomeren van 6-MeCL met hoge enantiomere zuiverheid.

In Hoofdstuk 4 wordt ITC geïntroduceerd als een nieuwe polymerisatiemethode voor de synthese van goedgedefinieerde materialen. Met ITC is het mogelijk om optisch zuivere polyesters te synthetiseren vanuit het racemische monomeer met volledige omzetting (zie schema). Het principe is bewezen met de synthese van *R*-oligomeren uit *S*-6-MeCL in een twee-pots-systeem. Hydrogenatie van 6-MeCL en dehydrogenatie van de alcohol eindgroepen zijn belangrijke zijreacties gebleken die het molecuulgewicht negatief beïnvloeden. In een één-pots-systeem zijn alleen korte oligomeren verkregen. Onvoldoende compatibiliteit van de beide katalysatoren was hiervan de oorzaak. Uiteindelijk is ook de één-pots ITC van 6-MeCL gelukt door het gebruik van een andere racemisatiekatalysator. Deze resultaten staan beschreven in het proefschrift van Jeroen van Buijtenen.



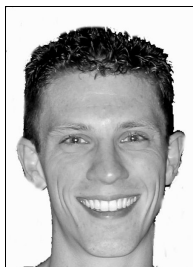
Vervolgens is ITC uitgebreid met de polycondensatie van een diol en een diester; dit wordt dynamische kinetische resolutiepolymerisatie genoemd (DKRP). Deze resultaten staan beschreven in Hoofdstuk 5. Met 1,1'-(1,3-fenyleen)diethanol en diisopropyladipaat als monomeren zijn chirale polymeren verkregen. Een optimalisatiestudie resulteerde in polymeren met redelijk hoog molecuulgewicht en hoge enantiomere zuiverheid. Ook de polymerisatie met de para-isomeer 1,1'-(1,4-fenyleen)diethanol resulteerde in een chirale polyester. Het gebruik van alifatische diolen in DKRP was ook mogelijk, maar leidde niet tot optisch zuivere polymeren. Dit kon verklaard worden vanuit de lage enantioselectiviteit van CALB ten opzichte van de secundaire alcoholgroepen van alifatische diolen.

De kinetiek van tandemkatalytische systemen die gebruik maken van lipases is complex. In Hoofdstuk 6 wordt gekeken naar de kinetiek van enzymatische ringopeningspolymerisatie. In het bijzonder wordt er aandacht besteed aan de dissociatieconstanten voor de complexen die ontstaan tussen het katalytische centrum en enerzijds een lacton of anderzijds een polyestermolecuul. Als deze niet gelijk zijn, is er geen sprake van (pseudo) eerste orde kinetiek. Met behulp van het Langmuir-Hinshelwood mechanisme is de kinetiek van de ITC van 6-MeCL beschreven. De voorspelde kinetiek komt goed overeen met de experimentele data.





# Curriculum Vitae



In Nijmegen, op zaterdag 7 mei 1977, werd Bart van As geboren. Na de eerste 12 jaar van zijn leven in Nijmegen gewoond te hebben, verhuisde hij in 1989 naar Deurne. Daar spendeerde hij zijn middelbare school periode aan het Sint Willibrord Gymnasium. Na een korte periode van 3 maanden aan de Universiteit Twente zette hij zijn studie Scheikundige Technologie voort aan de Technische Universiteit Eindhoven. Een afstudeerproject bij de vakgroep Homogene Katalyse en Coördinatiechemie onder leiding van prof. dr. Dieter Vogt resulteerde in 2002 in de afronding van deze studie. Vanaf november 2002 heeft Bart als promovendus gewerkt in de vakgroep Macromoleculaire en Organische Chemie aan de Technische Universiteit Eindhoven onder leiding van prof.dr. Bert Meijer en dr.ir. Anja Palmans. Dit proefschrift bevat de belangrijkste resultaten van het onderzoek.

On Saturday May 7<sup>th</sup> 1977, Bart van As was born in Nijmegen. After living in Nijmegen for 12 years, he moved in 1989 to Deurne. There he followed secondary education at the Sint Willibrord Gymnasium. After a short stay of 3 months at Twente University, he continued his study Chemical Engineering at the Eindhoven University of Technology. Bart finished his study with a graduation project at the Laboratory of Homogeneous Catalysis and Coordination Chemistry under guidance of prof.dr. Dieter Vogt. Since November 2002, Bart worked as a PhD student at the Eindhoven University of Technology under guidance of prof.dr. Bert Meijer and dr.ir. Anja Palmans. This thesis describes the most important results of his work.





# Nawoord

Tsja, daar zit je dan. Na vier jaar proeven doen en een aantal maanden schrijven aan dit proefschrift heb ik nu nog een uurtje en een lege pagina over. Te vullen met wat overdenkingen, en een bedankje aan een aantal personen. Maar dat laatste bewaar ik even voor het einde. Ik vind het namelijk een mooi moment om eerst even terug te blikken. Normaal gesproken kijk ik liever vooruit, het is ten slotte de toekomst die je nog gaat beleven, maar voor deze gelegenheid maak ik een uitzondering. Ik sluit met dit proefschrift toch een periode van vier jaar af.

Vier jaar lijkt een lange tijd. Toch heb ik het gevoel dat het voorbijgevlogen is. Dat maakt me een beetje angstig, want laatst vertelde iemand mij dat, naarmate je ouder wordt, de tijd steeds sneller lijkt te gaan. De meesten van jullie weten dat ik ouder worden niet echt waardeer, ik waan mezelf liever wat jonger dan ik ben. Schijnt in de familie te zitten, hè mam? Maar als ik wat dieper nadenk, schieten er ontelbare herinneringen in gedachten. Die vier jaar mogen achteraf dan kort lijken, ik heb ontzettend veel meegemaakt in die tijd. Weekendjes weg, vakanties, sporten, verjaardagen, stapavonden, vrienden gemaakt en ook uit het oog verloren...teveel om op te noemen. En dat zijn alleen nog de dingen van buiten werktijd. Bij de vakgroep heb ik ontzettend veel geleerd, niet alleen op inhoudelijk gebied, maar vooral ook op het persoonlijke vlak. Eén ding tegelijk en afmaken waar je mee bezig bent, een hele uitdaging voor Bart! Ach, uiteindelijk ben ik daar redelijk in geslaagd. Nou ja, ik heb vooruitgang geboekt, zullen we maar zeggen. D'r ligt een proefschrift, dus ik heb toch iets goed aangepakt.

Dat had ik niet kunnen bereiken zonder de hulp en toewijding van een aantal personen. Anja, volgens mij heb ik je af en toe slapeloze nachten bezorgd, maar onze samenwerking heeft mij een hoop geleerd en ik heb veel waardering voor de manier waarop je mij begeleid hebt. Bert, jouw input was van onschatbare waarde. We waren het niet altijd eens, al moet ik toegeven dat je achteraf toch regelmatig gelijk bleek te hebben. Ben ik misschien soms iets té eigenwijs? (Open vraag, geen antwoord graag!) Jeroen, we hebben de afgelopen jaren intensief samengewerkt aan de ontwikkeling van ITC. Ik heb dat altijd heel prettig en gezellig gevonden, al vraag ik me sinds het lezen het dankwoord in jouw proefschrift af waarom je onze samenwerking 'uitdagend' vond ;-). Kalle, you gave me the opportunity to visit your group in Stockholm twice. I really enjoyed your hospitality and the atmosphere at KTH, thank you very much for that experience. And, of course thank you for your willingness to take place in my committee. Dat laatste geldt ook voor Jan van Hest: hartelijk dank voor het

plaatsnemen in mijn commissie en voor de tijd en moeite die je in het lezen van mijn proefschrift hebt gestoken. Emmo Meijer, Jan Meuldijk en Jef Vekemans wil ik hartelijk danken, zowel voor het plaatsnemen in mijn commissie als voor hun voortdurende interesse in mijn werk en resultaten en hun aanstekelijke enthousiasme. Dat heeft mij heel erg gestimuleerd en gemotiveerd om er iets moois van te maken!

Nu ik toch aan het bedanken ben, er komen een heleboel namen in mij op van personen die mijn leven hebben gemaakt tot wat het was de afgelopen jaren. Als ik iedereen apart zou noemen, was ik nog wel even bezig. Daarom hier een lijst, al ben ik bang dat hij onvolledig is. Mocht ik jou vergeten zijn te noemen, sorry! Ik denk vaak aan je, maar op dit moment net even niet! Komt 'ie: pa, ma, Hanneke, Koen, Nicole, Marco, Anna, Tijmen, Jurre, Oma, Harry, Mieke, Daan, Carlijn, Marloes, Bram, Menno, iedereen van SMO nu en vroeger (ja, daar maak ik me makkelijk van af zo ;-), Bart, Bert, Harm, Freek, René, Wil, Marloes, Hein, Linda, Bart, Barbara, Bart, Joke, Marcel, Mara, Jordi, Wilbert, Joris, Leon, Bas, Oscar, Bart, Marian, Reinder, Bianca, Pieter, Wilm, Woutjan, Martijn, Sjef, Vusal, Ramses, Renze, Elise, Raymond, Stefan, Doris, Bart B (2x), Jurgen, Lotte, Debby, Bas, Tess, Manon, Frank, Marlies, Janny, Marleen, Susan, Maartje, Tristan en Jessica: ik vond en vind het supergezellig met jullie en hoop dat het nog lang zo blijft!

Eens kijken, ik heb nog een paar regels over. Is er nog iets wat ik kwijt wil, waarvan ik denk dat ik de lezer ermee verblijd? Er schiet mij niets te binnen, en anders vertel ik het jullie persoonlijk wel. Ik heb gelukkig niet zo'n moeite met praten, dus dat moet lukken. Het is nu mooi geweest. Ik sluit een proefschrift af, en een stuk van mijn leven. En op beiden kijk ik met een goed gevoel terug. Mooi toch?

